Preparation and Characterization of Conjugated Polymer Thin Films for the Fabrication of Electrochromic Rear-view Mirror

THESIS

Submitted in partial fulfilment
of the requirements for the degree of

DOCTOR OF PHILOSOPHY

by

SIJU C.R.
2009PHXF029P

Under the Supervision of

Prof. S. SINDHU

BIRLA INSTITUTE OF TECHNOLOGY AND SCIENCE

PILANI (RAJASTHAN) INDIA

2015

Preparation and Characterization of Conjugated Polymer Thin Films for the Fabrication of Electrochromic Rear-view Mirror

THESIS

Submitted in partial fulfilment
of the requirements for the degree of

DOCTOR OF PHILOSOPHY

by

SIJU C.R.
2009PHXF029P

Under the Supervision of

Prof. S. SINDHU

BIRLA INSTITUTE OF TECHNOLOGY AND SCIENCE

PILANI (RAJASTHAN) INDIA

2015

BIRLA INSTITUTE OF TECHNOLOGY AND SCIENCE
PILANI (RAJASTHAN)

CERTIFICATE

This is to certify that the thesis entitled "Preparation and Characterization of Conjugated Polymer Thin Films for the Fabrication of Electrochromic Rear-view Mirror" which is submitted for the award of Ph.D. degree of the Institute embodies original work done by Siju C.R, ID No 2009PHXF029P, under my guidance and supervision.

Signature of the supervisor   :

Name of the supervisor   : Prof. S. SINDHU

Designation   : Associate Professor

Date:

ACKNOWLEDGEMENTS

ABSTRACT

Conjugated polymers (CPs) have been paid more attention in electrochromic device applications due to their high color contrast, fast response time, low operation potential, higher coloration efficiency, better optical memory, good switching stability, and offering color variability. The main challenge of conducting polymers based electrochromic window and rear-view mirror is to change a color from highly transparent state to highly dark/opaque state under redox potential. Nowadays, design and synthesis of novel functionalized conjugated polymers and tuning their optoelectronic properties are exploring area in organic electronics.

This thesis is focusing on design, synthesis, and characterization of conducting polymers to enhance the electrochromic performances of the materials and to fabricate a single type electrochromic window and rear-view mirror based on these newly functionalized conducting polymers. Herein, the electrochromic properties of CPs are mainly tuned by various approaches such as doping, treated with electrochemically exfoliated graphene, structural modifications of monomers, and the copolymerization.

A simple and cost-effective one step cyclic voltammetry technique for the polymerization of poly(3,4 ethylenedioxythiophene) (PEDOT) and PEDOT doped polystyrene sulfonate (PSS) films in aqueous electrolyte medium was presented. The influence of polymerization conditions and dopants on electrochromic properties of PEDOT was observed. The potentio-statically polymerized PEDOT doped with PSS (PEDOT:PSS) film exhibits uniform morphology, and good electrochemical and electrochromic performance compared to its conventional polymer (PEDOT).

Electrochemical and electrochromic (EC) properties of PEDOT film were further tuned by incorporating ion enriched graphene (IEGR) into polymer matrix. The PEDOT-IEGR films showed very high electrical conductivity (~3968 Scm^{-1}) and showed optical response both in the visible and near-IR regions. The electrochromic coloration of the PEDOT-IEGR film changed between greyish purple to transmissive blue while compared to conventional PEDOT. The electrochromic devices (ECDs) based on the PEDOT-IEGR provide a faster response time, good optical stability, broad absorption in the entire visible region, and stable optical memory.

Novel solution-processable di-isopropylbenzyl substituent on poly(3,4 propylenedioxythiophene) nanobelts (PProDOT-IPBZ$_2$) is prepared by reverse mircoemulsion polymerization method. The PProDOT-IPBZ$_2$ polymer appeared as thin nanobelts structures with high aspect ratio (3:100) and found to be soluble in common organic solvents. The polymer films were prepared by spray coating, solution casting, and electropolymerization methods. The electropolymerized PProDOT-IPBZ$_2$ films showed a higher color contrast of 48 % with response time of <1 s and coloration efficiency was calculated as 305 cm^{2}C^{-1}. This PProDOT-IPBZ$_2$ film showed higher transparency at +1.0 V and dark purple color at −1.0 V. The PProDOT-IPBz$_2$ based electrochromic window showed a good optical contrast (40%), fast response time (~2 s), excellent switching stability, low switching voltage (±1.0 V), and outstanding optical memory. The PProDOT-IPBz$_2$ based EC rear-view mirror exhibited a high reflectance contrast (47%), good absorption of yellow color, and better switching stability without any distortion of efficiency after 1000 cycles.

A new π-conjugated monomer unit containing structural components of thiophene and carbazole as a single molecule entity was synthesized by stille coupling method. The corresponding polymer, P(Th-Cbz-Th) (P1) and its copolymer with PEDOT, P(Th-Cbz-Th)-PEDOT (P2) were electrochemically polymerized by cyclic voltammetry technique between the potential of −1.0 and 1.4 V at a scan rate of 100 mVs^{-1}. The spectroelectrochemical and electrochromic properties of P1 and P2 films were studied. We noted that P(Th-Cbz-Th) film is anodically coloring, and showed electrochromic coloration between blackish blue (1.5 V) and pale yellow (−1.0 V). However, P(Th-Cbz-Th)-PEDOT copolymer film exhibits multi-electrochromic coloration from reddish brown to blue; in intermediate colors of brown, yellowish brown, yellowish green, and yellow were observed. The P(Th-Cbz-Th)-PEDOT films showed good color contrast in visible (43 %) and near IR (57 %) regions, applicable response time (2–3 s), good optical memory (8–10 % memory loss), and better optical switching stability over 500 cycles. A single-type electrochromic rear-view mirror and window based on these polymer films were fabricated and their EC performances were tested. Electrochromic rear-view mirrors showed a significant reflection contrast at visible (33% T) and near IR regions (48% T), faster response time (2–4 s), applicable coloration efficiency, good open circuit memory, and better long-term electrochemical stability (>250 cycles). EC windows also showed a good optical contrast both in visible (28–33%) and near IR regions (40–43 %), faster response time (2–4 s), applicable coloration efficiency, stable optical memory, and better optical switching stability.

CONTENTS

LIST OF FIGURES

function of different applied potentials between −1.5 V and 2.0 V.

various applied potentials from −1.5 V to 1.2 V in 0.1 M TBAP/ACN solution, and (b) photographs of PEDOT-IEGR film in the reduced and oxidized states

mVs^{-1}

LIST OF SCHEMES AND TABLES

LIST OF ACRONYMS

ACN	Acetonitrile
AgNO$_3$	Silver nitrate
Al	Aluminium
AOT	Sodium bis (2 ethyl hexyl) sulfosuccinate
BSE	Backscattered electrons
CB	Conduction band
CDCl$_3$	Deuterated chloroform
CE	Counter electrode
CIE	Commission Internationale de l'Eclairage
CMY	Cyan- magenta-yellow
CP	Conducting polymer
CPE	Constant phase element
CSA	R-camphor sulphonic acid
CV	Cyclic voltammetry
CVD	Chemical vapour deposition
D-A	Donor-acceptor
DCM	Dichloromethane
DMF	Dichloromethane
EA	Electron affinity
e-beam	Electron beam
EC	Electrochromic
ECD	Electrochromic device
ECM	Electrochromic rear-view mirror
ECW	Electrochromic window
EDOT	3,4 ethylenedioxythiophene
EIS	Electrochemical impedance spectroscopy

FeCl$_3$	Ferric chloride
FTIR	Fourier transform infrared spectroscopy
HCl	Hydrochloric acid
HOMO	Highest occupied molecular orbital
IEGR	Ions enriched graphene
IP	Ionization potential
IR	Infra-red
ITO	Indium tin oxide
K$_3$Fe(CN)$_6$	Potassium ferricyanide
KNO$_3$	Potassium nitrate
LCDs	Liquid crystal displays
LED	Light emitting diodes
LiClO$_4$	Lithium perchlorate
LUMO	Lowest unoccupied molecular orbital
Lu(Pc)$_2$	Lutetium bis(phthalocyanine)
MgSO$_4$	Magnesium sulfate
MPc	Metal phthalocyanines
NBS	N-bromosuccinimide
n-BuLi	n-butyllithium
NMR	Nuclear Magnetic resonance
PA	trans-polyacetylene
PANI	Polyaniline
PB	Prussian blue
PC	Propylene carbonate
PD	Potentiodynamic
PEB	Poly(3,4-ethylenedioxythiophene-didodecyloxybenzene)
PEDOP	Poly(3,4ethylenedioxypyrrol)
PEDOT	Poly(3,4 ethylenedioxythiophene)

PMMA	Poly methyl methacrylate
PProDOP	Poly(3,4 propyledioxypyrrol)
PProDOT	Poly(3,4 propylenedioxythiophene
PProDOT-IPBZ$_2$	Isopropylbenzyl derivative of Poly(3,4 propylenedioxythiophene
Ppy	Polypyrrol
ProDOT	3,4 propylenedioxythiophene
PS	Potentiostatic
PSS	Poly(styrenesulfonate)
PTh	Polythiophene
P(Th-Cbz-Th)	Poly 2,7-dithienylcarbazole
p-TSA	p-toluene sulfonic acid
PXDOP	Poly(alkylenedioxypyrrol)
PXDOT	Poly(3,4 alkylenedioxythiophene)
RE	Reference electrode
RGB	Red-Green-Blue
SCE	Saturated calomel electrode
SDS	Sodium dodecyl sulphate
SEM	Scanning Electron Microscopy
SnBu$_3$Cl	tri-butylchlorostannane
TBAB	Tetrabutylammonium bromide
TBAP	Tetrabutylammonium perchlorate
TMS	Tetramethylsilane
UV	Ultraviolet
VB	Valence band
WE	Working electrode
WO$_3$	Tungsten oxide
XPS	X-ray photo electron spectroscopy

LIST OF SYMBOLS & UNITS

A	Absorbance
a*	Hue
b*	Color intensity
c	Concentration of the electrolyte
c	Speed of light
C	Capacitance
cm	Centimeter
D	Diffusion constant
E_{BLA}	Bond length alternations
Eg	Energy band gap
E_{Inter}	Inter-molecular interaction
E_{pc}	Cathodic peak potential and
E_{pa}	Oxidation anodic peak potential
E^{on}_{oxd}	Onset oxidation potential
E^{on}_{red}	Onset reduction potential
E_{Res}	Resonance stabilization energy
E_{Sub}	Electron-acceptor/donor substituents
E_{θ}	Planarity
eV	Electron Volt
F	Faradays constant
h	Planck constant
Hz	Hertz
I	Current
I	Intensity
i_p	Peak current
I_{pa}	Anodic peak current

I_{pc}	Cathodic peak current
l	Pathlength
L*	Brightness or luminance
mA	Milliampere
mg	Milligram
mL	Milliliter
mm	Millimeter
M	Molar concentration
M_w	Molecular weight
n	Number of electrons
nm	Nanometer
psi	Pound per square inch
Q_d	Charge injected/ejected per unit area
R	Reflection
R_{ct}	Charge-transfer resistance
rpm	Rotation per minute
t or d	Thickness
T	Transmission
Tb	Transmittance at bleached state
Tc	Transmittance at colored state
tb	Response time for bleaching
tc	Response time for coloring
s	Second
S	Siemens
V	Voltage
W	Warburg Impedance
Z	Impedance
Z'	Real Impedance

Z"	Imaginary Impedance
λ_{max}	Absorption maxima
α	Alpha
β	Beta
δ	Chemical shift
ΔT%	Color contrast/Contrast ratio
η	Coloration efficiency
C	Columb
Γ	Concentration of the surface bound electroactive species
ºC	Degree centigrade
υ	Frequency
σ	Ionic Conductivity
μA	Mircoampere
ε	Molar extinction coefficient
Ω	Ohm
ω	Omega (Angular frequency)
ΔOD	Optical density
θ	Phase angle
π	Pi
ΔR	Reflection contrast
ρ	Resistivity
ν	Scan rate
λ	Wavelength

CHAPTER 1

INTRODUCTION

1.1. An Overview about Conducting Polymers

1.1.1. Brief History of Conducting Polymers

Commonly, polymers have been considered poor electronic conductors and have been used extensively as insulators in electronics applications. The first report of conducting polymer (CP), carbon black (currently known as polyaniline) synthesis was reported in 1862 by H. Letheby using anodic oxidation of aniline [1]. But the real application of CPs started in 1977, when trans-polyacetylene (PA) was discovered by A. Heeger, A. MacDiarmid and H. Shirakawa [2–4] who were awarded the Nobel Prize in Chemistry in the year 2000. They reported that the electrical conductivity of PA can be increased by many orders of magnitude to reach metallic-like behaviour by simply doping it with Iodine [2]. Even though PA exhibits high conductivity in the doped state, it is unstable in air and insoluble in common organic solvents, resulting in a lack of processability. To resolve this drawback, researchers have focused on the synthesis of new conjugated polymers, which are stable, highly conductive, easy processable, and inexpensive.
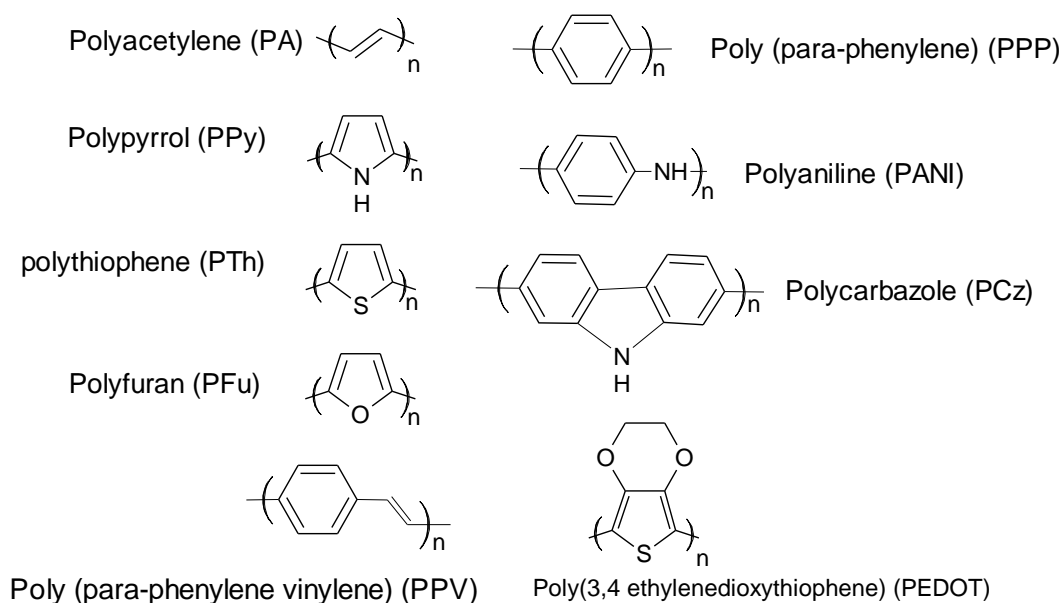
Figure 1.1: The chemical structures of some common conducting polymers

Conducting polymers based on aromatic hetero cycle compounds such as polyaniline (PANI), polypyrrol (Ppy), polythiophene (PTh) and their derivatives were prepared and studied over the last few decades [5]. These conducting polymers have been paid more attention due to their environmental stability, light weight, high conductivity, and ease of processability. In addition, the opto-electronic properties of CPs can be tuned by modifying monomer structures, and with various doping conditions [6]. The chemical structures of commonly used CPs are shown in Figure 1.1.

Many methodologies have been used to design and synthesise conductive polymeric materials to achieve good electrical, optical, and mechanical properties along with environmental stability and high processability [7–13]. A basic understanding of how the structural modification is related to characteristic material properties is required while synthesising a new material for end-user applications. Recent research indicates that the magnitude of the band gap and position of the conduction and valence band are important factors that control the optical and electrical properties of CPs [14, 15]. Nowadays, a fine tuning of the band gap is a significant feature for conducting polymers in advanced optoelectronic applications.

1.2. Electrical Properties of Conducting Polymers

1.2.1. Band Theory

Generally, materials can be classified into three states based on their electrical conductivity-insulators, semi-conductors and conductors. The comparison of energy level diagrams of a conductor, semiconductor and insulator are shown in Figure 1.2. CPs are usually insulators in the neutral stage; however, the electrical properties of CPs can be increased from the insulating state to the conducting state using oxidation (p-doping) or reduction (n-doping). The conduction mechanism of conjugated polymers is different from that of metals and inorganic semi-conductors. In conductive polymers, the main chain is mainly formed by carbon atoms with alternate single and double bonds. The one 2s orbital and the two 2p orbitals of the carbon atoms overlap to form a 3 sp2 hybridized orbital. Two of the hybridized sp2 orbitals bonded covalently (σ–bond) and one unhybridized p_z orbital present on the neighbouring carbon atoms overlap by weak π- bonds. These weakly bound π- bonds can be easily delocalized during doping, and provide better conduction in conjugated polymers.

According to band theory, when two identical atoms with half-filled orbitals are attracted together, they form two new discrete energy bands, in which one has the highest occupied

electronic energy level (valence band, VB) and another with the lowest unoccupied energy level (conduction band, CB). The difference between the highest occupied molecular orbital (HOMO) and the lowest unoccupied molecular orbital (LUMO) is called energy band gap (E_g) [16]. The energy band gap determines the intrinsic electrical and optical properties of the materials. Most conjugated polymers are semi-conductors due to their narrower energy band gap that can be easily altered by doping [17,18].
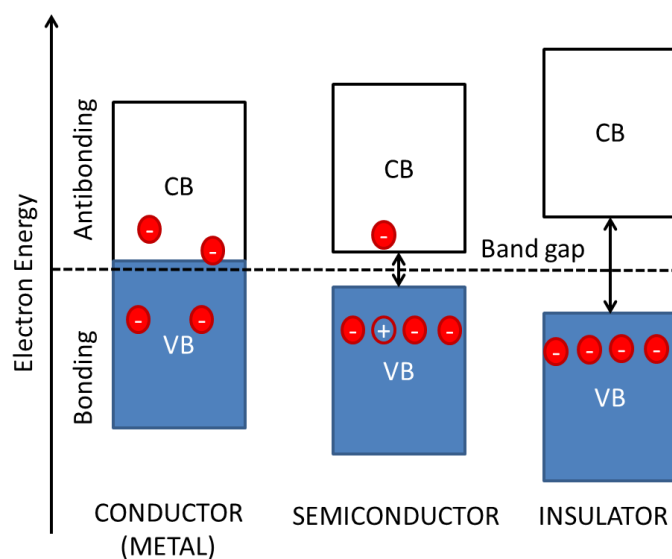
Figure 1.2: Comparison of energy level diagrams of conductor, semiconductor and insulator

1.2.2. Conduction Mechanism

1.2.2.1. Doping and Charge Carriers

The modification of electrical conductivity of CPs from insulating to conducting state upon oxidation/reduction is usually referred to as doping. The materials which are used for the doping process are called dopants and may be either anionic or cationic materials. Doping can be classified as chemical doping and electrochemical doping. Chemical doping is an efficient process even though it is difficult to control. This can be overcome by electrochemical doping that is a simple and easy process and can be controlled by applying the appropriate potential. During the doping, CPs possess an intermediate band between the CB and VB that can modify the band gap of materials and hence alter the aromaticity. Figure 1.3 shows the conductivity values in various materials.
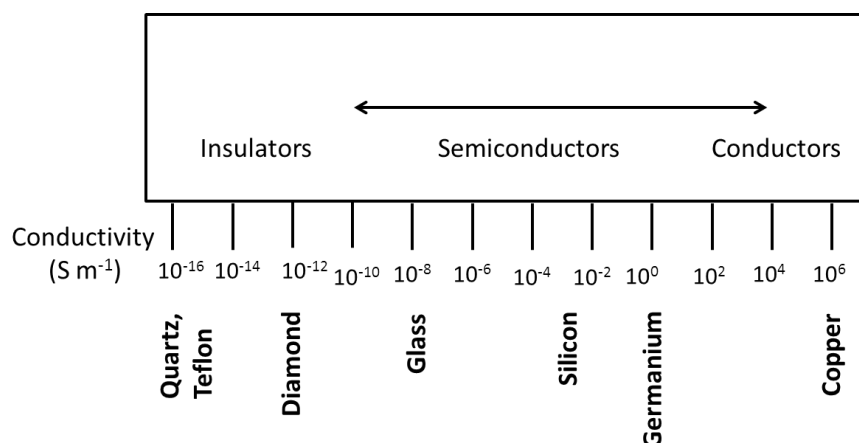
Figure 1.3: The conductivity chart of various materials
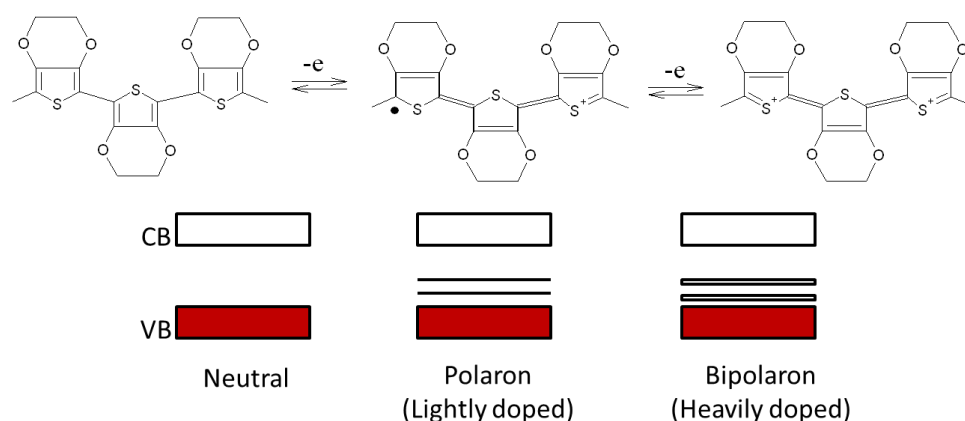
Figure 1.4: The formation of polarons and bipolarons on conjugated poly(3,4 ethylenedioxythiophene) and corresponding schematic band structures.

During oxidative doping, the removal of an electron from the neutral polymer chain results in the generation of polarons (radical cations) and transforms the structure from benzenoidal state to quinoidal state that leads to a charge transfer along the main polymer chain. On further doping, more electrons are removed from the polymer backbone and are then converted to bipolarons (bications). Polarons may be either radical cations or radical anions depending on the redox doping. Both polarons and bipolarons can transfer along the polymer chain in an electric field, and, hence, conduct electricity. The charge carriers are reversible and can be reverted back when the polarity of the potential is changed [19]. The formation of polarons and bipolarons on conjugated poly(3,4 ethylenedioxythiophene) (PEDOT) and its schematic band structures is given in Figure 1.4.

1.3. Factors Affecting Band Gap and Color Control

The electrochromic coloration of conductive polymers is directly related to the energy gap between CB and VB. Therefore, several structural aspects should be taken into consideration to modify the band gap (E_g) of the conducting polymers. An overview of the parameters affecting the band gap of conducting polymers is schematically represented in Figure 1.5. The energy band gap of the linear π-conjugated system is determined by the sum of several factors: bond length alternations (E_{BLA}), planarity (E_θ), electron-acceptor/donor substituents (E_{Sub}), inter-molecular interaction (E_{Inter}) and resonance stabilization energy (E_{Res}) [15].

$$Eg = E_{BLA} + E_\theta + E_{Sub} + E_{Inter} + E_{Res}$$

However, the exact fine tuning of the band gap is not an easy process because all the afore mentioned factors influence and are also closely related to each other. This may affect other important characteristic properties of the materials. Bond length alternation is defined as the difference between the single and double bond length of the polyacetylene. However, this may not be appropriate for polyaromatic materials as they show two different states like benzenoid and quinoid with a non-degenerate ground state [20]. Bredas et al. stated that the bond length alternation is the maximum difference between the lengths of the C-C bond relative to the chain axis and the C-C bond parallel to the chain axis [21]. The E_g value will decrease as the contribution of the benzenoid geometry decreases, or the quinoid geometry increases on polymer chain. The presence of single bond between two aromatic rings causes a twist in the conductive polymers, and this rotational defect around the single bond leads to decrease in the effective conjugation length. Thus, any alteration from planarity exhibits an increase in the band gap [22]. The band gap of the polymer generally decreases on decreasing the resonance energy that influences π-electron confinement within the aromatic rings and delocalization along the chain. The position and behaviour of the substituents have a major influence on the band gap of the polymer main chain. The electron withdrawing groups usually lower the energy of LUMO and electron donating groups increase the energy of HOMO. The intermolecular and inter-chain interactions of polymer chains affect their orientation in the solid state and decrease the band gap of polymers [23]. A donor-acceptor type (D-A Type) synthetic approach has been developed to reduce the band gap of polymer. In this approach, the incorporation of electron rich (donor) and electron deficient (acceptor) groups in the main polymer conjugation chain results in the modulation of the band gap, and multi-coloration of the resulting D-A type polymers [24–28].
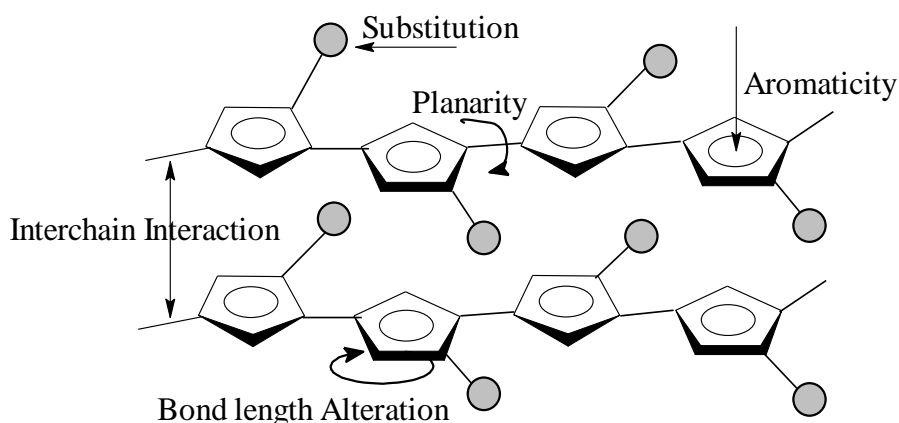
Figure 1.5: An overview of the parameters affecting band gap of conducting polymers

1.4. Synthesis of Conductive Polymers
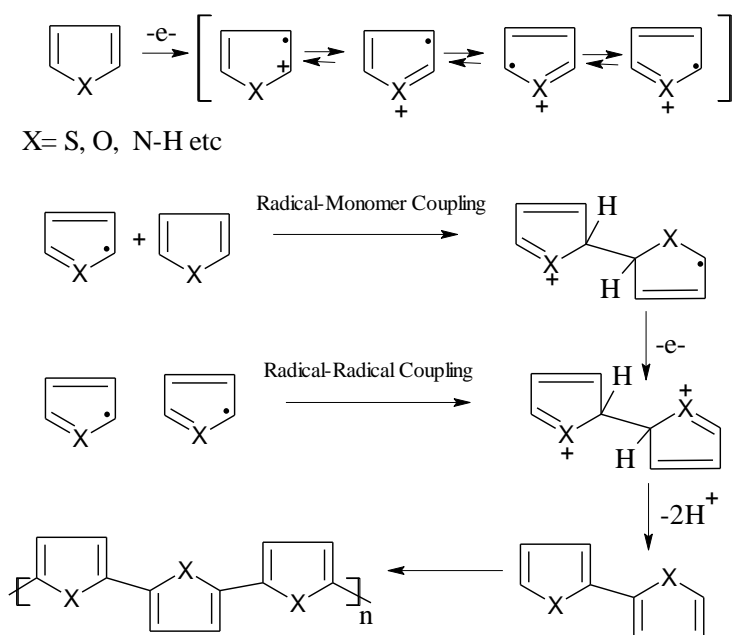
Figure 1.6: Mechanism of oxidative polymerization of heterocyclic materials

Conducting polymers have been generally polymerized by chemical or electrochemical methods [29].When bulk production is required, chemical polymerization is a suitable method. Even though the purification of final products requires more attention and reactions of chemical reagents, by-products and unreacted monomers may sometime affect the properties of CPs. Electrochemical polymerization is a simple, reproducible and convenient method when the formation of uniform polymer films and various nanostructures is desired.

6

The fine control of film thickness and the morphology of the film can be obtained by altering the experimental parameters of electrochemical polymerization such as applied potential, solvent, concentration of reagents, charge, and polymerization time. The other relatively rare techniques such as metathesis polymerization, stille polymerization, photochemical polymerization, vapour phase polymerization, and pyrolysis are also used for the synthesis of CPs [5]. A typical mechanism of oxidation polymerization for thiophene is illustrated in Figure 1.6.

1.4.1. Chemical Polymerization

In oxidative chemical polymerization, a stoichiometric number of oxidative agents are used to produce a polymer that will be either neutral or conductive. The most commonly used oxidative agents are $FeCl_3$ and other Lewis acids. The reduction of the neutral polymer is achieved by the addition of strong base like ammonium hydroxide and hydrazine hydrate. In the first step, the radical cations are generated by the oxidation of monomers. After the initial oxidation, radical-radical cation coupling and de-protonation between the neighbouring radical cations lead to the formation of dimers. The oxidation and propagation processes are then repeated alternately. When the nucleophilic reaction occurs on polymer chains, the polymerization process is terminated. Chemical oxidative polymerization is a widely used synthesis technique for the production of large quantities of polymers at a low cost. However, there are other possibilities of side reactions in the chemical oxidative polymerization of heterocycles resulting in coupling defects on the polymer main chain that reduce the linearity and planarity of polymers.

1.4.2. Electrochemical Polymerization

In electrochemical polymerization, the monomer is first oxidized as a delocalized radical cation (or anion) while applying a positive (or negative) potential to the working electrode. This process is considered the rate determining step in electrochemical polymerization, and it is much slower than the electron transfer reaction. The further rate of this radical species depends on experimental conditions such as monomer concentration, electrolyte composition, temperature, applied potential, nature of the substrate etc. Then, the dimerization process occurs by a reaction between two radical cations (or anions) that leads to dimers. The propagation and termination reactions are relatively the same as the chemical polymerization discussed in the previous section. These electrochemical oxidation and radical coupling processes are repeated continuously and result in the formation of oligomers. These formed

oligomers become insoluble in the electrolyte medium, and are then deposited onto the working electrode due to its lower oxidation potential than the corresponding monomer. Electrochemical polymerization is a widely-used method for the preparation of small uniform thin films. However, this method is not applicable to large scale preparation and large area films.

The electropolymerization of heterocyclic materials have two possible reactions through α−α couplings and α−β couplings. If the polymerization occurs through α−α couplings, linear backbone polymers and enhanced electrical properties are produced. However, the polymerization occurrence of α−β linkage in a normal chain modifies its electronic distribution. This linkage defect generates a twist in adjacent chains, and leads to an increase in the number of undesired couplings, and decreases the effective mean conjugation length of the polymer chain [29].

1.5. Common Applications of Conductive Polymers

The common application areas of conductive polymers are broadly classified into two types based on their conductivity and electro-activity. The ability to tune both the electrochemical and optoelectronic properties of conducting polymers has been used in a wide range of applications. Some of the potential applications of these materials are the photovoltaic cell [30], light emitting diodes (LED) [31], storage batteries[32], super capacitors [33], transistors [34], fuel cells [35], sensors [36], corrosion protection [37], smart pixels displays[38], electrochromic devices [39], actuators [40], conductive textiles [41], and artificial muscles [42].

1.6. Chromic Phenomena

In the late 17th century, Newton discovered the relationship between light and colour, and the utilization of this fundamental science in both art and technology has become a booming area of interest to many researchers. Colour changes in chromic materials are due to many reasons, especially by both physical and chemical stimuli; this can be grouped into the five following fundamental chromic phenomena [43]:

1. Reversible color change (e.g. electrochromism, photochromism)
2. Absorption and reflection of light (e.g. classical organic/inorganic dye and pigments)
3. Absorption of energy and emission of light (e.g. phosphorescence, fluorescence)
4. Absorption of light and energy transfer/conversion (e.g. photosensitizer, solar energy conversion)

5. Manipulation of light (e.g. liquid crystals, lasers)

Chromism is defined as a reversible change in the colour of a material as a result of an external stimulus such as heat, light, solvent and electrical potential. Conjugated polymers are well known to show such chromic phenomena especially solvatochromism, thermochromism, photochromism, and electrochromism. Except electrochromism, the other major types of chromism can be due to conformation-induced chromism. This is defined as the change of effective conjugation length by altering the planarity of the backbone and the degree of π-orbital overlap by external forces. That alters the effective band gap due to the change in the electronic states of the molecules, and eventually the optical properties of the material.

Solvatochromism is the reversible color change induced by solvents and this is often due to changes in the polarity of various solvents. Thermochromism is the reversible optical property of a substance induced by temperature change that changes the overall conformation of the materials. A large variety of substances such as organic, inorganic, organometallic, supramolecular, and polymeric systems exhibit this phenomenon. Photochromism is also due to conformation-induced chromism by electromagnetic radiation; however, it exists in different mechanisms. In brief, a photochromic moiety should be incorporated into the polymer chain and a reversible chemical change like isomerization occurs on this photochromic group that leads to the conformation changes of the polymer backbone [43].

The color of a material is observed only when photons absorb a part of the region in the visible region of the electromagnetic spectrum. In fact, the color of the material seems to be the complementary color of that which is absorbed. Thus, materials absorbing energy in the visible region correspond to shorter wavelengths and appear as red-orange, whereas materials absorbing longer wavelengths look blue-purple. When photon absorption occurs, simultaneously, the electron present in the ground state of the system transfers to the first excited level. According to Planck's relation, the energy required for the transition of electrons ($\pi \rightarrow \pi^*$) is directly related to the wavelength of light absorbed,

$$E = h\upsilon = hc/\lambda,$$

where h is the Planck constant, υ is the frequency at wavelength λ, and c is the speed of light. A color wheel of the visible region with corresponding wavelengths is shown in Figure 1.7.
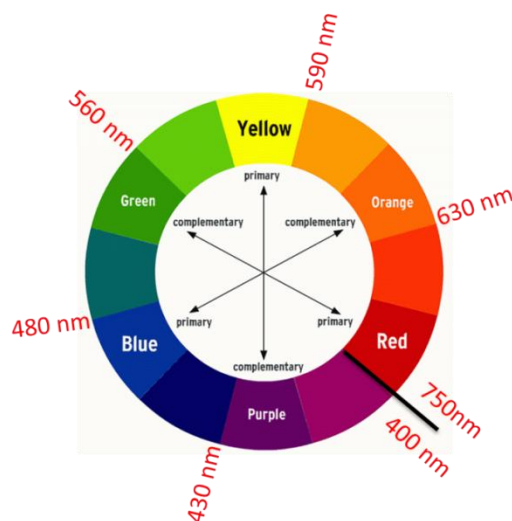
Figure 1.7: A color wheel of the visible region in electromagnetic spectrum

1.7. Electrochromism

1.7.1. Concept and a Brief Literature Review

Electrochromism is defined as the change in optical properties reversibly during electrochemical redox reactions as a function of applied potential. This phenomenon occurs due to the electronic transitions between the HOMO and LUMO (energy band gap) energy levels under electrochemical doping. Generally, conjugated molecules possess a low energy band gap, and the electron present in the lower energy π orbitals can easily be excited to a higher energy π^*orbital as a $\pi \rightarrow \pi^*$ transition during the redox reaction. As a result, the EC materials absorb energy mostly in the visible region and show a corresponding color in reduced/oxidized state. Some of the materials show coloration during the injection of ions in a redox reaction that is called cathodical coloring and those materials are referred to as cathodically colored materials. When the materials show coloration during the ejection of ions in the redox process, it is termed anodical coloring and those materials are referred to as anodically colored materials [44].

1.7.2. Type of Electrochromic Materials

Basically, there are three main types of EC materials presented due to their electronically available optical states and nature of colorations.

Type I: This type of material consists of at least one colored and one bleached state while applying the redox potentials. Typical examples of this type of material are metal oxides, Prussian blue, viologens and some conjugated polymers (eg: PEDOT and poly(3,4

10

propylenedioxythiophene (PProDOT) derivatives). The main applications of these materials are in optical shutters, architectural windows and mirrors.

Type II: These materials consist of two distinct colored states at various redox states and in the absence of a transmissive state. However, these materials are highly applicable in display type devices where different colors are appreciated. A typical example of this type of material is polythiophene.

Type III: These materials consist of two or more different colored states depending on the redox states of the materials and they are a growing field in the electrochromic area. PANI is one of the examples for this type of material. Commonly, conjugated polymers and some copolymers have played a key role in this type of material due to their color tunability by structural modification [39]

1.7.3. Electrochromic Materials

Many inorganic and organic materials show electrochromism while applying external potentials [45–48]. The first study on EC materials and devices was reported by Dev [49], which is considered as the real origin of electrochromic technology. Some common EC materials are briefly explained below.

1.7.3.1. Inorganic EC Materials

1.7.3.1.1. Metal Oxides

Most metal oxide thin films show electrochromic phenomena that have been widely studied in the last decades. The oxides of following transition metals were studied for electrochromism: cerium, chromium, cobalt, copper, iridium, iron, manganese, molybdenum, nickel, niobium, palladium, praseodymium, rhodium, ruthenium, tantalum, titanium, tungsten and vanadium. The preparation, redox chemistry, and optical properties of those metal oxides have been explained in detail by P.M.S. Monk and his co-workers [50]. Granqvist also reviewed the electrochromic properties of all the well-known electrochromic metal oxides. They explained how the solid state crystals of metal oxides are composed of octahedral arrangements in various corner sharing and edge sharing arrangements, and systematic analyses of these structural units exhibit electrochromism. Among the metal oxides, the semiconductor tungsten oxide (WO_3) has been extensively considered as a promising inorganic EC material for more than two decades due to its higher contrast ratio and better optical switching stability. Many research groups have been reviewed in the literature for the

electrochromism of WO_3 based films and devices. However the metal oxide shows more brittle, instability with moisture, high photoactivity, and a slower response. Lower coloration efficiencies are reduced in its application in fast and flexible EC devices [45]. The mechanism involved in the electrochromic coloration of WO_3 is mentioned below:

$$WO_3 + xM^+ + xe- \rightarrow M_XWO_3 \qquad\qquad (1.1)$$
$$\text{(Very pale yellow)} \qquad \text{(Deep blue)}$$
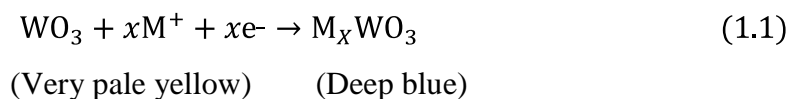
where M+ can be mostly H+, Li+, Na+ or K+.

1.7.3.1.2. Prussian Blue

Prussian blue (PB), [iron(III) hexacyanoferrate(II)]is the prototype of polynuclear transition-metal hexacyanometallates, which contain iron with different oxidation states, Fe^{III} and Fe^{II}. PB is extensively used as a pigment in paints, lacquers and printing inks. The PB film is commonly prepared by the electrodeposition method using cyclic voltammetry in an acid medium containing ferric chloride and potassium ferricyanide. However, Ho.et al. noted that this method was not suitable for making PB films over larger surfaces because of non-uniformity [51]. A new electroless deposition mechanism using the reducing agent H_3PO_2 was introduced to overcome this problem. The electrochemistry and electrochromism of PB was first reported by Neff in 1978 [52], and followed by this research. Other numerous studies on the electrochromic applications and basic structural properties of PB were reported. PB has been widely used in electrochromic devices (ECDs) as a sole electrochrome, or an auxiliary electrode especially with a complementary for WO_3 based device [53]. PB is an anodical colored electrochromic material and changes the color to blue and a colorless state [54]. The brown/yellow soluble complex is present in solutions containing Fe (III) and Hexacynaoferrate (III) ion as a result of the following equilibrium:

$$Fe^{3+} + Fe^{III}(CN)_6{}^{3-} \leftrightarrow FE^{III}FE^{III}(CN)_6{}^0 \qquad\qquad (1.2)$$

1.7.3.1.3. Phthalocyanine

Many years ago, molecular metallo-organic phthalocyanines were used as a pigment in the dye and paint industries. However, new rare-earth metal-based phthalocyanines (Pcs) have been investigated and studied for electrochromic applications since the first report of lutetium bis(phthalocyanine) (Lu(Pc)$_2$). In metal phthalocyanines (MPc), a metal ion is located at the

center of a single phthalocyanine ring or between two rings in a sandwich type compound, commonly called bis(phthalocyanines). The molecular structure of copper phthalocyanines is shown in Figure 1.8.
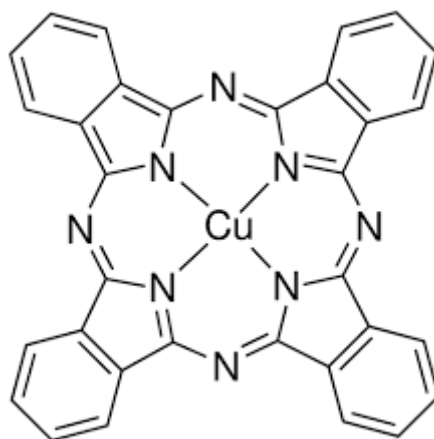
Figure 1.8: The molecular structure of copper phthalocyanine

The rare earth phthalocyanines are generally prepared by a vacuum sublimation method that was first reported by Moskalev and Kirin [55]. The phthalocyanine compounds of more than 30 metals have been studied for solid state electrochromic applications [46]. Among those compounds, Lu(Pc)$_2$ has received more attention because it provides a full range of colors from orange to violet and the films can easily be prepared by vacuum sublimation [55]. Many other MPcs based on neodymium, europium, gallium, cobalt, tin, molybdenum, copper, aluminium, chromium, magnesium, manganese, zinc, titanium, uranium, ytterbium, thorium, vanadium, zirconium have been prepared and their the electrochromic properties have been studied by various research groups [56,57].

1.7.3.2. Organic Electrochromic Materials

1.7.3.2.1.Viologens

The di-quaternisation a of 4,4'-bipyridyl to form a 1,1'-disubstituted-4,4'- bipyridilium salt is commonly known as viologens. Michaelis and Hills named 4,4-dipyridium compounds viologen because they become deeply blue-purple during reduction [58]. Viologens have three common bipyridilium redox states as shown in Figure 1.9. Among all these states, the dication(bipm^{2+}) is the most stable and is a colorless state. Radical cation (bipm$^{+}\cdot$) is the intermediate redox state and shows an intense blue-violet color, whose stability depends upon the delocalization of the radical electron present in aromatic system. The reductive electron transfer to a radical cation forms an unstable neutral state/reduced state (bipm^{0}) that shows a

pale coloration. The preparation and characterization of viologens by electrodeposition of 1, 1'-substituted-4,4'-bipyridinium salts were reported by R.J. Mortimer et al [59].
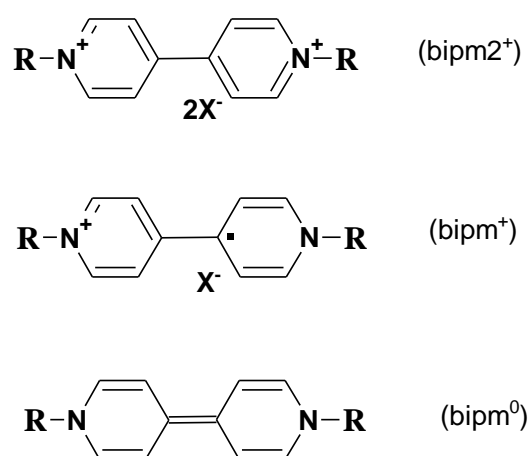
Figure 1.9: The molecular structures of three common bipyridyl redox states. X^- is a singly charged anion.

Viologens have received significant attention in the last 30 years for electrochromic applications due to their good environmental stability and better color contrasts that have been well studied and reported [60]. Because of a slow switching response, instability, and an inability to work in solid state, these compounds are not suitable for fast display device applications. These drawbacks can be improved by substituting various alkyl/aryl groups on viologen which improve the electrochromic (EC) properties [61]. Viologens with mesoporous nanoparticles of metal oxides have shown improved electrochromic properties [62]. More recently, viologen with graphene quantum dots provides an electrolyte-free flexible electrochromic device with high durability and better stability [63].

1.7.4. Electrochromism in Conducting Polymers

In recent years, CPs gained more attention in electrochromic applications than in inorganic EC materials due to their fast response time, high optical contrast, better switching stability, ease of processability, and color tunability [64–66]. Color tunability has been achieved by the modification of a polymer through monomer functionalization and copolymerization [67–70]. Nowadays, major researchers are focusing on the EC polymer to control its color by the modification of the main backbone and pendant group of chains [71–74]. The electrochromism of conducting polymers is induced by delocalized π- electron band structures with lower energy intra-band transitions that occur by the insertion/extraction of

ions during an electrochemical reduction/oxidation that provides different absorption of energies. The colors exhibited by the polymers are mainly related to the band gap of the systems and the conjugation length of the polymers. In the neutral (insulating) state, the CPs exhibit semiconducting states with an appropriate energy gap between the HOMO and LUMO levels. However, upon oxidative doping with counter ions, the band structure of the neutral polymer is modified and generates a new absorption band between HOMO and LUMO due to the formation of charge carriers such as polarons and bipolarons that modulate the optical properties of the polymer. This is the main cause of electrochromism in such materials during the redox process. Among the conjugated EC polymers, poly(thiophene)s, poly(aniline)s, poly(pyrrole)s and their derivatives were widely studied and reported for EC applications.

1.7.4.1. Polythiophene

Polythiophenes are interesting candidates as electrochromes due to their ease of chemical and electrochemical synthesis, environmental stability and facile processability [75,76]. The electrochromic properties of new polythiophene derivatives particularly on poly(3-substituted thiophene)s and poly(3,4 disubstituted thiophene)s have been studied and reported [29]. Polythiophene is blue in the oxidized state and red in the reduced state. The substituted polythiophene has been more extensively studied than the unsubstituted thiophene due to its lower oxidation potential. The alkyl substitutions at the 3rd and 4th positions of the thiophene rings provide a significant increase in conjugation length and result in higher electronic conductivity [77, 29]. The substitutions at the 3,4-position have limited study due to their steric interaction between substituents that reduce the polymer conjugation length. The poly(3,4 dialkylthiophene)s showed a higher band gap, lower conductivities, and higher oxidation potentials than 3-alkyl substituted thiophenes. The alkoxy-substituted poly(thiophene)s can overcome those issues and is being widely studied for electrochromic properties [78, 6].

The poly(3,4 ethylenedioxythiopne) and its derivatives are more promising EC materials because of a lower band gap due to the presence of two electron donating oxygen atoms near to thiophene ring [79]. The band gap of PEDOT which is lower by 0.5 eV than poly(thiophene) results in maximum absorbance in the red region and shows a blue film in the neutral state. Compared to other substituted thiophenes, these alkylenedioxy based thiophenes show an outstanding stability and higher conductivity in the doped state [50]. The

highly stable PEDOT was first developed by Bayer AG research laboratories [80]. However, the insolubility of the PEDOT can be rectified by using water soluble polyelectrolyte, poly(styrenesulfonate) (PSS) as a counter ion with PEDOT, which forms a dispersion in water [81].Other numerous substituted EDOT monomers were synthesized and polymerized by oxidative or electrochemical methods that have led to a polymer with a range of variable band gaps [79]. The characteristic properties of PEDOT based materials can be improved by secondary dopants [82], acid treatment [83], annealing [84], various polymerization conditions [85], nanocomposite [86,87], and graphene [88].

The changes in the size of the alkylenedioxy ring of poly(3,4 alkylenedioxythiophene), (PXDOT) materials and their alkyl and aryl substituted derivatives were extensively studied [89,81,6]. Their electrochromic properties can be improved by increasing the alkylenedioxy ring size and substituting bulky or rigid groups on the ring which increases the inter chain separation and results in a higher color contrast [90]. The electrochromic coloration from highly opaque states to highly transparent states is greatly desirable for the potential application of electrochromic devices. Recent research efforts with poly(3,4 propylenedioxythiophene)s (PProDOT) and its derivatives have achieved electrochromic coloration from a highly transparent to a highly opaque state [91–95]. The di-substituted PXDOT showed better EC properties than the corresponding mono-substituted polymers [96]. The longer alkyl chain substituents such as the dihexyl and di dodecyl derivatives of PProDOT were found to be soluble in organic solvents and have improved processability[97]. The color tuning of the PProDOT achieved by the donor-acceptor approach is also reported for EC applications [98, 74]. More recently, the full color palette of polymeric electrochromism achieved by the color mixing theory with additive primary colors and fine-tuning of colors is possible by controlling film thickness [99].

1.7.4.2. Polypyrrol

Polypyrrol (Ppy) is usually prepared by the chemical or electrochemical polymerization of the pyrrol monomer. Polypyrrol and its derivatives have also been widely studied for their electrochromic properties and their optical properties can be tuned by alkyl or alkoxy substitution [100]. The thin film of parent Ppy is green/yellow color in its neutral state and violet/blue in its oxidation state. Normally, Ppy shows lower oxidation potentials than the corresponding thiophene-based polymers [101]. The dialkoxy substituted Ppy shows again a lowering of the band gap by raising the HOMO level of the resulting polymers due to the

presence of oxygen at the third and fourth positions of the Ppy ring. At p-type doping, poly(alkylenedioxypyrrol)s (PXDOP)s show the lowest oxidation potential in conducting electrochromic polymers [102]. Similar to PEDOT, Poly(3,4ethylenedioxypyrrol) (PEDOP) was also studied for electrochromic applications due to its lower oxidation potential, and good optical properties [103]. The effect of the ring size of the alkylenedioxy bridge was also studied and shows that increasing the alkylendioxy ring size generates another electronic band with new colored states at low doping levels. This multi-coloration is also observed in propylenedioxy and butylenedioxy pyrrols derivatives. The poly(3,4 propyledioxypyrrol) (PProDOP) is orange in the neutral state, brown during the intermediate doping, and light gray/blue in the fully oxidised state [102].

The alkyl or alkoxy substitution at the nitrogen in PXDOPs exhibits higher band gap polymers while retaining its lower oxidation potentials [104]. Those substitutions led to a twist in the polymer backbone resulting in a decrease of the effective π-conjugation that increases in the band gap of the polymers. This increase in the band gap due to the blue shift of π-π^* transitions to the lower wavelength region and charge carries transitions that occur in the visible region. The N-methyl PProDOP is purple in the neutral state, dark green in the intermediate state and finally blue in the fully oxidized state. The N-methyl PProDOP exhibits a higher band gap as 3.0 eV compared to the PProDOP polymer (E_g =2.2 eV) [104]. The N-substituted anodically colored PXDOP polymers have been effectively used in dual polymer electrochromic devices due to their electrochemical and optical compatibility with various polyalkylenedioxythiophenes [105].

1.7.4.3. Polyaniline

Polyaniline (PANI) has emerged as one of the most promising conducting polymers because of its excellent chemical stability and electrical properties. PANI has been easily synthesized by chemical or electrochemical polymerization methods [106]. PANI is a typical Phenylene - based polymer having – NH – group in a polymer chain linked on either side by a phenylene ring. The electrical properties of PANI are influenced by the oxidation state and the degree of protonation. PANI films show polyelectrochromism due to their different redox mechanisms involving a protonation/deprotonation process [107]. Polyaniline can exist in three different redox states such as (i) leuco-emeraldine (fully reduced form) (ii) pernigraniline (fully oxidized form) and (iii) emeraldine (intermediate oxidized form). Upon oxidation, PANI shows electrochromic coloration from transparent yellow to green, dark blue and black at different applied potentials [108]

PANI film shows two maximum absorption peak regions around 300–500 nm and above 500 nm due to an aromatic π-π* transition and formation of radical cations. The absorption peak at a wavelength above 500 nm shifts toward a lower wavelength region when the polarity is changed from negative to positive potentials. This blue shift is due to the corresponding absorption band with color changes of yellow, green, blue, and brown. The electrochromic coloration of PANI is very close to the primary colors except for red. When the absorption of PANI shifts to a shorter wavelength up to 500 nm, it would have showed all three primary colors (Red-Green-Blue (RGB) colors). The incorporation of substituents or another monomer unit on a polymer back bone might lead to all the three primary colors [109].

Many research groups have studied the electrochromic property of polyaniline and its derivatives. The fabrication of electrochromic devices based on PANI with inorganic Prussian blue as a complementary electrode showed deep blue to green coloration [110]. The substituted PANIs have also received much attention for their electrochromic properties. Poly(*o*-toluidine) and poly(*m*-toluidine) showed better stability of polyelectrochromic responses in comparison with the parent PANI. The maximum absorption and redox potential of the ortho- and meta- substituted poly(toluidine)s shift from the parent polymer values may be due to the lower conjugation length [111]. Even though electrochemical polymerization is a good method for the preparation of small area PANI film, it may not be appropriate for large area device applications. Much effort has been made to synthesize soluble polymers such as poly(*o*-methoxyaniline) that can be dispersed in a solution and deposited as a thin film by a solution processable method [112]. Large area electrochromic films of PANI based materials have been prepared with polyacrylate-silica hybrid sol-gel network solutions and that can be deposited by spray, dip or brush-coating onto the substrates [113].

1.8. Electrochromic Devices

Electrochromic devices (ECDs) can control optical properties such as transmission, reflection, and absorption by an external applied potential. An electrochromic device can also be considered an electrochromic cell in which the electrochromic working electrode and charge balancing counter electrode (or complementary EC electrode) are separated by a transparent ionic conductive gel. Solid state ECDs are typically fabricated with at least one transparent conductive electrode coated with an electrochemically reversible cathode /anode material. While applying an external potential to the electrodes, one of the electrodes gets oxidized, while the other electrode is reduced, this leading to a change of the color of the EC

device. The conductive gel electrolyte should be transparent and be a source of cations and anions to balance the redox reactions. The conductive gel electrolyte consists of inorganic salt dissolved in a suitable solvent with a plasticizer [64, 50].

The device fabricated with only one electrochromic species coated on a working electrode and a counter electrode used as a conventional transparent conductive electrode is called a single-type electrochromic device. Such devices may have fewer of redox states compared to a device having more than one electrochromic species. A single-type electrochromic device typically exhibits high transparency because the corresponding counter electrode will be a transparent conductive electrode layer [114]. The dual-type electrochromic device consists of two different kinds of electrochromic species; usually, one with cathodically colored and the other with anodically colored materials coated on working and counter electrodes respectively or vice-versa. The dual type electrochromic device has multi-colorations in a low applied potential, and can also improve the color-contrast of the device [115].

The performance of ECDs is restricted by the diffusion of ions in each layer and also depends on the interface behavior of each electroactive species involved. Over the past decades, liquid crystal displays (LCDs) where optical changes occur by the alignment of molecules at applied electric fields are more commercially accessible for display applications; however, due to the viewing angle dependency, expensive process, and lack of multi-colorations, they are limited for future exploration [64]. A study of ECDs based on conducting polymers showed interesting due to fast response, outstanding stability, easy processability, low cost, high contrast, and the possibility of a full color palette [50]. While comparing them with LCDs, non-emissive electrochromic technologies in ECDs have the practical advantage on objects accessible from any angle. Nowadays, tremendous efforts have been reported in the design and modification of EC device architectures to enhance the color contrast, response time and switching stability [64, 74]. By the suitable selection of electrochromic materials and by novel device designs, the optical modulations of the ECDs can be improved [116,117]. ECDs can be used either in transmissive or reflective mode applications by varying the nature of the counter electrode. If working and counter electrodes in ECDs are prepared on transparent conductive substrates (Indium tin oxide (ITO)/glass substrate), then the device can be used for transmissive applications. If the counter electrode is coated with reflective material (eg: silver, aluminum or gold), then the device is usually used for EC mirror applications [50].

1.9. Applications Areas for Electrochromic Devices

The phenomenon of electrochromism provides numerous applications mainly in transmission and reflection-based devices. Nowadays, ECDs have many commercial applications such as smart windows, rear-view mirrors, displays, optical shutters, and e-papers [50]. The schematic diagrams of ECDs with transmissive and reflective modes are shown in Figure 1.10.
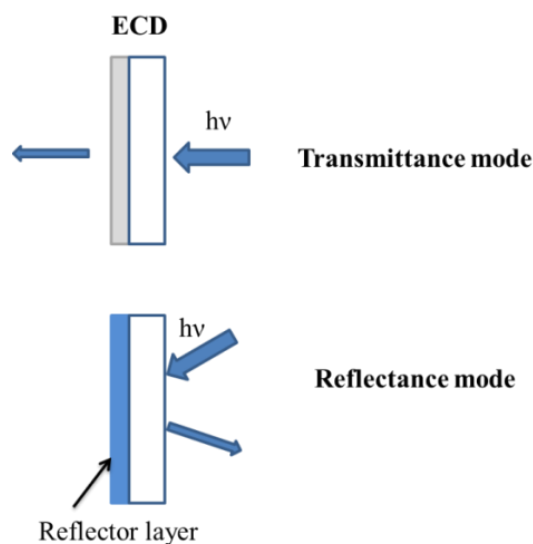
Figure 1.10: Schematic diagrams of ECD at two different modes of operation: Arrows indicate incoming and outgoing electromagnetic radiation and the thickness of the arrows shows intensity of radiation.

1.9.1. Transmissive Electrochromic Device

A transmission type ECD shows reversible optical switching of EC materials between a highly transparent (bleached) and a highly opaque state (colored) on transparent conducting substrates by applied potentials. In such devices, both the electrode materials should be highly transmissive to the visible region. The schematic representation of conventional dual type transmission based ECDs at the colored state is represented in Figure 1.11.Due to the redox stability and chemical compatibility concerns, ECDs with good electrochromic performance can only be obtained by using an appropriate combination of EC species and the supporting gel electrolyte [118,119]. Thus, pairs of electrochromic complementary materials must be selected carefully to not only enhance the color requirements but also balance the redox process to improve the device stability upon repeated switching. To achieve high

optical contrast in this type of device, the transparent gel electrolyte is sandwiched between two complementary EC materials, namely a cathodically colored polymer and anodically colored polymer deposited on transparent conductive electrodes. Mostly, the cathodically colored polymers occur in the low band gap region and exhibit coloration in the neutral state (undoped) which becomes transmissive upon oxidation. Cathodically colored materials should have a band gap around 1.8–2.2 eV revealing a $\pi-\pi^*$ transition within the range of 550–650 nm, where the human eye is highly sensitive. The anodically colored polymers have a high band gap and appear transmissive in the neutral state. Upon oxidation, the polymers become colored in the visible region. Therefore, both the electrochromic active electrodes presented in ECDs show intense colored or bleached states at the same potential [39]. This type of ECD concept is mostly used in applications such as smart windows in buildings and automobiles [120], e-paper [121], optical shutters [122], and electrochromic displays [123].

In 1985, Granqvist et al. named 'smart window' the device, which has been used to restrict the transmission of light by applying a small external voltage [124]. Many research groups have reviewed the fabrication and design architecture of EC windows [125–127]. Based on the theory of ECDs, Granqvist and his co-workers have developed car sunroofs, motorcycle helmets, and goggles [128]. Recently, transmissive EC devices based on conducting polymers such as polythiophene [129], polypyrrol [130, 65], polyaniline [131, 132], PEDOT [133,134] and PProDOT [135,136] have been studied. Prussian blue was used as a complementary EC species along with many cathodically colored polymeric systems in ECDs to improve EC performances [135,137,138]. PANI was usually used as a complementary electrode with a metal oxide EC layer [139,140]. The layer-by-layer assembly method was used to deposit soluble EC polymers on ITO substrates and has fabricated complementary ECDs with PEDOT and PANI reported by DeLong Champ and Hammond [141]. J.R Reynolds et al. reported a charge balanced device of poly(3,4-ethylenedioxythiophene-didodecyloxybenzene) (PEB) as the catholically colored material using WO_3 [142]. Recently, PEDOT and PB based ECDs showed good EC properties and reported a coloration efficiency of ~300 cm^2/C [143]. Flexible and polymer-based ECDs with many complementary colored EC polymers were investigated using ITO coated plastic substrates [119,144–146]. The fabrication of ECDs using PProDOT-Me$_2$ as cathodically colored polymer and number of complementary anodically colored materials such as PB [147], a high-band-gap pyrrole-based polymer, *N*-PrS-PPro-DOP (E_g: 2.9 eV) could give an optimized contrast ratio and high stability [105]. Systematic material strategies and black to transmissive switching of polymer

ECDs were designed using a set of spray-processable cathodically colored polymers [74]. ITO-free polymer ECDs have also been recently reported where the ITO layer was replaced by highly conducting PEDOT-PSS material [148].
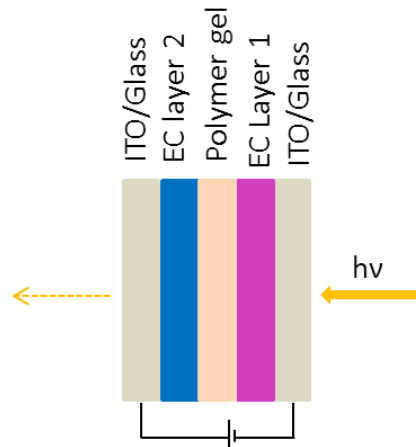
Figure 1.11: Schematic representation of conventional dual type transmissive based ECD at colored state.

1.9.2. Reflective Electrochromic Device
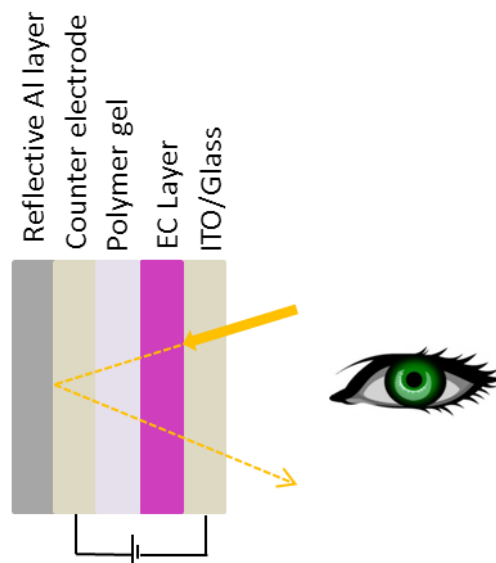
Figure 1.12: Schematic diagram of conventional reflection type ECD at colored state.

Reflective type ECDs have been mostly used in electrochromic rear-view mirror applications for automotives at night to reduce the glare of light from the following vehicles and thereby improve the driver's safety and comfort [50]. The design of reflective ECDs are almost like transmissive ECDs except that an extra reflective metal layer must be incorporated on the

counter electrode as showed in Figure 1.12. The reflecting electrodes should be inert during the electrochemical process in the adjacent layer, must have excellent optical quality, and low cost. These requirements are met by a few metals like aluminium, silver, gold and platinum [116]. The presence of an electrochromic layer would be absorbed in maximum light in their colored state and hence reduce the intensity of reflection. As the back electrode is a reflective layer, it allows reflection as in a conventional mirror in the bleached state of the EC layer.

Baucke and his co-workers have studied a different solid state electrochromic mirror based on WO_3 in the early 1990s. The basic design and important aspects of reflecting solid state devices were systematically investigated by Bange. K.et al. [149,150]. All solid state green-yellow reflective electrochromic devices containing Prussian blue as an electrochromic layer, CeO_2–TiO_2 as a counter-electrode thin film and a PVB-based membrane as an electrolyte were fabricated [151]. A reflective electrochromic device based on polymeric microspheres was proposed, and its feasibility for a display was investigated [152]. More recently, C. Kocabas et al. have fabricated graphene-based flexible reflective ECDs and the key goal of these devices were simplicity of device architecture and high optical contrast [153].A new design approach and spray processable polymer films based reflective type ECDs have been constructed by Reynolds and his co-workers [154,155]. The conducting polymer-based reflective ECDs have also been used in the visible, NIR, and mid-IR regions of the electromagnetic spectrum [156].

1.10. Gap in Existing Research

In India, research on the fabrication and performance analysis of highly efficient and stable electrochromic rear-view mirror based on conducting polymers is very rare; however, this area has been studied and reported internationally for practical applications. Gentex Corporation (Zeeland, USA) and Magna-Donnelly International Inc. (Holland) are the main manufacture for automatic dimming electrochromic rear-view mirrors for automobile applications, but these mirrors are very expensive. Internationally, some research groups have worked on electrochromic materials for electrochromic device applications. Though several patents have been reported exclusively for electrochromic rear-view mirrors [157–160], the characteristics study for electrochromic mirrors and windows based on conductive polymers and those related publications/patents are very limited. Currently, there is a great deal of interest in the design and synthesis of electrochromic CPs due to their high optical contrast, rapid response time, good optical memory, higher processability, and better long-term

stability, which have made them more attractive materials for transmissive/reflective type ECDs. Recent research efforts have focused on tuning the spectral characteristics using structural modifications of the polymer backbone. However, the biggest challenges of electrochromic CPs are their solution processability and to attainment of the coloration from a highly transparent to an opaque state between redox states, which are growing research demands in ECD applications such as aircraft and automotive windows, goggles, e-papers, auto dimming mirrors, signage, and displays. In the national and international scenario, this research area would be a highly significant and promising technology for academic and industrial applications.

1.11. Objectives

The main objective of this research is the design, synthesis and characterization of conductive polymers and their applications in transmissive and reflective electrochromic devices such as EC windows and rear-view mirrors. Moreover, it is to modify the optical modulations of conducting polymers by simple, facile, and cost-effective methods using mainly dopants, functionalized graphene, structural modification of monomers, and copolymerization approaches. A chemical polymerization method, reverse microemulsion polymerization, will be introduced as this would be a suitable method for preparing solution-processable, one-dimensional nanostructured conducting polymers at room temperature. The objective is also to characterize the structural, morphological, electrochemical, spectroelectrochemical and electrochromic properties of prepared conducting polymer films and to fabricate electrochromic windows and rear-view mirrors and test their electrochromic performance.

1.12. Thesis Outline

Chapter 1 is an overview about conducting polymers and their synthesis, properties, and applications. The general background of this research and the literature review are also discussed. Electrochromism, different electrochromic materials, and electrochromism in conjugated polymers are briefly explained. In the last section, transmissive and reflective type electrochromic devices and their applications are also discussed. Chapter 2 describes experimental methods and characterization techniques that are mainly used for electrochromic polymers and devices. The key layers present in electrochromic devices and the process of device fabrication are also discussed.

Chapter 3 introduces a simple and cost-effective electropolymerization of PEDOT and studies the effect of dopant and polymerization methods. This chapter also describes the fabrication and characterization of transmissive and reflective type electrochromic devices based on PEDOT and PEDOT:PSS and systematically compares their electrochromic performances.

Chapter 4 presents the preparation and characterization of PEDOT-Ions enriched graphene (IEGR) film using the electropolymerization method and analyzes its electrochromic properties. The effects of IEGR on the PEDOT matrix are also studied. Additionally, fabricated electrochromic windows and rear-view mirrors based on PEDOT-IEGR films are studied and their EC performance is tested.

Chapter 5 describes the design, synthesis and characterization of a new solution-processable di-isopropyl benzyl derivative of a (3,4 propylenedioxythiophene) monomer. This chapter introduces solution-processable one dimensional PProDOT-IPBZ$_2$ nanobelts prepared by reverse microemulsion polymerization method at room temperature. The PProDOT-IPBZ$_2$ films are prepared by electropolymerization, spray coating, and solution cast methods and their electrochromic performance is compared. Solid state electrochromic windows and rear-view mirrors are fabricated based on electropolymerized PProDOT-IPBZ$_2$ film and their EC performance is analyzed.

The design and synthesis of a new conjugated monomer based on thiophene and carbazole groups using stille coupling is introduced in Chapter 6. The corresponding polymer, P(Th-Cbz-Th) and its multi-colored copolymer with poly(3,4ethylenedioxythiophene), P(Th-Cbz-Th)-PEDOT are electrochemically polymerized and characterized. The electrochemical and electrochromic properties of the resulting polymer films are studied and compared. Moreover, fabricated electrochromic windows and rear-view mirrors based on P(Th-Cbz-Th) and P(Th-Cbz-Th)–PEDOT films studied and their electrochromic performance is tested.

The thesis ends with a chapter on conclusions attained from the individual studies of the various approaches of electrochromic materials for transmissive and reflective electrochromic devices. The future scope and recommendations that could improve the electrochromic properties for advanced opto-electronic technologies are also discussed.

1.13. References

[1]   Letheby H., *J. Chem. Soc.*, 1862, 15: 161–163.

[2]   Chiang C. K., Fincher C. R., Park Y. W., Heeger A. J., Shirakawa H., Louis E. J., Gau S. C., Macdiarmid A. G., *Phys. Rev. Lett.*, 1977, 39: 1098–1101.

[3]   Macdiarmid A. G., Akhtar M., Chiang C. K., Cohen M. J., Kleppinger J., Heeger A. J., Louis E. J., Milliken J., Moran M. J., Peebles D. L., Shirakawa H., *J. Electrochem. Soc.*, 1977, 124: C304–C304.

[4]   Shirakawa H., Louis E.J., Macdiarmid A. G., Chiang C. K., Heeger A. J., *J. Chem. Soc.*, *Chem. Commun.*, 1977, 578–580, DOI: 10.1039/C39770000578.

[5]   Skotheim T. A., Reynolds J. R., *Handbook of conducting polymers*. 3rd ed. CRC Press: New York, 2007.

[6]   Groenendaal L. B., Jonas F., Freitag D., Pielartzik H., Reynolds J. R., *Adv. Mater.*, 2000,12: 481–494.

[7]   Walczak R.M., Reynolds J. R., *Adv. Mater.,* 2006, 18:1121–1131.

[8]   Tung T.S., Ho K.C., *Sol. Energ. Mat. Sol. Cells,* 2006, 90: 521–537.

[9]   Deepa M., Ahmed S., *Eur. Polym.,* 2008, 44: 3288–3299.

[10]   Lu W., Fadeev A.G., Qi B., Mattes B R., *Synth. Met.*, 2003, 139:135–136.

[11]   Akoudad   S.,   Roncali   J.,   *Chem.   Commun.*,   1998,   2081–2082, DOI: 10.1039/A804992K

[12]   Igor F.P., Dmitrii F. P., *Handbook of Thiophene-based Materials: Applications in Organic Electronics and Photonics* , Wiley, John Wiley & Sons Ltd ,UK, 2009.

[13]   Gordon G.W., Geoffrey M. S., Leon A.P. K., Peter R.T., *Conductive electroactive polymers: Intelligent Polymer systems*, 3rd Edition, CRC press, Taylor and Francis Group, Newyork, 2009.

[14]   Bredas L., Street G. B*., Acc. Chem. Res.*, 1985, 18: 309–315.

[15]   Roncali J., *Chem. Rev.,* 1997, 97: 173–205.

[16]   Furukawa Y., *J Phys Chem*., 1996, 100: 15644–15653.

[17]   Reynolds J. R., Schlenoff J. B., Chien J. C. W., *J. Electrochem. Soc*., 1985, 132: 1131–1135.

[18]   De-Leeuw D. M., Simenon M. M. J., Brown A. R., Einerhand R. E. F., *Synth. Met*., 1997, 87: 53–59.

[19]   Bredas J.L., Street G.B., *Acc. Chem. Res*., 1985, 18: 309–315.

[20]   Lowe J. P., Kafafi S. A., *J. Am. Chem. Soc*.,1984, 106: 5837–5841.

[21]   Bredas J. L., *J. Chem Phys.*, 1985, 82: 3808–3811.

[22]   Liu B., Yu W. L., Lai Y. H., Huang W., *Chem. Mater.*, 2001, 13: 1984–1991.

[23]   Roncali J., *Macromol Rapid Commun.*, 2007, 28: 1761–75.

[24]   Durmus A., Gunbas G. E., Camurlu P., Toppare L., *Chem.Commun.*, 2007, 3246–3248, DOI: 10.1039/B704936F.

[25]   Palas B. P., Soumyajit D., Sanjio S. Z., *J. Polym. Sci. A Polym. Chem.*, 2012, 50, 3996–4003.

[26]   Ki-Ryong L., Gregory A. S., *Chem. Commun.*, 2013, 49: 5192–5194.

[27]   Izuhara D., Swager T. M., *J. Mater. Chem.*, 2011, 21: 3579–3584.

[28]   Braunecker W. A., Owczarczyk Z. R., Garcia A., Kopidakis N., Larsen R. E., Hammond S. R., Ginley D. S., Olson D. C., *Chem.Mater.*, 2012, 24: 1346–1356.

[29]   Roncali J., *Chem Rev.*, 1992, 92: 711–738

[30]   Alexander W. H., Ziqi L., Michael A. W., Brian A. G., *Chem. Rev.*, 2010, 110 : 6689–6735.

[31]   Andrew C. G., Khai L. C., Rainer E. M., Pawel G. J., Andrew B. H., *Chem. Rev.*, 2009, 109 (3): 897–1091.

[32]   Suga T., Ohshiro H., Sugita S.; Oyaizu K., Nishide H., *Adv. Mater.*, 2009, 21: 1627–1630.

[33]   Pandey G. P., Rastogi A. C., *J. Electrochem. Soc.*, 2012, 159(10): A1664–A1671.

[34]   Sarah H., Jenny E. D., Iain M., *Chem.Mater.*, 2014, 26: 647–663.

[35]   Wu S., Qiu Z., Zhang S., Yang X., Yang F., Li Z., *Polymer,* 2006, 47: 6993–7000.

[36]   McQuade D. T., Anthony E. P., Timothy M. S., *Chem. Rev.*, 2000, 100 : 2537–2574.

[37]   Antonio F. F., Roderick B. P., Rigoberto C. A., *Ind. Eng. Chem. Res.*, 2010,49: 9789–9797.

[38]   Andersson P., Nilsson D., Svensson P.O., Chen M., Malmstrom A., Remonen T., Kugler T., Berggren M., *Adv. Mater.*, 2002, 14: 1460–1464.

[39]   Avni A. A., Pierre-Henri A., Barry C. T., Irina S., Carleton L. G., Jungseek H., Nicholas J. P., David B. T., MacDiarmid A. G., Reynolds J. R., *Chem. Mater.*, 2004, 16: 4401–4412.

[40]   Elisabeth S., *Adv. Mater.*, 2003, 15: 481–494.

[41]   Dierk K., Eckhard S., *Synth Met.*, 2009, 159: 1433–1437.

[42]   Otero T.F., Sansinena J.M., Bioelectrochem. Bioener., 1995, 38: 411–414.

[43]   Peter B., *Chromic Phenomena: The Technological Applications of Colour Chemistry,* Royal Society of Chemistry, Thomas Graham House, Cambridge, UK, 2001.

[44] Monk P.M.S., Mortimer R.J, Rosseinsky D.R., *Electrochromism:Fundamentals and applications* VCH Pub, Newyork, USA, 1995.

[45] Granqvist C.G., *Hand book of Inorganic electrochromic Materials*, Elsevier, Newyork, USA, 1995.

[46] Somani P.R, Radhakrishnan S., *Mater. Chem. Phys.*, 2002, 77: 117–133.

[47] Ruben B., Bjorn P.J., Arild G., *Sol. Energ. Mat. Sol. Cells*, 2010, 94: 87–105.

[48] Vijay K. T., Guoqiang D., Jan M., Lee P.S., Xuehong L., *Adv. Mater.*, 2012,1–25. DOI: 10.1002/adma.201200213.

[49] Deb S.K., *Philos. Mag.*, 1973, 27: 801–822.

[50] Monk P.M.S., Mortimer R.J., Rosseinsky D.R., *Electrochromism and Electrochromic devices*, Cambridge University Press, Cambridge, UK, 2007.

[51] Ho K.C., *Proc.Electrochem.Soc.*, 1994, 94: 170–184.

[52] Neff V.D., *J. Electrochem. Soc.*, 1978, 125: 886–887.

[53] Tada H, Bito Y., Fujino K., Kawahara H., *Sol. Energ. Mat.* 1989, 16: 509–516.

[54] Cheng-Lan L., Li-Chun L., *Surf. Coat. Technol.*, 2014, 259: 330–334.

[55] Moskalev N., Kirin I.S., *Opt. Spektrosk.,* 1970, 22: 414–415.

[56] Collins G.S.E., Schiffrin D.J, *J. Electroanal. Chem.*, 1982, 139: 335–369.

[57] Moskalev P.N., Shapkin G.N., Darovskikh A.N., *Russ. J. Inorg. Chem.*, 1979, 24: 188–192.

[58] Michaelis L., Hill E.S., *J Gen Physiol.*, 1933, 16: 859–873.

[59] Mortimer R.J., *Electrochim. Acta,* 1999, 44: 2971–2981.

[60] Kenworthy J.G., ICIC Ltd, 1973, British patent, 1314049.

[61] Van-Da H.T., Ponjee J.J., *J. Electrochem. Soc.*, 1974, 121: 1555–1558.

[62] Bach U., Corr D., Lupo D., Pichot F., Ryan M., *Adv. Mat.,* 2002, 14: 845–848.

[63] Hwang E., Seo S., Bak S., Lee H., Min M., Lee H., *Adv. Mater.*, 2014, 26: 5129–5136.

[64] Beaujuge P.M., Reynolds J.R., *Chem. Rev.*, 2010, 110: 268–320.

[65] Pinar C., *RSC Adv.*, 2014, 4: 55832–55845.

[66] Huiying Q., Hangchuan Z., Na L., Zhongqiu T., Jing W., Jiupeng Z., Yao L., *RSC Adv.*, 2015, 5: 803–806.

[67] Beverina L., Pagani G. A., Sassi M., *Chem. Commun.*, 2014, 50: 5413–5430.

[68] Fahad A. A., Michael T. O., Yujie D., Sotzing G. A., *Adv. Mater.*, 2013, 25: 6256–6260.

[69] Merve I.O., Melek P. A., Zahide O., Fatih A., Ahmet M. O., Cihaner A., *Macromolecules*, 2012, 45: 729−734.

[70] Beaujuge P.M., Chad M. A., Reynolds J.R., *Acc. Chem. Res*., 2010, 43: 1396–1407.

[71] Tanmoy D., Michael A. I., Yujie D., Zeki B., Sotzing G.A., *Macromolecules*, 2011, 44: 2415–2417.

[72] Ki-Ryong L., Sotzing G.A., *Chem. Commun*., 2013, 49: 5192–5194.

[73] Li-Ting H., Hung-Ju Y., Guey-Sheng L., *Macromolecules*, 2011, 44: 9595–9610.

[74] Svetlana V. V., Beaujuge P. M., Shujun W., Joseph E. B., Vincent W. B., Reynolds J.R., *ACS Appl. Mater. Interfaces*, 2011, 3: 1022–1032.

[75] Roncali J., *J. Mater. Chem*., 1999, 9: 1875–93.

[76] Barbarella G., Melucci M., Sotgiu G., *Adv Mater.*, 2005, 17: 1581–93.

[77] Mastragostino M., Arbizzani C., Bongini A., Barbarella G., Zambianchi M., *Electrochim. Acta*, 1993, 38: 135–40.

[78] Groenendaal L., Zotti G., Aubert P.H., Waybright S. M., Reynolds J. R., *Adv. Mater.*, 2003,15: 855–79.

[79] Andreas E., Stephan K.,Wilfried L., Udo M., Knud R., *PEDOT: Principles and applications of an Intrinsically conductive polymer*, CRC Press Taylor & Francis Group, Broken Sound Parkway, NW, 2011.

[80] Jonas F., Schrader L., *Synth. Met*., 1991, 41: 831–836.

[81] Heywang G., Jonas F., *Adv. Mater*., 1992, 4: 116–18.

[82] Fabretto M., Hall C., Vaithianathan T., Innis P.C., Mazurkiewicz J., Wallace G.G., Murphy P., *Thin Solid Films*, 2008, 516: 7828–7835.

[83] Xia Y., Ouyang J. *ACS Appl. Mater. Interfaces*, 2010, 2: 474–483.

[84] Taekyung A., Haiwon L., Sien-Ho H., *Appl. Phys. Lett*., 2002,80: 392–394.

[85] Elena P., Li M., Arkady B., Michael B., *Chem. Mater.*, 2010, 22: 4019–4025.

[86] Movaffaq K., Vahid A., Mohsen M., *Sol. Energ. Mat. Sol. Cells*, 2013, 112: 57–64.

[87] Long J.M., Yong X. L., Xiao F. Y., Qun B. Y., Chang-Ho N., *Sol. Energ. Mat. Sol. Cells,* 2008, 92: 1253–1259.

[88] Saxena A.P., Deepa M., Amish G. J., Shweta B., Avanish K. S., *ACS Appl. Mater. Interfaces*, 2011, 3: 1115–1126.

[89] Stephen E. B., Gabriel G. R., Michael A. L., Yasuyuki K., Richard G. H., Abruna H.D., *J. Phys. Chem. C,* 2010, 114: 16776–16784.

[90] Kumar A., Welsh D. M., Morvant M. C., Piroux F., Abboud K. A., Reynolds J. R., *Chem Mater*., 1998, 10: 896–902.

[91]   Dietrich M., Heinze J., Heywang G., Jonas F., *J. Electroanal. Chem.*, 1994, 369: 87–92.

[92]   Welsh D.M., Kumar A., Morvant M.C., Reynolds J.R., *Synth. Met.*, 1999, 102: 967–968.

[93]   Welsh D.M., Leroy J. K., Luis M., Mauricio R. P., Barry C. T., Kirk S. S., Khalil A. A., David P., Reynolds J.R., *Macromolecules*, 2002, 35: 6517–6525

[94]   Welsh D.M., Kumar A., Meijer E.W., Reynolds J.R., *Adv. Mater.*, 1999, 11: 1379–1382.

[95]   Krishnamoorthy K., Ambade A.V., Kanungo M., Contractor A.Q., Kumar A., *J. Mater. Chem.*, 2001, 11: 2909–2911.

[96]   Mishra S.P., Krishnamoorthy K., Sahoo R., Kumar A., J. *Polym. Sci. A Polym. Chem.*, 2005, 43: 419–428.

[97]   Benjamin D. R., Christophe R. G. G., Avni A. A., Cirpan A., McCarley T D., Reynolds J.R., *Macromolecules,* 2004, 37: 7559–7569.

[98]   Pengjie S., Chad M. A., Eric P. K., Emily J. T., David Y. L., Jianguo M., Aubrey L. D. Reynolds J.R., *Adv. Mater.*, 2010, 22: 4949–4953.

[99]   Aubrey L. D., Emily J. T., Reynolds J.R., *ACS Appl. Mater. Interfaces,* 2011, 3: 1787–1795.

[100] Genies E. M., Bidan G., Diaz A. F., *J. Electroanal. Chem.*, 1983, 149: 103–113.

[101] Diaz A. F., Castillo J. I., Logan J. A., Lee W. I., *J. Electroanal. Chem.*, 1981, 129: 115–132.

[102] Schottland P., Zong K., Gaupp C. L., Thompson B. C., Thomas C. A., Giurgiu I., Hickman R., Abboud K. A., Reynolds J.R., *Macromolecules*, 2000, 33: 7051–61.

[103] Gaupp C. L., Zong K.W., Schottland P., Thompson J. R., Thomas C. A., Reynolds J. R., *Macromolecules*, 2000, 33: 1132–1133.

[104] Sonmez G., Schwendeman I., Schottland P., Zong K. W., Reynolds J.R., *Macromolecules*, 2003, 36: 639–647.

[105] Schwendeman I., Hickman R., Sonmez G., Schottland P., Zong K., Welsh D.M., Reynolds J. R., *Chem. Mater.*, 2002,14: 3118–22.

[106] Akheel A. S., Dinesan M.K., *Talanta,* 1991, 38: 815–837.

[107] Ray A., Richter A.F., MacDiarmid A.G., Epstein A.J., *Synth. Met.*, 1989, 29: 151–156.

[108] Mortimer R.J., Aubrey L. D., Reynolds J.R., *Displays*, 2006:27: 2–18.

[109]   Kaneko M., Nakarmura H., Shimomura T., *Makromol. Rapid. Commun.*, 1987, 8: 179-180.

[110]   Deepa M., Awadhia A., Bhandari S., *Phys. Chem. Chem. Phys.*, 2009, 11: 5674–5685.

[111]   Mortimer R.J., *J. Mater. Chem.*, 1995, 5: 969–973.

[112]   Jing J., Lun-Hong A., *J. Macromol. Sci., Phys.*, 2011, 50: 890–896.

[113]   Jang G-W., Chen C.C., Gumbs R.W., Wei Y., Yeh J-M., *J. Electrochem. Soc.*, 1996, 143: 2591–2596.

[114]   Tsutsumi H., Nakagawa Y., Tamura K., Sol. Energy Mater.Sol. Cells, 1995, 39: 341–348.

[115]   Sapp S.A., Sotzing G.A., Reynolds J. R., *Chem. Mater.,* 1998, 10: 2101–2108.

[116]   Bange K., Gambke T., *Adv.mater.,* 1990, 2: 10–16.

[117]   Gurunathan K., Vadivel M. A., Marimuthu R., Mulik U.P., Amalnerkar D.P., *Mater. Chem. Phys.*, 1999, 61: 173–191.

[118]   Seshadri V., Padilla J., Bircan H., Radmard B., Draper R., Wood M., Otero T. F. Sotzing G. A., *Org. Electron.* 2007, 8: 367–381.

[119]   De Paoli M.A., Nogueira A. F., Machado D. A., Longo C., *Electrochim. Acta*, 2001, 46: 4243–4249.

[120]   Rauh R. D., *Electrochim. Acta*, 1999, 44: 3165–76.

[121]   Monk P.M.S., Delage F., Costa-Vieira S.M., *Electrochim. Acta*, 2001, 46: 2195–2202.

[122]   Freeman W., Rosseinsky D., Jiang H., Soutar A., Finisar Corporation. 2005, US Patent 6,940,627 B2.

[123]   Sonmez G., Meng H., Wudl F., *Chem. Mater.*,2004,16: 574–580

[124]   Svensson J. S. E. M., Granqvist C. G., *Sol. Energy Mater.*, 1985, 12: 391–402.

[125]   Azens A., Granqvist C. G., *J. Solid State Electrochem.*, 2003, 7: 64–8.

[126]   Mbise G. W., Le Bellac D., Niklasson G. A., Granqvist C. G., *J. Phys. D: Appl. Phys.*,1997,30: 2103–2122.

[127]   Demiryont H., *Proc. SPIE*, 1991, 1536: 2–28.

[128]   Azens A., Gustavsson G., Karmhag R., Granqvist C. G., *Solid State Ionics*, 2003, 165: 1–5.

[129]   Ribeiro A. S., Machado D. A., Filho P. F. S., De Paoli M.A., *J. Electroanal. Chem.,* 2004, 567: 243–248.

[130]   Ana J. C. D, Fred A. R N., Josealdo T., Adriana S. R., Solar *Sol. Energ. Mat. Sol. Cells* 2011, 95: 2255–2259

[131] Montazami R., Jain V., Heflin J.R., *Electrochim. Acta,* 2010, 56: 990–994.

[132] Bernard M.C., Hugot-Le G. A., Zeng W., *Electrochim. Acta,* 1998, 44: 781–796.

[133] Jain V., Yochum H. M., Montazami R., Heflin J. R., *Appl. Phys. Lett.*, 2008, 92, DOI: 10.1063/1.2834818.

[134] Chih-Wei H., Kun-Mu L., Vittal R, Dung-Jing Y., Kuo-Chuan H., *J. Electrochem. Soc.*, 2010, 157: 75–78.

[135] Padilla J., Seshadri V., Filloramo J., Warren K. M., Mishra S.P, Radmard B, Kumar A., Sotzing G. A., Otero T. F., *Synth. Met*., 2007, 157: 261–268.

[136] Otley M.T., Alamer F.A., Zhu Y., Singhaviranon A., Zhang X., Li M., Kumar A., Sotzing G.A., *ACS Appl. Mater. Interfaces,* 2014, 6: 1734–1739.

[137] Sydam R., Deepa M., Srivastava A. K., *RSC Advances*, 2012, 2: 9011–9021.

[138] Kang J.H., Paek S.M., Choy Y.B,, Hwang S.J., Choy J.H., *J. Nanosci. Nanotechnol.* 2007, 7: 4131–4134.

[139] Jelle B. P., Hagen G., Oedegaard R., *Electrochim. Acta*, 1992,37: 1377–1380.

[140] Jelle B. P., Hagen G., Birketveit O., *J. Appl. Electrochem.*, 1998, 28: 483–489.

[141] DeLongchamp D., Hammond P. T., *Adv. Mater.,* 2001, 13: 1455–1459.

[142] Rauh R. D., Wang F., Reynolds J. R., Meeker D. L., *Electrochim. Acta,* 2001, 46: 2023–2029.

[143] Tung T.S., Ho K.C., *Proc. Electrochem. Soc.* 2003, 17: 254–265.

[144] Arbizzani C., Mastragostino M., Meneghello L., Morselli M., Zanelli A., *J. Appl. Electrochem.* 1996, *26*: 121–123.

[145] De Paoli M. A., Casalbore-Miceli G., Girotto E. M., Gazotti W. A., *Electrochim. Acta* 1999, 44: 2983–2991.

[146] Ferraris J. P., Henderson C., Torres D., Meeker D., *Synth. Met.* 1995, 72: 147–152.

[147] Kun-Chieh C., YuHsu C., WeiHub C., Kuo-Chuan H., *Sol. Energ. Mat. Sol. Cells,* 2011, 95: 2238–2245.

[148] Argun A. A., Cirpan A., Reynolds J. R., *Adv. Mater.,* 2003, 15: 1338–1341.

[149] Baucke F. G. K., *Sol. Energy Mater.*, 1987,16: 67–77.

[150] Baucke F. G. K., *Proc. Electrochem. Soc.*, 1990, 20: 298–311.

[151] Assis L.M.N., Ponez L., Januszko A., Grudzinski K., Pawlicka A., *Electrochim. Acta*, 2013,111: 299–304

[152] Ryu J.H., Shin D., Suh K., *J. Polym. Sci. A Polym. Chem,* 2005, 43, 6562–6572.

[153] Emre O. P., Osman B. & Coskun K., *Sci. Rep.*, 2014, 4 : 6484(1–8). DOI: 10.1038/srep06484.

[154] Cirpan A., Argun A. A., Grenier C. R. G., Reeves B. D., Reynolds J.R., *J. Mater. Chem.*, 2003, 13: 2422–2428.

[155] Aubert P.H., Argun A.A., Cirpan A, Tanner D.B., Reynolds J.R., *Chem. Mater.*, 2004, 16: 2386–2393.

[156] Schwendeman I., Hwang J., Welsh D.M., Tanner D.B, Reynolds J.R., *Adv. Mater.*, 2001, 13: 634–637.

[157] OFarrell D.J, Gahan R.J, Donnelly Corporation, Holland, 1995, US patent no:5,406,414.

[158] Ash K.L., Tonar W. L.,. Bauer F.G.T., Gentex Corporation, 1999, US patent no: 5,940,201.

[159] Desaraju. V.V., Ian A.M., Habibi H., Lynam N.R., Zhao M., Dornan C.A., Donnelly Corporation, Holland, 1998, US patent no:5,724,187.

[160] Schofield K., Larson M., Donnelly Corporation, Holland, 1996, US patent no:5,550,677.

CHAPTER 2

EXPERIMENTAL

This chapter provides an overview of experimental methods and the basic concepts of characteristic techniques, which are used to analyse the structural, electrochemical, and electrochromic properties of the materials, films and devices presented in this research. Additionally, the processes of the fabrication of transmissive and reflective electrochromic devices are also described. These analyses would be most commonly used in the following chapters. A detailed synthesis procedure and the preparation of each compound can be found in the respective chapters.

2.1 Chemicals and Materials

3,4, dimethoxy thiophene, 3,4 ethylenedioxythiophene (EDOT), thiophene, carbazole, diethyl malonate, 4-isopropyl benzyl bromide, poly(sodium 4-styrene sulfonate) (PSS)-25 wt % of water (molecular weight,M_w-1,000,000), lithium perchlorate (LiClO$_4$), tetra butyl ammonium perchlorate (TBAP), R-camphor sulphonic acid (CSA), sodium bis (2 ethyl hexyl) sulfosuccinate (AOT), p-toluene sulfonic acid (p-TSA), poly methyl methacrylate (PMMA), N-bromosuccinimide (NBS), dichloromethane (DCM), propylene carbonate (PC), dichloromethane (DMF), acetonitrile (ACN), n-butyllithium (n-BuLi), tributylchlorostannane (SnBu$_3$Cl), ethyl acetate, anhydrous MgSO$_4$, and indium tin oxide (ITO) coated glass plates (surface resistivity 8–12 and 30 Ω/Sq) were purchased from Sigma-Aldrich Chemie, Germany. Potassium nitrate (KNO$_3$) was purchased from S.D fine-chem. Ltd India, and tetrabutylammonium bromide (TBAB) was purchased from Spectrochem Pvt Ltd India. Graphite rods (6mm x 50mm) were purchased from HHV Equipment Co, Bangalore, India and ethanol (AR, 99.9%) was purchased from Les Alcools De Commerce, Boucheville, Que. All Chemicals and solvents were used without any further purification unless otherwise mentioned.

2.2. Solution Processing Techniques

2.2.1. Spray Coating

The processing of conjugated polymers in solution by a spray coating technique is a simple and low cost method to form uniform film on any kind of substrate and is applicable to

prepare a large area of films. In this method, the previously prepared homogenous polymer solution is transferred to the cup of the spray gun (Air bush, Model: Artmaster) and sprayed through a small nozzle (0.3 mm) using an air compressor. The resulting polymer film is uniform and fully covers the substrate without pores/agglomeration. The thickness and uniformity of the film have been optimized by parameters such as pressure (10–15 psi), polymer concentration (5–10 mg/ mL), distance between the substrate and nozzle (minimum 15–20 cm) and the solvent (as toluene).

2.2.2. Solution Casting

Solution casting is a low cost, easy method to make thin film on substrates. However, this method exhibits lack of film quality and inhomogeneity. Herein, the polymer solution was prepared by dissolving 10 mg of polymer powder in 1 mL of toluene and two drops of this solution were placed onto a pre-cleaned ITO substrate. Because to the wettability of the solution on ITO substrate is very low, the solution tends to concentrate and is deposited at a specific area. To improve the quality of the film, a thin blade can be used to spread the solution on entire area of the substrate as the solvent dries up and the process can be repeated if required.

2.2.3. Electron Beam Evaporation

2.2.3.1. Deposition of Aluminium Layer
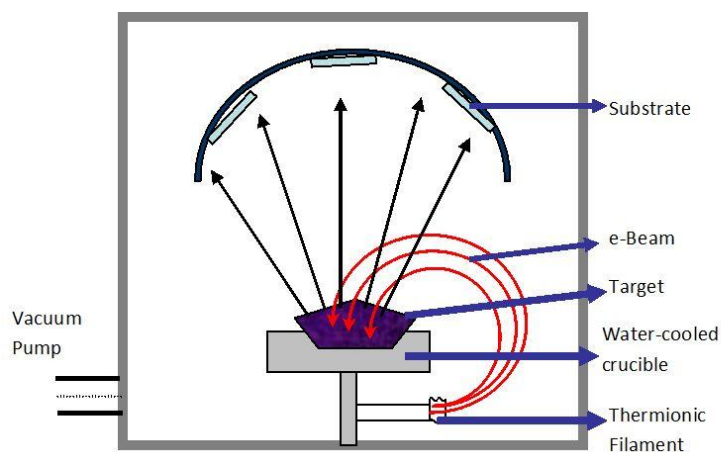
Figure 2.1: Schematic diagram of e-beam evaporation system

Electron beam (e-beam) evaporation is a technique in which the source material is bombarded with an electron beam and the evaporated atoms condense on a substrate under

high vacuum conditions. The e-beam deposition unit mainly consists of a vacuum chamber with vacuum pumps, a substrate holder, an electron beam gun, ingots (crucible), magnetic beam deflection, and a water-cooling system. The main advantages of electron beam evaporation are the low degree of contamination, better adhesion, high deposition rate, and alternating layers of different materials without a break in the vacuum. A schematic diagram of an e-beam evaporation unit is showed in Figure 2.1.

In e-beam deposition, a required amount of evaporation material is placed in the crucible. The pre-cleaned substrate to be coated is kept on top of the vacuum chamber. The distance between the crucible and the substrate can be adjusted by a shaft, which is connected with substrate holder. The substrate is pre-heated before the deposition which allows better film adhesion. The vacuum chamber should be evacuated to a pressure of $10^{-5} - 10^{-6}$ Torr that provides an easy movement of electrons from the electron gun to the evaporation material. The diffusion and rotary pumps are used under liquid nitrogen to get a high vacuum in the chamber. Once an appropriate vacuum is obtained, we applied a large voltage to the tungsten filament that generated an e-beam, generally, by the thermionic emission method. This electron beam attained high kinetic energy and focused on the evaporation material using a magnetic field. The attained kinetic energy of the electron beam is transformed to heat when it interacts with the target material. At sufficient temperatures/ sublimation temperatures, the material tends to melt and evaporate at atoms level, and then it is directly transferred to the top of the chamber. The vapours are condensed on the substrate to form a uniform thin film. In this research, the Al layer has been deposited on the rear side of ITO substrate with a thickness ~150 nm at a vacuum of 10^{-6} Torr.

2.3. Characterization Techniques and Instruments

The prepared materials presented in this dissertation were characterized by ^{1}H NMR and 13C NMR, FT-IR spectroscopy, Raman, and XPS techniques.

2.3.1. Nuclear Magnetic Resonance Spectroscopy

Nuclear magnetic resonance spectroscopy (NMR) is a powerful technique for determining the structure of organic compounds. NMR can exploit the magnetic properties of certain atomic nuclei (carbon/ proton) and help to determine the physical and chemical properties of atoms or the molecules in which they are presented.^{1}H NMR, and ^{13}C NMR spectra of materials were obtained by Bruker 500 MHz High Resolution Multinuclear FT-NMR Spectrometer

(Model-AV500) using CDCl$_3$ as a solvent and tetramethylsilane (TMS) as the internal standard related to the chemical shift (δ).

2.3.2. FT-IR Spectroscopy

FT-IR spectroscopy has been widely used in the laboratory and industry for several years as a non-destructive technique for the identification of chemical compounds in liquids, gases, powders and films. FT-IR spectra can be observed when the materials absorb electromagnetic radiation in the wavelength range of 400 to 4000 cm^{-1}.The functional groups present in the molecule absorb radiation at characteristic wavelengths in the IR region. The FT-IR spectrum represents fingerprints of a sample with absorption peaks, which correspond to the frequencies of vibrations between the bonds of the atoms. Like a finger print, the infrared spectrum provides a unique identification peak even if the same functional groups present in the materials due to the change in molecular environment. Therefore, infrared spectroscopy can provide information about functional groups, qualitative analysis, and the amount of material present in a mixture. The FT-IR spectra of the materials were studied by Perkin Elmer, Model Spectrum GX.

2.3.3. X-ray Photo Electron Spectroscopy

X-ray photo electron spectroscopy (XPS) is a widely used technique to investigate the elemental composition, chemical state, and electronic state of the elements that exist within a material. The XPS spectra of materials are obtained by irradiating them with a beam of X-rays, then simultaneously measuring the kinetic energy and number of electrons that escape from the surface of the material being analysed. Since core level electrons in solid-state atoms are quantized, the resulting energy spectra exhibit resonance peaks characteristic of the electronic structure of atoms at the sample surface. An X-ray photoelectron spectroscopy analysis of material was performed with a SPECS GmbH spectrometer (Model-Phoibos 100 MCD Energy Analyzer).

2.3.4. Raman Spectroscopy

Raman spectroscopy is molecular spectroscopy, and it relies on the in-elastical scattering (Raman scattering) of monochromatic light, usually from a laser in the visible, near infrared, or near ultraviolet range. As a result, Raman spectroscopy provides a valuable analytical tool for molecular finger printing as well as monitoring changes in the molecular bond structure.

The laser light interacts with molecular vibrations, phonons or other excitations in the system that resulting in the energy of the laser photons being shifted up or down in comparison with the original monochromatic frequency, which is called the Raman Effect. This shift in energy gives information about the vibrational modes in the system. The Raman Spectroscopy of the compounds was studied by a Horiba *LABRAM* Instrument, Model- HR800.

2.3.5. Scanning Electron Microscopy

Scanning Electron Microscopy (SEM) is a surface analytical technique, which is used to study the surface topography of the material, its chemical composition, crystalline structure and orientation of materials. SEM analysis provides morphological images of a sample by scanning it with a focused beam of high energy electrons. The electrons interact with the atoms in the sample, producing various signals that can be detected at a resolution of nanometer to micrometer scales. These signals include secondary electrons, backscattered electrons (BSE), diffracted backscattered electrons, photons, and heat. Scanning the sample and detecting secondary electrons are most valuable for showing the surface morphology and topography of materials. The surface morphological properties of the materials were studied by Quantum microscope Model Raith E-line with varying levels of magnification as per the requirements.

2.3.6. Conductivity Measurement

A conductivity measurement of the sample was performed by four-point probe conductivity measurements. The four-point probe method is a simple technique to measure the resistivity of materials especially for semi-conductors. In this technique, four probes of the instrument are arranged at an equal distance on top of the testing sample as shown in Figure 2.2. The current is passed through two of the outer probes and the corresponding voltage drop into the two inner probes that can provide resistance of the material is measured. The four-probe technique offers a broad range of applied current (between 1 µA and 1 mA) and reduces error due to contact resistance. Agilent Technologies B1500A Semiconductor device analyzer was used to measure the conductivity of the film.

The resistivity of the materials was calculated by the following equation

$$\rho = \frac{\pi}{\ln(2)} \ t \ \frac{V}{I} \qquad (2.1)$$

Where ρ is the resistivity, I the current applied through the outer probe, V the voltage drop measured across the inner probes and 't' the thickness of the sample.
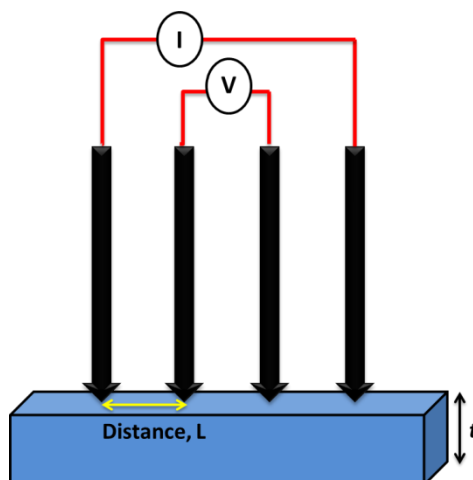
Figure 2.2: Schematic diagram of four point probe circuit to measure the sheet resistivity of a sample

2.4. Electrochemical Cell

Electrochemical analyses are normally carried out in a single-compartment three electrode cell. The electrochemical cell consists of electrodes, an electrolyte, and a power supply. A standard three electrode configuration comprises a working electrode (WE), reference electrode (RE), and a counter electrode (CE). WE is defined as the interface under study and it acts as the substrate to be tested. The main requirement of RE is that it should provide a stable potential and not substantially deviate during the experiment. The purpose of CE is to supply the current required to the WE. The CE is a conductive material that is chemically inert, like platinum, and it should have a large area compared to the working electrode.

An electrolyte refers to a medium of ionized salts that dissociate into ions by the application of an electric field. Electrolytes provide charge transport between the working and counter electrodes and are responsible for ionic conductivity through the electrolyte medium. All electrochemical reactions are studied in an electrochemical cell with at least two electrodes placed in an electrolyte. Usually, an electrolyte solution contains salts of sodium, potassium, chloride, calcium, and phosphate that are dissolved in suitable solvents such as water, acetonitrile, and dichloromethane. The electrolyte can be either liquid or solid electrolytes. The liquid electrolytes are used for the characterization of film, and solid electrolytes are mostly used in solid state devices. Herein, we have used lithium perchlorate,

tertabutylammonium perchlorate, and KNO_3 as ionic salts, and water, acetonitrile, and dichloromethane as suitable solvents. The PMMA-LiClO$_4$ based gel electrolyte was used for solid state ECDs.

2.5. Electrochemical Characterizations

Electrochemical analyses are very important in gaining a better understanding of the redox properties of materials. Various types of electrochemical techniques to characterize the electrochemical properties of conducting polymers were discussed in detail by Doblhofer et al. [1]. The electrochemical polymerization and electrochemical characterizations were performed using a single-compartment three electrode electrochemical cell, CH Instrument Electrochemical analyzer model-CHI 6005D. The most important electrochemical techniques such as cyclic voltammetry and electrochemical impedance spectroscopy employed for electrochromic materials are discussed below.

2.5.1. Cyclic Voltammetry
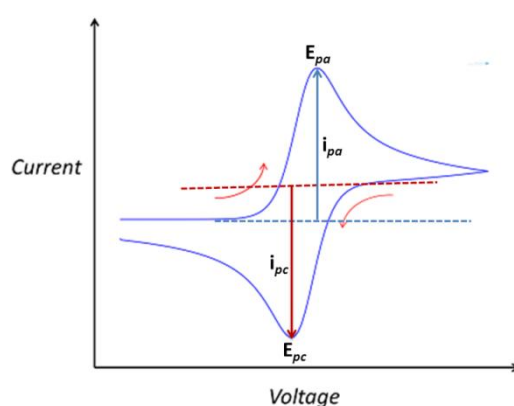
Figure 2.3: Typical cyclic voltammogram under dynamic potential; where i$_{pc}$ and i$_{pa}$ show the cathodic and anodic peak current respectively for a reversible reaction.

Cyclic voltammetry (CV) is a potentiodynamic electrochemical technique that is widely used for the electropolymerization of monomers and to study the redox properties of a material due to its simple and versatile approach. In CV, the potential across to the working electrode and the counter electrode is cycled between higher and lower potential limits at a constant scan rate (*v*). The range of potentials is at the figure at which redox processes are expected. The current passing through the electrode is continuously monitored and recorded with respect to

a reference electrode. The current versus applied potentials are usually plotted in a cyclic voltammogram as shown in Figure 2.3. The reduction potential (cathodic peak potential, E_{pc}) and oxidation (anodic peak potential, E_{pa}) peak potentials are obtained from the cathodic and anodic peaks of the cyclic voltammogram. Usually, the corresponding anodic (oxidation) peak current and the cathodic (reduction) peak current are represented as I_{pa} and I_{pc} respectively.

Electrochemical polymerization using CV is a potentially dynamic technique, and it is an irreversible process. The monomer is irreversibly oxidized under cyclic potentials and an electro active polymer film is deposited on the conductive working electrode. Typical electropolymerization usually starts from a low applied potential to an anodic direction where no redox reactions occur. While increasing the potential, the monomer gets oxidized to form radical cations at sufficient potential. The anodic current increases rapidly until the concentration of monomers at the vicinity of the electrode surface becomes zero, that resulting significant peak of current response in a cyclic voltammogram. During cyclic potential, the monomer gets oxidized and is followed by a coupling of monomer radicals to form oligomers. Once oligomers reach a specific chain length where they become insoluble in an electrolyte medium, they are deposited on the conductive electrode surface. When the potential is reversed (cathodic scanning), the reduction of the conductive polymer occurs at the electrode surface. Upon consecutive anodic-cathodic cycling, a new oxidation-reduction peak is observed due to polymer redox reactions. Repeated cycling provides more polymer deposition on to the electrode surface and this is evident from the increase of current density [2].

The onset potentials can be defined as the lowest (for the anodic reactions) or the highest (for the cathodic reactions) potentials at which a redox process occurs at a given electrode. The onset potentials of oxidation (E^{on}_{oxd}) and reduction (E^{on}_{red}) of a material can be correlated to the ionization potential (IP) and electron affinity (EA) as per the empirical relationship proposed by Bredas et al. [3]. They also indicate that these values refer to the first oxidation and reduction potentials, which correspond to the onset potential values of the electrochemical process.

The electrochemical band gap of the materials can be calculated from a cyclic voltammogram using onset oxidation and reduction potentials by the following equations:

$$EA = (E_{LUMO}) = (E^{on}_{red} + 4.8) \text{ eV} \qquad (2.2)$$

$$IP = (E_{HOMO}) = (E^{on}_{oxd} + 4.8) \text{ eV} \qquad (2.3)$$

Then, electrochemical band gap (Eg) = IP−EA

Where E^{on}_{red} and E^{on}_{ox} are the onset reduction and oxidation potentials versus the Ag/AgNO$_3$ reference electrode. Electrochemical potentials (vs SCE) are obtained by adding the work function of the ferrocene system (4.8 eV), which is considered an internal standard while calculating the electrochemical band gap by CV technique [4,5]. The electrochemical band gap of the materials is usually higher than the optical band gap because the electrochemical band gap may be a combination of optical band gap and the interface barrier for charge injection [6]. Both slow and fast reactions can be achieved as the rate of potential scan rates varies in consecutive cycles. In a diffusion-controlled electrochemical system, the peak current (i_p) can be calculated by the Randles-Sevcik equation [7],

$$ip = (2.69 \times 10^5) \, n^{3/2} \, AD^{1/2} \, C \, v^{1/2} \qquad (2.4)$$

Where n is the number of electrons, A the area of the electrode (cm^2), D the diffusion constant (cm^2/s), C the concentration of the electrolyte (mol/cm^3), and v the scan rate (Vs^{-1}). When the reaction is diffusion-controlled, the peak current should be proportional to the square root of the scan rate. If the redox processes of conjugated polymers are not diffusion controlled, they cannot be described by the Randles-Sevick equation and the peak current is represented by the following equation [8],

$$i_p = n^2 F^2 \Gamma \, n/4RT \qquad (2.5)$$

Where n is the number of electrons, Γ is the concentration of the surface bound electroactive species (mol/cm^2) and F is Faradays constant (96,485 C/mol). The linear relationship between the peak current with increasing scan rates shows that the redox process is non-diffusion controlled, and that the electroactive polymers have adhered to the working electrode.

In general, the oxidation and reduction process of conjugated polymers is a rapid process. However, the switching response is dependent upon film thickness, electrolytes, and the

structure of the polymer. Therefore, scan rate dependent studies are important for determining whether a polymer can be switched between redox states rapidly without a loss of current response or switching stability. Furthermore, CV reveals information regarding the redox stability of the materials during multiple redox cycles.

2.5.2. Electrochemical Impedance Spectroscopy

Electrochemical impedance spectroscopy (EIS) is a method to study the electrochemical process that occurs on electrode surfaces. According to Ohms law, the resistance (ability to resist a flow of current) can be represented in terms of the ratio between the voltage and current for a single circuit cell. However, the resistance for a complex system will be expressed by impedance, which is a measure of circuit resistance to resist the flow of an alternative electrical current. In EIS, a small potential is applied to an electrode-solution interface, and the resulting ac current is then measured. An electrochemical impedance spectrum is obtained as a function of frequency. The obtained impedance data can be represented in two types of plots: Nyquist plot (Imaginary [Z''] versus Real [Z']) and bode plot (log complex impedance, [$|Z|$] or phase angle, [θ] versus log frequency [ω] in Hz). The schematic representation of the Nyquist and Bode plot for a parallel resistor-capacitor circuit are shown in Figure 2.4a & b, respectively. Each point represented in the Nyquist plot denotes the complex impedance at a particular frequency. When drawing a vector through the zero-point to those points, the magnitude ($|Z|$), and the phase angle (θ) can be analysed. The frequency ω decreases from right to left in the plot.

The equivalent circuit of the system also can be attained from impedance data. Generally, an equivalent circuit is composed of a resistor, capacitor, Warburg Impedance (W) and other special components like a constant phase element (CPE), which serve as the electrical model for the physical interface. Those components are then correlated with physical processes occurring at the electrode-solution interface by fitting it to a suitable theoretical modelling. The impedance study of electrochromic systems provides information such as charge transfers and the diffusion processes of conducting polymers on electrodes [9].
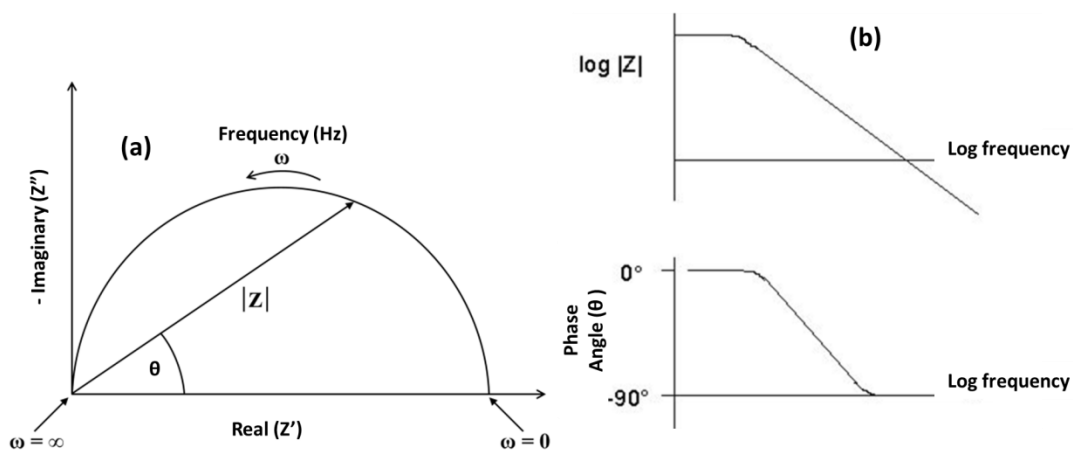
Figure 2.4: Schematic representation of (a) Nyquist and (b) Bode plot for a parallel resistor-capacitor circuit

2.6. Electrochromic Characterizations of Film and Device

2.6.1. Spectroelectrochemistry

Spectroelectrochemistry is an important study for the characterization of electrochromic polymers. The study of the spectral changes of EC films (in solution) and EC devices (in solid state) upon a redox process by applying different potentials is known as spectroelectrochemistry. According to the Beer Lambert law for absorption spectroscopy, the optical absorbance is expressed as the logarithmic ratio of intensities at the initial (I_0) and final states (I). This is equal to the molar extinction coefficient (ε) of the absorbing species being evaluated along with the concentration of chromophores, *c* and the optical path length, *l* of the sample.

$$A = \log (I_0/I) = \varepsilon c l \qquad (2.6)$$

In the case of electrochromic films, the path length, *l* is the film thickness. Spectroelectrochemical and electrochromic characterizations were performed using an ocean optics spectrophotometer (Model DH 2000-BAl) by passing a UV-Vis light source through an EC electrode which was connected to a CH analyser to allow various step-wise potentials. The spectroelectrochemistry of EC materials are usually monitored by absorbance versus wavelength of light/photons as a function of different applied potentials. This study provides specific properties of EC materials like absorption maxima (λ_{max}), band gap, intra-band states under doping and evaluation of polarons and bipolaron bands (charge carriers). The spectra

also give some insight in to the color of the polymer through the region of absorption maxima and degree of regularity along the polymer backbone. Figure 2.5 shows the spectroelectrochemistry of PProDOT-Hx$_2$ in 0.1 TBAP/ACN as a function of different applied potentials.
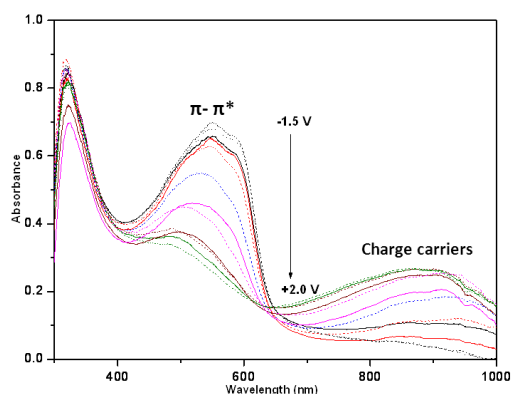
Figure 2.5: Spectroelectrochemistry of PProDOT-Hx$_2$ in 0.1 TBAP/ACN as a function of different applied potentials between −1.5 V and 2.0 V. Reproduced from reference [10].

The spectroelectrochemistry of EC film is studied in a monomer-free electrolyte solution and the EC polymer film coated on the ITO electrode is placed in the cuvette (to keep in a sample compartment of UV-Vis instrument) along with a counter and reference electrode. For solid state devices, a device without an EC polymer layer was used as the reference and ECDs were directly placed in the sample holder and their performance was studied.

2.6.2. Optical / Electrochromic Switching
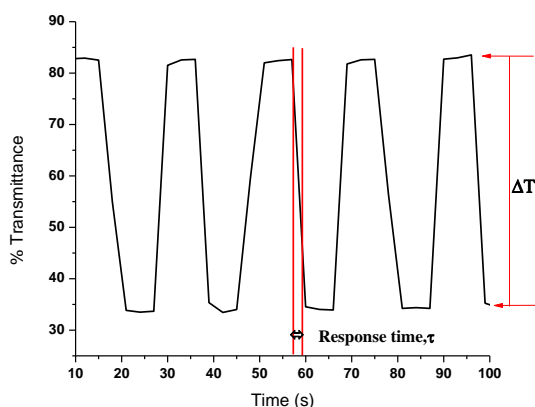
Figure 2.6: Electrochromic switching studies of representative conductive polymer as a function of applied potentials.

The fast optical switching response, better efficiency and high color modulations are the characteristic parameters for electrochromic applications. The optical switching study of EC films/devices has proven to be a simple and most efficient method to investigate the optical color contrast, response time and durability (cycle life time). In optical switching study, the EC polymer film deposited on ITO/glass substrate was used as working electrode and platinum foil as counter electrode and Ag/Ag+ used as reference electrode. These electrodes were immersed in the cuvette containing 0.1 M supporting electrolyte (usually LiClO$_4$) in organic solvents like ACN or DCM. A square wave potential step technique together with UV-Vis absorption spectroscopy is used to analyse the switching properties of EC materials. The polymer films switched between their fully oxidation-reduction potentials with a constant time interval (preferably 5-10 s) using chronoamperometry. The corresponding electrochromic switching studies are performed by monitoring the % transmittance (or reflectance) vs. time at a specific wavelength (λ_{max}) using Uv-Vis spectroscopy. A typical electrochromic switching studies are performed by monitoring the % transmittance changes as a function of stepped potentials as shown in Figure 2.6.

Color Contrast: The optical contrast is measured from the difference of % transmittance between bleached (oxidized, T$_{bleached}$) and colored (reduced, T$_{colored}$) states at a specific wavelength.

$$\text{Opitcal contrast,} (\%\Delta T) = T_{bleached} - T_{colored} \qquad (2.7)$$

Optical contrast is a prime tool in the characteristic property of an electrochrome. The wavelength is the maximum absorption wavelength at which the electrochrome exhibits the highest color contrast. Normally, optical contrast is measured as a function of square wave potential steps; however, spectroelectrochemical technique also can be used to monitor transmittance changes over a broad range of wavelengths.

Response Time: Response time (τ) is usually calculated as the time required for an EC film/device to change from its colored to its bleached state (or vice versa). It is an important parameter for applications such as fast displays and electrochromic mirrors, in which response time should be as low as possible or require a fast response. In applications like electrochromic windows that do not necessitate rapid color changes, a response time of few seconds can be accepted. The response time of electrochromic material is dependent on ionic conductivity of the electrolyte, ion diffusion in EC films, magnitude of the applied potential, film thickness and the morphology of the film [11]. Heflin et al. reported a millisecond

(coloration and decoloration times of 31 and 6 ms) response time of solid state ECD based on PEDOT and poly(allylamine hydrochloride) [12]. Similarly, Reynolds and his co-workers prepared a series of poly(3,4-alkylenedioxythiophene)s switched between their reduced and oxidized forms in 0.8–2.2 s with a color contrast of 44–63% [13].

2.6.3. Electrochromic Stability

Electrochromic switching stability is an experimental study for the durability of ECD, which is continuously switched between the reduced and oxidized states as a function of time. Electrochromic stability is usually related to electrochemical redox stability as the degradation of active redox states results in the loss of electrochromic color contrast, and, hence affects the performance of the electrochrome. Typical degradation processes include irreversible redox at extreme potentials, degradation of electrode materials or electrolytes, resistive heating due to repeat switching and side reactions due to the presence of water/oxygen and interference with EC components. Defect-free and effectiveness of the processing techniques, careful conditions of the redox process, and air-free sealing of the devices are the most important factors for better quality and long term operations of ECDs. Long term switching stability measurements of ECDs, which are usually carried out by repeated square wave step potentials (chronoamperometry) or by repeated potential cycling (cyclic voltammetry) are represented in Figure 2.7 a & b, respectively. Though the electrochromic stability of the devices are reported up to 10^6 cycles without a significant loss of performance [14], the lack of durability is one of the drawbacks for the commercialization of ECDs while compared to LCDs.
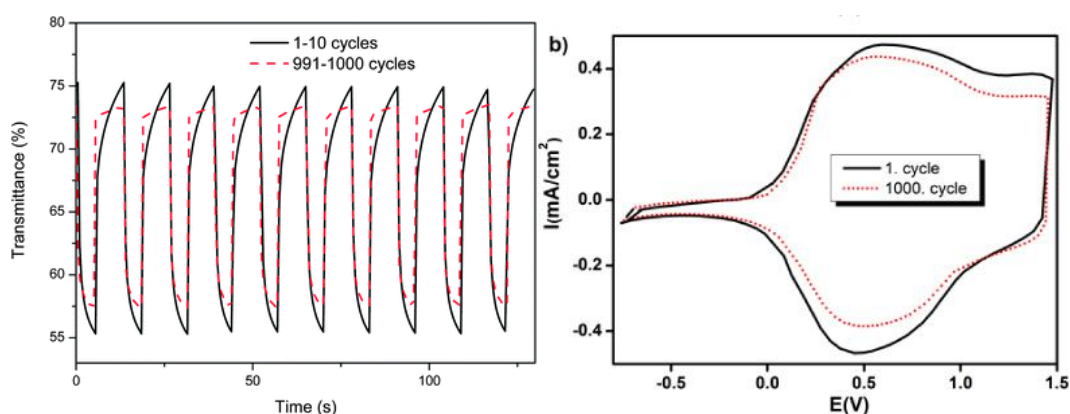
Figure 2.7: (a) Switching stability testing of ECD using square-wave potential step chronoamperometry (Reproduced from reference [15]); and (b) redox stability testing of ECD using cyclic voltammetry (Reproduced from reference [16].

47

2.6.4. Coloration Efficiency

Coloration efficiency (η) is a quantitative method to measure the amount of charge required to achieve maximum optical changes, and it is a fundamental parameter to measure the power requirement of electrochromic materials. Coloration efficiency is defined as the ratio of change in optical density (ΔOD) at a specific wavelength (λ_{max}) induced as a function of charge injected/ejected per unit area (Q_d).

$$\eta = \frac{\Delta OD}{Q_d} = \frac{\log \frac{T_{Bleached}}{T_{Colored}}}{Q_d} \qquad (2.8)$$

where $T_{bleached}$ and $T_{colored}$ are the transmittance values at the bleached and colored states. Coloration efficiency can be used to evaluate for a specific degree of coloration for practical applications. For the application of electrochromic materials in fast and efficient displays, the value of coloration efficiency should be as high as possible. Reynolds et al. reported spray coatable dioxythiophene derivatives with high coloration efficiencies up to 1365 cm^2/C [17]. A high coloration efficiency (930 cm^2/C) was also reported by a dual-polymer electro-chromic device (ECD) composed of poly(3,4-(1,4-butylene-(2-ene)dioxy)- thiophene) (PBueDOT) and polyaniline (PANI) [18].

2.6.5. Colorimetry (Chromaticity)

To describe the color of a material is very subjective with respect to humans and that can change in different circumstances such as surrounding colors and lighting conditions. Colorimetry analysis is a method to measure the quantitative information about color of EC material more accurately. Colorimetry can provide more accurate color measurement than spectroelectrochemistry and it measures the human eye's sensitivity to light over the visible regions. Generally, humans have a three-dimensional color space and many of the existing colors have three primary color coordinates. The red, green, blue (RGB) primary color system is a practical color space approach for creating a display, but this actually is not a perfect description of the full color space accessible to the human eye.

In 1931, The Commission Internationale de l'Eclairage (International Commission on Illumination,CIE) introduced the CIE 1931 *Yxy* system, which is a well-known and most widely used color system to represent a color. However, in 1976, a modified CIE L* a* b* system (CIELAB) of colorimetry was implemented by CIE. This is used for all possible quantitative measurements of color and allows colored objects to be described and compared,

where 'L*' corresponds to brightness or luminance (where a perfect black is zero and a perfect white is 100), 'a*' refers to hue (dominant wavelength where the maximum color contrast occurs), and 'b*' is known as saturation, which is the color's intensity or purity [19, 20]. The two-dimensional *xy* color diagram is known as the chromaticity diagram (Figure 2.8a). It has the shape of a horseshoe, with the wavelengths of light in the visible region found on the surrounding line called the spectral locus. The line connecting the shortest and longest wavelengths is called the purple line. The area surrounded by spectral locus and the purple line is called color locus, where all possible colors can exist. The point, where three primary color coordinates associate within the color locus region, is known as white point (W) and its location depends on the light source. The 3D image of a color sphere with color coordinates is shown in Figure 2.8b.
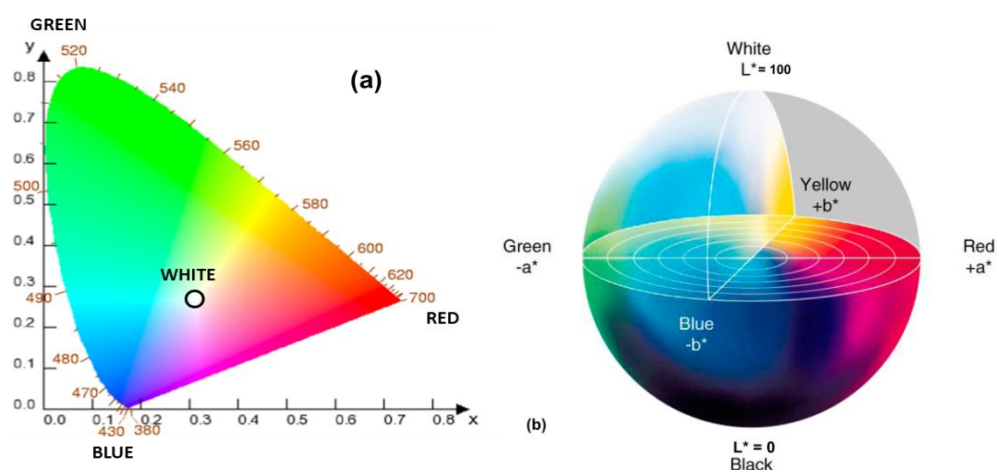
Figure 2.8: (a) CIE Chromaticity diagram with color wavelength and (b) CIE lab color sphere.

2.6.6. Open Circuit Memory (Optical Memory)

The unique importance of ECDs compared to other displays (LCDs and OLEDs) is its optical memory, which is defined as the ability of an EC material to retain its coloring/bleaching state after the electric circuit is opened (Figure 2.9). This memory effect is induced due to the stable electrochemical doping/dedoping process and is an important parameter in energy-saving electrochromic devices. In this study, initially a potential is applied (for e.g.; −1.0 /+1.0 V for 5 s) to an EC film/device and the circuit is opened for a period of time (say 200 s). Then, transmittance (reflectance), which changes as a function of time under open circuit conditions, is monitored.
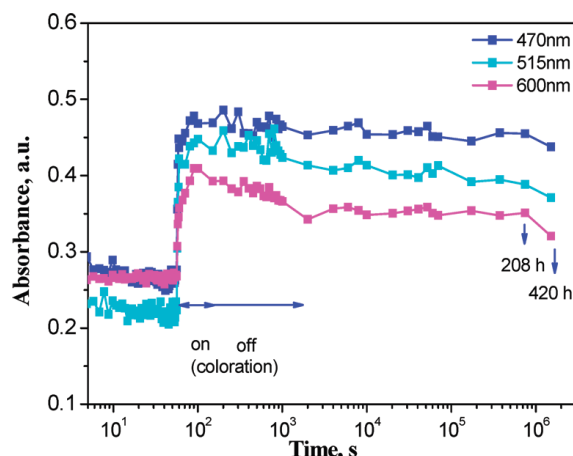
Figure 2.9: Typical optical memory of ECD in an open circuit condition at three different wavelengths. Reproduced from reference [21].

2.7. Fabrication of Electrochromic Device

Electrochromic devices (ECDs) are considered a type of electrochemical cells having a generally five-layered structure. ECD mainly consists of two ITO coated glass electrodes along with EC layers; the electrochromic films are either coated on one of the ITO or both electrodes. An electrochromic device, which has been fabricated using an electrochromic electrode is separated from a charge balancing counter electrode (or complementary EC electrode) by a polymer gel electrolyte. The key layers present in a typical electrochromic device are the electrochromic layer, complementary/counter electrode layer, transparent conductive oxide (TCO) layer, and polymer gel electrolyte.

2.7.1. Electrochromic Layer

The electrochromic (EC) layer is an electrochemically active working electrode that changes the optical coloration while applying a potential to the device. Usually, EC materials are deposited on a transparent ITO coated glass substrate which is used as a transparent conductive layer due to its high transparency and conductivity. In this study, conducting polymer films have been used as EC layers, and are deposited on an ITO substrate by electropolymerization/spray coating techniques as discussed previously.

2.7.2. Complementary/Counter Electrode Layer

The counter electrode (ion storage electrode) /complementary electrode should offer a fast kinetics for electrochemical reactions. There can be two types of counter electrodes: One can be optically passive in which optical changes remain the same under redox process. It is also

called an ion storage layer. The other type of counter electrode is complementary to the electrochromic layer and it helps to improve the optical properties of the device. When devices are operating in a transmissive mode, such as windows or goggles, the counter electrode must be a transparent conducting substrate. When electrochromic devices function for the reflecting mode such as mirrors, the counter electrode must be a reflective substrate, which is prepared by Al/Ag metals deposited on ITO to act as a mirror in a reflecting ECD.

2.7.3. Polymer Gel Electrolyte

The electrolyte between the two electrodes should be ionically conductive but electronically used as an insulator. The electrical and electrochemical properties of ion conducting polymers, which have been used as electrolytes for ECDs were studied by Linford [22]. The electrolyte can be either liquid or solid; however, liquid electrolytes were more favoured due to their greater transparency, high ionic mobility and high ion concentration. Since liquid electrolytes exhibit long-term sealing problems and are unable to operate in a wider range of temperatures and potentials, various solid/ polymer gel type electrolytes have been used in ECDs [23–25]. The solid gel electrolyte consists of three components, ionic salt, a polar solvent and polymer. The ionic salt used must have low electrochemical interference, low lattice energy, better ionic mobility, and good thermal stability that provides ions for conduction. The solvents act as a medium for conduction and dissolution of salts. The polymer acts as a stiffener and provides mechanical durability and flexibility. Lithium perchlorate ($LiClO_4$) is used as a supporting electrolyte due to its good solubility, and high ionic conductivity. Acetonitrile (ACN) is one of the most used polar aprotic solvents for both cathodic and anodic reactions. It also has a high dielectric constant ($\varepsilon=37$) that dissolves common electrolytes and has a large diffusion coefficient. The poly methyl methacrylate (PMMA) has been chosen as a plasticizer in gel electrolytes because of its light weight, rigidity, and high transparency in the visible region. The lower concentration of polymers (< 30 wt%) in electrolytes is a suitable polymer matrix for ionic conduction that has been proved by Bohnke [26]. The higher concentration of polymer restricts ion motion resulting in a decrease in ionic conductivity.

2.7.3.1. Preparation of gel electrolyte

The gel electrolyte has been prepared by using the following electrolyte compositions: 3wt % $LiClO_4$, 7 wt% poly(methyl methacrylate) PMMA, 70wt % ACN, and 20wt % propylene carbonate (PC). The $LiClO_4$ is completely dissolved in an ACN solution, and then PMMA

polymer is slowly added to it. The whole solution is stirred overnight using a magnetic stirrer and is heated (<70ºC) continuously until a honey-like transparent gel is obtained [27].

2.7.4. Process of Device Construction

The steps involved in ECD fabrication are important, and strongly affect performance and the characteristic properties of ECD. A schematic representation of the steps involved in construction of the device is shown in Figure 2.10.
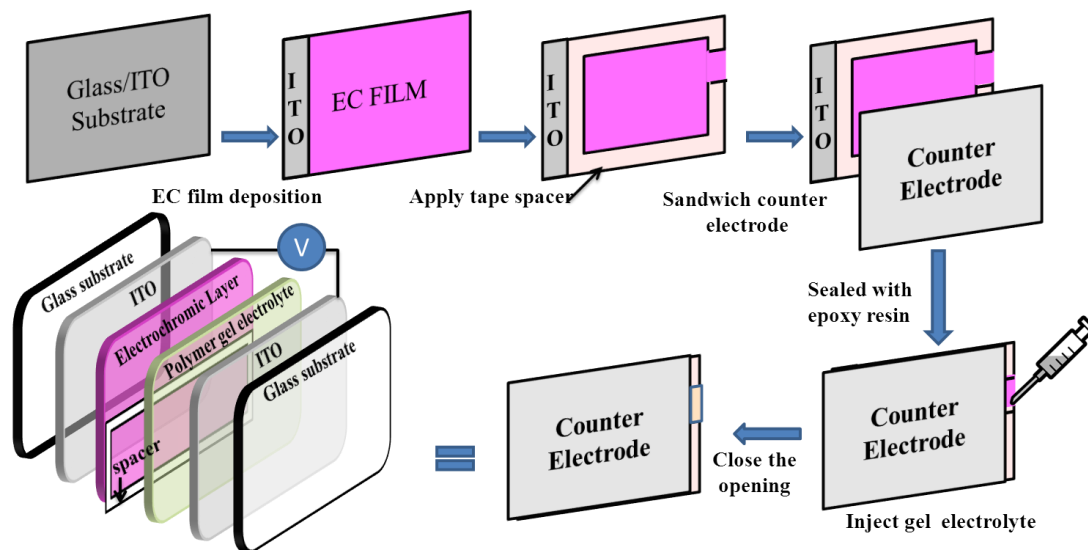
Figure 2.10: Schematic representation of steps involved in electrochromic device construction.

The ITO-coated substrates were used as transparent conducting oxide layers. The electrochromic conducting polymer layer is coated on a pre-cleaned ITO substrate that acts as an electrochromic layer. Then the double-side tape spacer is placed on the top of the electrochromic electrode, which is surrounded by the whole electrochromic layer except for a small opening to inject the electrolyte. This spacer maintains a constant separation between the two electrodes, has better adhesion and limits the volume of the electrolyte. Then the counter electrode/complementary electrode is placed face inward to the electrochromic electrode and they are combined together like a sandwiched structure. In the next step, the device is sealed properly by thermoplastic glues/epoxy resin (it must be chemically inert) and heated at 60ºC for 2 hr. The PMMA based gel electrolyte is uniformly injected in to the device through the small opening using a syringe with a needle, and care in taken prevents air bubbles inside the device. Finally, opening is closed by epoxy resin and electric connections on both ITO substrates are attracted for further device characterizations.

2.8. References

[1] K. Doblhofer, K. Rajeshwar, *Electrochemistry of conducting polymers*, in Handbook of Conducting Polymers; 3rd ed.; Skotheim T. A., Elsenbaumer R. L.,Reynolds J.R., (Ed.), Marcel Dekker , New York, 1997, 531–588.

[2] Sonmez G., Schwendeman I., Schottland P., Zong K., Reynolds J. R., *Macromolecules*, 2003, 36: 639–647.

[3] Bredas J.L., Silbey R., Boudreaux D.S., Chance R.R., *J. Am. Chem. Soc*., 1983, 105: 6555–6559.

[4] Xiao S., Zhou H., You W., *Macromolecules*, 2008, 41: 5688–5696.

[5] Shi Q., Fan H., Liu Y., Hu W., Li Y., Zhan X., *J. Phys. Chem*., 2010, 114: 16843–16848.

[6] Aparna M., Pankaj K., Ritu S., Dhawan S.K, Kamalasanan M.N., Subhas C. *Indian J. Pure Appl. Phys*., 2005, 43: 921–925.

[7] Abruna H., *Coord. Chem. Rev*., 1998, 86: 135–189.

[8] Sharp M., Petersson M., Edstrom K. J., *J. Electroanal.Chem*., 1979, 95, 123–130.

[9] Mark E. O., Bernard T., *Electrochemical Impedance Spectroscopy*. Wiley, John Wiley &Sons, Inc., Hoboken, New Jersey, 2008.

[10] Siju C. R., Saravanan T. R., Rao K. N., Sindhu S., *Int. J. Polym. Mater. Polym Biomater*., 2014, 63: 374–379.

[11] Argun A. A., Aubert P.H., Thompson B. C., Schwendeman I., Gaupp C. L., Hwang J., Jungseek P., Nicholas J., Tanner D. B., MacDiarmid A. G., Reynolds J. R., *Chem. Mater*., 2004, 16: 4401–4412.

[12] Jain V., Yochum H. M., Montazami R., Heflin J R., *Appl. Phys. Lett*., 92, 033304, 2008, DOI:10.1063/1.2834818

[13] Welsh D.M., Kumar A., Morvant M. C.,Reynolds J.R., *Synth. Met*.,1999, 102: 967–968.

[14] Miles M.H., Henry R.A., Fine D. A., 1996, US patent no: US5516462 A.

[15] Neo W. T., Loo L. M., Song J., Wang X., Cho C. M., Chan H. S. O., Zong Y., Xu J., *Polym. Chem*., 2013, 4: 4663–4675.

[16] Yagmur I., Ak M., Bayrakceken A., *Smart Mater. Struct*., 2013, 22: 115022, DOI: doi:10.1088/0964-1726/22/11/115022.

[17] Reeves B.D., Grenier C. R. G., Argun A. A., Cirpan A., McCarley T. D., Reynolds J. R., *Macromolecules*, 2004, 37: 7559–7569

[18]   Kang J.H., Xu Z., Paek S.M., Wang F., Hwang S.J., Yoon J., Choy J.H., *Chem. Asian J.*, 2011, 6: 2123–2129.

[19]   Witker D., Reynolds J.R., *Macromolecules*, 2005, 38: 7636–7644.

[20]   De Paoli M. A., Gazotti W. A., *J. Braz. Chem. Soc.*, 2002,13, 410–424.

[21]   Shin H., Kim Y., Bhuvana T., Lee J., Xu Yang., Park C., Kim E., *ACS Appl. Mater. Interfaces*, 2012, 4: 185−191.

[22]   Linford R. G., *Electrical and electrochemical properties of ion conducting polymers*. In Scrosati, B. (ed.), Applications of Electroactive Polymers, London, Chapman and Hall, 1993, 1–28.

[23]   Thakur V.K., Ding G., Ma J., Lee P.S., Lu X., *Adv. Mater.*, 2012, 24: 4071–4096.

[24]   Reiter J., Krejza O, Sedlarikova M., *Sol. Energy Mater. Sol. Cells*, 2009, 93: 249–255.

[25]   Barbosa P. C., Silva M. M., Smith M. J., Gonçalves A., Fortunato E., *Thin Solid Films*, 2008, 516: 1480–1483.

[26]   Bohnke O., Frand G., Rezrazi M., Rousselot C., Truche C., *Solid State Ionics*, 1993. 66: 97–104.

[27]   Gustaffsson G.C, Liedberg B., Inganas O., *Solid state Ionics*, 1994, 69: 145–152.

CHAPTER 3

A Study on Effects of Dopants and Polymerization Conditions on Characteristics of PEDOT and its Application in Electrochromic Devices

3.1 Introduction

Poly(3,4 ethylenedioxythiophene) (PEDOT) has emerged as a promising material in many applications such as optoelectronic devices [1,2], sensors [3,4], actuators [5,6], electrochromic devices [7–10], photovoltaic cells [11,12], anti-corrosion [13,14], and biomedical applications [15], due to its excellent conductivity, high transparency in the visible range, good thermal stability, moderate band gap, and lower oxidation potential [16]. However, powder insolubility and the decrease of electrical conductivity of PEDOT during long time usage have had limited applications in industrial and commercial areas. The insolubility of PEDOT can be rectified by polymerizing EDOT with a water-dispersible polyelectrolyte, polystyrene sulfonate (PSS) resulting in a dark blue colored aqueous dispersion. The Bayer AG research group chemically developed a water soluble poly(3,4 ethylenedioxythiophene) : poly(styrene sulfonate) (PEDOT:PSS) system with good electrical and better optical properties [17–19]. PSS is used as a charge balancing counter ion during polymerization in water medium to yield a composite of PEDOT-PSS [20–22]. In PEDOT: PSS dispersion, the polymer chains are probably attached by randomly coiled negatively charged PSS ions with positively charged PEDOT molecule chains under ionic attractions [23–26]. Instead of PSS doped PEDOT, other anionic surfactants like camphorsulphonic acid (CSA) [27,28], p-toluenesulfonic acid (PTSA) [29,30], dodecylbenzenesulfonic acid (DBSA) [31], sodium bis(2-ethylhexyl) sulfosuccinate (AOT), [32,33] and sodium dodecyl sulphate (SDS) [34,35] doped with PEDOT have also been reported to improve the characteristic properties of PEDOT. The anionic PSS doped polymer film has many advantages over other surfactants such as high processability, good transparency in the visible region, high contrast ratio, superior electrical and mechanical properties, and better environmental stability, which provides more applications in organic based optoelectronic devices, light emitting diodes, and photovoltaic cells [36]. Many research groups have extensively studied the synthesis, characterization, properties, and applications of PSS doped PEDOT film via chemical and electrochemical methods [37–45]. It was observed that the incorporation of water soluble polyelectrolytes on PEDOT affects the morphological and electrical properties of the PEDOT

films [46]. The addition of polyelectrolytes on PEDOT polymer chains affected the electrochromic performance of the devices, and this was reported by Pennisi et al. [47]. The molar ratio of PEDOT and PSS in dispersion strongly affects the electrical conductivity of PEDOT: PSS films. A larger PEDOT ratio showed higher conductivity and is expected to be a good charge transporting medium [48].

Nowadays electropolymerization method has been used as convenient method mainly because of its accuracy, repeatability, low monomer concentration, and facile film controllability by controlling experimental parameters such as scan rate, applied potential, concentration of electrolyte, and the number of repeating cycles [49–51]. Unlike an organic electrolyte medium, aqueous electrolyte media are more attractive due to their low cost, non-toxic, and environmental stability. The electropolymerization of PEDOT film in the presence of PSS on working electrodes in an aq. phosphate buffer solution using CV was first reported by Yamato et al. [52]. The electropolymerized PEDOT films showed better electrical conductivity than the film prepared by commercially available PEDOT-PSS aqueous dispersions [18]. The electropolymerized PEDOT:PSS film using one-step cyclic voltammetry in aqueous media was recently reported and its influence on polymerization potentials and dopants on the resulting polymers was studied [53]. On consideration of all the above aspects, in this chapter, we presents a simple, and cost-effective one-step cyclic voltammetry technique for the preparation of polymer film in an economically promising aqueous electrolyte medium and a low cost supporting electrolyte, KNO_3 for electrochromic device applications. The dopant PSS, was used as an anionic surfactant and electropolymerization methods such as potentiostatic (PS) and potentiodynamic (PD) techniques were used for the electropolymerization of EDOT. The effects of dopant and polymerization techniques on the electrochemical and morphological properties of the PEDOT polymer were systematically studied. The electrochromic performances of the films as well as devices based on PEDOT and PEDOT:PSS films were studied.

3.2. Electrochemical Polymerization

An ITO coated glass substrate (resistivity 15–930 $\Omega/\square$) was used as a working electrode, platinum foil as a counter electrode, and an Ag rod as a reference electrode. The electropolymerization was carried out using cyclic voltammetry (CV) (potentiodynamic, PD) and the constant applied potential (potentiostatic, PS) method. The CV was conducted by applying a potential between +1.2 V and −1.2 V at a scan rate of 50 mVs^{-1} for two cycles. A

static potential of 1.2 V was applied for 20–30 s for the constant potential technique. An electrolyte solution was prepared by 0.01M of EDOT monomer in 0.1M KNO_3 as supporting electrolyte. Then 0.01M of PSS dopant was added to the electrolyte solution. The entire solution was stirred continuously untill it became completely homogenous and the polymerization was then performed. The resulting dark blue PEDOT films were rinsed thoroughly with de-ionized water to remove unreacted monomers, surfactants, and electrolytic molecules and dried under a vacuum oven at 70°C for 1 h [54].

3.3 Preparation of Prussian Blue

Prussian blue (PB) film was electrodeposited on an ITO substrate by potentiodynamic technique using an equal volume of ferric chloride ($FeCl_3$, 10 mM) and potassium ferricyanide ($K_3Fe(CN)_6$, 10 mM) in 0.01 N aq.HCl solution (pH 2). The deposition was conducted under applied potential between −0.4 and 1.0 V at a scan rate of 100 mV s^{-1}. The PB films were rinsed with double distilled water and dried at room temperature for 30 min.

3.4. Results and Analysis

3.4.1. Cyclic Voltammetry

The electrochemical behaviour of polymer films was studied by cyclic voltammetry in a monomer-free electrolyte medium between applied potential of −1.2 V and +1.2 V at a scan rate of 100 mVs^{-1}. Cyclic voltammograms of PEDOT and PEDOT: PSS films prepared by two different polymerization techniques are shown in Figure 3.1 a & b respectively. The oxidation-reduction behaviour of PEDOT thin film was recorded as anodic and cathodic peaks in the cyclic voltammogram. The potential difference of oxidation and reduction peak values of the PEDOT:PSS film changed with a change in polymerization techniques. The PEDOT films prepared by the PS method showed a higher peak current value (i_p) than the film prepared by the PD method. This clearly reveals that the PEDOT films prepared by the PS method show a higher electrical response than with the PD method. This is due to the EDOT monomers which attained a constant oxidative potential (1.2 V) at a time that would lead to the ease of monomer oxidation during polymerization. This provides good adhesion of particles and uniform polymer film deposition on an ITO/glass surface without any preference [55].
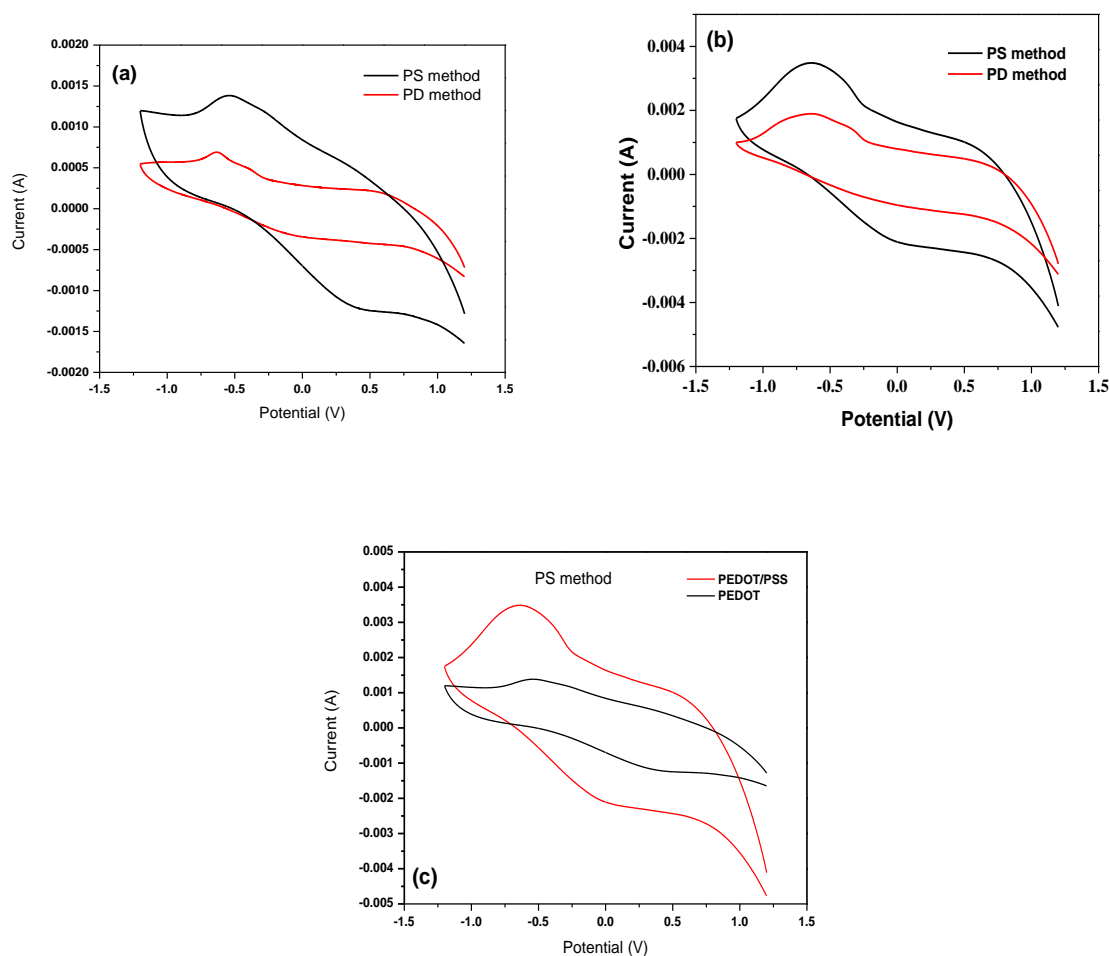
Figure 3.1: Cyclic voltammograms of (a) PEDOT and (b) PEDOT: PSS thin films at two different polymerization techniques at a scan rate of 100 mVs^{-1} in aqueous 0.1M KNO$_3$ solution. (c) Comparison of electrochemical response of PEDOT and PEDOT: PSS films prepared by PS method.

The electrochemical behaviour of PEDOT and PEDOT:PSS prepared by the PS method at applied potential between −1.2 V and +1.2 V at a scan rate of 100 mVs^{-1} is shown in Figure 3.2. We have noticed that the polymerization conditions strongly affect the nucleophilic character of the counter anion present in the polymer:dopant films. The dopant PSS showed much influence on the electrochemical properties of the PEDOT polymer. The higher electrochemical response of the PEDOT:PSS polymer reveals the easy transportation of small cations (K$^+$) upon a redox process through open morphology of the PEDOT:PSS film.

3.4.2. FTIR Spectral Analysis

An FTIR spectral analysis was carried out for further confirmation of the molecular structure of the resulting PEDOT and PEDOT: PSS films prepared by PS method. The FTIR spectra of electropolymerized PEDOT and PEDOT:PSS films on an ITO/glass are shown in Figure 3.2. The IR bands at 634 cm^{-1}, 790 cm^{-1}, and 978 cm^{-1} were ascribed to the C-S bond stretching vibration in the thiophene rings. The vibrations at 1088 cm^{-1} and 1154 cm^{-1} were attributed to the C-O-C band stretching modes of the ethylenedioxy group in the molecules. The peaks at 1361 cm^{-1} and 1449 cm^{-1} were due to the C-C and C=C stretching vibration of the quinoidal structure of thiophene rings, respectively. The presence of peak at 1683 cm^{-1} was attributed to the C-O bond out of plane deformation in ethylenedioxy ring. The bands at 1255 cm^{-1} and 913 cm^{-1} correspond to $^-SO3^-$ and S-OH stretching in the molecule of PSS. The FTIR spectral results indicated that the PSS anion was incorporated successfully into the backbone of the PEDOT polymer [56].
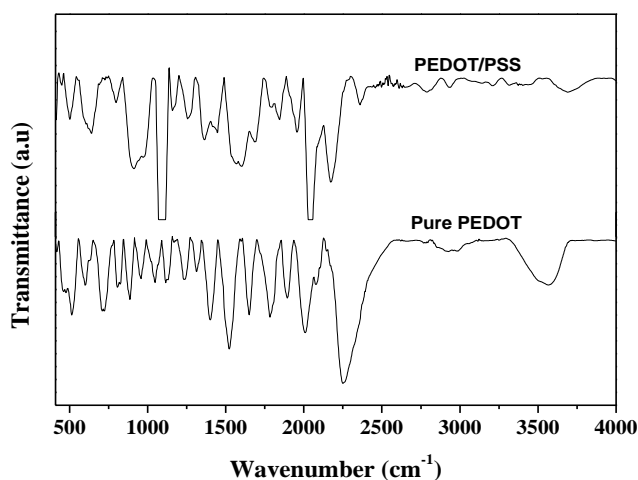
Figure 3.2: FTIR Spectra of PEDOT and PEDOT: PSS prepared electrochemically in 0.01M EDOT and 0.01 M PSS in 0.01M aq.KNO_3 solution.

3.4.3. Scanning Electron Microscopy (SEM)

A comparison of the morphological images of PEDOT, PEDOT:PSS, PEDOT:CSA, and PEDOT:AOT thin films prepared by potentiodynamic and potentiostatic techniques are shown in Figure 3.3. The SEM images of PEDOT films prepared by the PD method show very rough morphological structures and many more particles agglomerated on the polymer surface than in the films polymerized by the PS technique. The polymer films prepared by the

PS method exhibit uniform and homogenous films. PEDOT doped with PSS film by the PS method shows a more highly uniform and smoother film than the other polymer films. However, the SEM images of normal PEDOT films (without dopants) prepared by two different polymerization methods show the same morphological properties. We observed that the dopants have significant influences on the morphological properties of the polymers and the polymerization techniques showed a minor effect on morphology.
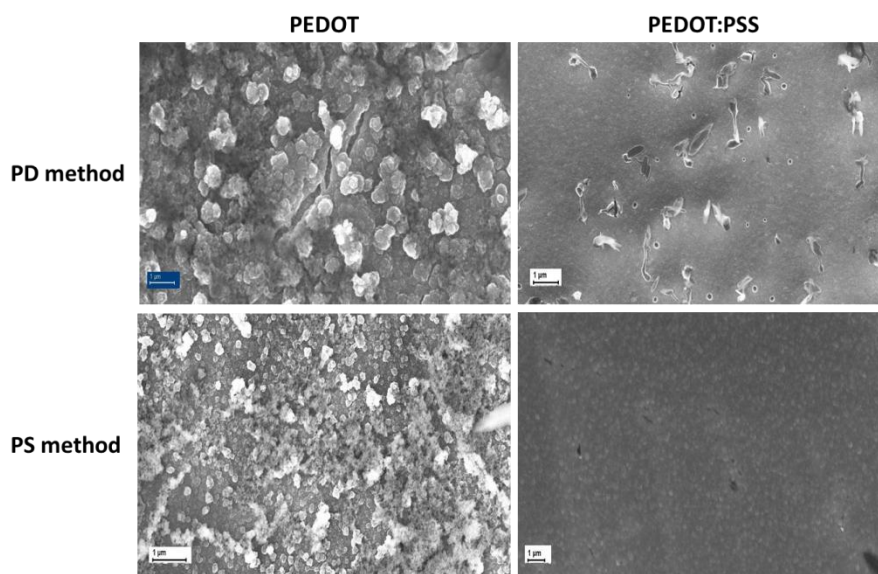
Figure 3.3: SEM images of pure PEDOT, and PEDOT:PSS thin film polymerized from 0.01M EDOT monomer in aqueous 0.1M KNO$_3$ at different polymerization techniques.

3.4.4. Spectroelectrochemistry

The spectroelectrochemical studies of PEDOT and PEDOT:PSS films recorded as a function of different applied potentials ranging between −2.5 V and 2.0 V in 0.1M LiClO$_4$/ACN solution are shown in Figure 3.4 a&b respectively. At −2.5V, the PEDOT film was fully reduced and showed a broad absorption peak at λ_{max} of 575 nm due to the inter-band π-π* transition. Upon step-wise oxidation of the PEDOT film, the absorption due to the π-π* transition peak decreased and a peak due to the polaronic/ bipolaronic transitions was formed towards higher wavelength region. At oxidized state (+2.0 V), the absorbance at the visible region was fully diminished, and a peak due to charge carriers appeared near IR region. These same spectroelectrochemical properties were observed for the PEDOT:PSS film. However, at a reduced state (−2.5 V), the intensity of absorption was increased compared to PEDOT film and the absorption peak due to π–π* transition at λ_{max} of 590 nm was observed

that covered the entire area of the visible region (400–850 nm) of the electromagnetic spectrum.
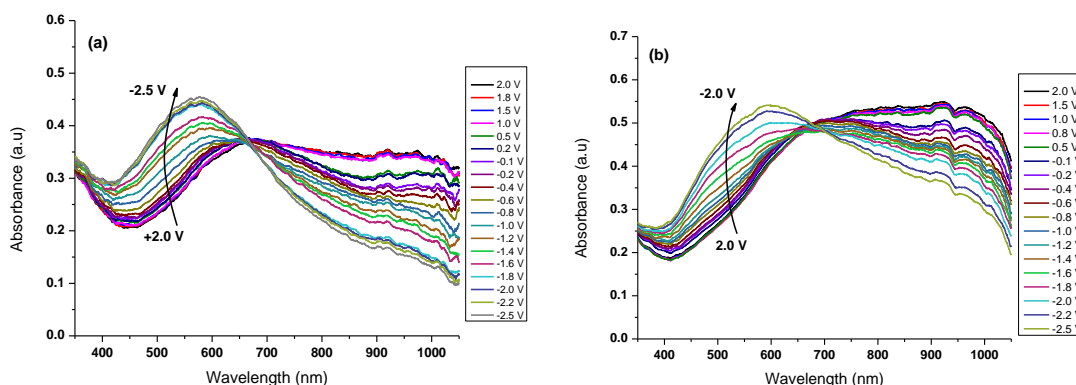
Figure 3.4: Spectroelectrochemistry of (a) PEDOT and (b) PEDOT:PSS films in 0.1M $LiClO_4$/ACN electrolyte at different applied potentials.
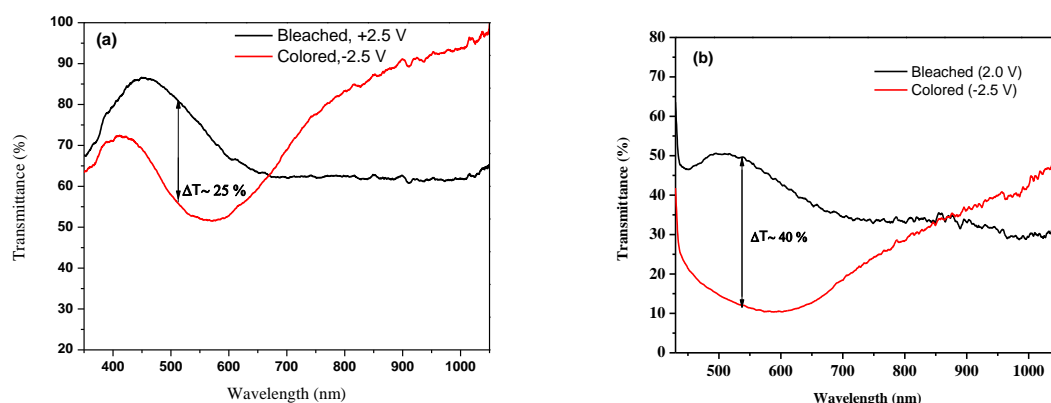
Figure 3.5: Transmittance spectra of (a) PEDOT and (b) PEDOT: PSS film on ITO coated glass in 0.1M $LiClO_4$/ACN electrolyte at fully bleached and reduced states.

The redox process of PEDOT:PSS film can be represented as;

$$(PEDOT: PSS)Li_n \leftrightarrow (PEDOT: PSS) + ne^- + nLi^+$$

$$\text{(Deep Dark Blue)} \qquad \text{(Pale sky blue)}$$
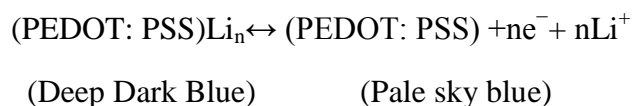
The color contrast of PEDOT and PEDOT: PSS film was calculated to be ~ 25 % T (520 nm) and 40 % T (535 nm) respectively, from transmittance spectra (Figure 3.5). However, the value is acceptable for most optoelectronic device applications where $\Delta T \approx 40\%$.

3.4.5. Optical Switching Studies

The optical switching properties of PEDOT and PEDOT:PSS films were studied by repeatedly switching potential between reduced (−1.5 V) and oxidized states (+1.5 V) at regular interval of 5 s and monitoring the % transmission as a function of time at 500 nm in 0.1 M of LiClO$_4$/ACN solution as shown in Figure 3.6 a & b, respectively. The color contrast calculated from the difference in percentage transmission (%T) between the completely reduced and oxidized states of PEDOT and PEDOT:PSS films were ~20 % (520 nm) and ~27 % T (535nm) respectively, which is reasonable in electrochromic device applications. The coloration efficiency of PEDOT and PEDOT:PSS films were found to be 56 cm^{2}C^{-1} and 123 cm^{2}C^{-1} with response time of <2 s for both the films.
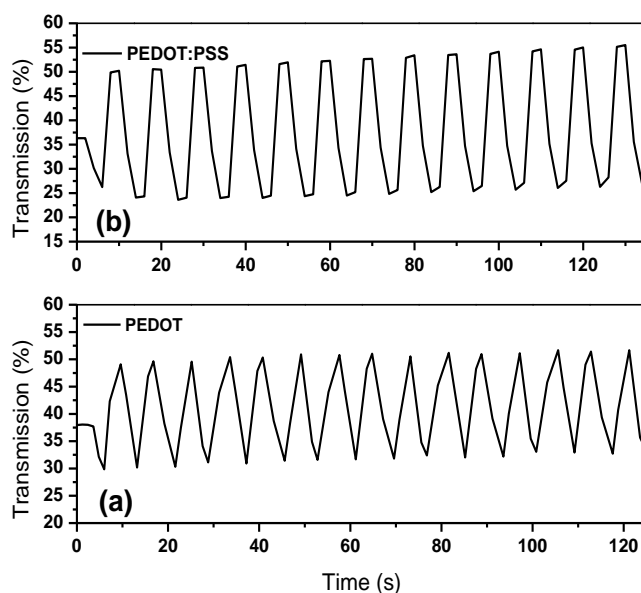
Figure 3.6: Optical switching of (a) PEDOT and (b) PEDOT:PSS films prepared by PS method in 0.1M LiClO$_4$/ACN medium at a potential between −1.5 V and +1.5 V.

3.5. Performance Testing of Electrochromic Window

3.5.1. Spectroelectrochemistry

The PEDOT and PEDOT:PSS films were electropolymerized by the potentiostatic method from 0.01M EDOT monomer in an aq. 0.1 M KNO$_3$ solution and these electropolymerized PEDOT and PEDOT: PSS films were used as active EC layers for electrochromic windows, represented as PEDOT-ECW and PEDOT:PSS-ECW. An ITO coated glass substrate was used as a counter electrode and PMMA based gel was used as a conductive gel electrolyte.

The optical properties of ECWs based on PEDOT and PEDOT:PSS films was studied by transmittance versus wavelength spectra as shown in Figure 3.7 a & b, respectively. The color contrast of PEDOT-ECW was measured to be ~25% T at 520 nm. The PEDOT:PSS-ECW shows a significant color contrast as ~30% T at λ_{max} of 520 nm. We have noticed that a sharp transmittance (%) peak was observed at 520 nm for PEDOT-ECW; however, a broad peak (450–700 nm) was observed for PEDOT:PSS-ECW device.
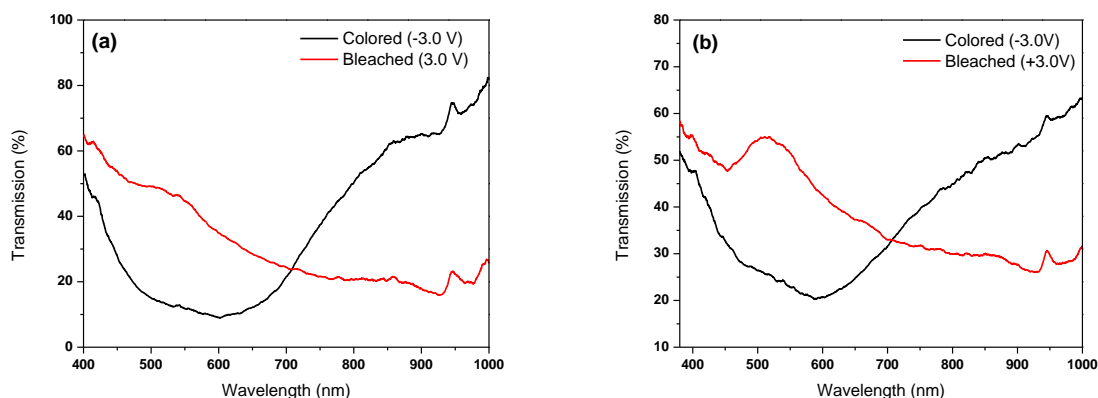
Figure 3.7: Transmittance spectra of (a) PEDOT-ECW and (b) PEDOT:PSS-ECW at fully colored and bleached states.
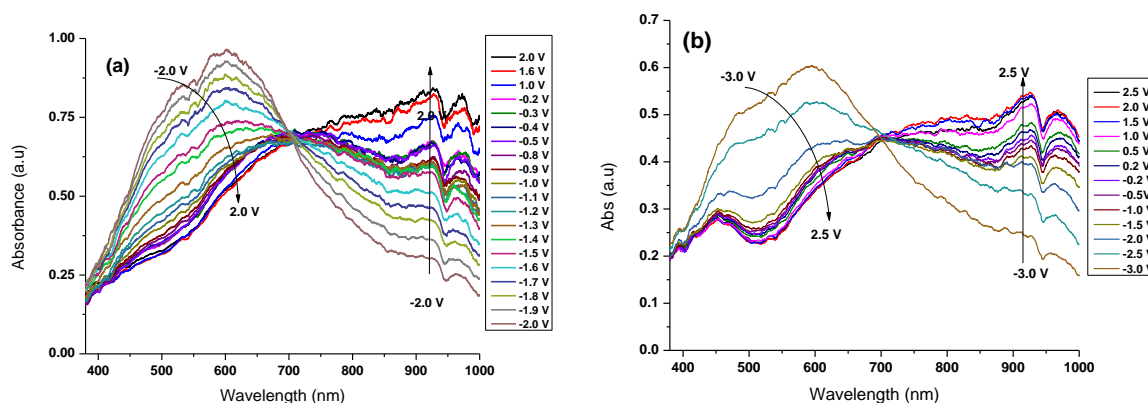
Figure 3.8: The spectroelectrochemical studies of (a) PEDOT-ECW and (b) PEDOT:PSS-ECW as a function of different applied potentials.

The spectroelectrochemical properties of PEDOT-ECW and PEDOT:PSS-ECW were studied by monitoring the absorbance changes as a function of different applied potentials as shown in Figure 3.8 a & b, respectively. Both devices showed nearly similar characteristic behaviour as like their corresponding films. At −3.0 V, the PEDOT:PSS-ECW gets fully reduced with

strong absorption (450–750 nm) that is attributed to the distinct π to π^* inter band transition of the EC material. During stepwise oxidation, the absorbance due to π–π^* transition decreases in the visible region and slightly increases towards the longer wavelength region (850–900 nm). At the fully oxidized state (+2.5 V), the absorbance due to the π to π^* transition in the visible region is fully diminished, and a new peak is observed at 850 nm because of polaronic transitions. The PEDOT:PSS-ECW showed high intense and a broad absorption peak in the visible region when compared to the PEDOT based device, which improved the color contrast of the device. However, PEDOT-ECW also shows significant spectroelectrochemical properties at various applied potentials between −2.0 V and +2.0 V. The PEDOT-ECW and PEDOT:PSS-ECW showed a single well- identified isosbestic point at 705 and 710 nm, respectively.

3.5.2. Optical Switching Kinetics

The optical switching stability and the chronoamperometry of PEDOT-ECW and PEDOT:PSS-ECW which were studied by repeatedly switching the potential between −2.5 V and +2.5 V at a regular interval of 15 s are shown in Figure 3.9 a & b, respectively. The PEDOT-ECW showed a stable reversible switching and its color contrast was calculated to be 28% T without a complementary electrode. The response time of PEDOT-ECW for bleaching and coloration were about 2.5 s and 1.7 s respectively. The PEDOT:PSS-ECW also showed a highly stable and better optical switching stability with optical contrast of 32% T. The bleaching and coloring time were calculated as ~3.0 s and ~3.5 s respectively. Both the devices showed stable and repeatable cyclic current response (chronoamperometry) as a function of time during optical switching. The color contrast of PEDOT-ECW and PEDOT:PSS-ECW which can be changed as functions of pulse width (5–15 s) are shown in Figure 3.10 a & b, respectively. When the pulse width was increased from 5 s to 15 s, the color contrast of PEDOT-ECW and PEDOT:PSS-ECW was increased by 3% T and 8% T, respectively. A photograph of PEDOT and PEDOT:PSS based ECW at colored (−3.0 V) and bleached states (+3.0 V) is shown in Figure 3.11 c & d, respectively.
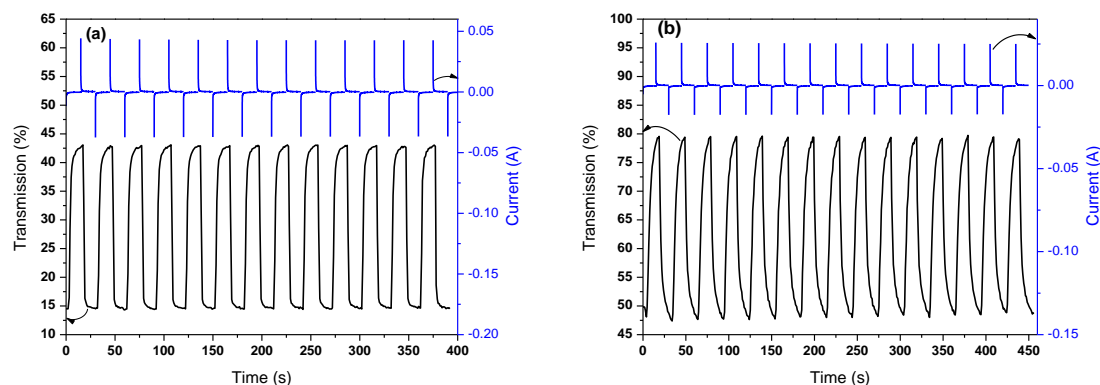
Figure 3.9: The optical switching stability and corresponding cyclic current response of (a) PEDOT-ECW and (b) PEDOT:PSS-ECW between the applied potential of −2.5 V and +2.5 V at 520 nm.
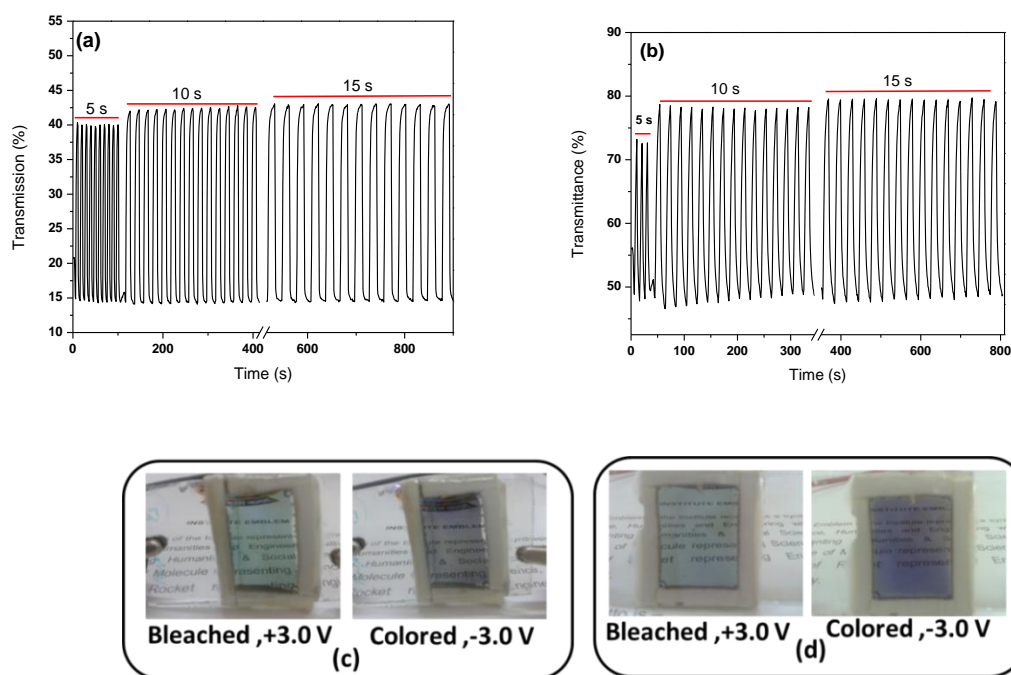
Figure 3.10: Optical switching study of (a) PEDOT-ECW and (b) PEDOT:PSS-ECW between the applied potential of −2.5 V and +2.5 V at different pulse width; Photograph images of (c) PEDOT-ECW and (d) PEDOT:PSS-ECW at redox potential (Active area of the device: ~2.5 cm^2)

A dual-type electrochromic window was fabricated using Prussian blue (PB) film as a complementary counter electrode in the PEDOT:PSS-ECW device structure. The color

contrast of PEDOT:PSS-ECW can be enhanced by incorporating PB layer as a counter electrode to the PEDOT:PSS based window (PEDOT:PSS/PB-ECW). The optical switching response of PEDOT:PSS/PB-ECW was studied at a switching potential between −3.0 and 3.0 V at a regular interval of 5 s and 10 s, and the %T was monitored as a function of time at 520 nm as shown in Figure 3.11a. The color contrast of this dual-type ECW was calculated to be 45% T at a pulse width of 10 s. The dual-type ECW enhanced the color contrast from 32 % T to 45% T while compared to the single type PEDOT:PSS-ECW. The response time of PEDOT:PSS/PB-ECW for bleaching and coloration was about 3.0 and 3.3 s respectively. The coloration efficiency of this ECW was found to be 25 cm^2C^{-1} in the fully reduced state. The photograph of PEDOT:PSS/PB-ECW at the fully colored and bleached states is shown in Figure 3.11b.
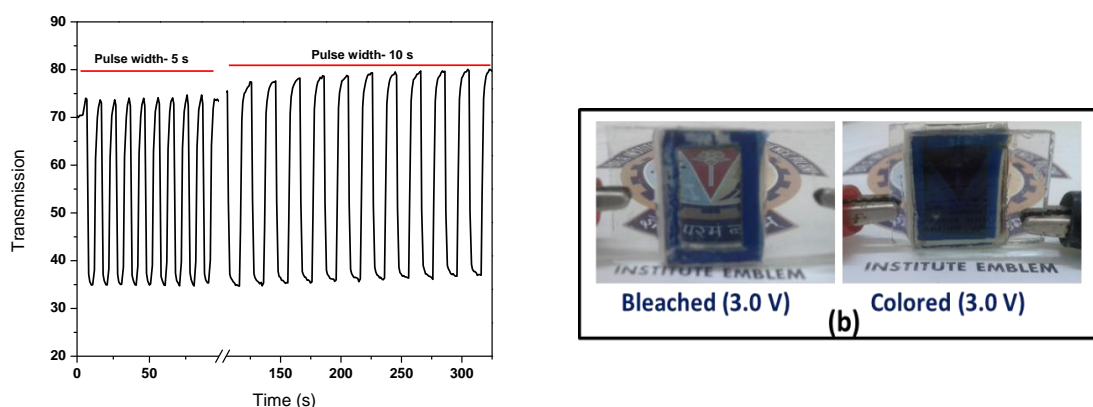
Figure 3.11: Optical switching study of (a) dual type electrochromic device based on PEDOT:PSS:PB-ECW and (b) photographs of this ECW at fully colored and bleached states (Active area of the device: ~2.5 cm^2)

3.5.3. Open Circuit Memory and Electrochemical Long-term Stability

The open circuit memory of PEDOT- ECW and PEDOT:PSS-ECW was monitored at 520 nm as a function of time at an applied potential of ±2.5 V for 30 s to stabilize the color (or bleach) and then the circuit potential was opened up to 300 s (Figure 3.12). At the bleached state (+2.5 V), PEDOT-ECW and PEDOT:PSS-ECW showed good optical stability and exhibited better optical memory without much deviation in %T (<3–5%) under open circuit conditions. But in the reduced state, both the devices showed a small degradation in terms of color and, therefore, increase of transmittance when the potential was opened. However, this

limitation could be overcome by applying a negative potential to retain the fully colored state. The redox switching stability of PEDOT- ECW and PEDOT:PSS-ECW were studied using CV by applying the potential between −1.2 and +1.2 V at a scan rate of 300 mVs^{-1} (Figure 3.12 c & d). After 200 cycles, the electroactivity of both ECWs were retained, revealing that the devices have good long-term electrochemical stability and an excellent redox response.
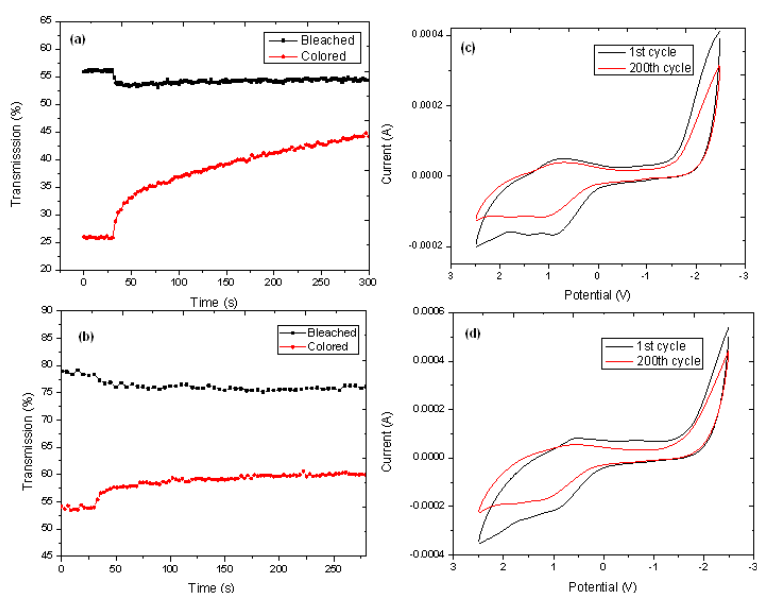
Figure 3.12: The open circuit memory and long-term electrochemical stability of PEDOT-ECW (a&c) and PEDOT:PSS-ECW (b &d) devices.

3.6. Performance Testing of Electrochromic Rear-view Mirror

The electrochromic rear-view mirror (ECM) was constructed by sandwiching polymer gel electrolyte between both a PEDOT:PSS based working electrode and an ITO/glass/Al counter electrode. The reflectance spectra of ECM which monitored the % of reflection at the colored and bleached states are shown in Figure 3.13a. At −3.0 V, the active EC layer in the mirror has reached to fully reduced state, and the maximum absorption peak was noticed at 500 nm due to the π–π* transition that leads to a reduction in the reflectance (~40%). At the fully oxidized state (+3.0 V), the absorption due to π–π* transition was decreased and a new peak was formed at a higher wavelength region due to polaronic transition. This can increase the reflectivity of ECM in the visible region, and then the Al layer achieves higher reflectivity (~75%) like a normal mirror. A photograph of a rear-view mirror at the fully colored and bleached states is shown in Figure 3.13 b.

67
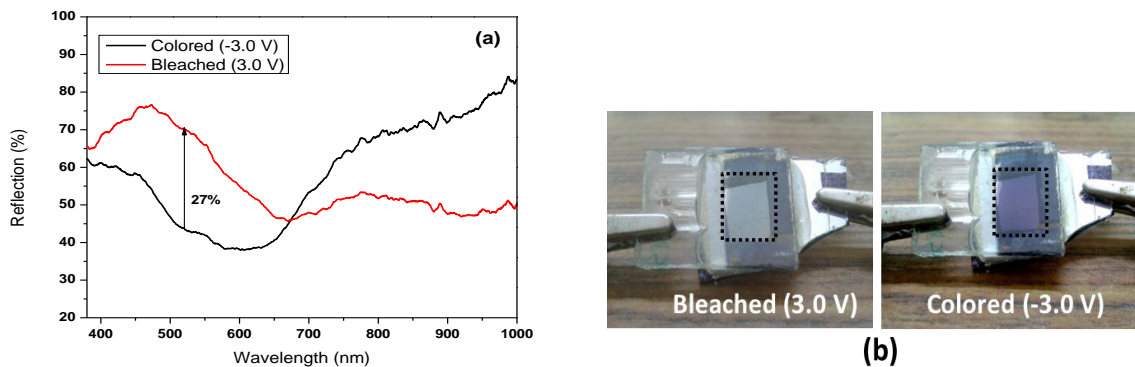
Figure 3.13: (a) Reflectance spectra of electrochromic rear-view mirror at applied potential between −3.0 V and 3.0 V; and (b) photographs of rear-view mirror at bleached and colored states (Dotted column represents active area of mirror: 2cm^2).
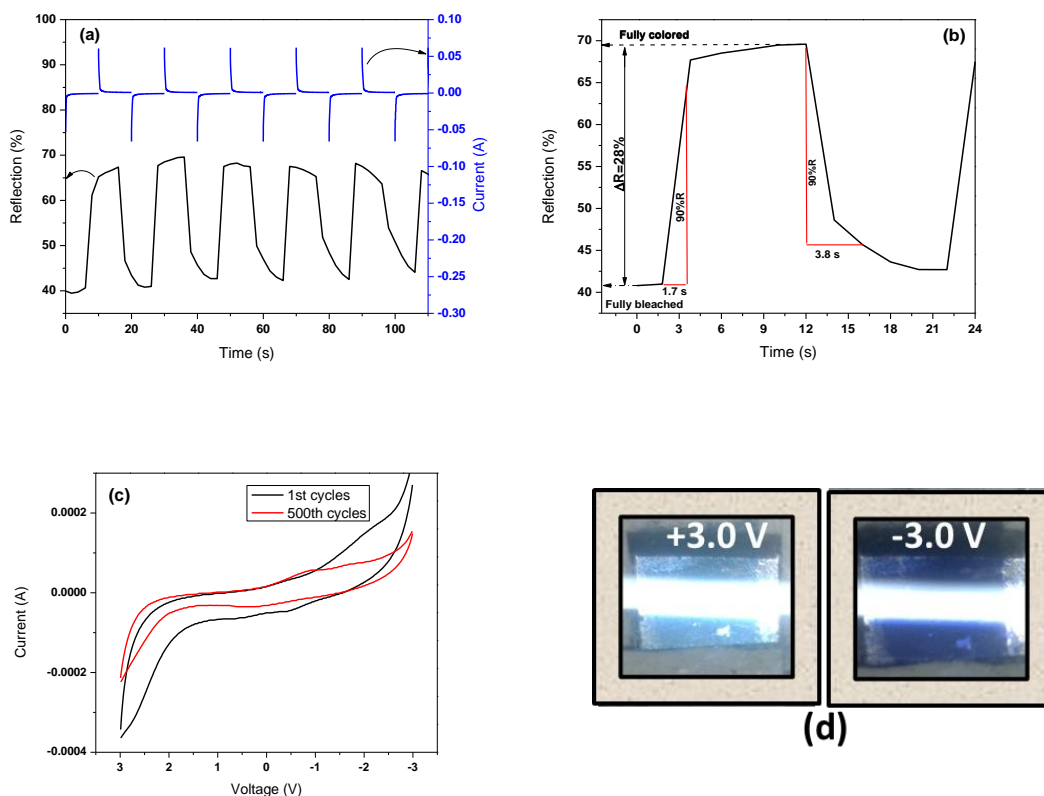
Figure 3.14: (a) Optical switching kinetics, and (b) Calculation of reflectance ratio and response time of electrochromic rear-view mirror based on PEDOT:PSS film at λ_{max} of 520 nm between the potential of −3.0 V and +3.0V with regular interval of 10 s. (c) Long term electrochemical stability of ECM by CV and (d) Photograph of glare reduction in electrochromic rear-view mirror between redox potentials (Active area of the device: ~2.5 cm^2)

The optical switching response of a PEDOT:PSS based EC rear-view mirror was studied at a switching potential between −3. 0 V and +3.0V at a regular interval of 10 s, and the % reflection as a function of time at λ_{max} of 520 nm was monitored, as shown in Figure 3.14a. The reflection contrast of ECM was calculated to be 27% at 520 nm. The response time for bleaching and coloring was calculated as 1.7 s and 3.8 s respectively (Figure 3.14 b). The coloration efficiency of ECM was found to be 15 cm^2C^{-1} in the reduced state (charge =0.023 C & area= 1.5 cm^2). In Figure 3.14c, the long-term redox switching stability of PEDOT:PSS-ECM was studied using CV by applying the cyclic potential between −3.0 and +3.0 V at a scan rate of 300 mVs^{-1}. This ECM was successfully switched for more than 500 cycles, revealing that this mirror is highly reversible and retained electrochemical stability without much degradation of the redox response. A Photograph of glare reduction in ECM at the fully colored and bleached states is shown in Figure 3.14d.

3.7. Summary

We have introduced a fast, simple and cost effective electrochemical polymerization route for the preparation of PEDOT using one-step cyclic voltammetry in an aqueous KNO_3 medium. The effect of the morphological and electrochemical properties of PEDOT and PEDOT:PSS films were studied. The electrochemical and morphological properties of the PEDOT films influenced by surfactants and polymerization techniques were observed. The polymer films electropolymerized by the potentiostatic method showed higher electrical conductivity and a better electrochemical response than the films polymerized by the potentiodynamic method. The PSS dopant has influenced the electrochemical and morphological properties of PEDOT film. The PEDOT film doped by PSS showed smooth and well-uniform homogenous film formation on the working electrode. The spectroelectrochemistry, optical switching studies, and the long-term stability of these films were also studied. The optimized PEDOT film was used to fabricate a prototype of a cost effective electrochromic window and rear-view mirror and their EC performance was tested. The ECDs showed significant optical contrast, good optical switching stability, and an applicable response time. This easy processable and economically promising electropolymerized PEDOT:PSS could be used for practical applications of low-cost electrochromic devices.

3.8. References

[1]   Friend R. H., *Pure Appl. Chem.*, 2001, 73:425–430.

[2]   Ouyang J., Chu C W., Chen F.C., Xu Q., Yaintervang Y., *J. Macromol. Sci., Pure Appl. Chem*, 2004, 41: 1497–1511.

[3]   Lin C.Y., Chen J. G., Hu C. W., Tunney J. J., Ho K. C., *Sens. Actuators. B*, 2009, 140: 402–406.

[4]   Kwon O. S., Park E., Kweon O. Y., Park S.J., Jang J., *Talanta*, 2010, 82: 1338–1343.

[5]   Okuzaki H., Suzuki H., Ito T., Synth. Met., 2009, 159: 2233–2236.

[6]   Plesse C., Khaldi A., Wang Q., Cattan E., Teyssi D., Chevrot C., Vidal F., *Smart Mater. Struct.*, 2011, 20: 124002, DOI:10.1088/0964-1726/20/12/124002.

[7]   Sindhu S., Rao K.N., Gopal E.S. R., *Bull. Mater. Sci. B*, 2008, 31: 15–18.

[8]   Sindhu S., Rao K.N., Ahuja S., Kumar A., Gopal E.S.R., *Mater. Sci. Eng., B*, 2006, 132: 39–42.

[9]   Vergaz R., Barrios D., Pena J.M.S., Marcos C., Pozo C., Pomposo J. A., *Sol. Energy Mater. Sol. Cells*, 2008, 92: 107–111.

[10]   Mecerreyes D., Marcilla R., Ochoteco E., Grande H., Pomposo J.A., Vergaz R., Sánchez Pena J. M., *Electrochim. Acta*, 2004, 49: 3555–3559.

[11]   Schmidt-Mende L., Fechtenkotter A., Mullen K., Moons E., Friend R. H., Mackenzie J. D, *Science*, 2001, 293: 1119–1122.

[12]   Liscio A., De Luca G., Nolde F., Palermo V., Meullen K., Samori P. J., *J. Am. Chem. Soc.*, 2008, 130: 780–781.

[13]   Liesa F., Ocampo C., Aleman C., Armelin E, Oliver R., Estrany F., *J. Appl. Polym. Sci.*, 2006, 102: 1592–1599.

[14]   Ocampo C., Oliver R., Armelin E., Alemanm E., Estrany F., *J. Polym. Res.*, 2006 13: 193–200.

[15]   Ravichandran R., Sundarrajan S., Venugopal J.R., Mukherjee S., Ramakrishna S., *J. R. Soc. Interface,* 2010, 7: S559–S579, DOI: 10.1098/rsif.2010.0120.

[16]   Skotheim T. A., Reynolds J. R., *Handbook of Conducting Polymers- Conjugated Polymers: Synthesis, Properties and Characterization*. CRC Press: Boca Raton, FL, 2007.

[17]   Jonas F., Heywang G., Schmidtberg W., Heinze J., Dietrich M., 1990, US 4959430 Patent No.4959430.

[18]   Groenendaal L., Jonas F., Freitag D., Pielartzik H., Reynolds J.R, *Adv Mater*., 2000, 12: 481–494.

[19]   Groenendaal L., Zotti G., Jonas F., *Synth.Met*., 2001, 118: 105–109.

[20]   Pigani L., Heras A., Colina A., Seeber R., Palacios J.L., *Electrochem. Commun*. 2004, 6: 1192–1198.

[21]   Li G., Pickup P.G., *Phys. Chem. Chem.Phys*., 2000, 2: 1255–1260.

[22]   Cui X., Matrin D., *Sens. Actuators. B*, 2003, 89: 92–102.

[23]   Travers J.P., Sixou B., Berner D., Wolter A., Rannou P., Beau B., Pepin-Donat B., Barthet C., Guglielmi M., Merilliod N., Gilles B., Djurado D., Attias A.J., Vautrin M., *Synth. Met*., 1999, 101: 359–362.

[24]   Kohlman R.S., Joo J., Wang Y.Z., Pouget J.P., Kaneko H., Ishiguro T., Epstein A.J., *Phys. Rev. Lett*., 1995,74: 773. DOI:10.1103/PhysRevLett.74.773.

[25]   Prigodin V.N., Epstein A.J., *Synth. Met*., 2001, 125: 43–53.

[26]   Jonsson S.K.M, Birgerson J., Crispin X., Greczynski G., Osikowicz W, Denier van der Gon A.W.,Salaneck W. R., Fahlman M., *Synth. Met*., 2003, 139: 1–10.

[27]   Feng W, Li Y., Wu J., Noda H., Fujii A., Ozaki M., Yoshino K., *J. Phys.: Condens. Matter*, 2007, 19: 186220, DOI:10.1088/0953-8984/19/18/186220.

[28]   Bhandari S., Deepa M., Singh S., Gupta G., Kant R., *Electrochim. Acta*, 2008, 53: 3189–3199.

[29]   Aasmundtveit K.E., Samuelsen E.J., Inganas O., Pettersson L.A.A., Johansson T., Ferrer S., *Synth. Met*. 2000, 113: 93–97.

[30]   Aasmundtveit K.E., Samuelsen E.J., Pettersson L.A.A., Inganas O., Johansson T., Feidenhans R., *Synth. Met*., 1999, 101: 561–564.

[31]   Choi J.W., Han M.G., Kim S.Y., Oh S.G., Im S.S., *Synth. Met.*, 2004, 141: 293–299.

[32]   Bhandari S., Deepa M., Srivastava A.K., Kant R., *J. Mater. Chem.*, 2009, 19: 2336–2348.

[33]   Mao H., Liu X., Chao D., Cui L, Li Y., Zhang W., Wang C., *J. Mater. Chem*., 2010, 20: 10277–10284.

[34]   Sakmeche N., Aeiyach S., Aaron J.J., Jouini M., Lacroix J.C., Lacaze P.C., *Langmuir*,1999, 15: 2566–2574.

[35]   Chun L., Toyoko I., *Macromolecules*, 2004, 37: 2411–2416.

[36]   Elschner A., Kirchmeyer S., Lovenich W., Merker U., Reuter K., *PEDOT: Principles and Applications of an Intrinsically Conductive polymers*. CRC Press Taylors & Francis group, Boca Raton,London, 1st ed, 2011.

[37] Tamburri E., Orlanducci S., Toschi F., Terranova M.L., Passeri D., *Synth. Met.*, 2009, 159: 406–414.

[38] Fan B., Mei X., Ouyang J., *Macromolecules*, 2008, 41: 5971–5973.

[39] Okuzaki H., Suzuki H., Ito T., *J.Phys.chem.B*, 2009, 113: 11378–11383.

[40] Louwet F., Groenendaal L., Dhaen J., Manca J., Van Luppen J., Verdonck E., Leenders L., *Synth. Met.*, 2003, 135: 115–117.

[41] Zotti G., Zecchin S., Schiavon G., Louwet F., Groenendaal L., Crispin X., Osikowicz W., Salaneck W., Fahlman M., *Macromolecules*, 2003, 86: 3337–3344.

[42] Crispin X., Marciniak S., Osikowicz W., Zotti G., Van Der Gon A.W.D., Louwet F., Fahlman M., Groenendaal L., DeSchryver F., Salaneck W.R., *J. Polym. Sci., Part B: Polym. Phys.*, 2003, 41: 2561–2583.

[43] Aleshin A.N., Williams S.R., Heeger A.J., *Synth. Met.*, 1998, 94: 173–177.

[44] Ouyang J., Chi-Wei C, Fang-Chung C., Xu Q., Yang, Y., *Adv. Funct. Mater.*, 2005,15: 203–208.

[45] Lefebvre M., Qi Z., Danesh R. D., Pickup P.G., *Chem.Mater.*,1999,11: 262–268.

[46] Liao Y.H., Laakso J., Osterholm J.E., *Macomol. Rapid Commun.,* 1995, 16: 23–25.

[47] Di-Marco G., Lanza M., Pennisi A., Simone F., *Solid State Ionics*,2000, 127: 23–29.

[48] Jonsson S.K.M., Birgerson J., Crispin X., Greczynski G., Osikowicz W., Danier Van der Gon A.W., Salaneck W.R., Fahlman M., *Synth. Met.*, 2003, 139: 1–10.

[49] Merve I., Pamuk M., Algi F., Onal A.M., Cihaner A., *Chem. Mater.*, 2010, 22: 4034–4044.

[50] Du X., Wang Z., *Electrochim. Acta*, 2003, 48: 1713–1717.

[51] Han D.H., Kim J.W., Su-Moon P., *J. Phys. Chem. B*, 2006, 110: 14874–14880.

[52] Yamato H., Ohwa M., Wernet W., *J. Electroanal. Chem.*, 1995, 397: 163–170.

[53] Han D., Yang G., Song J., Niu L., Ivaska A., *J. Electroanal. Chem.*,2007, 602: 24–28.

[54] Zhou C., Liu Z., Du X., Ringer S.P., *Synth. Met.*, 2010, 160: 1636–1641.

[55] Morikita T., Yamamoto T., *J. Organomet. Chem.*, 2001, 637: 809–812.

[56] Wen Y., Jingkun X., Haohua H., Baoyang L., Yuzhen L, Dong B., *J. Electroanal. Chem.* 2009, 634: 49–58.

CHAPTER 4

Fabrication of Electrochromic Devices based on Electropolymerized PEDOT-Ions Enriched Graphene Film

4.1. Introduction

Graphene, a single layer of two-dimensional honeycomb structure of carbon atom has recently attracted interest because of its remarkable electrical, thermal, and mechanical properties [1−3]. This single-atom-thick sheet of carbon atoms is the thinnest, strongest, and stiffest material, as well as being an excellent conductor of both heat and electricity [4–7]. Moreover, inexpensive sources of graphene (graphite) will allow its use as potential candidate for energy storage [8,9], photovoltaic devices [10,11], field effect transistors [12−14], memory devices [15,16], and optoelectronics applications [17,18]. Efforts are concentrated on producing graphene sheets in a controlled and accessible manner, to emphasize its wide range of unique properties and applications.

Mechanically exfoliated graphene films exhibit high quality but are not suitable for large-scale production [19,20]. Recently, chemical vapour deposition (CVD) methods have been shown to be capable of growing large area graphene sheets in highly transparent and conducting films [21−23]. However, more effort is required for reducing production costs using sophisticated process conditions and inexpensive substrates. Reduced graphene oxide derived from chemical exfoliation has received much attention because of its advantages of low-cost solution-processed fabrication [24−27]. Nevertheless, the oxidation process damages the honeycomb structure of grapheme, and requires a very high temperature to improve/modify the graphene structures [28−30]. Several other exfoliation methods, for example, liquid phase exfoliation, intercalation, and expansion of graphite have been reported by different research groups [31−34]. We have chosen electrochemical exfoliation because of its specific unique properties, such as low toxicity, high chemical and thermal stability, and facile synthesis, which maintain the graphene honeycomb structure, with high transparency and good conductivity [35]. Lui et al. synthesized ionic liquid functionalized graphene with conductivity of 13.84 S m^{-1} directly from graphite using one-step electrochemical route [36]. The incorporation of electrochemically exfoliated graphene into poly(3,4-

ethylenedioxythiophene) (PEDOT) showed high electrochemical activity, ionic/electric conduction, and better electrochromic properties [37].

PEDOT has been extensively used in many potential applications for organic optoelectronic devices [39–41], photovoltaic [42,43], sensors [44,45], batteries [46], actuators [47], biomedical devices [48,49], anti-corrosion devices [50,51], electrochromic windows [52–54], and light emitting diodes [55], because of its good conductivity, high transparency, good thermal stability, and moderate band gap [56]. However PEDOT has several limitations to be considered for some electrical and optical applications due to its reduced conductivity with long time usage, high optical band gap, slow response time, and poor mechanical properties. Conducting polymer nanocomposite with graphene could improve such limitations and might be used in many potential applications in electronic and optoelectronic devices where high electrical conductivity, fast response, and good transparency are the most critical requirements [57]. The conductivity and thermal stability of the composite of polystyrene sulfonic acid (PSS) and graphene-PEDOT is increased compared with that of PEDOT:PSS [58]. Recently graphene/conducting polymer composites have been studied for other potential applications, e.g., transparent electrodes, supercapacitors, and organic solar cells [59–61].

In this chapter, a supporting electrolyte based on lithium perchlorate has been functionalized with graphene (Ions Enriched Graphene, IEGR) by a facile electrochemical exfoliation of graphite rods in aq. $LiClO_4$ solution. Poly(3,4-ethylenedioxythiophene) (PEDOT)-IEGR films were prepared using electropolymerization of EDOT with as-prepared IEGR as the supporting electrolyte in ethanol using a constant potential method. The effect of incorporation of IEGR on the morphological, electrochemical and electrochromic properties of PEDOT- IEGR films were studied. Moreover, electrochromic devices (ECDs) such as electrochromic window and rear-view mirror were fabricated and characterized.

4.2. Preparation of Ions Enriched Graphene (IEGR)

Two graphite rods of 5 mm diameter and approximately 4 cm length were partially immersed in a solution containing 1 g of $LiClO_4$ and 10 ml of distilled water in a 25 ml beaker. A dc potential of 16 V was continuously applied to the graphite rods, and the rods were subjected to continuous corrosion at room temperature for 6 h. The resulting black-brown colloid was

subjected to centrifugation at ~1200–1500 rpm and washing with isopropanol to remove the superfluous ionic liquid until pure IEGR was formed.

4.3. Electropolymerization of PEDOT-IEGR Film

An electrolytic solution of 0.01 g of prepared IEGR with 0.1 M EDOT in 10 mL of ethanol was used for electropolymerization PEDOT- IEGR films. The solution was ultrasonicated for 2 h prior to use. A three electrode system with a platinum foil as a counter electrode, a non-aqueous Ag/AgNO$_3$ (in acetonitrile, ACN) electrode as the reference electrode and an ITO coated glass substrate was used as the working electrode for film deposition. A constant potential of 1.5 V was applied to the working electrode for 200 s at room temperature. The resulting blackish-blue films of PEDOT- IEGR were immediately rinsed with ethanol and dried at room temperature. The relative current with time for oxidative polymerization of EDOT with IEGR in ethanol solution at a constant potential of 1.5 V is shown in Figure 4.1a. There is a small reduction in relative current at short times, which is followed by a constant increase in current with time. This may be due to the oxidation of monomer occurring while applying static potentials initially. Thereafter the current increased due to the deposition of a PEDOT-IEGR film on the working electrode. A schematic representation of IEGR on PEDOT layers is shown in Figure 4.1b.
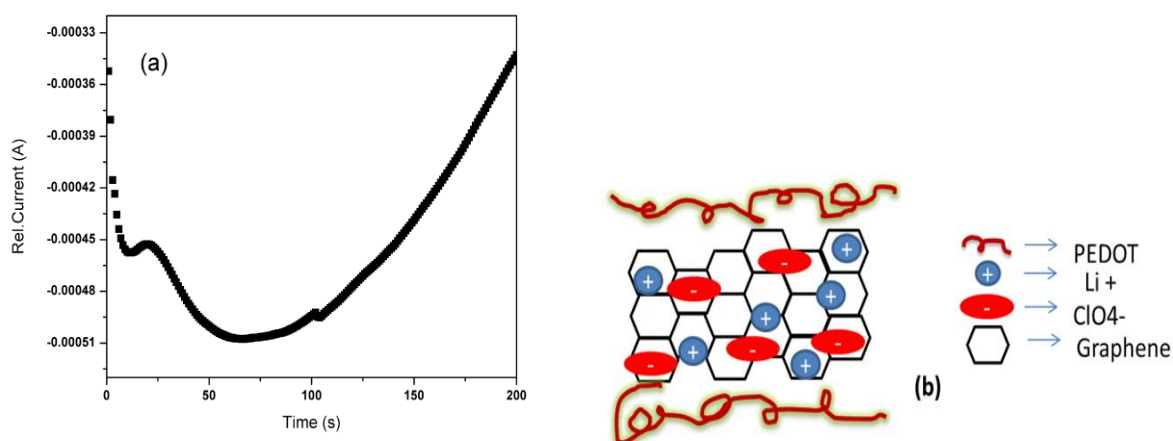
Figure 4.1: (a) Relative current - time plot for oxidative electropolymerization of EDOT with IEGR; and (b) schematic representation of ions enriched functionalized graphene on PEDOT layers.

4.4. Results and Analysis

4.4.1. Raman Spectroscopy

The Raman studies of IEGR powder and PEDOT-IEGR films were carried out in the wavenumber range of 400 to 4000 cm^{-1}, as shown in Figure 4.2 a & b, respectively. The carbon molecules show their fingerprints under Raman spectroscopy mostly by *D*, and *2D* peaks around 1360, 1590, and 2710 cm^{-1}, respectively due to the change in electron bands. In Figure 4.2a & b, the peaks at 1360 and 1365 cm^{-1} (*D*) result from the presence of disordered sp^3 hybridized atomic arrangements or defects/impurities in carbon materials. A low defect-related *D* peak indicates that the graphene incorporated polymer films are of good crystalline quality. The Raman spectra of bulk IEGR shows two characteristic peaks at 1590 cm^{-1} (*G*) and 2710 cm^{-1} (*2D*). These peaks are associated to the doubly-degenerate E_{2g} vibrational mode of sp^2 bonded carbon and second-order vibration by the Raman scattering of photons at the zone boundary. The intensity of the *2D* peak is related to the stacking order/layer number. The low-intensity *2D* peak is attributed to the presence of graphene as a multilayer. The most intense peak at 1452 cm^{-1} observed only in PEDOT-IEGR films (Figure 4.2b) corresponds to the symmetrical stretching of $C_\alpha = C_\beta$ present in the PEDOT molecules [61−63].
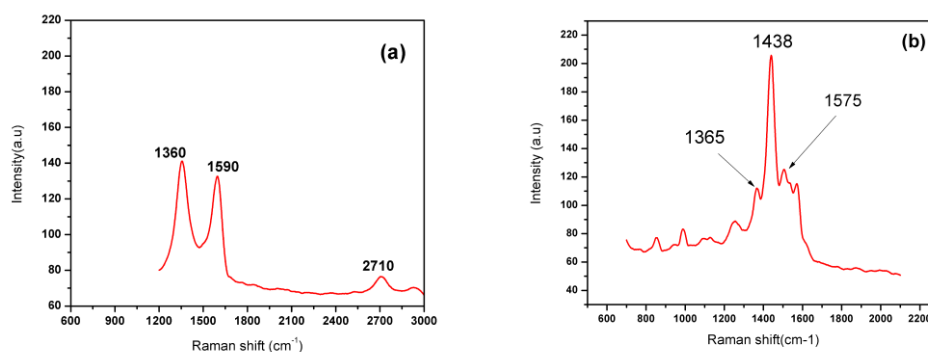
Figure 4.2: Raman spectra of (a) exfoliated IEGR powder and (b) electropolymerized PEDOT- IEGR film.

4.4.2 X-ray Photoelectron Spectroscopy (XPS)

XPS studies of PEDOT- IEGR film were conducted for elemental analysis and to identify the incorporation of anions/cations in graphene on polymer matrix. The deconvoluted C1s, O1s, and S2p core level spectra of PEDOT- IEGR are presented in Figure 4.3 a–c, respectively. The C1s core level spectrum of PEDOT- IEGR is deconvoluted into three peaks at 284.1,

285.4, and 287.6 eV that can be assigned to the C-C bond in the graphene/PEDOT chain, C-S from sulphur in the PEDOT ring, and the C-O-C bond of PEDOT molecules respectively.
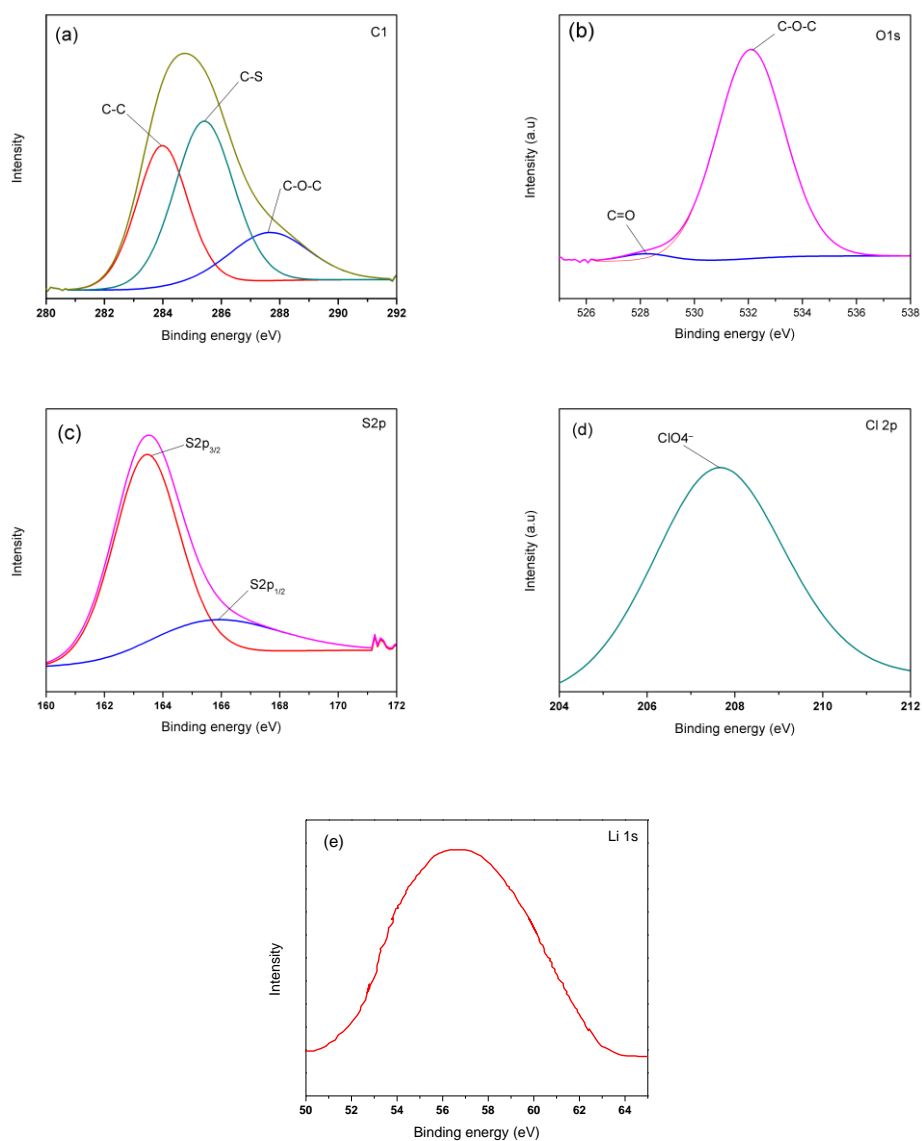
Figure 4.3: Deconvoluted XPS core level spectra of (a) C1s, (b) O1s, (c) S2p, (d) Cl 2p, and (e) Li 1s of PEDOT- IEGR film.

The O1s core spectra of PEDOT-IEGR are split into two peaks at 532.10 and 528.12 eV, corresponding to the C-O-C from PEDOT/Graphene and C=O of graphene sheets, respectively. The intensity of the C=O peak in graphene is very low, which may be explained by the lower oxidation of graphene with water. The core level S2p spectra of PEDOT-IEGR shows the contribution of the $Sp^{3/2}$ and $Sp^{1/2}$ spin-spin doublet observed at 163.48 and 165.84 eV respectively, with an energy difference of ~ 2.36 eV [64–66]. The core level spectra of

chlorine, 'Cl' at 207.65 eV is shown in Figure 4.3d. The 'Cl' originates from the perchlorate anions (ClO_4^-) of the ion entrapped by the inter gap between graphene layers [67]. The core level spectrum of Li 1s appears at 56 eV, as shown in Figure 4.3e. The spectrum shows broadening towards higher binding energy and is shifted by about 1 eV to the higher energy side compared to that of pure Li metal. This shift may be due to the environment of graphene network system [68].

4.4.3. Scanning Electron Microscopy
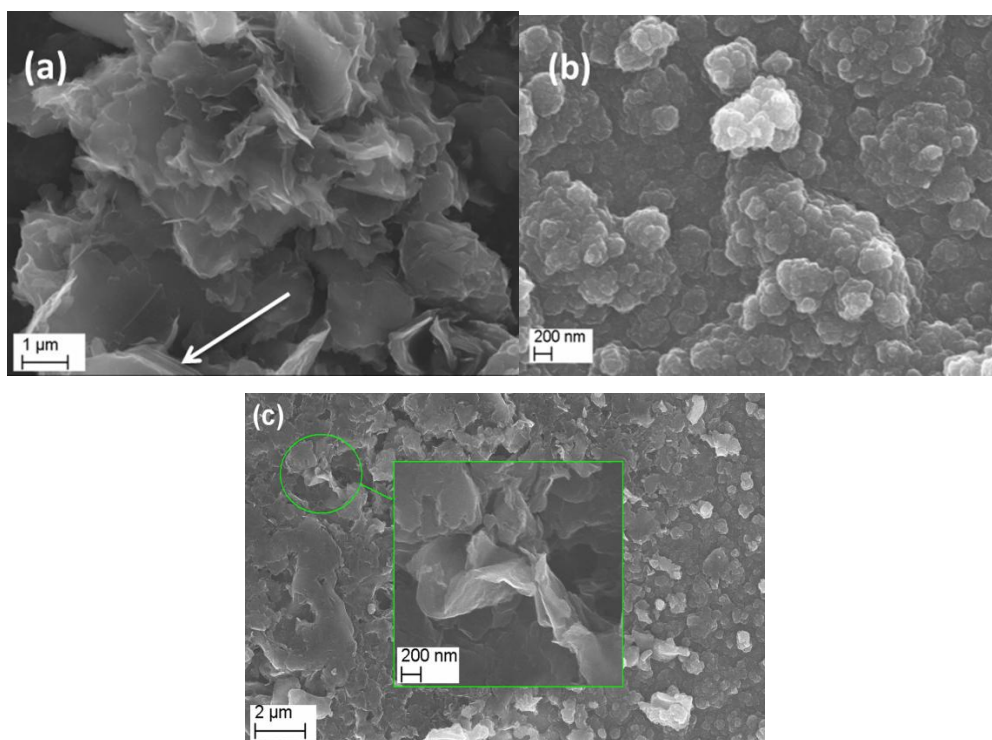
Figure 4.4: SEM images of (a) IEGR powder (arrow shows the multi sheets of graphene), (b) PEDOT film, and (c) PEDOT-IEGR film; Inset shows a magnified view of the foils.

The surface morphological properties of IEGR (powder), PEDOT, and PEDOT-IEGR films were studied by SEM analysis. The SEM images of IEGR appeared as thin foils and flakes of nanometer size. The IEGR layers also appear to be stacked one over the other, and the peripheries are crumpled as highlighted by the arrow in Figure 4.4a. Pure PEDOT (prepared without IEGR) shows that the particles are agglomerated and appear as flower/cauliflower like structures (Figure 4.4b). After the incorporation of IEGR into PEDOT, we see the presence of interconnected grains as well as stacked graphene layers (~500 nm) on the

polymer surface (Figure 4.4c). At higher magnification, the PEDOT-IEGR film showed the presence of lengthy foils a few micrometers in size with rippled edges. The SEM images of PEDOT-IEGR films show good evidence for the incorporation of graphene layers into PEDOT films [69, 70].

4.4.4. Cyclic Voltammetry

The redox properties of PEDOT-IEGR film were studied by cyclic voltammetry at applied potential between −1.0 and +1.2 V in 0.1 M of tetra butyl ammonium perchlorate (TBAP)/ACN solution as shown in Figure 4.5a. A sharp reduction and oxidation peak at around −0.35 and 0.2 V respectively, although there was an anodic shift of the oxidation peak with increasing scan rate, was observed. A weak shoulder appears at +0.21 V in the voltammogram, which corresponds to cation extraction from the polymer film.
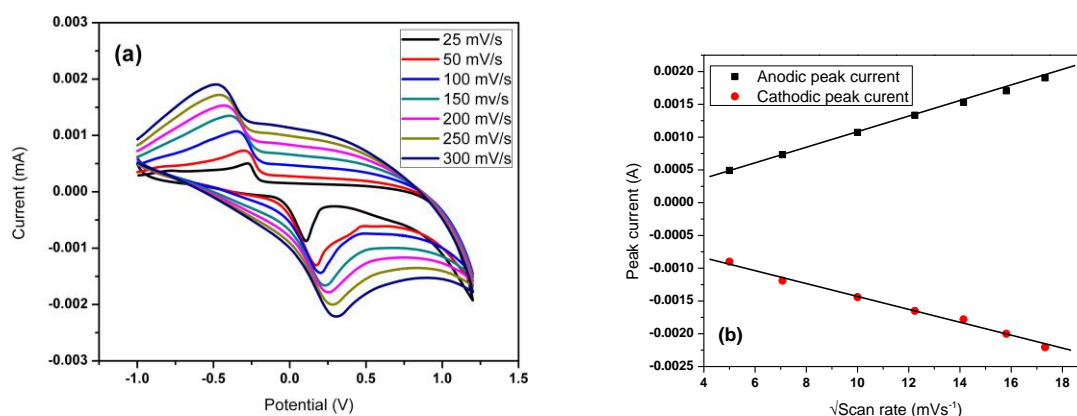
Figure 4.5: Cyclic voltammogram of (a) PEDOT-IEGR film at different scan rates and (b) scan rate dependence of anodic and cathodic peak currents.

The peak currents dependence on the square root of scan rate (Figure 4.5b) indicates the formation of a well-adhered electroactive PEDOT-IEGR film on the working electrode. The peak current increases with an increase in the square root of the scanning rate, indicating that the electrochemical processes are diffusion-limited and quasi-reversible. The diffusion coefficient (D) was calculated to be 1.5867×10^{-14} $cm^2 s^{-1}$ from the CV curve (in TBAP/ ACN medium at a scan rate of 100 mVs^{-1}) using the Randles-Sevcik equation, which is close to the value reported by Deepa et al. [37]. The PEDOT-IEGR films showed significantly higher diffusion coefficients, which are attributed to the facile ion transport in the PEDOT-IEGR films during the redox reactions.

4.4.5. Four Probe Conductivity Studies

Figure 4.6 shows the I-V characteristics curves of PEDOT-IEGR films. The resistance of the PEDOT-IEGR films (~12.6 Ω cm^{-1}) was reduced after the incorporation of graphene into the PEDOT matrix. This enhances their conductivity and ion transport through the polymer. The conductivity of the PEDOT-IEGR film was measured as ~3970 Scm^{-1} which is excellent and higher than those given in recent reports [71–72]. The increased conductivity is believed to result from a conformation change in PEDOT-IEGR. This conformation change enhances the inter-chain separation of polymer layers and provides faster diffusion of the counter ion during the redox process. Due to the presence of graphene in the PEDOT matrix, a conductive network structure is formed by interaction between PEDOT molecules and the two-dimensional honeycomb structure of graphene. This is because of strong covalent bonding and attractive van der Waals forces between PEDOT and grapheme, resulting in more rapid conduction in PEDOT-ILFG.
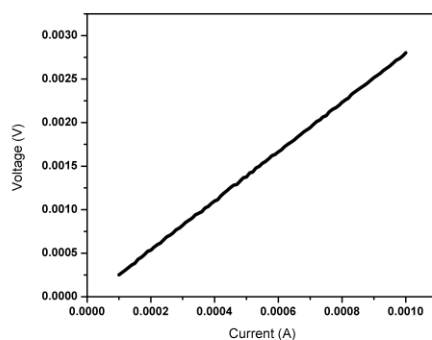
Figure 4.6: The I-V characteristic curve of PEDO-IEGR film.

4.4.6. Electrochemical Impedance Spectroscopy

The electrochemical impedance spectra of PEDOT and PEDOT-IEGR film was studied at 1.0 V in 0.1M TBAP/ACN solution. The relation between the real (Z') and the imaginary (Z") impedance of PEDOT and PEDOT-IEGR films at frequency range of 10^5–1 Hz is shown in Figure 4.7 a, & b, respectively. An unfinished semicircle with high resistance was observed for PEDOT film in the high frequency region. A semicircle at high frequency, followed by a vertical line of 45$^°$ angle at low frequency, was observed for PEDOT-IEGR film. The semicircle present at high frequencies has been considered to be due to the charge-transfer process between the polymer surface and the ionic electrolyte. At low frequencies, the diffusion of charge in the polymer dominates, and a slope of 45$^°$ shows the good capacitance behaviour of the PEDOT-IEGR system. The difference in the real part of the impedance

between high and low frequencies can be used to calculate the charge transfer resistance associated within the material. These are about 4500 $\Omega.cm^{-2}$ and 200 $\Omega.cm^{-2}$ for PEDOT and PEDOT-IEGR [73,74]. The low resistance of PEDOT-IEGR results from the high electrical conductivity of the system, which is clear evidence of the role of graphene nanosheets in facilitating electron/charge transport throughout the films.
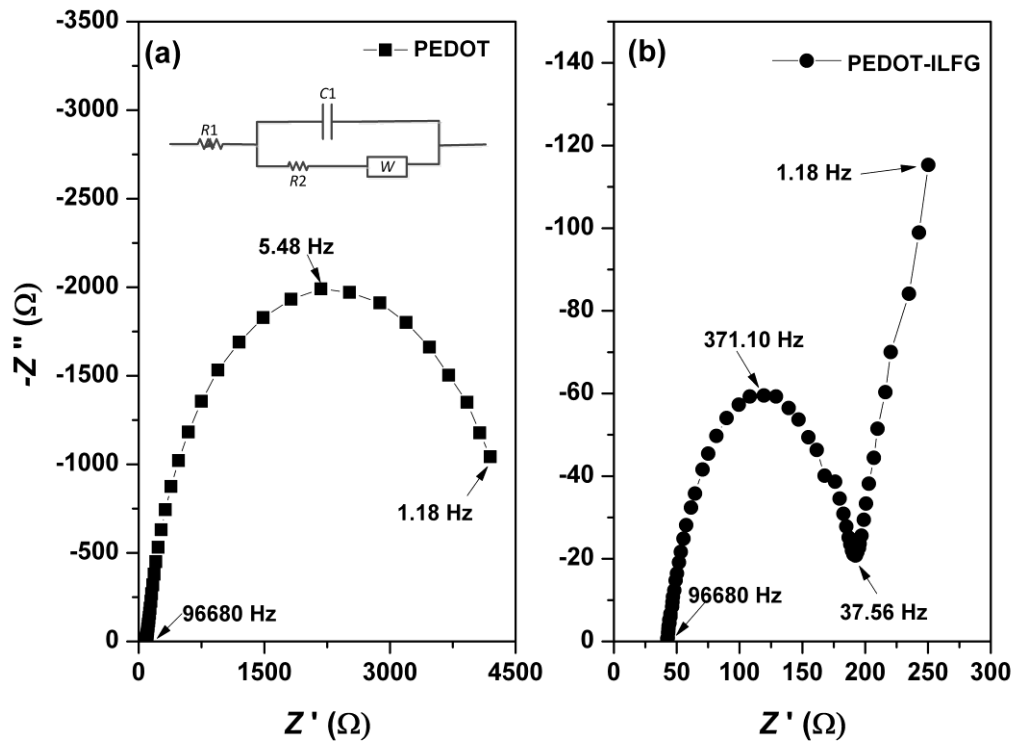
Figure 4.7: Electrochemical impedance spectra of (a) PEDOT and (b) PEDOT-IEGR film in 0.1 M TBAP/ACN solution with corresponding freequencies. Inset: Equivalent circuit of PEDOT and PEDOT-IEGR films.

An equivalent circuit of four elements represented in Figure 4.7a (inset) was used to simulate the impedance properties of PEDOT-IEGR and PEDOT film in 0.1M TBAP/ACN electrolyte medium. The $R1$ represents the electrolyte resistance, which depends on the ionic strength of the electrolyte solution. The parallel connection of $C1$ and $R2$ represent the impedance of the pores; $C1$ is the bulk electronic capacitance and $R2$ is the pore resistance. W is the Warburg impedance resulting from the mass transfer from the bulk electrolyte to the electrode interface. The ionic conductivity of the film was calculated to be 3.125 10^{-7} Scm^{-1} using the following equation:

$$\text{Ionic Conductivity, } \sigma = d/R_{ct}.A \tag{3.1}$$

where d is the thickness of the film, R_{ct} is the charge-transfer resistance, and A is the film area. Electrochemical impedance measurements show that the charge transfer resistance, R_{ct} of PEDOT-IEGR films is low compared to that of conventional PEDOT [75].

4.4.7. Spectroelectrochemistry

A series of UV-Vis absorbance spectra of PEDOT-IEGR film as a function of applied potential (−1.5 to +1.2 V) in 0.1 M of TBAP/ACN solution is shown in Figure 4.8a. The intensity of the absorption peak increased progressively as the reduction potential was raised from −0.2 to −1.5 V. At fully reduced state (−1.5 V), a strong, broad absorption peak was observed corresponding to $\pi-\pi^*$ transitions in the visible region, indicating the neutralization of bipolarons and the formation of reduced polymer with a blackish-grey color.
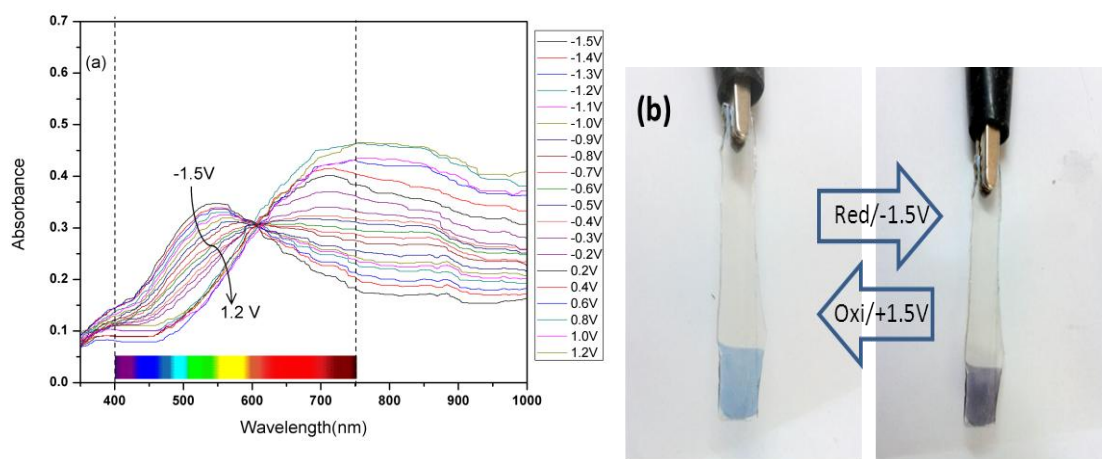
Figure 4.8: Spectroelectrochemistry of PEDOT-IEGR film (a) as a function of various applied potentials from −1.5 V to 1.2 V in 0.1 M TBAP/ACN solution, and (b) photographs of PEDOT-IEGR film in the reduced and oxidized states.

During stepwise oxidation of the polymer film, the absorbance due to the $\pi-\pi^*$ transition decreases in the visible region, and the peak due to polarons increases in the near IR region (800–1200 nm). In the fully oxidized state, a peak due to bipolaronic absorption was observed, which allows a significant transmissive color in the visible region. The PEDOT-IEGR film showed a good optical response in both the visible and NIR regions. The spectroelectrochemistry showed that IEGR influenced the optical absorption spectra of PEDOT by altering its electrochromic coloration from highly absorptive blackish-grey (reduced) to pale/transmissive blue (oxidized), as shown in Figure 4.8b. From the absorption spectra, an optical band gap of the PEDOT-IEGR film can be calculated to range from 1.58

eV to 2.75 eV in the fully reduced (−1.5 V) and oxidized (−1.2 V) states respectively. This shows the formation of different HOMO and LUMO energy levels, resulting in the possibility of tuning colors at different potentials.

4.4.8. Optical Switching Stability

The electrochromic switching properties of PEDOT-IEGR films were studied at λ_{max} of 485 nm to measure color contrast, response times, and coloration efficiency. Figure 4.9a shows the optical color contrast of the PEDOT-IEGR film in its fully reduced (−1.0 V) and oxidized (+1.0 V) states. The color contrast calculated from the difference in percentage transmission (%T) between the completely reduced and oxidized states of PEDOT-IEGR film was 25% at λ_{max} of 485 nm (film thickness about 100–150 nm), which is reasonable for electrochromic device applications [76]. However, the contrast ratio of the film can be increased further by increasing the thickness of the EC film [77].
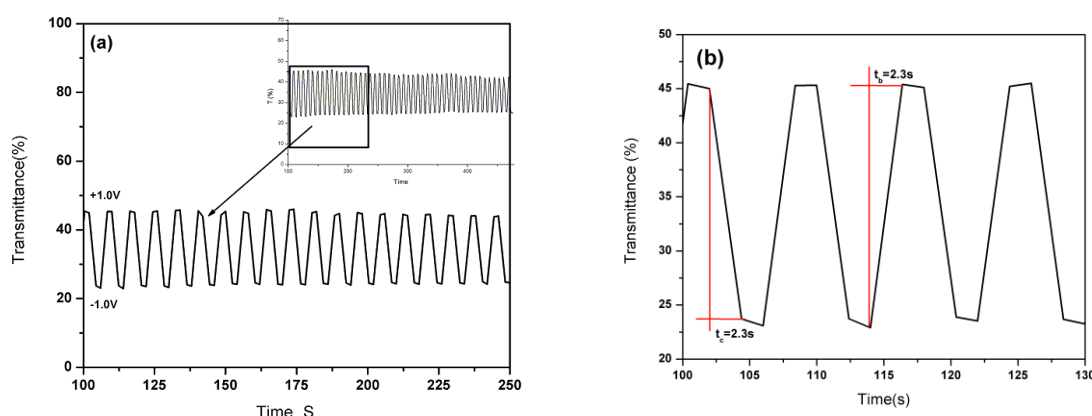
Figure 4.9: (a) The optical switching studies for PEDOT-IEGR film was stepped between its fully reduced (−1.0 V) and oxidized (1.0 V) states at λ_{max} of 485 nm in 0.1 M TBAP/ACN solution (Inset: 100 times switching of PEDOT-IEGR film); (b) Calculation of response time while switching from bleached to colored states and vice versa at 485 nm.

The bleaching and coloring time were almost same at 2.3 s (Figure 4.9b). The coloration efficiency of the films was calculated at ~30 cm^{2}C^{-1} at 485 nm. The optical switching stability of the PEDOT-IEGR film was observed between the application of a square wave potential of −1.0 V and +1.0 V using a pulse width of 4 s. The polymer film was stable even after 500 cycles. A loss of electrochromic color contrast of only <5% was observed after 500 cycles, when the response time increased by 0.12 s. The electrochemical redox stability of PEDOT-IEGR film was studied using cyclic voltammetry in 0.1 M TBAP/ACN solution at

applied potential between −1.0 V and +1.0 V is shown in Figure 4.10. The significant redox stability of PEDOT-IEGR film was retained over 500 cycles that reveals PEDOT-IEGR has better long-time electrochemical stability.
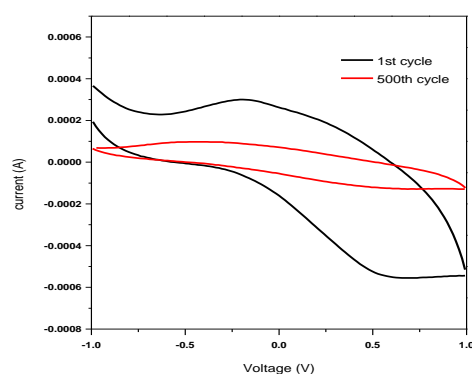
Figure 4.10: The electrochemical redox stability of PEDOT-IEGR film in 0.1 M TBAP/ACN solution at applied potential between −1.0 V and +1.0 V at a scan rate of 100 mVs^{-1}.

4.4.9. Open Circuit Memory
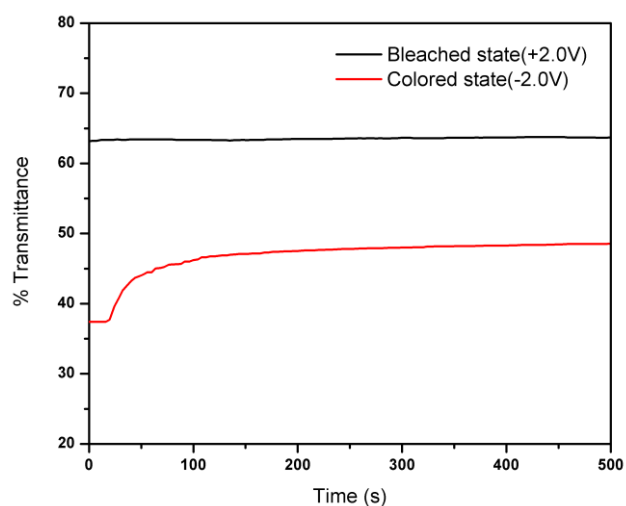
Figure 4.11: Open circuit memory of PEDOT-IEGR film monitored at 485 nm.

The open circuit memory of PEDOT-IEGR film was monitored at λ_{max} of 485 nm as a function of time under open circuit conditions as shown in Figure 4.11. Potentials of −2.0 V and +2.0 V were applied to a PEDO-IEGR film for 30 s to stabilize the color, following which the circuit potential was opened to 500 s. The PEDOT-IEGR film in the oxidized state

showed more stability and a very high optical memory without any change in %T under applied potential or open circuit conditions. In the reduced state, there was a small degradation of color after an open-circuit period for 30 s; however this could be overcome by applying a negative potential to recover the fully colored state. The film had good stability and constant optical memory over long time.

4.5. Performance Testing of Electrochromic Window

4.5.1. Spectroelectrochemistry

The spectroelectrochemical characteristics of PEDOT-IEGR based electrochromic window (ECW)was studied by absorbance changes as a function of different applied potentials are shown in Figure 4.12 (a).This EC window showed almost similar characteristic properties of PEDOT-IEGR film as discussed earlier. At −2.0 V, the electrochromic layer reached the fully reduced stage and maximum absorption peak was observed at 485 nm, this being due to the π–π* inter band transition of the EC layer present in ECW. Upon step wise oxidation of the device, the absorbance due to π–π* transition tends to decrease in the visible region and a new peak was formed towards higher wavelength region. At fully oxidized state (+2.0 V), the peak at the visible region was fully diminished and a broad peak was observed near the IR region because of polaronic-bipolaronic (charge carriers) transitions, this resulting in a high level of transmittance to the human eye. The transmittance spectra of ECW at fully colored (−2.0 V) and bleached (+2.0 V) states are shown in Figure 4.12 (b). The color contrast was calculated to be ~30% T between applied potentials at 485 nm.

The color coordinates of the electrochromic windows based on PEDOT-IEGR and PEDOT films were studied by CIELAB 1986 (l*a*b*) method, and plotted as shown in Figure 4.13a. In the colored state, both devices showed color coordinates in the +a* and −b* quadrant,whereas bleached state is in the −a* and −b* quadrant. However, we noticed that the color coordinate of PEDOT-IEGR based device at the colored stage was shifted to greyish purple region while compared with the PEDOT device, which provides a darker and better absorption to the PEDOT-IEGR device in the visible region. The photograph of the PEDOT-IEGR based window at colored (−2.0 V) and bleached (+2.0 V) states is shown in Figure 4.13b.
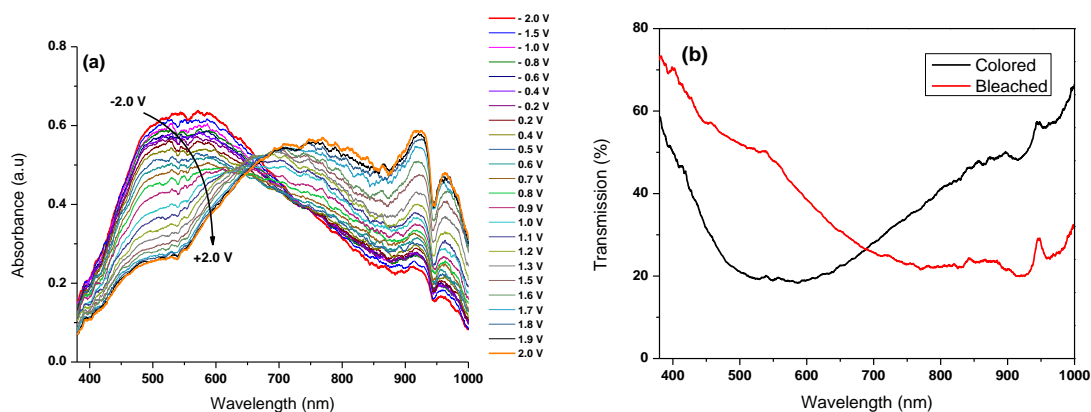
Figure 4.12: (a) Spectroelectrochemistry of PEDOT-IEGR based ECW as a function of various applied potentials, and (b) Transmittance spectra of ECW at colored (−2.0 V) and bleached (+2.0 V) states.
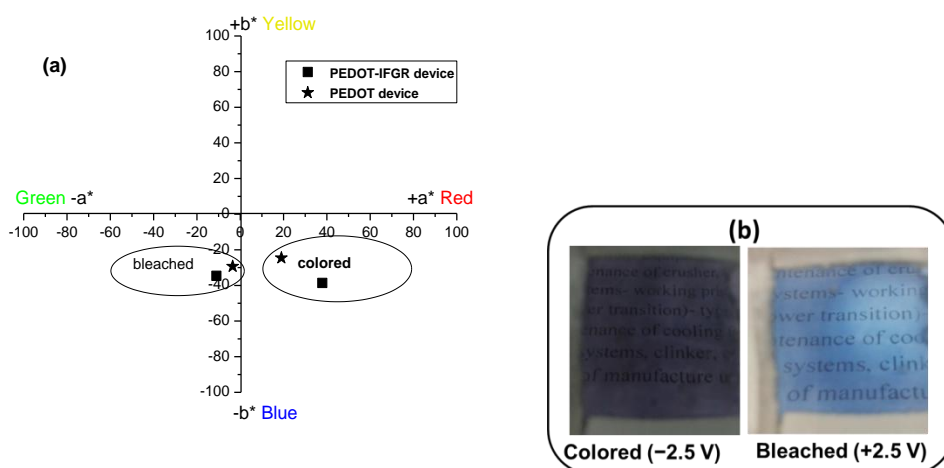
Figure 4.13: (a) CIE1986 a*b* plot showing the color coordinates of PEDOT-IEGR and PEDOT based windows and (b) photograph of PEDOT-IEGR based ECW at colored and bleached states under applied potentials.

4.5.2. Optical Switching

The optical switching properties of the PEDOT-IEGR based electrochromic window were studied by a change in transmittance as a function of time at λ_{max} of 485 nm during applied square-wave potentials at a regular interval of 10 s. The transmission (%) versus time properties of ECW as a function of applied redox potential and its corresponding cyclic current response monitored at 485 nm and 980 nm are shown in Figure 4.14 a&b, respectively.
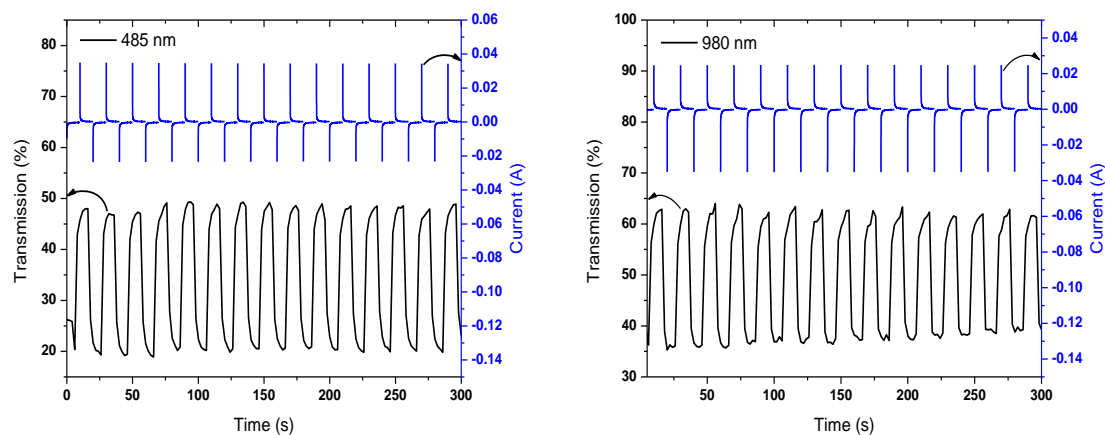
Figure 4.14: Electrochromic switching response and corresponding cyclic current stability of electrochromic window based on PEDOT-IEGR films were monitored at λ_{max} of (a) 485 nm and (b) 900 nm as a function of applied potential between −2.5 V and +2.5 V at a regular interval of 10 s.

This EC window is shown to have a highly stable cyclic current response without any destruction over 500 cycles under applied potential. It was noted that ECW shows excellent optical switching stability over a period of testing without much reduction of % transmittance under a redox switching potential. The color contrast of the window showed ~30% T at 485 nm with response times of 2.0 and 2.5 for bleaching and coloration respectively. This ECW also showed a good color contrast about 30% T near the IR region (950 nm). The bleaching and coloration time was about ~2.0 s and ~2.2 s respectively. The coloration efficiency of ECW was found to be 108 cm^2C^{-1} at 900 nm in the fully reduced state.

4.5.3. Open Circuit Memory and Electrochemical Long-term Stability

The open circuit memory of the PEDOT-IEGR based electrochromic window was monitored at 485 nm as a function of time by applying potential between ± 2.5 V for 30 s and then opened the circuit to 300 s as shown in Figure 4.15a. This electrochromic window showed a small deviation in % transmittance (<4–6%) when the circuit was opened, and, thereafter, the device showed a stable optical memory at bleached and colored states up to 300 s. The electrochemical redox stability of ECW was studied using cyclic voltammetry by applying a potential between −2.5 and +2.5 V with a scan rate of 250 mVs^{-1} as shown in Figure 4.15b. After 250 cycles, the electrochemical response of the device was retained and showed better long-term electrochemical stability without much destruction of redox activity.

87
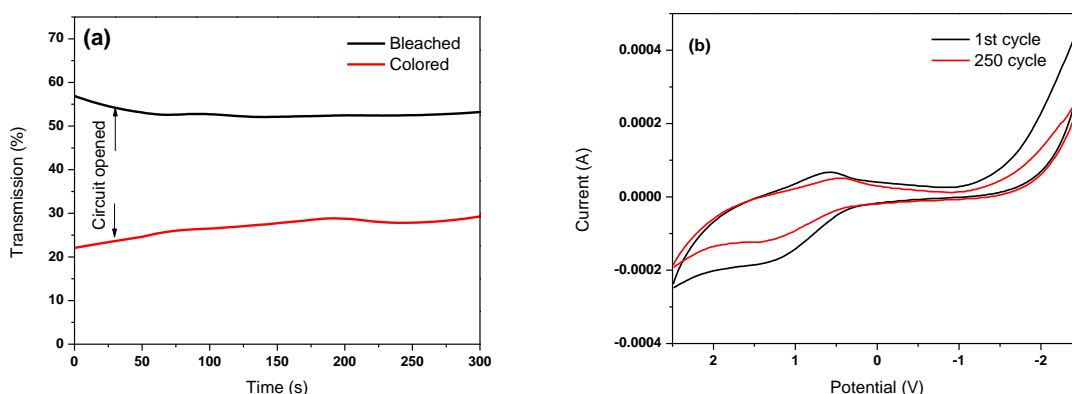
Figure 4.15: (a) Open circuit memory of the PEDOT-IEGR based window monitored at 485 nm at bleached and colored states, and (b) Long term redox stability of ECW using cyclic voltammetry as a function of applied potential between −2.5 V and +2.5 V at s scan rate of mVs^{-1}.

4.6. Performance Testing of Electrochromic Rear-view Mirror

4.6.1. Spectroelectrochemistry
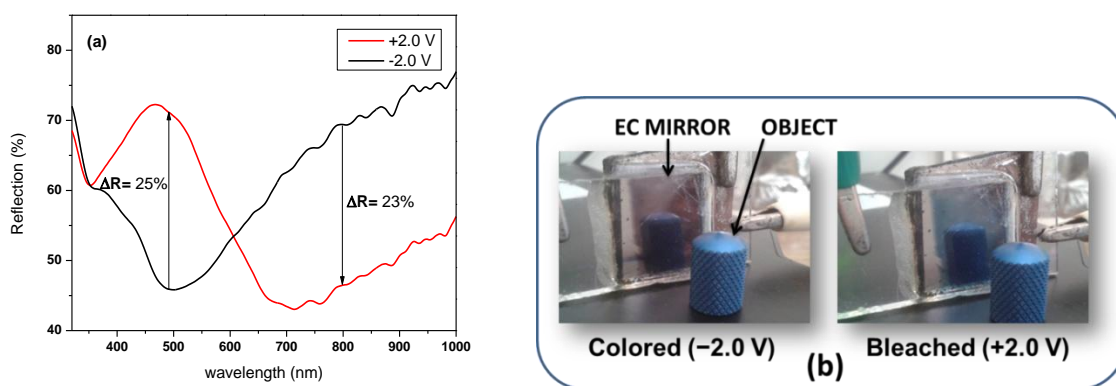
Figure 4.16: (a) The reflection spectra of ECM based on PEDOT-IEGR film at fully reduced and oxidized states, and (b) Photographs of ECM at colored and bleached states (Active area of the device: ~2.5 cm^2)

The spectroelectrochemical properties of electrochromic rear-view mirror (ECM) based on PEDOT-IEGR film was studied by change in reflection as a function of applied potential at +2.0 V and −2.0 V as shown in Figure 4.16a. This ECM showed a significant reflection contrast at the visible and near the IR region. At −2.0 V, a broad absorption was observed at 485 nm due to inter-band π–π* transition. At oxidized state (+2.0 V), the π–π* transition peak

88

was diminished and a new peak was formed due to polaronic transitions at higher wavelength (>750 nm). The reflection contrast was measured as 25% at 485 nm and 23% at 800 nm. At fully oxidized state (+2.0 V), this device showed a ~72% reflection at 485 nm, and that has been shortened to ~45% R at reduced state (−2.0 V). A photograph of the EC mirror at the colored and bleached states is shown in Figure 4.16b.

4.6.2. Optical Switching

The electrochromic switching stability of ECM was studied by measuring the reflection changes as a function of time while applying the redox potential as shown in Figure 4.17a.The reflection contrast (ΔR%) of this ECM measured about 25% R at 485 nm. The ECM showed a significant reflection contrast and good optical stability in visible region. The response time for bleaching and coloring was calculated as ~3.0 s and ~3.5 s respectively. This ECM was performed for more than 500 cycles without much decay of EC colouration and reflection contrast. Figure 4.17b shows the photographs of ECM regulate the reflection of light at colored and bleached states.
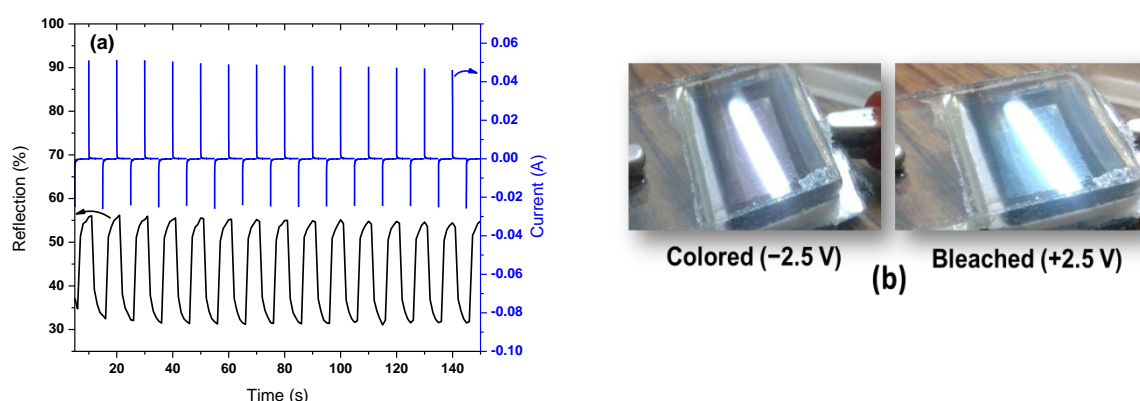
Figure 4.17: (a) The reflection switching stability and cyclic current response of ECM based on PEDOT-IEGR film were monitored at λ_{max} of 485 nm. (b) Photographs of electrochromic mirror regulate the reflection of light at fully colored and bleached states (Active area of the device: ~2.5 cm^2)

4.6.3. Open Circuit Memory and Electrochemical Long-term Stability

The open circuit memory of ECM was studied under open circuit potential condition. Initially, the redox potential was applied to the ECM for 30 s to stabilize the color (or bleach) and the circuit was opened to 300 s as shown in Figure 4.18a. The optical memory of the

device at reduced (colored) and oxidized (bleached) states are highly stable without much decrease in % reflection. However, in the oxidized state, the device showed very small variations in the reflection when the circuit was opened after 30 s. This limitation can be rectified by applying potential at regular intervals. The redox long term switching stability of PEDOT-IEGR based ECM was studied by CV between the applied potential between −2.0 and +2.0 V at a scan rate of 250 mVs^{-1} as shown in Figure 4.18b. The electro-activity of the device was retained after 500 cycles, revealing that ECM has good long term electrochemical stability and excellent electrochemical redox activity.
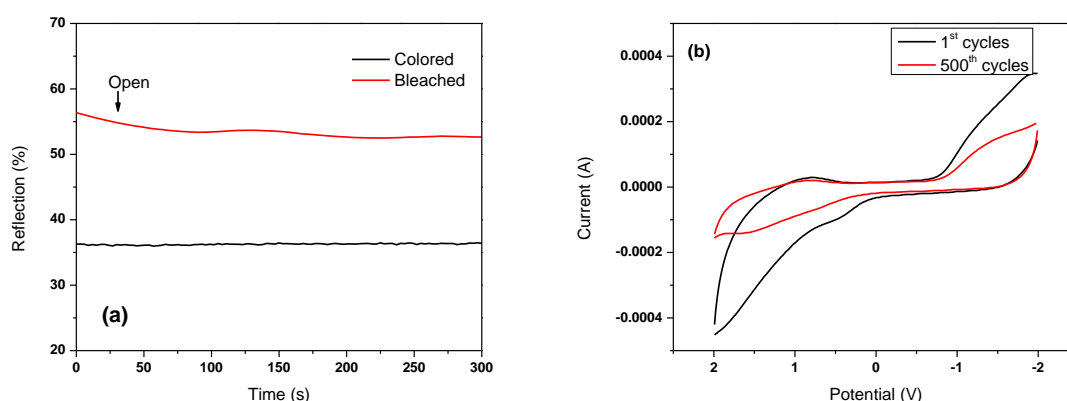
Figure 4.18: (a) The open circuit memory of electrochromic mirror based on PEDOT-IEGR films and (b) Electrochemical cyclic stability of mirror at 1st and 500th cycles.

4.7. Summary

Ions enriched graphene (IEGR) was prepared by simple electrochemical exfoliation of graphite rods in aqueous $LiClO_4$ solution. IEGR was effectively incorporated into a polymer matrix, as was clearly indicated by Raman, XPS, and SEM studies. It was noted that IEGR significantly influenced the electrochemical and optical properties of PEDOT. The PEDOT-IEGR films showed very high electrical conductivity (~3968 Scm^{-1}) and ionic conductivity (3.125×10^{-7} Scm^{-1}). The films had a noteworthy optical response both in the visible and NIR regions. Unlike conventional PEDOT, the electrochromic coloration of the PEDOT-IEGR film changed between greyish purple to transmissive blue. The electrochromic window and mirror based on PEDOT-IEGR films were fabricated and their electrochromic performance was characterized. The ECDs based on the PEDOT with multi-layered graphene provide a faster switching response, better electrochemical activities, good optical stability, low

operation voltage, broad absorption in the entire visible region, and stable optical memory, making it promising material for photovoltaic cells and electrochromic device applications.

4.8. References

[1] Geim A.K., Novoselov K.S., *Nat Mater*., 2007, 6: 183–191.

[2] Novoselov K.S., Geim A.K., Morozov S.V., Jiang D., Zhang Y., Dubonos S.V., Grigorieva I.V., Firsov A.A., *Science*, 2004, 306: 666–669.

[3] Lee C., Wei X.D., Kysar J.W., Hone J., *Science,* 2008, 321: 385–388.

[4] Berger C., Song Z.M., Li X.B., Wu X.S., Brown N., Naud C., Mayou D., Li T.B., Hass J., Marchenkov A.N., Conrad E.H., First P.N., Heer W.A., *Science*, 2006, 312: 1191–1196.

[5] Stankovich S., Dikin D.A., Dommett G.H.B., Kohlhaas K.M., Zimney E.J., Stach E.A., Piner R. D., Nguyen S.T., Ruoff R.S., *Nature*, 2006, 442: 282–286.

[6] Li D., Muller M.B., Gilje S., Kaner R.B., Wallace G.G., *Nat. Nanotechnol*., 2008, 3: 101–105.

[7] Hernandez Y., Nicolosi V., Lotya M., Blighe F.M., Sun Z.Y., De S., McGovern I.T., Holland B., Byrne M., Gunko Y.K., Boland J.J., Niraj P., Duesberg G., Krishnamurthy S., Goodhue R., Hutchison J., Scardaci V., Ferrari A.C., Coleman J. N., *Nat Nanotechnol*., 2008, 3: 563–568.

[8] Wang L., Lee K., Sun Y.Y., Lucking M., Chen Z., Zhao J.J., Zhang S.B., *ACS Nano*, 2009, 3: 2995–3000.

[9] Martin P., *Chem Rec*., 2009, 9: 211–223.

[10] Liu Z., Liu Q., Huang Y., Ma Y., Yin S., Zhang X., Sun W., Chen Y., *Adv Mater*., 2008, 20: 3924–3930.

[11] Gomez De A. L, Zhang Y., Schlenker C.W., Ryu K., Thompson M. E., Zhou C., *ACS Nano*, 2010, 4: 2865–2873.

[12] Li X. L., Wang X. R., Zhang L., Lee S.W., Dai H. J., *Science*, 2008, 319: 1229–1232.

[13] Liao L., Bai J., Lin Y.C., Qu Y., Huang Y., Duan X., *Adv Mater*., 2010, 22: 1941–1945.

[14] Barone V., Hod O., Scuseria G.E., *Nano Lett*., 2006, 6: 2748–2754.

[15] Zhuang X. D, Chen Y., Liu G., Li P.P., Zhu C.X., Kang E.T., Noeh K.G., Zhang B., Zhu J.H., Li Y.X., *Adv Mater*., 2010, 22: 1731–1735.

[16] Gunlycke D., Areshkin D. A., Li J., Mintmire J. W., White C. T., *Nano Lett*., 2007, 7: 3608–3611.

[17]   Chunder A., Pal T., Khondaker S., Zhai L., *J. Phys. Chem C*, 2010, 114:15129–15135.

[18]   Hwang J. O., Lee D. H , Kim J. Y., Han T. H., Kim B. H., Park M., *J. Mater. Chem*, 2011, 21:3432–3437.

[19]   Sutter P. W., Flege J. I., Sutter E. A., *Nat. Mater*, 2008, 7: 406–411.

[20]   Liang X., Fu Z., Chou S. Y., *Nano Lett*., 2007, 7: 3840–3844.

[21]   Reina A., Jia X., Ho J., Nezich D., Son H., Bulovic V., Dresselhaus M.S., Kong J., *Nano Lett*., 2009, 9: 30–35.

[22]   Li X., Cai W., An J., Kim S., Nah J., Yang D., Piner R., Velamakanni A., Jung I., Tutuc E., *Science*, 2009, 324:1312–1314.

[23]   Bae S, Kim H. K ., Lee Y. B., Xu X. F. , Park J. S., Zheng Y., Balakrishnan J., Lei T., Kim H. R, Song Y., *Nat. Nano. technol*., 2010, 5: 574–578.

[24]   Wassei J. K, Kaner R. B., *Mater. Today*, 2010, 13: 52–59.

[25]   Park S., Ruoff R.S., *Nat Nanotechnol*., 2009, 4: 217–224.

[26]   Park S., An J., Jung I., Piner R. D., An S. J, Li X., Velamakanni A., Ruoff R. S., *Nano Lett*., 2009, 9: 1593–1597.

[27]   Chen C. M., Yang Q. H., Yang Y. G., Lv W, Wen Y. F., Hou P. X., Wang M. Z., Cheng H. M., *Adv. Mater*., 2009, 21: 3007–3011.

[28]   Wu X., Sprinkle M., Li X., Ming F., Berger C., de Heer W. A., *Phys. Rev. Lett*., 2008, 101:026801-1–4.

[29]   Stankovich S., Piner R. D., Chen X., Wu N., Nguyen S. T., Ruoff R. S., *J. Mater. Chem*., 2006, 16: 155–158.

[30]   Su C. Y., Xu Y, Zhang W., Zhao J., Tang X., Tsai C.H., Li L. J., *Chem. Mater*., 2009, 21: 5674–5680.

[31]   Biswas S., Drzal L.T., *Nano Lett.*, 2009, 9: 167–172.

[32]   Hernandez Y., Nicolosi V., Lotya M., Blighe F. M., Sun Z., De S., McGovern I. T., Holland B., Byrne M., GunKo Y. K., *Nat. Nanotechnol*., 2008, 3: 563–568.

[33]   Li X., Zhang G., Bai X., Sun X., Wang X., Wang E., Dai H., *Nat. Nanotechnol*., 2008, 3: 538–542.

[34]   Lee J. H., Shin D. W., Makotchenko V. G., Nazarov A. S., Fedorov V. E., Kim Y. H., Choi J. Y., Kim J. M., Yoo J. B., *Adv. Mater*., 2009, 21: 4383–4387.

[35]   Gutowski K. E., Broker G. A., Willauer H. D., Huddleston J.G., Swatloski R. P., Holbrey J. D., Rogers R. D., *J. Am. Chem. Soc*., 2003, 125: 6632–6633.

[36]   Liu N., Luo F., Wu H., Liu Y., Zhang C., Chen J., *Adv. Funct. Mater.*, 2008, 18: 1518–1525.

[37]   Saxena A. P., Deepa M., Joshi A. G., Bhandari S., Avanish K. S., *ACS Appl. Mater. Interfaces*, 2011, 3: 115–1126.

[38]   Meng D., Yang T., Suyan M., Zhao C., Jiao K., *Anal. Chim. Acta*, 2011, 690: 169–174.

[39]   Siju C. R., Rao K.N., Sindhu S., J Opt., 2013, Doi: 10.1007/s12596-012-0113-x.

[40]   Friend R. H., *Pure Appl. Chem.*, 2001, 73 425–430.

[41]   Ouyang J., Chu C. W., Chen F. C., Xu Q., Yang Y., *J. Macromol. Sci. A Pure Appl. Chem.*, 2004, 41: 1497–1511.

[42]   Schmidt-Mende L., Fechtenkotter A., Mullen K., Moons E., Friend R. H., Mackenzie J. D., *Science*, 2001, 293, 1119–1122.

[43]   Liscio A., De Luca G., Nolde F., Palermo V., Meullen K., Samori P. J., *J. Am Chem. Soc.*, 2008, 130: 780–781.

[44]   Lin C. Y., Chen J.G., Hu C.W., Tunney J.J., Ho K.C., *Sens. Actuat*. B, 2009, 140:402–406.

[45]   Kwon O.S., Park E., Kweon O. Y., Park S. J. , Jang J., *Talanta*, 2010, 82: 1338–343.

[46]   Murugan A. V., Gopinath C. S., Vijayamohanan K., *Electrochem. Commun.*, 2005, 7:213–218.

[47]   Okuzakia H., Suzukia H., Itob T., *Synth Met.*, 2009, 159: 2233–2236.

[48]   Nagarajan S., Kumar J., Bruno F. F., Samuelson L. A., Nagarajan R., M*acromolecule*s, 2008, 41: 3049–3052.

[49]   Chikar J. A., Hendricks J. L., Richardson-Burns S. M., Raphael Y., Pfingst B. E., Martin D. C., *Biomaterials*, 2012, 33: 1982–1990.

[50]   Liesa F., Ocampo C., Aleman C., Armelin E., Oliver R., Estrany F., *J. Appl Polym. Sci.*, 2006, 102: 1592–1599.

[51]   Ocampo C., Oliver R., Armelin E., Aleman C., Estrany F., *J Polym Res.*, 2006, 13: 193–200.

[52]   Sindhu S., Rao K.N., Ahuja S., Kumar A., Gopal E.S.R., *Mat. Sci. Eng. B*, 2006, 132 39–42.

[53]   Vergaz R., Barrios D., Pena J.M.S., Marcos C., Pozo C, Pomposo J.A., *Sol. Energ. Mat. Sol. Cells.*, 2008, 92: 107–111.

[54]   Mecerreyes D., Marcilla R., Ochoteco E., Grande H., Pomposo J. A., Vergaz R., Sanchez Pena J.M., *Electrochim. Acta*, 2004, 49: 3555–3559.

[55] Kok M. M., Buechel M., Vulto S. I. E., Weijer P., Meulenkamp E.A., M de Winter S.H. P, Mank A.J.G., Vorstenbosch H.J.M., Weijtens C. H.L, van Elsbergen V., *Phys. Stat. sol. A.*, 2004, 201:1342–1359.

[56] Elschner A., Kirchmeyer S., Lovenich W., Merker U., Reuter K.,.*PEDOT: Principles and Applications of an Intrinsically Conductive polymers*, 1st (ed). CRC Press, London, 2011.

[57] Lewis I.N., *Chem Rev*., 1993, 93: 2693–2730 .

[58] Tarang L.K.H, Tung T.T., Kim T.Y., Yang W.S., Kim H., Suh K.S., *Polym. Int*., 2012, 61:93–98.

[59] Kiyoung J., Lee T., Choi H.J., Park J.H., Lee D.J., Lee D.W., Kim B.S., *Langmuir*, 2011, 27: 2014–2018.

[60] Nanjundan A. K., Hyun J.C., Andreas B., Jong-Beom B., Jeong Y.T., *J Mater Chem*., 2012, 22: 12268–12274.

[61] Xu Y., WangY., Liang J., Huang Y., Ma Y., Wan X., Chen Y., *Nano Res*., 2009, 2: 343–348.

[62] Sakmeche N, Aeiyach S, Aaron JJ, Jouini M, Lacroix JC, Lacaze PC (1999) *Langmuir*, 15: 2566–2574.

[63] Tamburri E., Orlanducci S., Toschi F., Terranova M.L., Passeri D., *Synth Met*., 2009, 159: 406–414.

[64] Du X.S., Yu Z.Z., Dasari A., Ma J., Mo M., Meng Y., Mai Y.W., *Chem Mater*., 2008, 20: 2066–2068.

[65] Yan H., Okuzaki H., *Synth Met*., 2009, 159: 2225–2228.

[66] Wang G.F., Tao X.M., Xin J.H., Fei B., *Nanoscale Res Lett*., 2009, 4: 613–617.

[67] Becerık I., Suzer S., Kadirgan F., *J. Electroanal. Chem*., 2001, 502: 118–125.

[68] Zhi W. S., Haotian W., Po-Chun H., Zhang Q., Weiyang L., Guangyuan Z., Hongbin Y., Yi C., *Energy Environ. Sci*., 2014, 7: 672–676.

[69] Schnyder B., Alliata D., Kotz R., Siegenthaler H., *Appl. Surf. Sci*., 2001, 173:221–232.

[70] Liu N., Luo F., Wu H., Liu Y., Zhang C., Chen J., *Adv. Funct. Mater*., 2008, 18: 1518–1525.

[71] Morkita T., Yamamoto T., *J Organo. Met. Chem*., 2001, 637–639: 809–812.

[72] Xia Y., Sun K., Ouyang J., *Adv. Mater*., 2012, Doi: 0.1002/adma.201104795.

[73] Reyes M.R., Cruz I.C., Sandoval R.L., *J. Phys.Chem C*, 2010, 114: 20220–20224.

[74]   Garreau S., Louarn G., Buisson J.P., Froyer G., Lefrant S., *Macromolecules*, 1999, 32: 6807–6812.

[75]   Hass R., Canadas J.G., Belmonte G.G., *J. Electroanal.Chem.*, 2005, 577: 99–105.

[76]   Tao Y.J., Zhang Z., Xu X., Wang N., Zhou Y.J., Cheng H.F., *Opt. Express*, 2012, 20: 15121–15125 .

[77]   Stefan H., Patrik H., Renee K., Ergang W., Mats R.A., *Org. Electron.*, 2011, 12:1406–1413.

CHAPTER 5

Synthesis and Characterization of Novel Solution-processable Di-isopropylbenzyl Derivative of Poly(3,4 propylenedioxythiophene) Nanobelts for Electrochromic Device applications

5.1. Introduction

Conductive polymers become promising candidates for electrochromic applications such as aircraft and automotive windows [1–4], e-paper [5,6], display devices [7–9], mirrors [10–14], and earth-tone chameleon materials [15,16] owing to their unique properties such as better environmental stability, good processability, low oxidation potential, less weight, and excellent electrochemical and optical properties. However, the biggest challenge of conductive polymers for opto-electronic applications is to change the color between highly transparent and highly opaque state under redox reactions. Design and synthesis of new monomers to enhance the electrochromic properties, are the current topics being studied by various research groups [17–26].

3,4-ethylenedioxythiophene based conjugated polymer and its derivatives have received much attention in EC applications due to its fast response time, good processability, high color contrast, excellent redox stability, better optical memory, and band gap tunability through structural modifications [27–29]. Alkylenedioxy substitution at 3rd and 4th positions of heterocyclic ring donates a π-electron to the heterocyclic ring, and prevents α-α and α-β interactions between the thiophene rings that offer more ordered polymer and low oxidation potential [30,31]. The electron donating nature of substituents present on alkylenedioxy ring has been studied theoretically and electrochemically by Abruna et.al [32]. Conjugated polymers prepared from 3,4 propylenedioxythiophene (ProDOT) exhibit higher color contrast in comparison to polymers from ethylenedioxythiophene (EDOT), which was first reported by Dietrich et al. [33]. The structural modifications of monomer to enhance the EC properties have been systematically studied by Reynolds and co-workers [34, 35]. They observed that EC properties have been enhanced by increasing ring size and incorporation of bulky groups on alkylenedioxy ring, which affects inter-chain spacing between polymer chains, hence better charge transfer at doping. EC properties of monosubstituted and disubstituted ProDOT derivatives have extensively been studied by Kumar et.al [36]. They observed that di-

substituted polymers showed very good EC properties than the corresponding mono substituted polymers. Further fine-tuning of EC coloration can be adjusted by film thickness and redox states to generate all possible colors [37]. Di-benzyl substituted ProDOT (PProDOT-Bz$_2$) was designed and synthesized by A. Kumar group [38], and that showed highest known contrast ratio (89%) reported till date and better stability after 5000 cycles. However, there was no information about the thickness of PProDOT-Bz$_2$ film, since is dependent on contrast ratio [39]. Our research group also studied the EC properties of PProDOT-Bz$_2$ film having thickness of about 250 nm and achieved the color contrast of 64% [40]. Cihaner and his co-workers carried pioneering studies on EC properties of PProDOT-Bz$_2$ film , which showed contrast ratio of 76% [41]. The long alkyl chain derivatives of regiosymmetric di-substituted ProDOT derivatives were soluble in common organic solvents, which enhanced the possibility of solution processable electrochromic materials, however this long alkyl chains substitutions reduce the extent of conjugation length [42].

Chemical synthesis of nanostructured conjugated polymers showed considerable attention in nano-sized sensor, opto-electronics, and energy storage applications [43–45]. In addition, these nanostructured conducting polymers are excellent materials for molecular wire applications due to their one dimensional transport properties and higher conductivity [46]. Most of the researchers have been focused on synthesis of nanostructures using inorganic or organic templates. Recently, PEDOT and polypyrrol nanostructures were synthesized by a hexane/water reverse microemulsion system using sodium bis(2-ethylhexyl) sulfosuccinate (AOT) cylindrical micelles as the template [47,48] and the micelles act as 'nano-reactors' [49]. However, the nanostructures of PProDOT derivatives have not yet been successfully synthesized using reverse micro emulsion system.

Based on these above aspects, we assume that combination of substituent like both rigid (benzyl) and small alkyl (isopropyl) group on propylenedioxy ring can be improved the solubility, and alter the inter chain distance, hence enhanced the intrinsic properties of the material. In this chapter, synthesized and characterization of a new monomer, di-4-isopropyl benzyl ProDOT and preparation of corresponding conjugated polymer by chemical and electrochemical method for the application of electrochromic devices. Chemical polymerization was carried out using a hexane/water reverse microemulsion system using AOT as self-assembling template and FeCl$_3$ as the oxidant. The spectroelectrochemical and electrochromic properties of ProDOT-IPBZ$_2$ films were studied. The effects of

polymerization cycles of the film on electrochemical and optical properties were systematically studied. In addition, a solid state single-type electrochromic window and rear-view mirror based on electropolymerized ProDOT-IPBZ$_2$ film were fabricated without any complementary EC layer and tested for their electrochromic performances. An efficient electrochromic rear-view mirror requires maximum absorption of selective-yellow light, better redox switching stability, excellent optical memory and fast switching response [50]. Synthesized purple/magenta colored ProDOT-IPBZ$_2$ film may absorb its complementary yellow color in wavelength region of 570–600 nm, and its EC rear-view mirror would be highly suitable for maximum absorption of commonly used yellow-orange colored head lamps in automobiles.

5.2. Experimental

5.2.1. Synthesis of 3, 3-Di (4-isopropylbenzyl)-3,4-dihydro-2H-thieno[3,4-b][1,4] dioxepine (ProDOT-IPBz$_2$)
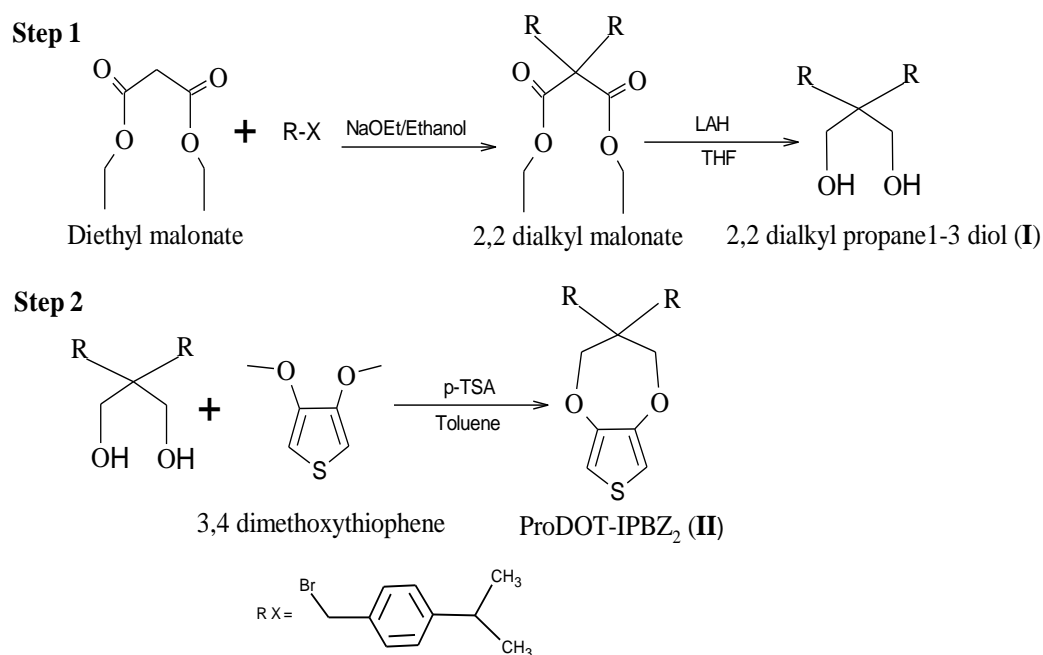
Scheme 5.1: Synthesis route of compound (**I**) and 3, 3-Di (4-isopropylbenzyl)-3,4-dihydro-2H-thieno[3,4-b][1,4] dioxepine(**II**).

The monomer was synthesized from 3,4-dimethoxy thiophene and di-4-isopropyl benzyl substituted propane 1, 3 diol (**I**) in the presence of catalytic amount of p-TSA in dry toluene by trans-etherification route according to previously reported procedure [36]. The preparation of compounds (**I**) and synthesis scheme of monomer (**II**) are shown in Scheme 5.1. The final

product was confirmed by ^{13}C NMR, ^{1}H NMR, and FT-IR spectroscopy. Yield: 81%. **^{13}C NMR** (CDCl$_3$, δ): 23.98, 33.66, 39.19, 45.24, 77.60, 106.18, 126.24, 130.63, 133.82, 147.04, 150.34. **^{1}H NMR:** (400 MHz, CDCl$_3$, δ): 1.29-1.30 (12 H, d, J=4 Hz), 2.86 (4H, s), 2.89–2.98 (2H, m), 3.89 (4H, s), 6.55 (2H, s), 7.20-7.15 (4H, dd, 8Hz), 7.31 (4H, s). **TOF-MS:** calculated for C$_{27}$H$_{32}$O$_2$S (m/z): 420.60; experimentally (M+Na): 443.20. **FT-IR** (KBr, cm^{-1}): 3110, 3012 (aromatic =C-H stretching), 2959, 2870 (aliphatic C-H stretching), 1654 (C=C stretching), 1485 (aromatic C-C stretch), 1376 (aliphatic CH bend), 1194 (C-O-C stretching), 820 (C-S stretching). A broad peak was observed at ~3500 nm due to the moisture presents in the monomer that may provide O-H stretching vibration of surface hydroxyl groups

5.2.2. Electrochemical Polymerization

The electrochemical polymerization of monomer ProDOT-IPBz$_2$ was carried out in a solution containing 10 mM monomer with 0.1 M of tetra butyl ammonium perchlorate (TBAP) in DCM: ACN (1:10 v/v) medium by applying potential between +1.5 V and −1.0 V *vs*. Ag/Ag$^+$ reference electrode at a scan rate of 100 mVs^{-1}. A three electrode system with a platinum foil was used as counter electrode, Ag/AgNO$_3$ electrode as a reference electrode, and ITO coated glass substrate was used as the working electrode. The monomer was electrochemically polymerized using cyclic voltammetry technique at various cycles such as 1, 2, 4, 6, and 8 cycles and respective films were referred to as PProDOT-IPBz$_2$-1, PProDOT-IPBz$_2$-2, PProDOT-IPBz$_2$-4, PProDOT-IPBz$_2$-6, and PProDOT-IPBz$_2$-8. The resulting purple colored polymer film was rinsed with ACN and dried at room temperature. The PProDOT-IPBz$_2$-2 was used for the studies of electrochemical and electrochromic properties of film as well as EC devices in this chapter, unless otherwise specifically mentioned.

5.2.3. Chemical Polymerization

Chemical polymerization of monomer, ProDOT-IPBZ$_2$ was carried out by reverse micro-emulsion method. In this synthesis, a reverse microemulsion is initially prepared by dissolving sodium bis (2-ethyl hexyl) sulfosuccinate, AOT (19.12 mM) in 20 mL of n-hexane in a glass beaker, and then adding 5 mL of aq. FeCl$_3$ solution (6.0 mM) drop wise into the AOT/hexane mixture. The resulting yellowish orange colored solution was gently stirred continuously for two days under room temperature. The polymer mixture was precipitated in methanol and filtered. The precipitated material was again mixed with chloroform, and the polymer reduced by adding excess

hydrazine hydrate. The suspension was allowed to stir for 1 h and again precipitated in methanol. The precipitated polymer was washed with methanol to remove the oligomers, surfactants, and inorganic impurities. Finally, purple colored solid powder was obtained by treatment with chloroform followed by evaporation of the chloroform. The overall synthetic procedure of PProDOT-IPBZ$_2$ nanobelts is presented in Scheme 5.2. **Molecular weight data:** M$_n$: 2835 g/mol, M$_w$: 5595 g/mol and polydispersity index (PDI=M$_w$/M$_n$): 1.97. This lower molecular weight polymer can be enhanced the dissolution rate and hence readily soluble in common organic solvents, resulting easier processing.
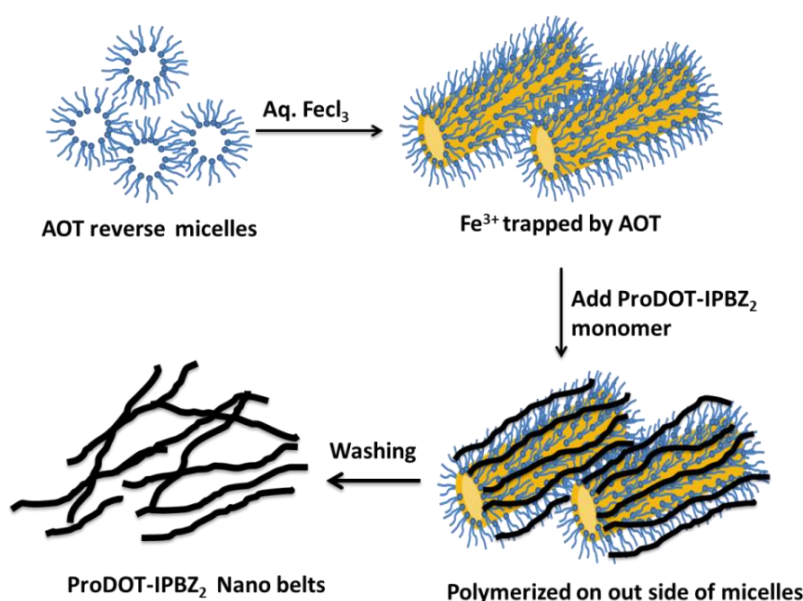
Scheme 5.2: Schematic diagram of the preparation of PProDOT-IPBZ$_2$ nanobelts using AOT reverse cylindrical mircoemulsion polymerization.

5.2.4. Preparation of Solution-processable Films

5.2.4.1. Spray Coating

In spray coating method, a homogenous solution of ProDOT-IPBZ$_2$ polymer in toluene (10 mg/ mL)was prepared and transferred to the cup of spray gun (Air bush, Model: Artmaster). The polymer solution was sprayed through small nozzle (0.3mm) using air compressor at a pressure of 10−15 psi on to clean ITO substrates. The resulting polymer film is uniform and fully covered over the substrate without much agglomeration. The film thickness of this polymer film was found in the range of 75−100 nm. The thickness and uniformity of the film have been optimized by parameters such as pressure (10−15 psi), polymer concentration (5−

10 mg/mL), distance between the substrate and nozzle (about 15–20 cm) and toluene as solvent.

5.2.4.2. Solution Casting

Solution-cast film of ProDOT-IPBZ$_2$ was prepared by dissolving 10 mg of ProDOT-IPBZ$_2$ solid powder in 1 mL of toluene, and two drops of this solution was uniformly placed onto pre-cleaned ITO substrate. The substrate is gently heated at 50-60º C for 2 min and cooled to room temperature. The process was repeated until appropriate thickness was obtained and the film dried at 60–70ºC under vacuum for 2 h. The film thickness of this polymer film was found to be in the range of 150–200 nm.

5.2.5. Fabrication of Electrochromic Devices

The electrochromic window (ECW) and mirror (ECM) were fabricated using electropolymerized PProDOT-IPBz$_2$ films/ITO/glass as electrochromic active electrode, ITO/glass as counter electrode and PMMA based polymer gel (LiClO$_4$:ACN:PMMA:PC in the ratio of 3:70:7:20) as conductive gel electrolyte. For EC rear-view mirror (ECM), an Aluminium (Al) layer was deposited additionally as reflective layer on rear side of ITO layer. All devices were fabricated using PProDOT-IPBz$_2$ layer, as active working electrodes and counter electrodes are sandwiched by polymer gel electrolyte. The gap between the two electrodes is controlled by placing double-side sticker tape (0.5mm) and then the devices sealed with acrylic resin. Finally, the gel electrolyte is injected into the device without any air bubbles. The ECW and ECM were assembled with the configuration of Glass/ITO/Gel electrolyte/PProDOT-IPBz$_2$/ITO/Glass and Al/Glass/ITO/Gel electrolyte/ PProDOT-IPBz$_2$/ITO/Glass, respectively.

5.3. Results and Analysis

5.3.1. Electrochemical Polymerization

The monomer was electrochemically polymerized from a solution containing 0.01 M monomer with 0.1 M of TBAP in DCM: ACN (1:10 v/v) medium by applying potential between +1.5 V and −1.0 V *vs*. Ag/Ag$^+$ at a scan rate of 100 mVs^{-1}as shown in Figure 5.1. The oxidation potential of the monomer was +1.2 V, which is similar to the value of other alkylenedioxythiophene derivatives [36].   During electropolymerization, oxidation and reduction peaks in 2nd cycle was observed at 0.10 V and −0.09 V respectively. Sharp redox peak was observed due to the presence of bulky side group substituted on the monomer

ProDOT [17]. The increase of redox current densities by successive CV scans indicates an increase in the surface area of working electrode owing to the deposition of conducting polymer on electrode.
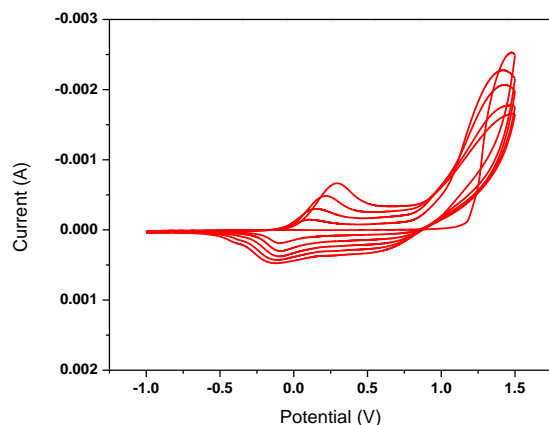
Figure 5.1: Electropolymerization of 0.01M of monomer in 0.1 M of LiClO$_4$/DCM:ACN solution at potential between −1.0 and 1.5 V at a scan rate of 100 mVs^{-1}.

5.3.2. Scanning Electron Microscopy
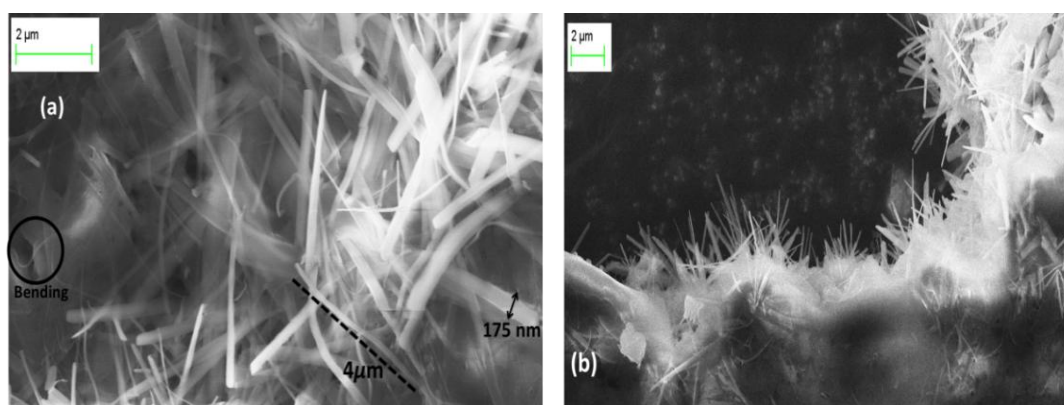
Figure 5.2: SEM images of chemically synthesized (a) PProDOT-IPBz$_2$ nanobelts using reverse microemulsion method and (b) edge-view of the nanobelts formation.

The morphological properties of chemically prepared PProDOT-IPBZ$_2$ powder were studied by scanning electron microscopy and the images are shown in Figure 5.2. The SEM images show the formation of PProDOT-IPBZ$_2$ as nanobelts with length of 4–6 μm having width of 25 ± 5 nm. PProDOT-IPBZ$_2$ nanobelts show high aspect ratio (3:100), indicating the presence of thin and long nanobelts. The nanobelts with thickness of 20±5 nm showed good flexibility and can be bent approximately in the range of 45–90º.

5.3.3. Cyclic Voltammetry
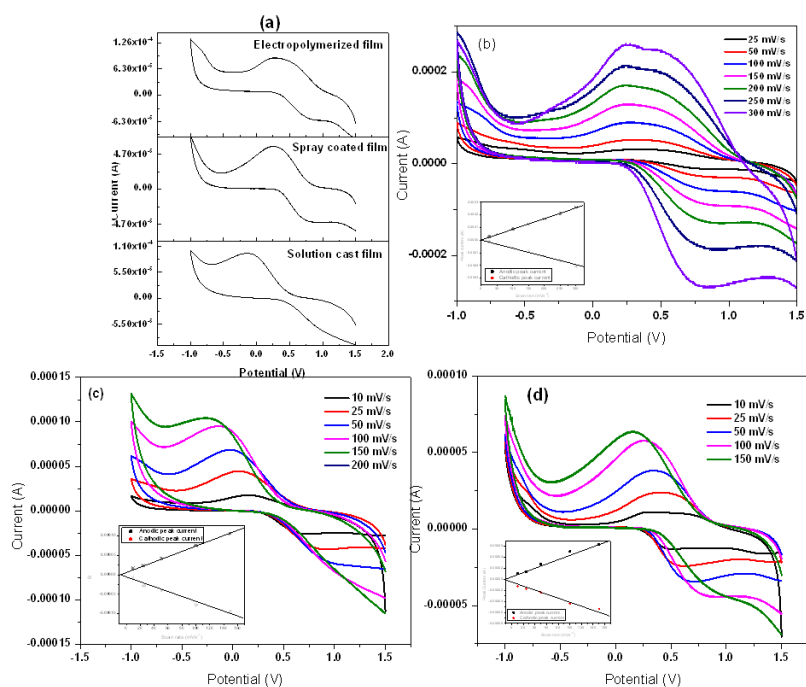
Figure 5.3: (a) Cyclic voltammogram of PProDOT-IPBz$_2$ film prepared at different methods in 0.1 M of TBAP/ACN solution at a scan rate of 100 mVs^{-1}. CV of (b) electropolymerized (c) solution cast, and (d) spray coated PProDOT-IPBz$_2$ films at potential between −1.0 V and 1.5 V at various scan rates in 0.1 M of LiClO$_4$/ACN solution, Inset (b-d): Plot of scan rates dependence redox peak currents.

The electrochemical behaviour of PProDOT-IPBz$_2$ films were studied by cyclic voltammetry (CV) in 0.1 M of LiClO$_4$/ACN solution at potential between −1.0 V and 1.5 V at a scan rate of 100 mVs^{-1} are shown in Figure 5.3a. All polymer films showed good electrochemical response and could be reversibly oxidized under redox reaction. The electropolymerized PProDOT-IPBz$_2$ film showed oxidation and reduction peaks at potential of 0.30 V and 0.84 V respectively. The respective anodic and cathodic peak currents observed for PProDOT-IPBz$_2$ film were 0.089 mA and −0.015 mA, respectively. However, the solution processed films showed low redox behaviour compared to electropolymerized film, which may be due to the difference in morphology and uniformity of those films. The electropolymerized films have an open morphology, whereas solution processed films tend to be more compact. This restricts the flow of ions in and out of the film during doping and reduced the electrochemical properties of solution processed films compared to the electrodeposited film [51].

The possible electrochemical redox mechanism on PProDOT-IPBz$_2$ film as mentioned below:

103

$$\text{PProDOT-IPBz}_2 \leftrightarrow (\text{PProDOT-IPBz}_2)^{n+} + ne^- + ClO4^-$$

(Neutral, dark purple)   (Oxidized, colorless)

Cyclic voltammogram of electropolymerized PProDOT-IPBz$_2$ film with various scan rates are shown in Figure 5.3b-d. Sharp redox peaks were observed with scan rates, revealing higher inter chain separation due to bulky groups, which lead to the faster transportation of counter ions. The oxidation peaks shift to more negative potentials, and reduction peaks shift towards positive potentials with increasing scan rates. This also confirms the facile transportation of counter ions with increasing scan rates during the redox process. At higher scan rates, the redox peaks were more prominent, followed the formation of a plateau in the oxidation scan. This reveals the increase of capacitive behaviour of PProDOT-IPBz$_2$ film at higher scan rates. A linear relationship between the redox peak current and scans rates indicated the formation of redox active polymer, and it adhered well to the working electrode. The peak current densities increased with increasing scan rates, which show the redox process of PProDOT-IPBz$_2$ to be reversible and not-diffusion limited.
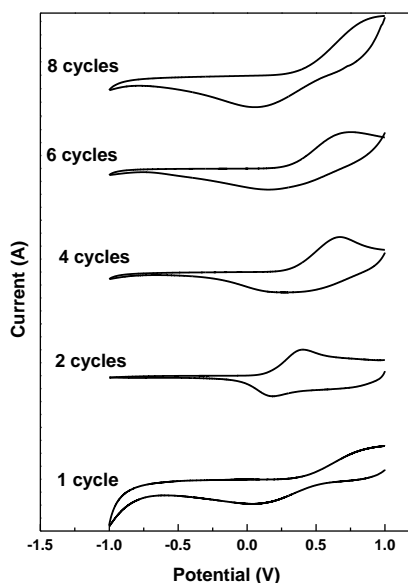
Figure 5.4: Cyclic voltammetry of PProDOT-IPBz$_2$ films electropolymerized at different polymerization cycles in 0.1 M of LiClO$_4$/ACN solution.

Cyclic voltammogram of PProDOT-IPBz$_2$ films electropolymerized at various deposition cycles at scan rate of 100 mVs^{-1} in 0.1M of LiClO$_4$/ACN medium are shown in Figure 5.4. The PProDOT-IPBz$_2$-1 film shows two broad oxidation and reduction peaks at about 0.12 and 0.80 V. It was noted that the redox peaks become broader and shift to a high potential on

increasing the no. of cycles during polymerization. The oxidation potential of PProDOT-IPBz$_2$ films shifts from -0.27 V to -0.72 V on increasing the deposition cycles from 1st to 8th cycles, revealing that the strong effect of polymerization cycles (film thickness) on the redox properties of polymer.

5.3.4. Spectroelectrochemistry

The UV-vis absorption spectra of the PProDOT-IPBz$_2$ in toluene solution and corresponding films at neutral state are shown in Figure 5.5. The shape of peaks (splitting) and absorption onset (λ_{onset}) of PProDOT-IPBz$_2$ in solution and polymer films are quite similar to one another, indicating that the polymer films prepared from solution could be processed to provide almost comparable characteristic as the electropolymerized film. The solution processed PProDOT-IPBz$_2$ films showed two absorption peaks (553 and 599 nm for solution cast film and 553 nm and 598 nm for spray coating film), which are considerably red shifted in comparison with absorption spectra of polymer in solution, where λ_{max} was observed at 542 and 580 nm. This may be due to better polymer chain packing in the solid state films as well as enhanced effective conjugation length; this similar behaviour also noticed for other polythiophene derivatives [52]. At neutral state, the electropolymerized PProDOT-IPBz$_2$ film showed maximum absorption (λ_{max}) at 497 nm (Figure 5.5b). The optical properties of polymer in solution and films are listed in Table 5.1

Table 5.1: Optical Properties of PProDOT-IPBz$_2$ in solution and PProDOT-IPBz$_2$ films at reduced state

Polymer	λ_{max}, $\lambda_{shoulder}$ (nm)	^{a}E$_g$ (eV)
PProDOT-IPBz$_2$ (in toluene)	542, 580	2.0
Solution-cast PProDOT-IPBz$_2$	553, 599	1.93
Spray coated PProDOT-IPBz$_2$	553, 598	1.90
Electropolymerized PProDOT-IPBz$_2$	555, 599	1.91

When the film is electrochemically oxidized and then reduced, the absorption peak red-shifted and split into two peaks with λ_{max} of 555 nm and shoulder at 599 nm. This red-shift and fine splitting are attributed to the formation of highly ordered polymer under doping.
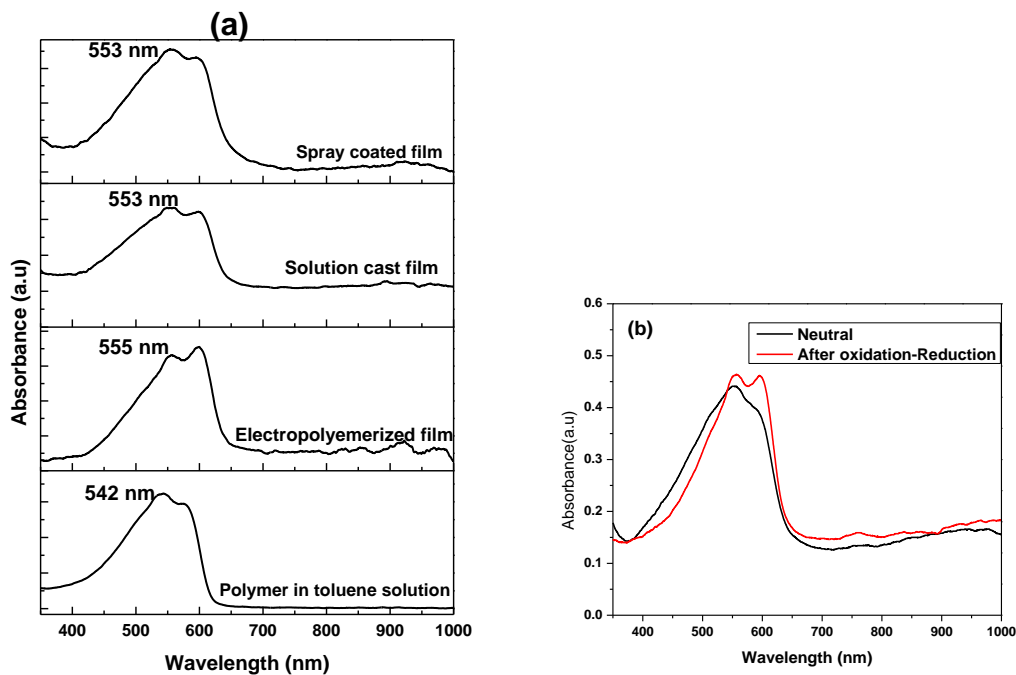
Figure 5.5: (a) UV-vis absorption spectra PProDOT-IPBz$_2$ in toluene solution and polymer films prepared by electropolymerization, spray coating, and solution casting methods, (b) Absorption spectra of electropolymerized film before (neutral) and after electrochemical oxidation and reduction process.

The spectroelectrochemical properties of PProDOT-IPBz$_2$ polymer films were studied by monitoring the absorbance changes with function of different applied potential in 0.1M of LiClO$_4$/ACN solution are shown in Figure 5.6a–c. The PProDOT-IPBz$_2$ film on ITO/glass substrate was used as the working electrode, platinum wire as a counter electrode, and Ag/Ag+ as the reference electrode. The PProDOT-IPBz$_2$ films prepared by different methods showed similar spectroelectrochemical behaviour; they were observed with same dark purple colored films at neutral/reduced stage and highly transmissive color at oxidized stage, but each spectrum showed differences in resolution and intensity. However, when the potential is increased, the splitting of two peaks was observed, which indicates the vibronic coupling due to high degree of molecules regularity along the polymer backbone and presence of bulky groups on polythiophene derivatives [17]. At fully reduced state potential, the polymer film showed dark purple color with intense absorption (450–650 nm), which is attributed to the distinct π to π* inter-band transition of the material. During stepwise oxidation of polymer film, the absorbance due to π–π* transition decreases in the visible region and polymer absorption increased slightly towards longer wavelength region (850–900 nm). At oxidized

106

state, the absorbance due to π to π^* transition in the visible region is fully diminished and a new broad peak was observed at about 850 nm because of polaronic transition. This provides significantly a high level of transmissivity to the human eye, and act as a high color contrast material. The PProDOT-IPBz$_2$ film shows a well-defined isosbestic point, which indicates that only one kind of chromophoric group present in polymer [53].
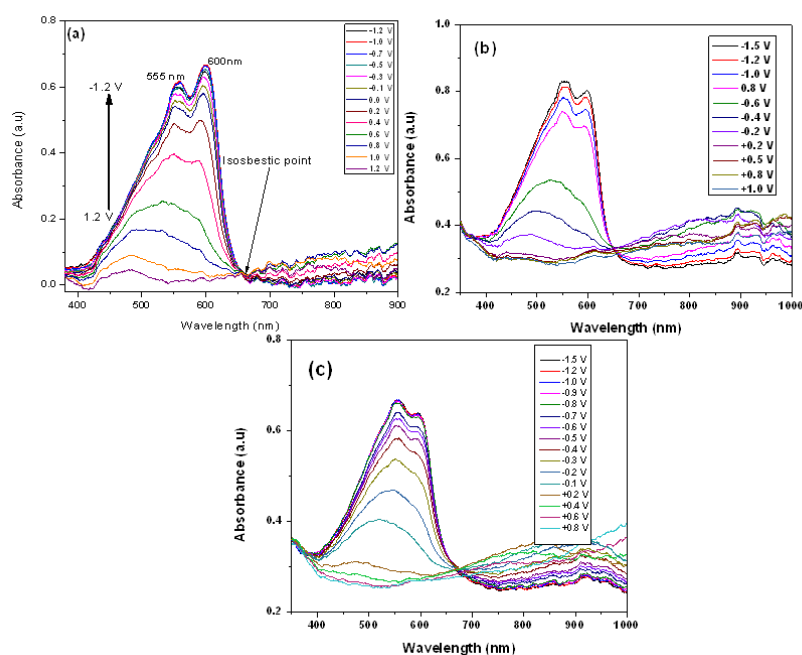
Figure 5.6: Spectroelectrochemistry of (a) electropolymerized PProDOT-IPBz$_2$ films, (b) solution cast film, and (c) spray coating film were studied as a function of various applied potential in 0.1M of LiClO$_4$/ACN solution.

The absorption spectra of PProDOT-IPBz$_2$ film were electropolymerized by different polymerization cycles as shown in Figure 5.7. The absorption spectra of PProDOT-IPBz$_2$-1film exhibit a broader peak at λ_{max} of 600 nm. On increasing the number of polymerization cycles, the absorption peaks became sharper and intensity of absorption increased. On increasing the film thickness, the absorption peak evidently split into two distinct peaks due to vibronic coupling, but λ_{max} value slightly blue shift may be due to the reduction in effective conjugation at a higher thickness. The electrochemical and electrochromic properties of electropolymerized films prepared at different potential cycles are listed in Table 5.2.
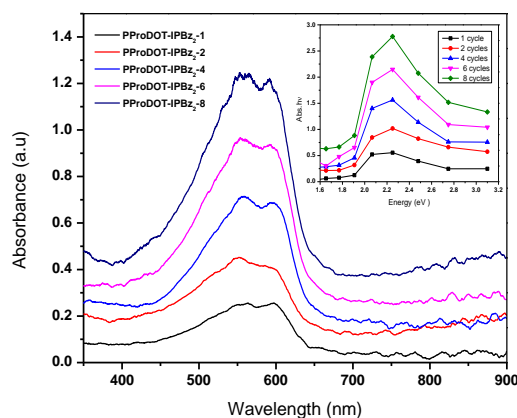
Figure 5.7: Absorption spectra of PProDOT-IPBz$_2$ film with various polymerization cycles at reduces state (−1.0 V). Inset: Absorption coefficient vs energy plot of PProDOT-IPBz$_2$ film at different polymerization cycles.

Table 5.2: The electrochemical and electrochromic properties of the PProDOT-IPBz$_2$ films

Polymer	Thickness[a] ±5nm (nm)	T_b[b] (%)	T_c[c] (%)	Color contrast (ΔT, %)	t_b[d] (s)	t_c[d] (s)	$\lambda_{max}/\lambda_{shoulder}$ (nm)	E_{onset}[e] (V)	E_{HOMO}[f] (eV)	E_{LUMO}[g] (eV)	E_g[h] (eV)
PProDOT-IPBz$_2$-1	75	94.11	63.48	30.63	0.40	0.40	562/597	−0.27	−5.07	−3.22	1.85
PProDOT-IPBz$_2$-2	154	83.34	34.66	48.68	0.68	0.41	550/591	−0.32	−5.12	−3.31	1.81
PProDOT-IPBz$_2$-4	430	57.52	16.80	40.72	0.69	0.42	557/596	−0.53	−5.33	−3.50	1.83
PProDOT-IPBz$_2$-6	662	42.43	14.72	27.71	1.78	1.18	555/594	−0.71	−5.51	−3.69	1.82
PProDOT-IPBz$_2$-8	928	31.80	10.37	21.43	1.75	1.98	558/590	−0.72	−5.52	−3.71	1.81

[a]Thickness of the film measured by Dektak surface profiler, [b]Transmittance at bleached state, [c]Transmittance at colored state, [d]response time for bleaching and coloring for 95% at constant interval of 10 s, [e]Oxidation onset potential, [f]E_{HOMO} = −e(E_{onset}+4.8 eV) (vs. SCE of ferrocene system), [g]E_{LUMO} = E_{HOMO}−E_g, [h] E_g-calculated the optical band gap from Abs.hυ/ Energy plot.
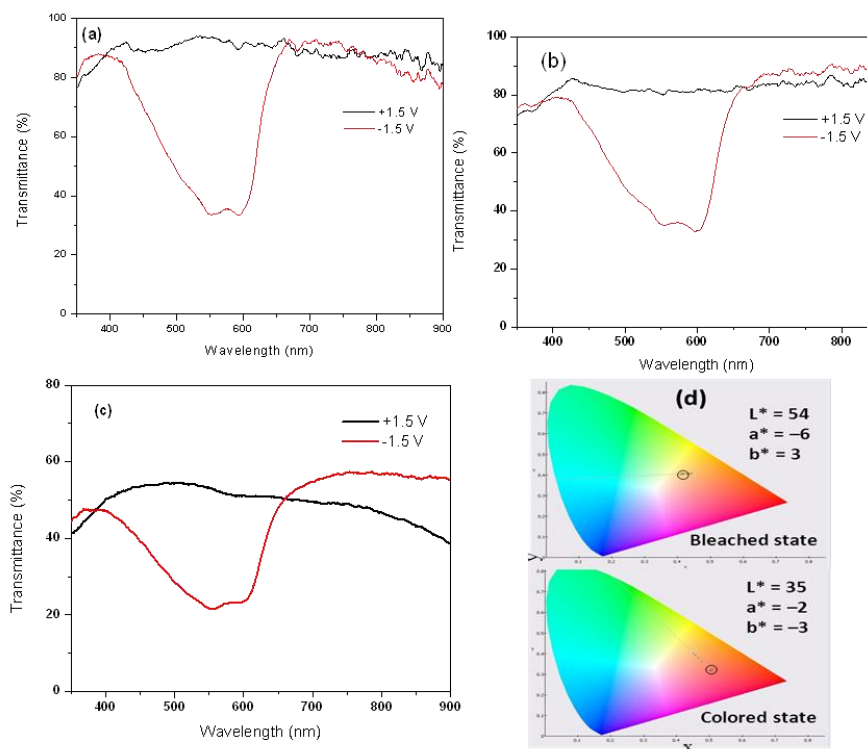
Figure 5.8: Transmittance spectra of PProDOT-IPBz$_2$ films prepared by (a) electropolymerization (b) solution cast, and (c) spray coating at fully oxidized (1.5 V) and reduced states (−1.5 V); (d) CIE 1986 chromaticity diagram of electropolymerized PProDOT-IPBz$_2$ films at bleached and colored states.

The transmittance spectra PProDOT-IPBz$_2$ films at colored and bleached states are shown in Figure 5.8 a–c. The color contrast of electropolymerized PProDOT-IPBz$_2$ film calculated from the difference in % transmittance between fully colored (−1.5 V) and fully bleached state (+1.5 V) at 550 nm was 60% T for electropolymerized film, 46% T for solution cast film, and 30% T for spray coated film. At 550 nm, where human eye is most sensitive, PProDOT-IPBz$_2$ film exhibits high color contrast and strong absorption. In Figure 5.8a, the polymer showed around 90 % transparency at fully oxidized state and exhibits 30% T at reduced state, which is highly appreciable in EC applications. The color contrast of solution processed films from toluene solution is less in comparison with electropolymerized film, and that is due to the inconsistent thickness and inhomogeneous morphology of solution-processed films. As described above (Section 5.3.2), these solution-processed compacted films may restrict the movement of ion upon redox process that directly influences the optical color contrast of the films.

5.3.5. Colorimetry

The quantitative color measurement of the PProDOT-IPBz$_2$ film during redox switching was measured colorimetrically using CIE lab 15.2-1986 (of L* a* b*), where L* represents light versus dark, a* represents red versus green, and b* represents yellow versus blue color of the material [54]. The chromaticity diagram of electropolymerized PProDOT-IPBz$_2$ film at fully colored and bleached states are shown in Figure 5.8d. At oxidized state, the PProDOT-IPBz$_2$ film exhibited L* a* b* color coordinates of 54, –6, and 3 respectively. A higher L* value reveals higher transparency of the film and lower values of a* and b* show loss of the respective colors [55, 56]. At colored state, the L* value of PProDOT-IPBz$_2$ film decreased to 35, revealing that the polymer film changed to more darkened state, which is comparable to the value reported previously [57]. The reversible changes of the L* a* b* values between redox states show a clear evidence of color switching of the PProDOT-IPBz$_2$ film.

5.3.6. Optical Switching Kinetics

The optical switching stability of PProDOT-IPBz$_2$ films were studied by repeated potential switching between redox potential at regular interval (5 s/10 s) , and monitoring of % transmission as a function of time at 550 nm in 0.1M of LiClO$_4$/ACN solution is shown in Figure 5.9 a–c. In Figure 5.9a, the PProDOT-IPBz$_2$ film showed high contrast ratio as 48%, switched at regular intervals of 10 s. The film showed good stability and successfully switched more than 1000 cycles without much failure in color contrast (<3%T) and deformation of film. The average response time of the film was calculated to be ~1 s; it implies that bulky substituents on propylenedioxy ring reduce the switching time and enhance the EC color contrast due to the higher inter-chain separation. The coloration efficiency (CE) value for electropolymerized PProDOT-IPBz$_2$ film was calculated as ~305 cm^{2}C^{-1}, which is more significant for EC device applications. The solution processed films also showed significant optical switching response at applied redox potentials. The color contrast of solution cast film was calculated to be ~37% T and spray coating film to be ~28% T. The electrochromic properties of PProDOT-IPBz$_2$ films are described in Table 5.3.
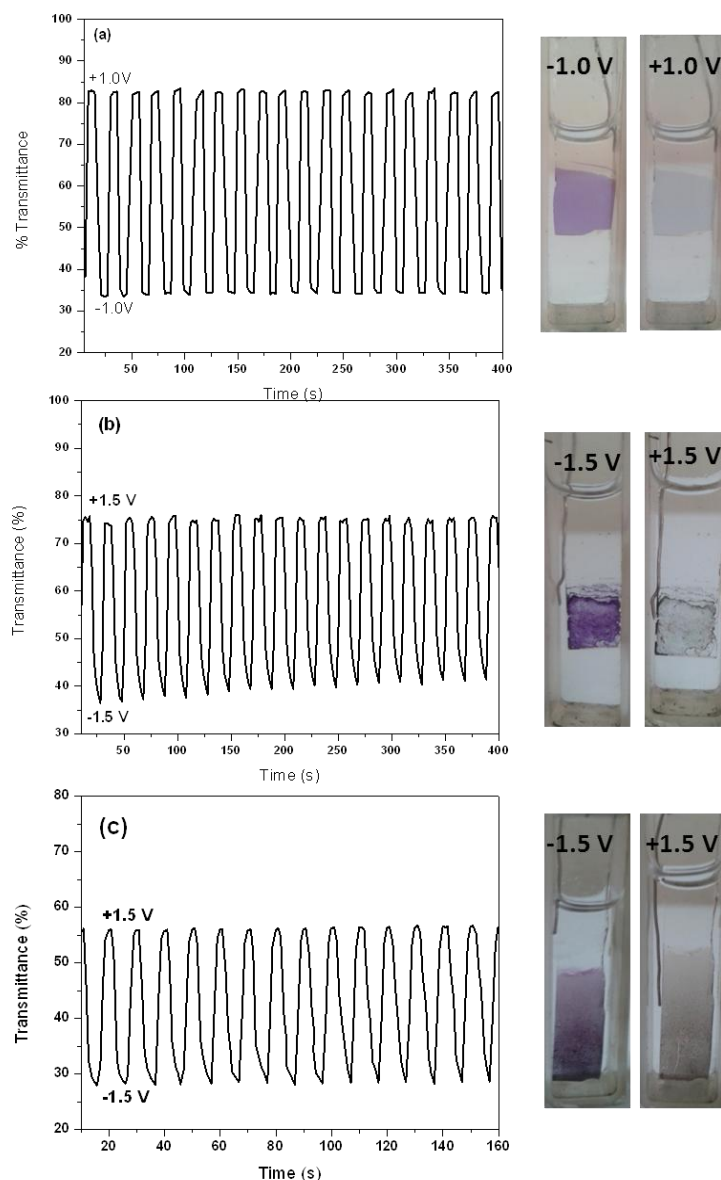
Figure 5.9: (a) Optical switching study of PProDOT-IPBz$_2$ films monitored at redox potentials with constant interval of 5 s (for spray coating and solution cast film) and 10 s (for electropolymerized film) at 550 nm in 0.1 M of LiClO$_4$/ACN solution using chronoamperometry technique. Right side: Photographs of the PProDOT-IPBz$_2$ films at bleached and colored states respectively.

The optical switching response of PProDOT-IPBz$_2$-2 and PProDOT-IPBz$_2$-8 films were recorded at 600 nm by applying square wave potential between −1.0 V and 1.0 V at switch time of 10 s as illustrated in Figure 5.10a. The color contrast of the PProDOT-IPBz$_2$-2 and PProDOT-IPBz$_2$-8 films was evaluated to be 48% and 21% respectively at 600 nm. The relationship between polymerization cycle and EC color contrast of PProDOT-IPBz$_2$ films is

shown in Figure 5.10b. While increasing the thickness of film, the color contrast decreased and a longer switching response was observed that was probably due to the higher diffusion distance required by counter ions during redox switching [58, 6].

Table 5.3: Electrochromic parameters of PProDOT-IPBz$_2$ films prepared by electropolymerization, solution cast, and spray coating methods.

PProDOT-IPBz$_2$	T_b (%)	T_c (%)	ΔT (%)	t_b(s)	t_c(s)	~Thickness (nm)	η^a (cm^2 C^{-1})
Electropolymerized film	82	34	48	1.0	1.2	180	305
Solution cast film	75	38	37	2.5	3.0	175-180	88
Spray coated film	56	28	28	2.0	2.5	175-180	30

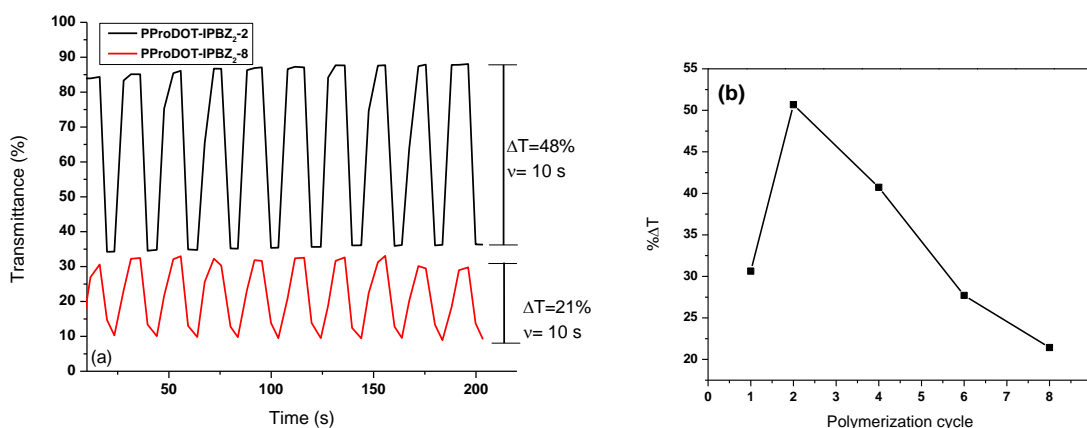Coloration efficiency,$(\eta) = \log(T_b/T_c)/ Q_d$, Where Q_d is Charge per unit area.

Figure 5.10: (a) Optical switching of PProDOT-IPBz$_2$-2 and PProDOT-IPBz$_2$-8 films at 600 nm by applying square wave potentials between −1.0 V and 1.0 V at switch time of 10 s. (b) Plot of color contrast (%ΔT) *vs* no. of electropolymerization cycles of PProDOT-IPBz$_2$ films.

5.4. Performance Testing of Electrochromic Window

5.4.1 Spectroelectrochemistry

The spectroelectrochemical studies of solid state ECW as a function of different applied potential are shown in Figure 5.11. The absorbance spectra of ECW were shown to be similar in characteristic spectra at different applied potentials. At −1.4 V, the polymer film gets fully reduced (purple color) and the absorption peak splits into two at 550 and 590 nm due to

vibronic coupling. Upon step wise oxidation, the absorption of π-π* decreased, and a new peak formed at higher wavelength region due to polaronic transition. At +1.6 V, the absorbance due to π to π* transition in the visible region diminished fully and the device appeared to be in a transparent color.
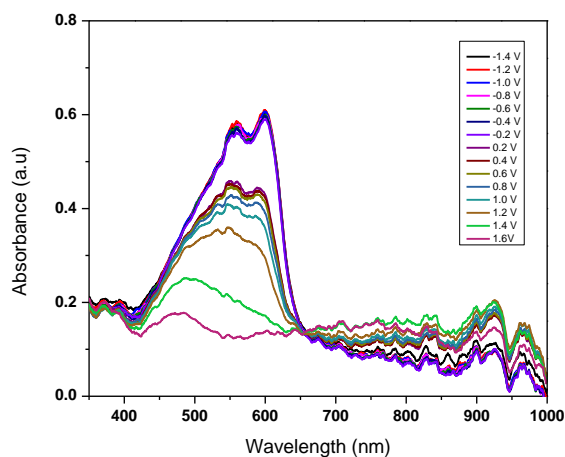
Figure 5.11: The spectroelectrochemistry of electrochromic window based on PProDOT-IPBz$_2$ film as a function of applied the potentials.

5.4.2. Optical Switching

The optical switching stability of ECW based on PProDOT-IPBz$_2$ film was studied by applying continuous stepped potential between −2.0 and +2.0 V at a regular interval of 10s, and % transmission was monitored as a function of time at λ_{max} of 600 nm (Figure 5.12a). The optical color contrast of the ECW was calculated to be 40% at 600 nm, the response time of ECW for bleaching and coloration was about 2 s and 2.5 s respectively. This single-type electrochromic window showed faster response time and significantly good color contrast without using any complementary counter electrode that is attributed to bulky isopropyl benzyl group provides faster counter-ion movement in open morphologies. The coloration efficiency of ECW was found to be 555 cm^{2}C^{-1} at 600 nm in the fully doped state, this value is much closer to the value reported by A. Kumar et al [39]. This ECW was successfully switched for more than 1000 cycles without much failure in color contrast (<5% T), and degradation of the film is attributed to better switching of PProDOT-IPBz$_2$based devices. Figure 5.12b shows the photographs of multi-colored ECW at different applied potentials. The ECW showed transmissive, magenta, and violet colored states at applied potentials of 1.5 V,−1.0 V and −2.0 V respectively.
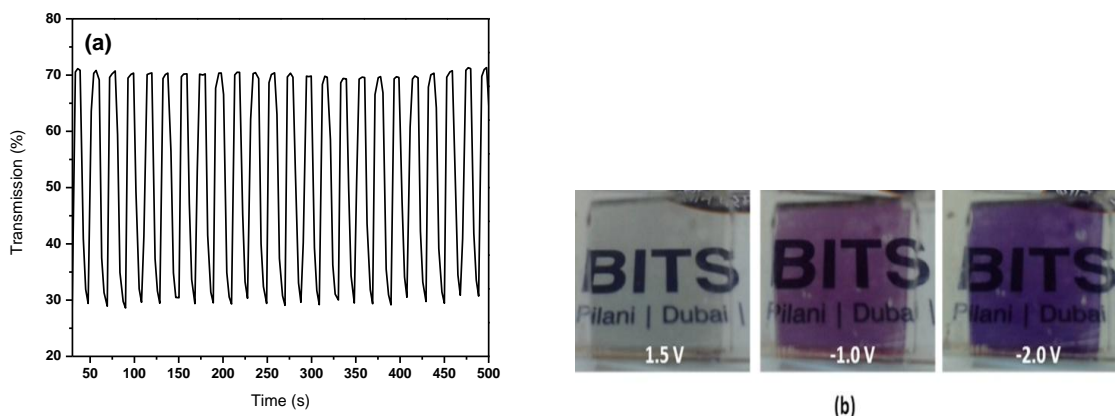
Figure 5.12: (a) The optical switching stability of ECW based on PProDOT-IPBz$_2$ at applied potentials between −2.0 V and +2.0 V at interval of 10 s at 600 nm, and (b) Photographs of multi-colored electrochromic window at different applied potentials (Active area: ~2.5 cm^2)

5.4.3. Open Circuit Memory and Electrochemical Long-term Stability
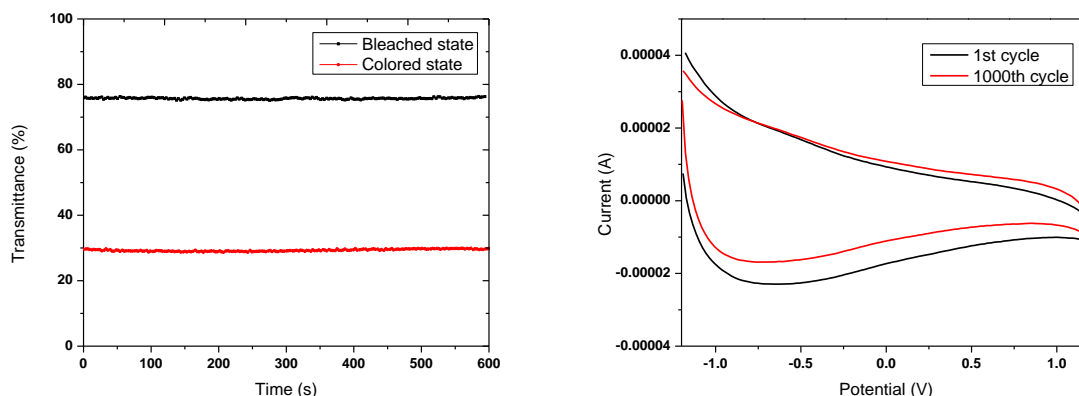
Figure 5.13: (a) The open circuit memory of the PProDOT-IPBz$_2$ based device monitored at 600 nm at reduced and oxidized states, and (b) Long term electrochemical stability of PProDOT-IPBz$_2$ based ECW using cyclic voltammogram as a function of applied potential between −1.2 and +1.2 V at a scan rate of 250 mVs^{-1}.

The open circuit memory of ECW based on PProDOT-IPBz$_2$ was monitored at 600 nm as a function of time at an applied potential of ±1.0 V for 30 s to stabilize the color (or bleach), and then circuit potential was opend to 600 s, are shown in Figure 5.13. This ECW showed a significant optical memory when compared with PDiBz-ProDOT/PBEDOT-NMCz device, reported by J.Padilla et.al [59]. Both transparent and colored states of the device have excellent optical memory without applying a voltage to retain the coloration. The redox long term switching stability of ECW based on PProDOT-IPBz$_2$ was studied by CV with applied

114

potential between −1.2 and +1.2 V at a scan rate of 250 mVs^{-1} (Figure 5.13b). The ECW showed excellent long term stability without any considerable change in redox properties after 1000 cycles.

5.5. Performance Testing of Electrochromic Rear-view Mirror

5.5.1. Spectroelectrochemistry

The EC rear-view mirror was constructed using both PProDOT-IPBz$_2$ based working electrode and ITO/glass/Al counter electrode; the two were sandwiched by polymer gel electrolyte. The spectroelectrochemical properties of ECM based on PProDOT-IPBz$_2$ monitored the % of reflection at different applied potential as shown in Figure 5.14a. At −0.4 V, the active layer of PProDOT-IPBz$_2$ in ECM reached a fully reduced state, and absorbed maximum wavelength at 600 nm due to π to π* inter-band transition that leads to lowest reflectance as 40%. Upon stepwise oxidation, the intensity of π to π* transition decreased at visible region, and a new peak was observed at higher wavelength region that achieved highly transmissive state at fully oxidized state (+1.6 V). Therefore, Al layer dominates with high reflectivity as normal mirror that increases reflectance up to ~85%. From absorption spectra, the reflectivity contrast, %ΔR (the % difference of reflection at reduced and oxidized states) of ECM between fully colored and bleached state was 45% at 600 nm and 25% in the near IR region (900 nm). This reflectivity contrast at visible region is relatively comparable with the result obtained by reflective ECD based on PProDOT-(CH$_2$OEtHx)$_2$ film [60]. The photograph of electrochromic mirror with an object at bleached and colored states are shown in Figure 5.14b.
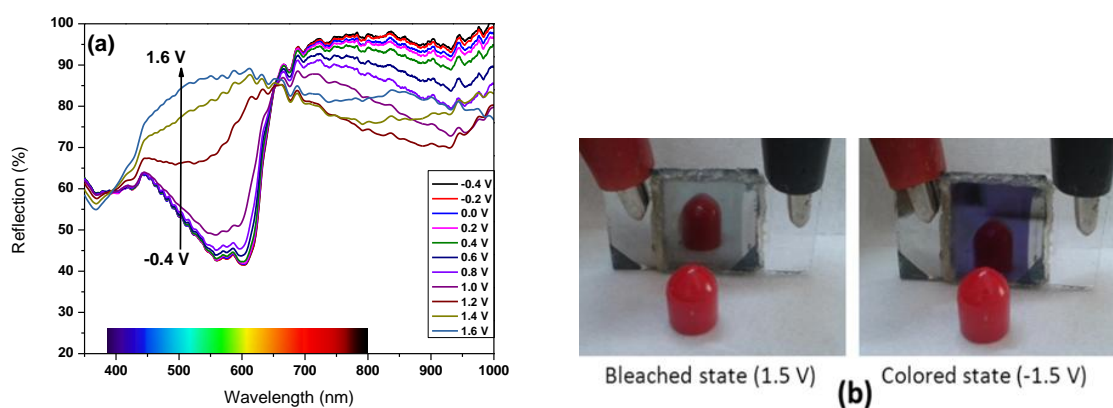
Figure 5.14: (a) Spectroelectrochemistry of PProDOT-IPBz$_2$ based ECM monitored at % reflection as a function of different applied potentials. (b) Photograph of ECM with an object at fully bleached and colored states (Active area of the device: ~2.0 cm^2)

5.5.2. Optical Switching
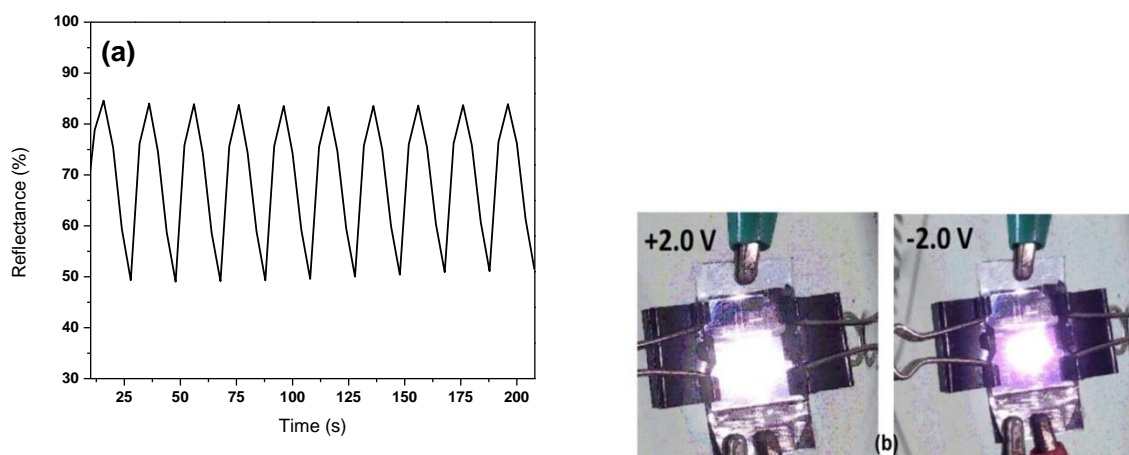
**Figure 5.15:** (a) The optical switching study of PProDOT-IPBz$_2$ based ECW at applied potential between −2.0 V and +2.0 V at interval of 10 s at 600 nm. (b) Photographs of ECM regulates the reflection of light at fully colored and bleached states Active area of the device: ~2.0 cm^2).

The optical switching response of PProDOT-IPBz$_2$ based ECM was studied at a switching potential between −2.0 and +2.0 V at interval of 10 s, and % reflection as a function of time at λ_{max} of 600 nm was monitored, as shown in Figure 5.15a.The PProDOT-IPBz$_2$ based ECM has been successfully switched for more than 1000 cycles, showing that ECM is indeed highly reversible and excellent optical switching stability without much failure in reflection contrast (<8%R). The reflective contrast (ΔR %) was calculated to be ~35% at 600 nm between the applied potential of −2.0 V and +2.0 V at interval of 10 s. The bleached and coloration time of ECM was calculated as ~3.0 s and 3.5 s respectively and coloration efficiency was found to be 138 cm^{2}C^{-1}. Figure 5.15b shows the photograph of the light regulation in ECM at fully bleached and colored states. This revealed that the reflection of light could be efficiently control by this ECM, which would be highly appreciable for rear-view mirrors in automobile industry.

5.5.3. Open Circuit Memory and Electrochemical Long-term Stability

The open circuit memory of PProDOT-IPBz$_2$ based ECM was examined at 600 nm as a function of time by applying potential between ±1.0 V for 30 s to stabilize the color (or bleach), and then opened the circuit potential up to 600 s. As shown in Figure 5.16a, the device showed a constant memory at reduced state (dark purple color, 42% R), as there was

no color change after the circuit was opened. But in the oxidized state, the device showed a very small variation in reflection (~2% R) when the potential was opened after 10 s. However, the device showed highly stable memory effect (%R= 88%) at bleached state throughout the experiment. The redox long term switching stability of PProDOT-IPBz$_2$ based ECM was studied by CV with applied potential between −1.2 and +1.2 V at a scan rate of 250 mVs^{-1} as shown in Figure 5.16b. After 1000 cycles, the electro-activity of the device was retained, revealing that ECM has good long term stability and excellent redox response.
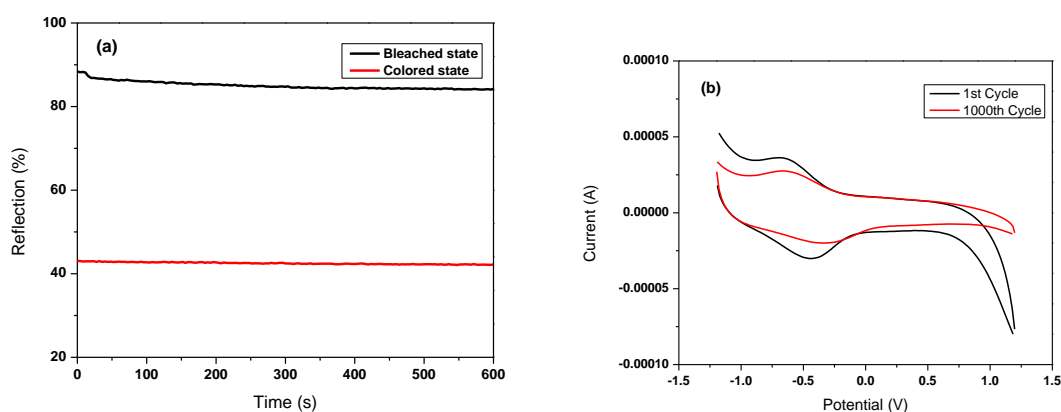
Figure 5.16: (a) The open circuit memory of ECM studied at 600 nm. (b) Long term redox stability using cyclic voltammogram of PProDOT-IPBz$_2$ based ECM as a function of applied potential between −1.2 and +1.2 V at a scan rate of 250 mVs^{-1}.

5.6. Summary

The di-4-isopropyl benzyl substituted (3,4 propylenedioxythiophene) monomer was synthesized and characterized. The corresponding PProDOT-IPBz$_2$ polymer was prepared by chemical and electropolymerization methods. The polymer was chemically synthesized by reverse micro emulsion method, and was appeared as thin nanobelt structures that showed higher solubility in toluene and chloroform. The electrochemical and electrochromic properties of PProDOT-IPBz$_2$ films were characterized. The effect of film thickness on electrochemical and electrochromic properties was systematically analysed and optimized. It has been noted that polymerization cycles play key roles on electrochemical, optical, and electrochromic performance of PProDOT-IPBz$_2$ films. The electropolymerized PProDOT-IPBz$_2$ film showed good color contrast (48% T), fast response time (~1s), and better optical switching stability. The substitution of bulky and flexible isopropyl benzyl group on propylenedioxy ring not only improves the solubility but also enhances the electrochromic

properties of the material. We have presented EC window and rear-view mirror having significant color contrast, fast response time, lower power consumption, excellent optical memory, and better optical switching stability for more than 1000 cycles without much failure in color contrast of the device. The electrochromic rear-view mirror proved to be superior light regulator in the visible and the near-IR regions under low applied potentials. The purple colored ECM has strong absorption of selective yellow color light (570–600 nm), which is commonly used color in automobile headlights. The new PProDOT-IPBz$_2$ derivative can be used as promising candidate in automobile window and mirror applications.

5.7. References

[1]   Monk P.M.S., Mortimer R.J., Rosseinsky D.R., *Electrochromism and Electrochromic devices*, Cambridge University Press, New york, 2007.

[2]   Rauh R.D., *Electrochim. Acta.* 1999, 44: 3165–3176.

[3]   Azens A., Granqvist C. G., *J. Solid State Electrochem.*, 2003, 7: 64–68.

[4]   Sonmez G., *Chem.commun.*, 2005, 42 5251–5259.

[5]   Xu C., Liu L., Susan E. L., Ning D., Taya M., *J. Mater. Res.*, 2004,19: 2072–2080.

[6]   Tehrani P., Hennerdal L., Dyer A.L. , Reynolds J.R., Berggren M., *J. Mater. Chem.* 2009,19: 1799–1802.

[7]   Granqvist C.G., *Nat. Mater.*, 2006, 5: 89–90.

[8]   Sonmez G., Meng H., Wudl F., *Chem. Mater.*,2004,16: 574–580.

[9]   Tehrani P., Isaksson J., Robinson N. D., Mammo W., Andersson M. R., Berggren M., *Thin Solid Films*, 2006, 515: 2485–2492.

[10]   Rosseinsky D. R., Mortimer R. J., *Adv. Mater,* 2001,13: 783–793.

[11]   Schierbeck K.L., *Digital electrochromic mirror system.* Donnelly Corporation, US Patent No.06089721, 2000.

[12]   Mortimer R.G.,*Chem. Soc. Rev.*, 1997, 26: 147–156.

[13]   Bange K., Gambke T., *Adv. Mater.*, 1992, 2: 10–16.

[14]   Baucke F.G.K., *Sol. Energy Mater*, 1987, 16: 67–77.

[15]   Brotherson I.D., Mudigonda D.S.K., Ocborn J.M., Belk J., Chen J., Loveday D.C., Boehme J.L, Ferraris J.P., *Electrochim. Acta*, 1999, 44: 2993–3004.

[16]   Invernale M.A., Ding Y., Sotzing G.A., *ACS appl. Mater interface.*, 2010, 2: 296–300.

[17]   Kumar A., Welsh D.M., Morvant M.C., Piroux F., Abboud K.A., Reynolds J.R.,*Chem. Mater.*, 1998, 10: 896–902.

[18]   Yildiz U.H., Sachin El., Akhamedov I.M., Tanyeli C., Toppare L., *J. Polym. Sci. A Polym. Chem.*, 2006, 44: 2215–2225.

[19]   Durmus A., Gunbas G.E., Toppare L., *Chem. Mater.*, 2007, 19: 6247–6251.

[20]   Kung Y.C., Liou G.S., Hsiao S.H., *J. Polym. Sci. A Polym. Chem.*, 2009, 47: 1740–1755.

[21]   Dyer A.L., Thompson E.J., Reynolds J.R., *ACS Appl. Mater. Interfaces*, 2011, 3: 1787–1795.

[22]   Xu C., Zhao J., Wang M., Wang Z., Cui C., Kong Y., Zhang X., *Electrochim. Acta*, 2012, 75: 28–34.

[23]   Hsiao S.H., Wang H.M., Chang P.C., Kung Y.R., Lee T.M., *J. Polym. Sci. A Polym. Chem.* 2013, 51: 2925–2938.

[24]   Aydın A., Kaya I., *Org. Electron.*, 2013, 14: 730–743.

[25]   Algi M.P., Tirkes, S. Ertan, Ergun E.G.C., Cihaner A., Algi F., *Electrochim. Acta*, 2013, 109, 766–774.

[26]   Groenendaal L.B., Zotti G., Aubert P.H., Waybright S.M., Reynolds J.R., *AdV. Mater.* 200,15: 855–879.

[27]   Jain V., Yochum H.M., Montazami R., Heflin J.R., *Appl. Phys. Lett.*, 2008, 92: 033304, DOI: 10.1063/1.2834818.

[28]   Cho S.I., Choi D.H., Kim S.H., Lee S.B., *Chem. Mater.*, 2005, 17: 4564–4566.

[29]   Aubert P.H., Argun A.A., Cirpan A., Tanner D.B., Reynolds J.R., *Chem. Mater.*, 2004, 16: 2386–2393.

[30]   Mc Culluough R.D., Williams S.P., *Polym.Prepr.*, 1994, 35: 300–301.

[31]   M. Blohm, J.E. Pickett, P.C. van Dort, Macromolecules 26 (1993) 2704–2710.

[32]   Burkhardt S.E., Rodriguez-Calero G.G., Lowe M.A., Kiya Y., Hennig R.G., Abruna H.D., *J. Phys. Chem. C*, 2010, 114: 16776–16784.

[33]   Dietrich M., Heinze J., Heywang G., Jonas F., *J. Electroanal. Chem.*, 1994, 369: 87–92.

[34]   Groenendaal L. B., Jonas F., Freitag D., Pielartzik H., Reynolds J. R., *Adv. Mater.* 2000, 12: 481–494.

[35]   Welsh D.M., Kumar A., Morvant M.C., Reynolds J.R., *Synth. Met.*, 1999, 102: 967–968.

[36]   Mishra S.P., Krishnamoorthy K., Sahoo R., Kumar A., *J. Polym. Sci. A Polym. Chem.*, 2005, 43: 419–428.

[37]   Sonmez G., Sonmez H.B., Shen K.F., Wudl F., *Adv. Mater.*, 2004, 16: 1905–1908.

[38]   Krishnamoorthy K., Ambade A.V., Kanungo M., Contractor A.Q., Kumar A., *J. Mater. Chem*. 2001, 11: 2909–2911.

[39]   Stefan H., Patrik H., Renee K., Ergang W., Mats R.A., *Org. Electron*. 2011, 12: 1406–1413.

[40]   Raja L., Raja P.P., Shivaprakash N.C., Sindhu S., *J. Appl. Polym.Sci*., 2014, DOI: 10.1002/APP.40717.

[41]   Ozkut M., Mersini J., Onal A.M., Cihaner A., *J. Polym. Sci. A Polym. Chem*., 2012,50: 615–621.

[42]   Welsh D. M., Kloeppner L. J., Madrigal L., Pinto M. R., Thompson B. C., Schanze K. S., Abboud K. A., Powell D., Reynolds J. R., *Macromolecules*, 2002, 35: 6517–6525.

[43]   Duan X., Huang Y., Cui Y., Wang J., Lieber C. M., *Nature*, 2001, 409: 66–69.

[44]   Tran H.D., Li D., Kaner R.B., *Adv. Mater*., 2009, 21: 1487–1499.

[45]   Kong J., Franklin N., Zhou C., Chapline M. G., Peng S., Cho K., Dai H., *Science*, 2000, 287: 622–625.

[46]   Feng W., Li Y., Wu J, Noda H, Fujii A, Ozaki M., Yoshino K., *J. Phys.: Condens. Matter*., 2007,19: 186220 (8pp) doi:10.1088/0953-8984/19/18/186220.

[47]   Zhang X., Lee J.S., Lee G. S., Cha D.K., Kim M. J., Yang D. J., Manohar S. K., *Macromolecules*, 2006, 39: 470–472.

[48]   Jang J., Yoon H., *Chem. Commun*., 2003, 6: 720–721.

[49]   Pileni M. P., *J. Phys. Chem.*, 1993, 97: 6961–6973.

[50]   Monk P.M.S., Mortimer R.J., Rosseinskly D.R., *Electrochromism Fundamental and Applications*, Weinheim, Newyork, VCH, 1995.

[51]   Reeves B. D., Grenier C. R. G., Argun A. A., Cirpan A., McCarley T. D., Reynolds J.R., *Macromolecules,* 2004, 37: 7559–7569.

[52]   Politis J. K., Nemes J.C., Curtis M.D.. *J. Am. Chem. Soc*., 2001, 123: 2537–2547.

[53]   Jain V., Sahoo R., Mishra S.P., Sinha J., Montazami R., Yochum H.M., Heflin J.R., Kumar A., *Macromolecules*, 2009, 42: 135–140.

[54]   Dyer A.L., Craig M.R., Babiarz J.E., Kiyak K., Reynolds J.R., *Macromolecules*, 2010, 43: 4460−4467.

[55]   Thompson B.C., Cshottland P., Zong K., Reynolds J.R., *Chem. Mater*., 2000, 12: 1563−1571.

[56]   Amb C. M., Dyer A. L., Reynolds J. R., *Chem. Mater.*, 2011, 23: 397−415.

[57]   Kim J., You J., Kim B., Park T., Kim E., *Adv. Mater*., 2011,23: 4168–4173.

[58] Shi P., Amb C.M., Dyer A.L., Reynolds J.R., *ACS Appl. Mater. Interfaces*, 2012, 4: 6512−6521.

[59] Padilla J., Seshadri V., Filloramo J., Mino W.K., Mishra S.P., Radmard B., Kumar A., Sotzing G.A., Otero T.F., *Synth. Met.*, 2007, 157: 261–268.

[60] Cirpan A., Argun A.A., Grenier C.R.G., Reeves B.D., Reynolds J.R., *J. Mater. Chem.*, 2003, 13: 2422–2428.

CHAPTER 6

Fabrication of Multi-Colored Electrochromic Devices Based on New Conjugated Copolymer Bearing Carbazole and Thiophene Groups

6.1. Introduction

Conjugated polymers have attracted considerable attention in molecular electronics due to their color modulation attained by structural modification. This makes conjugated polymers one of the desired electrochromic materials [1–3]. According to color mixing theory, primary additive red, green, and blue (RGB) and primary subtractive cyan, magenta, and yellow (CMY) are more important in electrochromic device applications due to the possibility of achieving full color palette by mixing two of these colors [4]. Recently, various colored EC materials in the neutral states have been reported by Reynolds and his co-workers [5,6] and Toppare and his co-workers [7,8]. However, a black/intense dark colored EC material has been considered as challenging due to complexity of designing a polymer that absorbs the entire visible spectrum in the neutral state and is effectively transparent at oxidized state. This is highly desirable in most of the ECD applications, such as smart windows, anti-glare mirrors, and display devices. In conjugated polymers, the color changes are induced by the alteration of band gap under the doping-dedoping process. Therefore, control of band gap is an efficient approach to achieve different colored electrochromic materials. Copolymerization is an easy method to modify the HOMO-LUMO bands and hence control the color of material. Thus, copolymerization has been used to develop new materials, which provide intermediate properties of individual homopolymers [9,10].

Polythiophene has attracted attention due to its environmental stability and electrical properties; however, its applications in optoelectronic devices are limited because of its higher oxidation potential. In order to reduce the oxidation potential, a new block copolymer approach, building by dimers and trimers, which have two or more hetero-atomic rings derived from thiophene, furan and pyrrol has been reported [11]. Researchers have noticed that the 'trimeric' block copolymer (e.g. thiophene- pyrrol- thiophene) reduces the steric hindrance using thiophene spacers and those can be polymerized at a lower oxidation potential. Additionally, a combination of electronic conjugation of both the groups provides a

change in band gap and causes color changes in materials from its corresponding homopolymers [12].

Here, in this chapter, we have designed and synthesized a new conjugated monomer with insertion of both a carbazole core and two outer thiophene subunits, namely 2,7-dithienylcarbazole (Th-Cbz-Th) using Stille coupling method [13,14]. The corresponding polymer, P(Th-Cbz-Th) and its copolymer with poly(3,4 ethylenedioxythiophene), P(Th-Cbz-Th)- PEDOT were electrochemically polymerized and characterized. The electrochemical and electrochromic properties of these polymer films were studied and compared. In addition, transmissive and reflective type electrochromic devices were fabricated based on P(Th-Cbz-Th) and P(Th-Cbz-Th)–PEDOT films and their electrochromic performances were tested.

6.2. Experimental Methods

6.2.1. Synthesis of 3,6-dibromo carbazole

2.0 g of carbazole (11.96 mM) was dissolved in 25 mL of dichloromethane (DMF) solution. A 20 mL solution of 4.2 g of N-bromosuccinimide (NBS) (23.92 mM) in DMF was added to a previously prepared reaction mixture at 0 °C under inert atmosphere. The resultant mixture was stirred for 4 h at 0 °C and the solution was poured into distilled water. The precipitated product was filtered and washed with distilled water and dried under vacuum. The filtrate was recrystallized from ethanol and the product was dried under vacuum. Synthesis route of 3,6 dibromo carbazole is shown in Scheme 6.1. Yield=83%.^{1}H NMR spectrum (CDCl3, δ in ppm): 8.128–8.123(2H, d), 8.098 (1H,S), 7.532–7.505 (2H, dd), 7.313–7.290 (2H, dd).
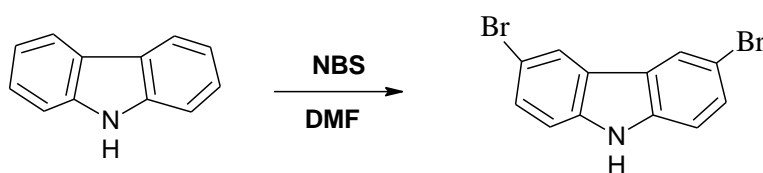

Scheme 6.1: Synthesis route of 3,6 dibromo carbazole

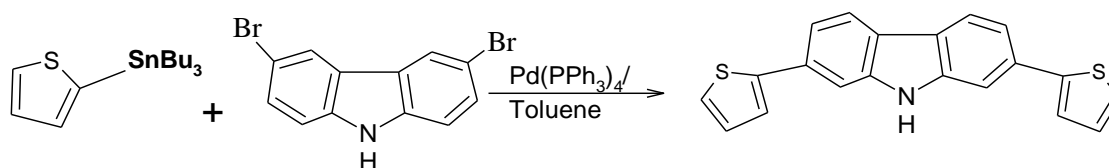### 6.2.2. Synthesis of tributyl(thiophen-2-yl) stannane

2.0 g of thiophene (23.77 mM) was dissolved in 15 mL of freshly distilled dry diethyl ether in 100 mL of two-necked flask under argon atmosphere. 1.6 g of n-BuLi (24.15 mM) was dissolved in hexane and added drop-wise to the previously prepared thiophene solution, then stirred for 1 h at 0 °C. The reaction mixture was then cooled to −78 °C using ethyl acetate and liquid nitrogen bath. 6.4 mL of tributylchlorostannane (SnBu3Cl) (23.7699 mM) was

then added to the reaction mixture. The mixture was slowly allowed to warm up to room temperature and stirred for another 12 h and then was poured into 100 mL of cooled water, and extracted with hexane. The organic layer was dried under anhydrous $MgSO_4$ and the solvent was removed by rotary evaporation to obtain the product brown oil. Synthesis route of tributyl (thiophen-2-yl) stannane is shown in Scheme 6.2. Yield: 88%. The crude product was used to next step without further purification. ^{1}H NMR spectrum (CDCl$_3$, δ in ppm): 8.10–8.08 (d, 1H), 7.47–7.39 (m, 1H), 7.25–7.19 (m, 1H), 1.90–1.27 (m, alkyl H, 27H).
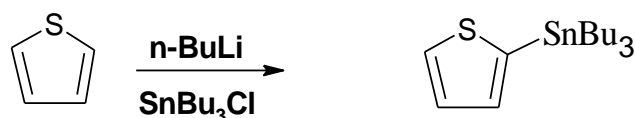
Scheme 6.2: Synthesis route of tributyl(thiophen-2-yl)stannane

### 6.2.3. Synthesis of 2,7-dithienyl carbazole (Th-Cbz-Th) monomer

Scheme 6.3: Synthesis route of 2,7-dithienyl carbazole monomer

A solution of 2.0 g of tributyl(thiophen-2-yl)stannane (5.3593 mmol) and 0.79 g of 3,6-dibromo carbazole (2.4360 mmol) and Pd(PPh$_3$)$_4$ (4 mol%) in dry toluene (15 mL) was prepared and was well purged under nitrogen atmosphere for 10 min. The entire reaction mixture was heated to 80 °C and stirred for 24 h under inert atmosphere. The reaction mixture was cooled to room temperature and poured in to cold water (100 mL). The organic layer was extracted with diethyl ether (3×50 mL) and dried over anhydrous $MgSO_4$. The solvent was removed by rotary evaporator. The crude product was purified by column chromatography with hexane and ethyl acetate as eluting solvent. The resulting product was further purified by recrystallization from ethanol. After recrystallization, the product was dried under vacuum. Synthesis route of 2,7-dithienyl carbazole monomer is shown in Scheme 6.3. **Yield: 72%.** ^{1}H NMR spectrum (CDCl$_3$, δ in ppm): 8.22-8.23 (d, J=4 Hz, 2H), 8.11 (s, 1H), 7.69-7.71 (dd, J=4 Hz, 2H), 7.49-7.51 (dd, J=4 Hz, 2H), 7.30 (s, 2H), 7.41-7.43 (dd, J=8 Hz, 2H), 7.09-7.12 (t, J=8 Hz, 2H).

6.3. Results and Analysis

### 6.3.1. Polymerization of (Th-Cbz-Th) and (Th-Cbz-Th)-PEDOT
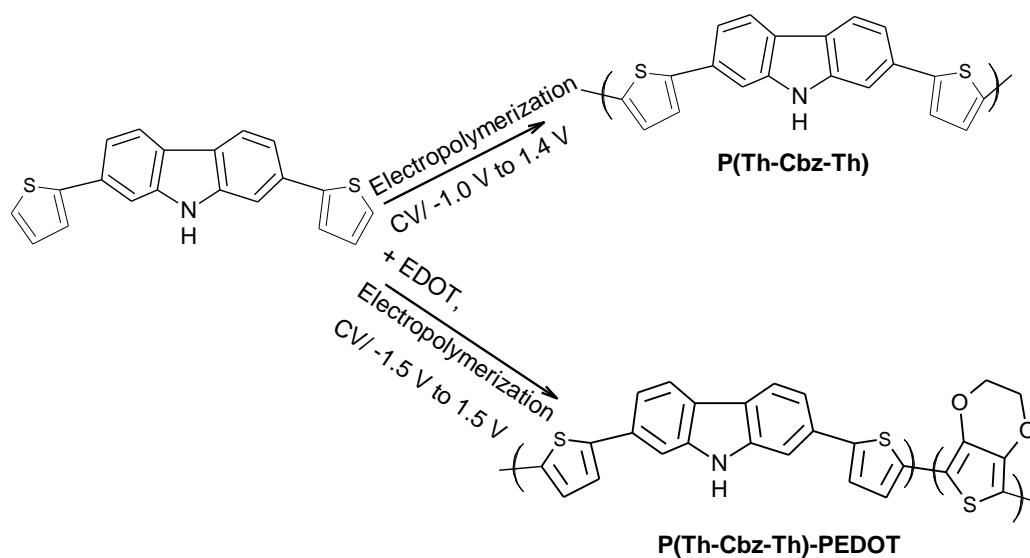
Scheme 6.4: Synthesis route of P(Th-Cbz-Th) and P(Th-Cbz-Th)-PEDOT polymers by electropolymerization method.

The monomer, Th-Cbz-Th was electrochemically polymerized from a solution containing 5mM of monomer and 10 mM TBAP as supporting electrolyte in DCM between the cyclic potentials of −1.0 and 1.4 V using cyclic voltammetry technique at a scan rate of 100 mVs^{-1}. Synthesis routes of P(Th-Cbz-Th) and P(Th-Cbz-Th)-PEDOT polymers using electropolymerization method are shown in Scheme 6.4. In copolymerization, an equimolar concentration of both monomers (5 mM of Th-Cbz-Th and EDOT) were dissolved in 0.1 M of TBAP in DCM solution with applied potential between −1.5 and 1.5 V. During the cyclic scan, the deposition of polymer films was appeared on the surface of ITO working electrode. The increase of current density by successive CV cycles indicates that the amount of polymer deposited on working electrode increases, as shown in Figure 6.1. Th-Cbz-Th monomer showed an oxidation peak at 1.2 V and two distinct reduction peaks at −0.40 V and 0.36 V, respectively. However, copolymer showed an oxidation peak at 1.36 V and corresponding two reduction peaks were observed at −0.45 and 0.55, respectively. The onset oxidation potential (E_{onset}) was drastically reduced from 0.82 for Th-Cbz-Th to −0.2 V for (Th-Cbz-Th)-PEDOT, which indicated that the latter can be easily oxidized than Th-Cbz-Th.
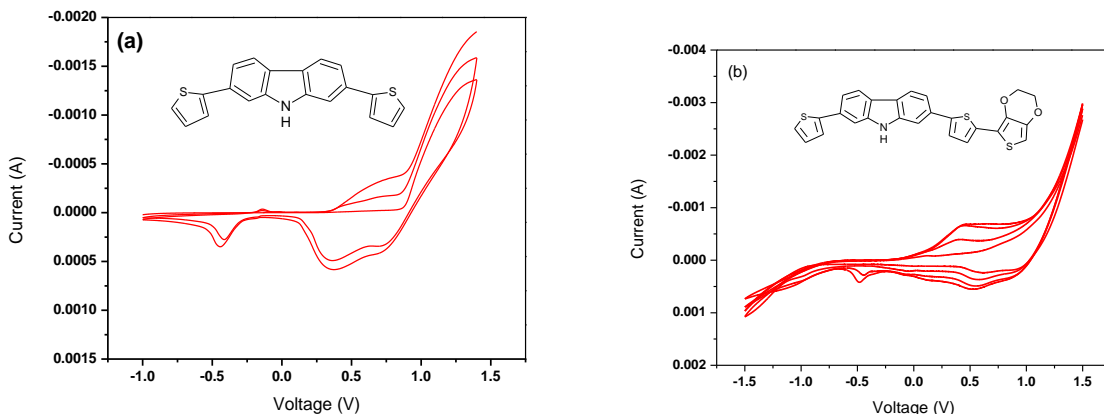
Figure 6.1: Potentiodynamic electropolymerization of (a) P(Th-Cbz-Th) and (b) P(Th-Cbz-Th)-PEDOT at a scan rate of 100 mVs^{-1} in 0.1M TBAP/DCM solution. Inset: Chemical structure of corresponding monomers.

6.3.2. Cyclic Voltammetry
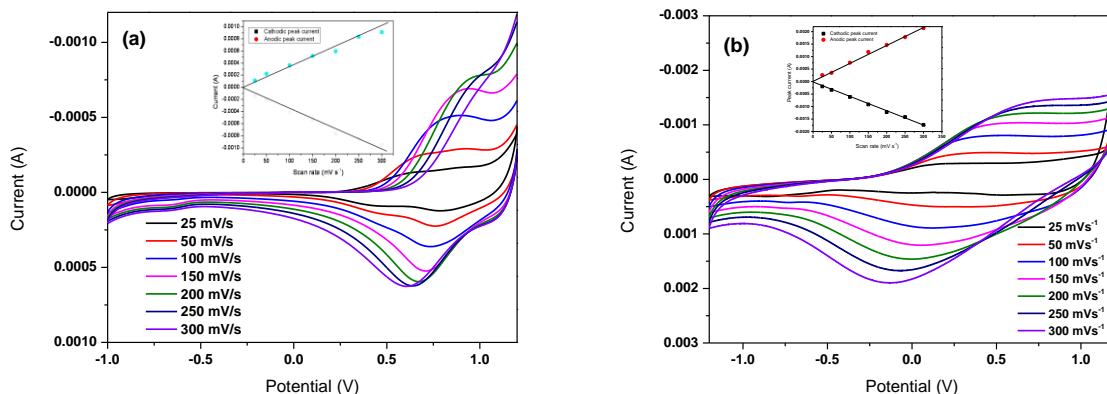
Figure 6.2: Cyclic voltammogram of (a) P(Th-Cbz-Th) and (b) P(Th-Cbz-Th)-PEDOT films at various scan rates in 0.1M LiClO$_4$/ACN solution. Inset: peak current vs. scan rate plot.

The redox behaviour of polymer films were studied by cycling the potential between −1.0 to 1.2 V for P(Th-Cbz-Th) and −1.2 to 1.2 V for P(Th-Cbz-Th)-PEDOT in 0.1M LiClO$_4$/ACN solution at different scan rates as shown in Figure 6.2. Both polymer films showed a well-defined redox peak; however, the reduction peak potential shifted from 0.62 V for P(Th-Cbz-Th) to −0.14 V for P(Th-Cbz-Th)-PEDOT film. The peak current density of polymer films increased upon increasing the scan rate indicating that polymer films are electroactive and adhered well to the electrode surface. P(Th-Cbz-Th) film and P(Th-Cbz-Th)-PEDOT film

exhibit a linear relationship between the scanning rate and peak current, indicating that the electrochemical process of polymer films is reversible and redox process is not diffusion limited.

6.3.3. Spectroelectrochemistry

A series of UV–Vis absorbance spectra of polymer films were recorded as a function of different applied potentials in 0.1 M of LiClO$_4$/ACN solution. The spectroelectrochemistry and the corresponding electrochromic coloration of P(Th-Cbz-Th) film and P(Th-Cbz-Th)-PEDOT film are shown in Figure 6.3. At neutral state (0.2 V), the P(Th-Cbz-Th) film showed a pale yellow color with strong absorption peak at λ_{max} of 390 nm with a shoulder located at 425 nm because of π–π^* transition. Upon stepwise oxidation from 0.2 V, the intensity of π–π^* transition peak decreased, and two new charge carrier absorption bands were observed at 580 nm and 900 nm due to polaronic and bipolaronic bands, respectively. At fully oxidized state (1.5 V), the films showed a dark greyish blue color at λ_{max} of 920 nm.

The P(Th-Cbz-Th)-PEDOT film showed a yellow color at neutral state (0.4 V) and a sharp absorption peak was observed at 454 nm due to π–π^* transition. Compared to P(Th-Cbz-Th), the P(Th-Cbz-Th)-PEDOT film had a red shift of π–π^* transition peak in the visible region, 390 nm to 450 nm. This shift can be attributed to the presence of higher electronic-rich nature of PEDOT moieties, which enhanced the π–π interactions on the polymer backbone and improved the effective conjugation length. At fully reduced state (−2.2 V), the film showed a broad absorption in the visible region centered at 594 nm. Upon oxidation, the intensity of this absorption peak decreased, and two charge carrier peaks were observed at 675 and 930 nm, indicating the formation of polaron and bipolaron bands. It was surprising to find that the P(Th-Cbz-Th)-PEDOT film showed a multi-colored electrochromism under different applied potentials. This film was reddish brown at fully reduced state (−2.2 V) and blue in the fully oxidized state (2.5 V). At intermediate potentials, yellowish green (1.5 V), yellow (0.6V), yellowish brown (−1.5 V), and brown (−2.0 V) appeared.
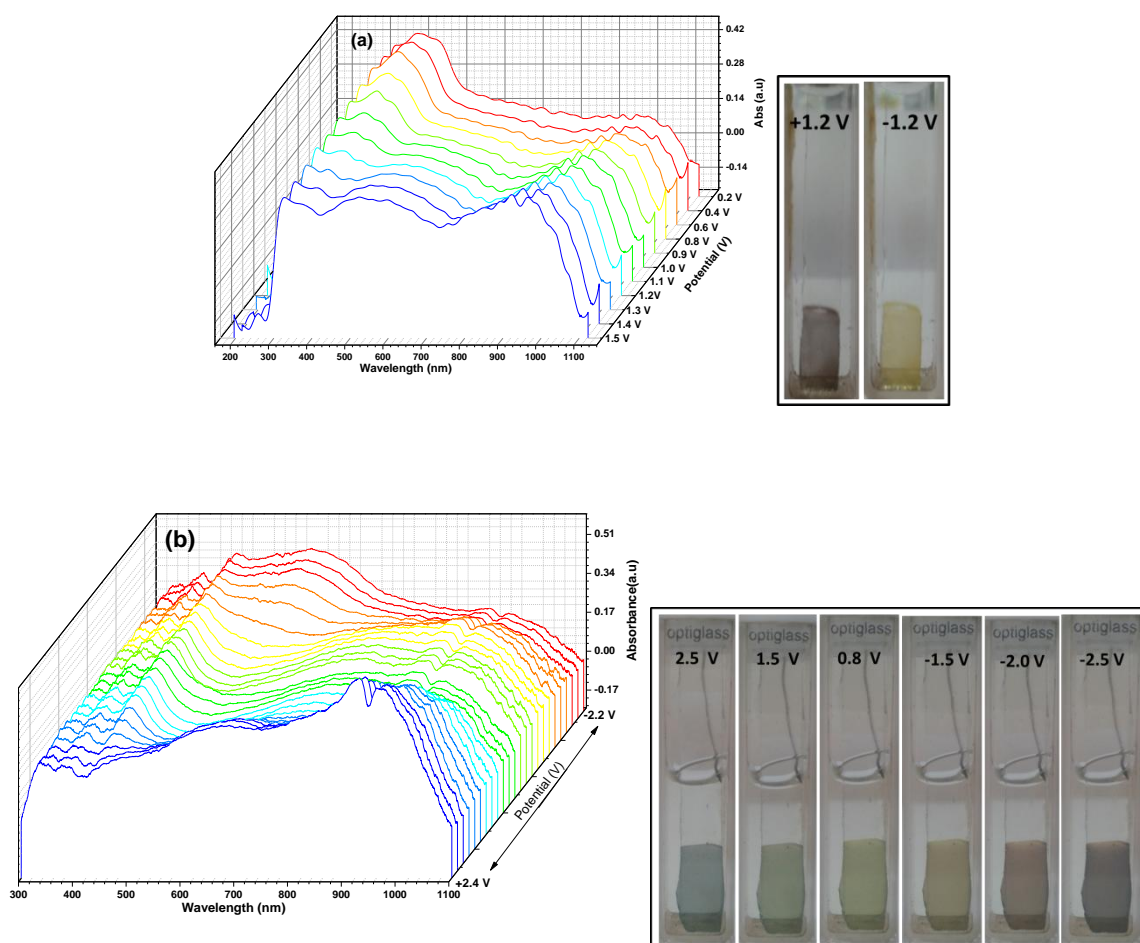
Figure 6.3: Spectroelectrochemistry and corresponding electrochromic colorations of (a) P(Th-Cbz-Th) film and (b) P(Th-Cbz-Th)-PEDOT film as a function of different applied potentials in 0.1 M of LiClO$_4$/ACN solution.

6.3.4. Colorimetry

The color coordinates of P(Th-Cbz-Th)-PEDOT film at different redox potentials were studied by CIELAB 1986 (l*a*b*) method, and plotted as shown in Figure 6.4. At oxidized state (+2.5 V), the film showed color coordinate in the −a* and −b* quadrant represented in the blue region, whereas reduced state (−2.0 V) is in the +a* and +b* quadrant represented in the dark brown region. At intermediate states (1.8 V and 0.8 V), the film appeared to have color coordinates in +a* and +b* quadrant for yellow region and −a* and +b* quadrant for green region, respectively. We have achieved a Red-Green-Blue (RGB) color space material by simple copolymerization with PEDOT to the P(Th-Cbz-Th) chain, which is highly significant since it provides more color combinations for full color electrochromic display applications.

128
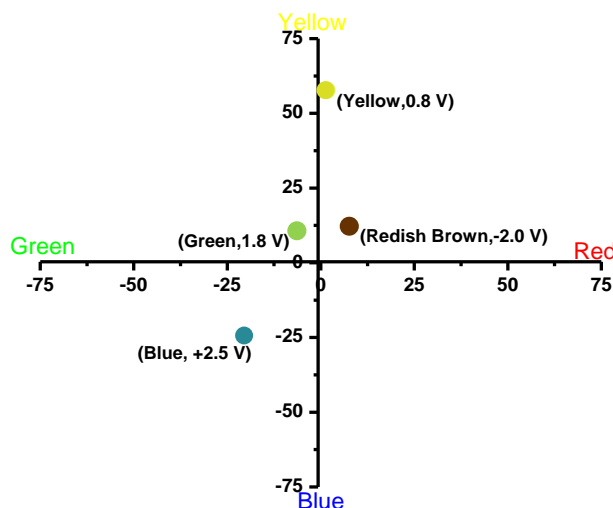
Figure 6.4: CIE 1986 a*b* plot showing the color coordinates of P(Th-Cbz-Th)-PEDOT film between redox potentials.

6.3.5. Optical Switching

The optical switching studies of polymer films were monitored by % transmittance (at λ_{max}) with time as a function of stepped potential between −1.5 to +1.5 V at a constant time interval of 10 s in 0.1 M of LiClO$_4$/ACN and are shown in Figure 6.5. These polymer films showed reasonable optical contrast at the visible and near IR regions, 650 nm and 950 nm for P(Th-Cbz-Th) film and 550 nm and 950 nm for P(Th-Cbz-Th)-PEDOT film. The color contrast of the P(Th-Cbz-Th) film was calculated to be 43 % and 47 % at 650 nm and 950 nm, respectively. The P(Th-Cbz-Th)-PEDOT film also showed a good color contrast both in visible and near IR regions as 43% (550 nm) and 56 % (950 nm), respectively. The good optical color contrast observed especially in near IR region is a significant property of these materials and can be utilized as a promising material for NIR applications. The response time of polymer films during electrochromic switching between −1.5 and +1.5 V was monitored and tabulated in Table 6.1.
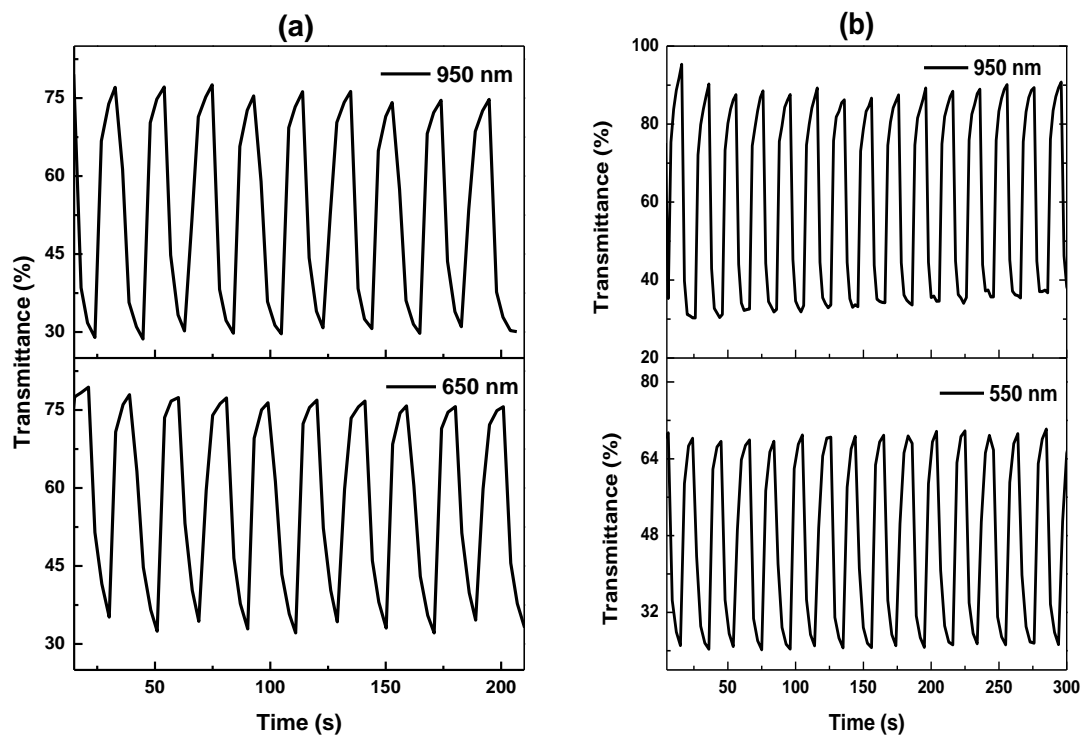
Figure 6.5: The optical switching study of P(Th-Cbz-Th) and P(Th-Cbz-Th)-PEDOT films monitored at different wavelength at applied stepped potential between −1.5 V and +1.5 V.

Table 6. 1: Color contrast and response time values of polymer films

Polymer	λ_{max} (nm)	~T_b (%)	~T_c (%)	ΔT^a (%)	$t_{b\ (s)}^{\ b}$	$t_{c\ (s)}^{\ c}$
P(Th-Cbz-Th	650 nm	76	33	43	3.2	4.2
	950 nm	77	30	47	2.8	3.6
P(Th-Cbz-Th)-	550 nm	68	25	43	2.5	3.0
PEDOT	950 nm	88	32	56	2.5	1.8

[a] $\Delta T = T_b - T_c$, where T_b- transmittance at bleached state, T_c-transmittance at colored state, [b&c] Calculated the response time for bleaching (t_b) and coloring (t_c) of polymer film at 95 % of full switch.

6.3.6. Open Circuit Memory

The open circuit memory of polymer films was monitored at λ_{max} of 600 nm for P(Th-Cbz-Th) film and 550 nm for P(Th-Cbz-Th)-PEDOT film as a function of time under redox potential as shown in Figure 6.6 a&b, respectively. The potential was applied to polymer film for 30 s to stabilize the color and then the circuit was opened up to 300–400 s. At oxidized state (−2.0 V), both polymer films showed a stable open circuit memory throughout the experiment without any change in %T after the circuit was opened. But in the reduced state, polymer films showed cumulative degradation of transmittance (~10% T) with time when potential was opened after 30 s. However this limitation can be overcome by applying a consecutive positive potential to maintain a fully colored state.
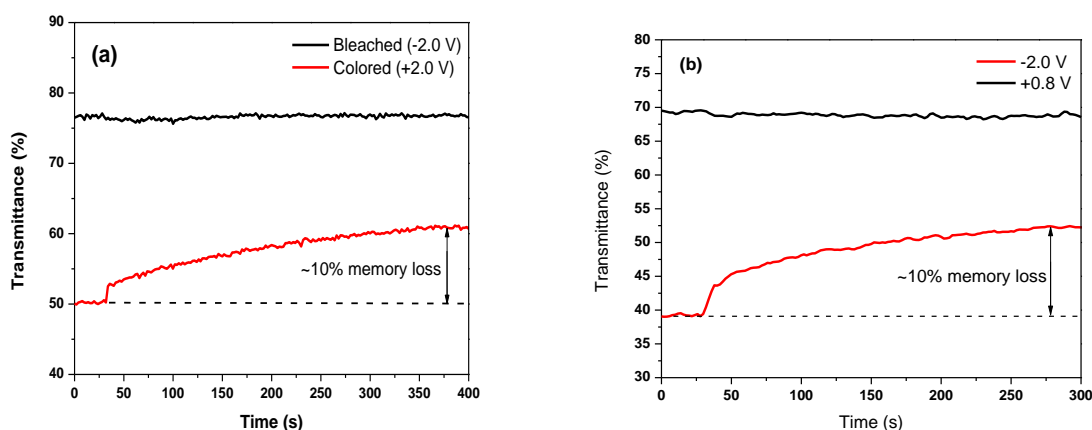

Figure 6.6: The open circuit memory of (a) P(Th-Cbz-Th) and (b) P(Th-Cbz-Th)-PEDOT films monitored at 600 nm and 550 nm, respectively at reduced and oxidized states.

6.4. Performance Testing of Electrochromic Window

6.4.1. Spectroelectrochemistry

A single-type electrochromic window (ECW) was fabricated based on P(Th-Cbz-Th) and P(Th-Cbz-Th)-PEDOT films and their spectroelectrochemical properties were studied as a function of different applied potentials as shown in Figure 6.7. At fully neutral state (0.0 V), the P(Th-Cbz-Th) based device showed a sharp peak at 396 nm that can be attributed to π–π* transition. During step-wise oxidation, the intensity of absorption due to π–π* transition gradually decreased and two new absorption peaks appeared at around 600 nm and 950 nm, due to the formation of polaronic and bipolaronic bands.

131
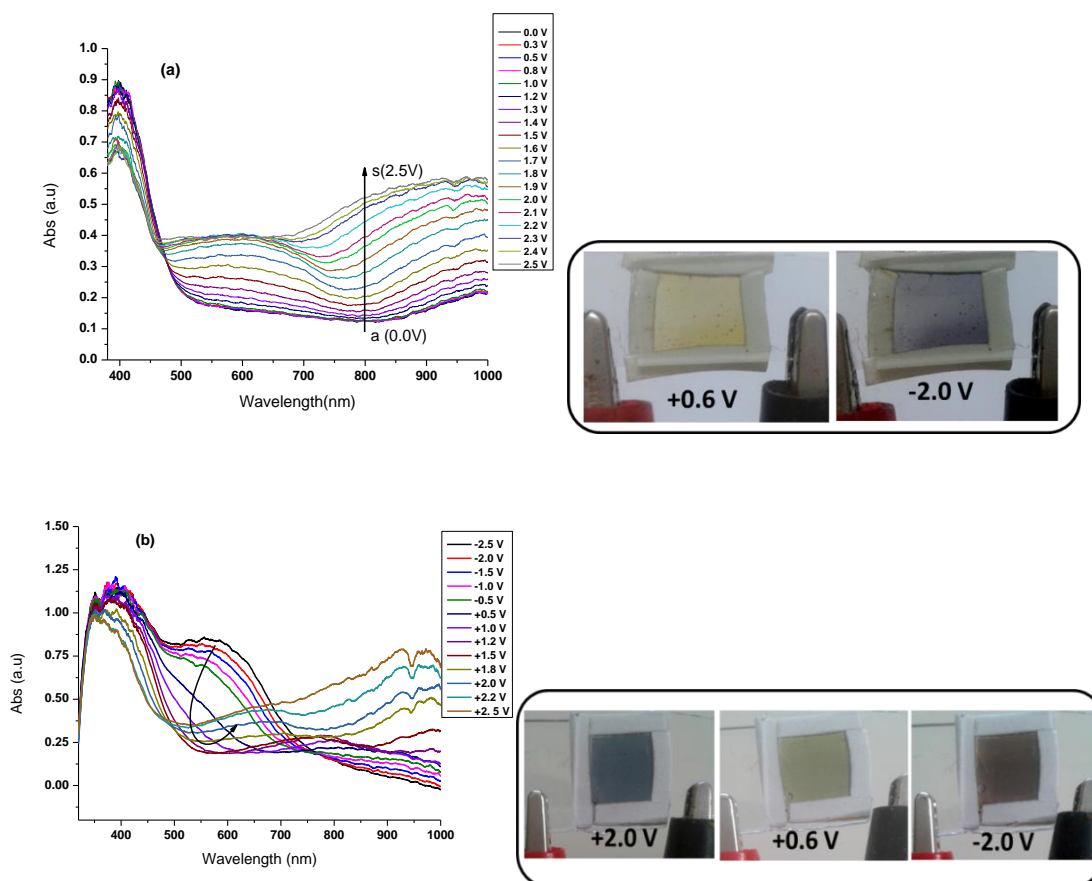
Figure 6.7: Spectroelectrochemistry of (a) P(Th-Cbz-Th) and (b) P(Th-Cbz-Th)-PEDOT based ECWs as a function of different applied potentials and its corresponding electrochromic colorations (Active area of the devices: ~2.0 cm^2).

At neutral state (+0.5 V), the P(Th-Cbz-Th)-PEDOT based electrochromic window showed a pale yellow color with strong absorption peaks at λ_{max} of 400 nm that were due to π–π* transition of P(Th-Cbz-Th)-PEDOT layer. During stepwise oxidation, the absorption due to π–π* transition peak decreased and two charge carrier absorption bands were observed at 680 nm and 950 nm due to polaronic and bipolaronic bands. At fully reduced state (−2.5 V), a broad absorption peak centered at 586 nm appeared, which covered the whole region of visible spectrum. This EC window showed multi-colorations like blue, yellow and brown at fully redox potentials of +2.0 V, 0.6 V, and −2.0 V respectively.

6.4.2. Optical Switching

The optical switching response of P(Th-Cbz-Th) and P(Th-Cbz-Th)-PEDOT based ECWs were monitored by % transmittance at different λ_{max} with time as a function of applied potentials at regular pulse intervals. The P(Th-Cbz-Th) device also showed a reasonable

optical contrast at 650 nm and 900 nm that was found to be about 28% and 43%, respectively (Figure 6.8a). The response time for bleaching and coloration were about 3.2 s and 4.2 s for 650 nm and 2.8 and 3.6 s for 950 nm, respectively. Figure 6.8 b shows the optical switching response of P(Th-Cbz-Th)-PEDOT device monitored at 550 and 950 nm. The optical contrast was calculated to be 33% and 40% for 550 nm and 950 nm, respectively. The bleached and coloration time was calculated as ~1.2 s and ~2.0 s for 550 nm and 2.2 s and 3.0 s for 950 nm, respectively.
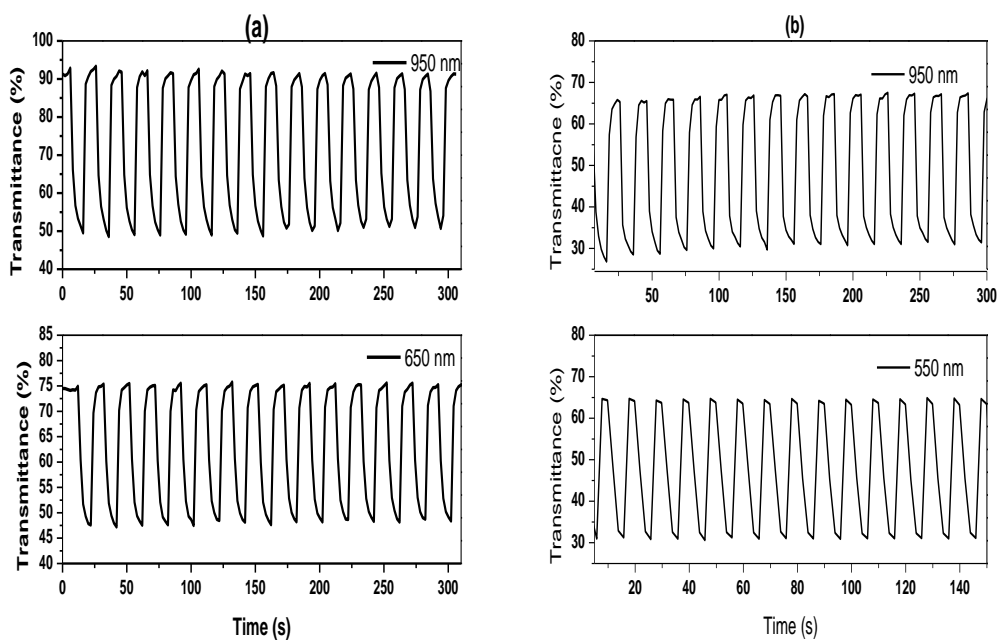


Figure 6.8: Electrochromic switching response of (a) P(Th-Cbz-Th) device monitored at different wavelength between the potential of −2.0 V and +2.0 V with a pulse interval of 10 s and (b) P(Th-Cbz-Th)-PEDOT device at applied potential between −1.5 V and +2.5 V with constant interval of 5 s (550 nm) and 10 s (950 nm).

### 6.4.3. Open Circuit Memory and Electrochemical Long-term Stability

The open circuit memory of electrochromic window was examined as a function of time by applying redox potentials for 30 s to stabilize the color (or bleach) and then the circuit potential was opened to 300–400 s. In Figure 6.9a, the P(Th-Cbz-Th) device showed a constant optical memory at reduced state (transparent yellow, 74% T) and there were no transmission changes observed after the circuit was opened. But in the oxidized state, the device showed lower stability in terms of color resolution that changed the % of transmittance from 36 % to 49%. Thereafter, the device exhibited constant memory throughout the experiment. The P(Th-Cbz-Th)-PEDOT device also showed a steady optical

memory at reduced state; however, a small variation in optical memory at oxidized state from 13 % to 25 % T, was observed. This limitation observed at oxidized state can be overcome by applying regular current pulses to retain its original colored state.
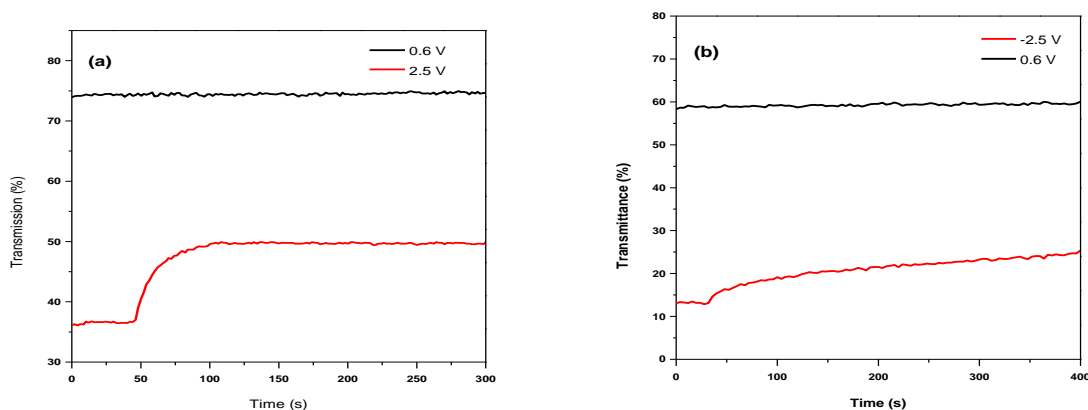
Figure 6.9: Open circuit memory of (a) P(Th-Cbz-Th) and (b) P(Th-Cbz-Th)-PEDOT based electrochromic windows monitored at 650 nm and 550 nm, respectively.

The electrochemical long-term stability of fabricated electrochromic windows were studied using cyclic voltammetry between the applied cyclic potentials for 250 cycles at a scan rate of 250 mVs^{-1} as shown in Figure 6.10. Both the devices showed good cyclic long term stability without much change in redox behaviour indicating that these devices have good long term stability and electrochemical redox response.
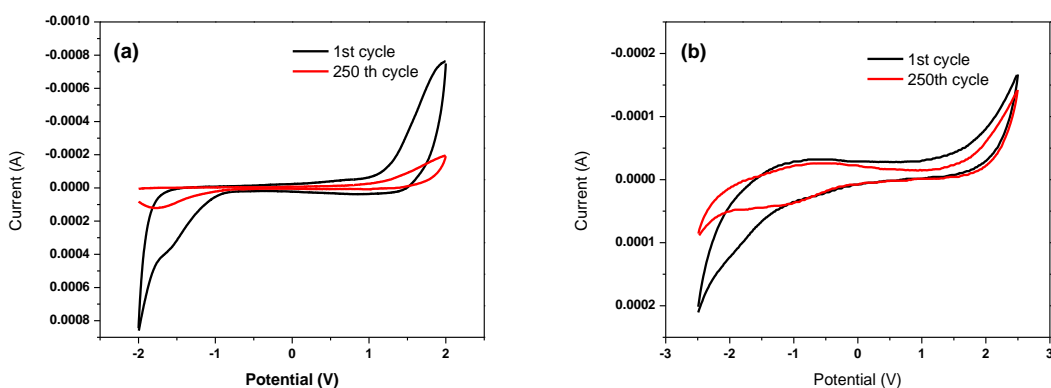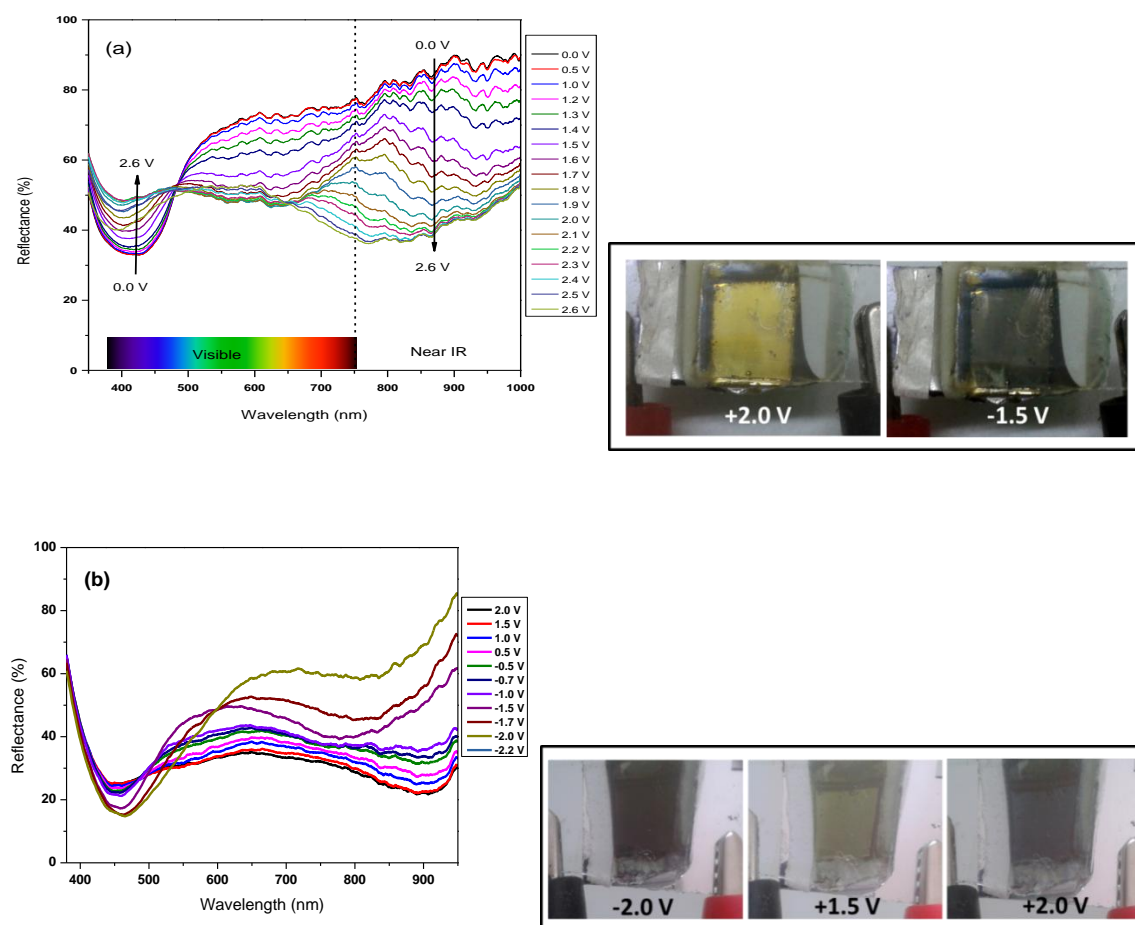

Figure 6.10: The electrochemical stability of (a) P(Th-Cbz-Th) and (b) P(Th-Cbz-Th)-PEDOT based electrochromic windows using cyclic voltammetry at a scan rate of 250 mVs^{-1}.

6.5. Performance Testing of Electrochromic Rear-view Mirror

6.5.1. Spectroelectrochemistry

Figure 6.11: Spectroelectrochemistry of (a) P(Th-Cbz-Th) and (b) P(Th-Cbz-Th)-PEDOT based electrochromic mirrors monitored at % of reflectance as a function of different applied potentials and their corresponding photographs of ECM between redox states Active area of the device: ~2.0 cm^2).

The spectroelectrochemical properties of electrochromic mirror based on P(Th-Cbz-Th) and P(Th-Cbz-Th)-PEDOT film monitored the % of reflectance at different applied potentials. At neutral potential (0.0 V), the P(Th-Cbz-Th) device turns to a transparent yellow (~75% R) with maximum absorption of light at 390 nm due to $\pi \rightarrow \pi^*$ inter band (Figure 6.11a). Upon step-wise oxidation, the peak due to π–π^* transition decreases and two broad absorption peaks are observed at higher wavelength regions, 650 nm and 950 nm due to charge carrier transitions. At fully oxidized state (2.5 V), the active EC layer becomes greyish blue and the reflectivity of the mirror is reduced to about 37%. Figure 6.11b shows the

spectroelectrochemistry of P(Th-Cbz-Th)-PEDOT based mirror at different applied potentials. At reduced state (−2.0 V), this device showed a maximum absorption at about 450 nm due to $\pi \to \pi^*$ transition. During step-wise oxidation, the intensity of peak at 450 nm decreased and a new peak appeared at 585 nm due to polaronic transition. These fabricated ECMs showed a good glare reduction of light both in the visible and the near IR region.

6.5.2. Optical Switching Study

The optical switching studies of P(Th-Cbz-Th) and P(Th-Cbz-Th)-PEDOT based electrochromic rear-view mirrors was monitored by % of reflectance with time as a function of applied stepped potential at regular pulse interval of 10 s. The reflectivity contrast (%ΔR) of ECM between fully colored and bleached states was calculated to be ~24%, and 28% at 550 nm and 950 nm (Figure 6.12a). This %ΔR of the ECM is relatively comparable and significantly useful for glare reduction in the visible as well as in the near IR region when compared with reflective ECD based on PProDOT-Me$_2$ active layer reported by Aubert et al. [15].
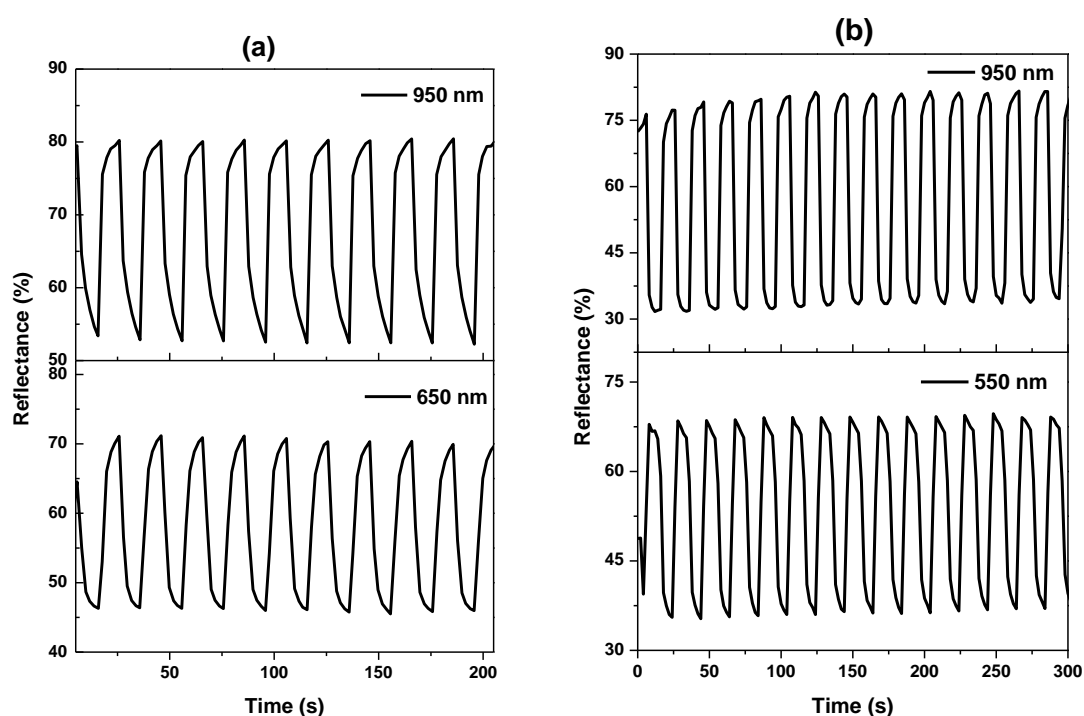
Figure 6.12: The optical switching stability of (a) P(Th-Cbz-Th) and (b) P(Th-Cbz-Th)-PEDOT based ECMs switched potential between −2.0 and +2.0 V.

The response time of ECM was measured at bleached and colored states as ~3.8 s and ~3.2 s at λ_{max} of 650 nm and ~ 2.4 s and 3.8 s for 950 nm, respectively. The coloration efficiency of the ECM was calculated as 57 cm^{2}C^{-1} (charge= 3.04 x 10^{-3} C, active area: 2 cm × 2 cm) at 950 nm in the reduced state, which is significant for practical applications of ECDs. Figure 6.12b shows the optical switching response of P(Th-Cbz-Th)-PEDOT mirror monitored at 550 and 950 nm. The optical contrast was calculated to be about 33% and 48% for 550 nm and 950 nm, respectively. The bleaching and coloring time was calculated as ~2.7 s and 3.5 s for 550 nm and 1.8 s and 2.0 s for 950 nm, respectively. The coloration efficiency of EC mirror was found to be 232 cm^{2}C^{-1} at 950 nm for reduced state (charge= 5.08x 10^{-3} C and active area: 2 x 1.5 cm^2). The P(Th-Cbz-Th)-PEDOT based mirror showed a good contrast ratio, fast response time and higher coloration efficiency when compared with P(Th-Cbz-Th). However, both the EC mirrors showed good optical switching stability and higher reversibility under applied redox potential.

6.5.3. Open Circuit Memory and Electrochemical long-term Stability
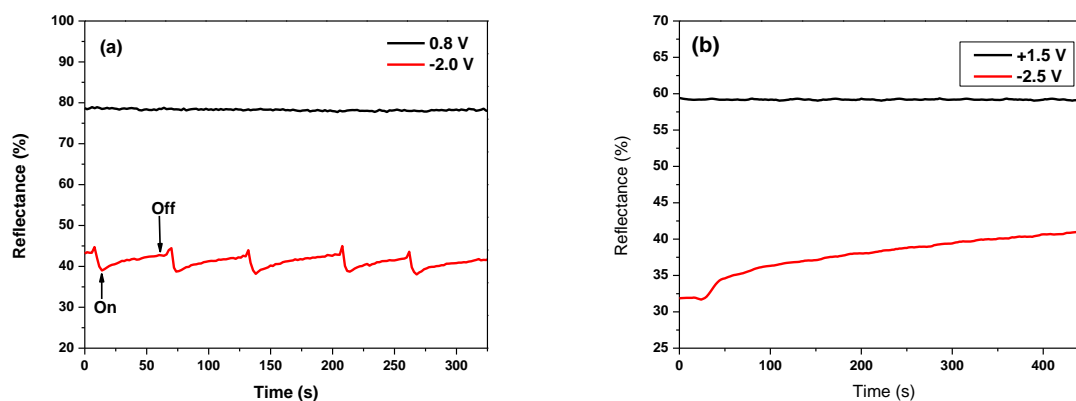

Figure 6.13: The open circuit memory of electrochromic mirror based on (a) P(Th-Cbz-Th) and (b) P(Th-Cbz-Th)-PEDOT film at λ_{max} of 650 nm and 550 nm, respectively.

The open circuit memory of P(Th-Cbz-Th) and P(Th-Cbz-Th)-PEDOT based mirrors was studied by monitoring the % reflectance change (at λ_{max}) as a function of time under applied redox potential for 30 s to stabilize the color (or bleach), and then the circuit potential was opened up to 300–400 s. As shown in Figure 6.13a, the P(Th-Cbz-Th) mirror showed a stable optical memory at bleached state after the circuit was opened. But in the colored state, this device showed poor stability of color and this drawback can be improved by applying the pulse at regular intervals to achieve the fully colored state. The P(Th-Cbz-Th)-PEDOT mirror

also showed similar optical memory properties at colored and bleached states. This device showed a constant optical memory at oxidized state (+1. 5 V) and relatively lower memory was observed at reduced state (−2.5 V).

The redox long term switching stability of fabricated ECM based on P(Th-Cbz-Th) and P(Th-Cbz-Th)-PEDOT film was studied using CV between the applied redox potential at a scan rate of 250 mVs^{-1} as shown in Figure 6.14. We noticed that both the mirrors retained their electrochemical activity after 250 cycles, revealing that mirrors have good long term electrochemical stability and significant electrochemical redox activity.
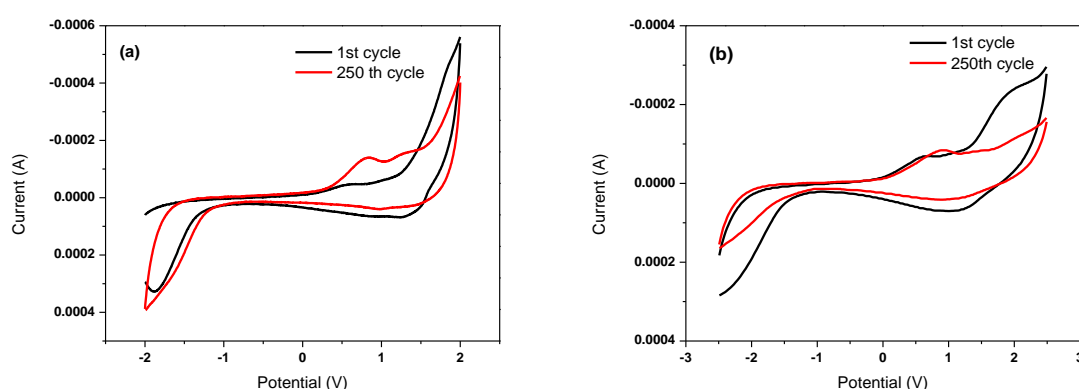
Figure 6.14: Redox long-term stability of (a) P(Th-Cbz-Th) and (b) P(Th-Cbz-Th)-PEDOT based ECMs as function of repeated cycles between applied potential at a scan rate of 250 mVs^{-1}.

6.7. Summary

We synthesized a new trimeric monomer based on thiophene-carbazole-thiophene units using stille coupling method. The corresponding polymer and its copolymer with PEDOT were electrochemically prepared and characterized. The spectroelectrochemical and electrochromic properties of P(Th-Cbz-Th) and P(Th-Cbz-Th)-PEDOT films were studied. Though P(Th-Cbz-Th) has only two colors (yellow and greyish blue) between redox state, its copolymer, P(Th-Cbz-Th)-PEDOT showed multi-colored (blue, greenish yellow, yellow, yellowish brown, brown, and reddish brown) electrochromism. However, both polymer films showed reasonable optical contrast in the visible and near IR regions, applicable response time, and better optical memory. The P(Th-Cbz-Th)-PEDOT film not only lowered the oxidation potential, but also enhanced the oxidation states of material compared to their corresponding homopolymer. In addition, the single type electrochromic window and mirror based on these

polymers were fabricated and characterized. The P(Th-Cbz-Th) based device showed two different colors, while P(Th-Cbz-Th)–PEDOT device displayed multi-colored between redox potentials. Both EC windows and rear-view mirrors also showed significant optical contrasts at visible and near IR regions, fast response time, applicable coloration efficiency, good open circuit memory, and better electrochemical stability. These multi-colored carbazole-thiophene based polymers can also be used as potential candidates for electrochromic display applications.

6.8. References

[1]   Liu D. Y., Chilton A. D., Shi P., Craig M. R., Miles S. D., Dyer A. L., Ballarotto V. W., Reynolds J. R., *Adv. Funct. Mater.*, 2011, 21: 4535–4542.

[2]   Beaujuge P. M., Reynolds J. R., *Chem. Rev.*, 2010, 110: 268–320.

[3]   Gunbas G., Toppare L., *Chem. Commun.*, 2012, 48: 1083–1101.

[4]   Dyer A. L., Thompson E. J., Reynolds J. R., *ACS Appl. Mater.Interfaces* 2011, 3: 1787–17995.

[5]   Beaujuge P. M., Ellinger S., Reynolds J. R., *Nat. Mater.*, 2008,7: 795–799.

[6]   Beaujuge P. M., Vasilyeva S. V., Ellinger S., McCarley T. D., Reynolds J. R., *Macromolecules*, 2009,42: 3694–3706.

[7]   Durmus A., Gunbas G., Camurlu P., Toppare L., *Chem. Commun.*, 2007, 3246–3248.

[8]   Durmus A., Gunbas G., Toppare L., *Adv. Mater.*, 2008, 20: 691

[9]   Ocampo C., Aleman C., Oliver R., Arnedillo M. L., Ruiz O., Estrany F., *Polym. Int.* 2007, 56: 803–809.

[10]   Chen S., Gao Q., Zhao J., Cui C., Yang W., Zhang X., *Int. J. Electrochem. Sci.*, 2012, 7: 5256–72.

[11]   Camarada M.B., Jaque P., Diaz F.R., and del-Valle M.A., *J. Polym. Sci. B*, 2011, 49: 1723–33.

[12]   Tarkuc S., Ak M., Onurhan E., Toppare L., *J. Macromol. Sci. A*, 2008, 45: 164–171.

[13]   Ranjith K., Swathi S. K., Kumar P., Ramamurthy P. C., *Sol. Energy Mater. Sol. Cells*, 2012, 98: 448–454.

[14]   Carsten B., He F., Son. H.J., Xu T., Yu L., *Chem. Rev.*, 2011, 111: 1493–1528.

[15]   Aubert P.H, Argun A. A., Cirpan A., Tanner D. B., Reynolds J. R., *Chem. Mater.*, 2004, 16: 2386–2393.

CHAPTER 7

Conclusions and Future Scope

7.1 Conclusions

This thesis includes a detailed study on the design, synthesis, and characterization of various electrochromic conducting polymers for electrochromic device applications. The optical properties of various electrochromic conducting polymers, which were tailored using dopant, functionalized graphene, structural modifications, and copolymerization method have been conducted and presented in this dissertation. We have also described about fabrication of transmissive and reflective type electrochromic devices based on the prepared conducting polymers.

Chapter 1 describes an overview about conjugated polymers, electrochromic concept, materials and applications. Thesis objective and outlines are also discussed in this chapter. Chapter 2 provides an overview of experimental methods and the basic concepts of characteristic techniques, which are used to analyse the structural, electrochemical, and electrochromic properties of the materials, films and devices presented in this research.

In Chapter 3, the effects of dopant and polymerization methods on morphological, electrochemical and electrochromic properties of PEDOT film were investigated. The PEDOT film prepared by potentiostatic method showed better optical properties than the film prepared by potentiodynamic method. The PEDOT doped with PSS showed a higher color contrast, faster response, good coloration efficiency, stable optical memory and better optical switching stability. The dual-type electrochromic window enhanced the color contrast from 32 % T to 45% T when related to the single type electrochromic window. These cost-effective ECDs can be used as economically promising devices for practical applications.

Chapter 4 addressed the incorporation of ion enriched graphene (IEGR) on PEDOT matrix and its influence on the intrinsic properties of PEDOT was studied. The PEDOT-IEGR film exhibits a higher conductivity (~3968 Scm^{-1}) and ionic conductivity (3.125×10^{-7} Scm^{-1}). This film also showed good capacitance behaviour and a higher diffusion coefficient value compared to PEDOT film. The PEDOT-IEGR film not only tuned the optical bandgap but also improved electrochromic properties. This film showed broad absorption (400–750 nm)

140

and the electrochromic coloration changed between greyish purple and transmissive blue while compared to conventional PEDOT. The PEDOT-IEGR showed reasonable color contrast both in the visible and near IR regions, a faster switching response, good optical memory, better optical switching stability and electrochemical long-term stability. Due to the good capacitance nature and broad absorption of PEDOT-IEGR film over entire visible spectrum, it can also be used as a promising material in energy storage, and photovoltaic applications.

The solution processable di-isopropylbenzyl derivative of poly(3,4 propylene dioxythiophene) nanobelts using reverse microemulsion method was introduced in Chapter 5. PProDOT-IPBZ$_2$ nanobelts exhibit length of 4–6 μm and a width of 25± 5 nm with higher aspect ratio (3:100). This nanobelt with thickness of 20±5 nm showed good flexibility and can be bent 45–90º angle. The chemically prepared, cathodically coloring PProDOT-IPBZ$_2$ showed good solubility in common organic solvents and its film can be prepared by solution processable techniques. The substitution of bulky and flexible isopropyl benzyl group on propylenedioxy ring not only improved the solubility but also enhanced the electrochromic properties of the material. This polymer can also be prepared by electropolymerization method and the effect of film thickness on electrochromic properties of PProDOT-IPBZ$_2$ film was studied. The direct influence of film thickness on color contrast and response time was observed. The electropolymerized PProDOT-IPBz$_2$ film exhibits a contrast ratio of 48% at 550 nm, faster switching speed (~1 s) and higher coloration efficiency (305 cm^2 C^{-1}). The PProDOT-IPBz$_2$ film showed a high transparency (~85% T) at fully oxidized state and dark purple color (~30% T) at fully reduced state. The PProDOT-IPBz$_2$ based electrochromic window and rear-view mirror showed a good optical contrast, low operation voltages (±1.0 V), excellent optical memory at the colored and bleached states, and better optical switching stability for more than 1000 cycles. The dark purple electrochromic mirror can be used as a superior light regulator in both the visible and near IR regions due to the strong absorption of selective complementary yellow (570–600 nm), which is commonly used color in automobile headlights.

In Chapter 6, a π-conjugated monomer unit containing structural components of thiophene and carbazole performed as a single molecule entity was synthesized by stille coupling method. The corresponding polymer, P(Th-Cbz-Th) and its copolymer with PEDOT, P(Th-Cbz-Th)-PEDOT were electrochemically polymerized. Spectroelectrochemical and

electrochromic properties of the polymer films were characterized. The anodically coloring P(Th-Cbz-Th) film shows electrochromic coloration between blackish blue (1.5 V) and pale yellow (−1.0 V). However, the P(Th-Cbz-Th)-PEDOT copolymer film exhibits multi-electrochromic colors from reddish brown to blue; intermediate colors of brown, yellowish brown, greenish yellow, and yellow were also observed. A surprising observation was that Red-Green-Blue (RGB) electrochromic coloration occurred by a simple copolymerization approach, which is highly significant as it offers more color combinations for full color electrochromic display applications. These polymer films showed a good color contrast both in the visible and near IR regions, applicable response time, good optical memory, and better optical switching stability. The electrochromic window and rear-view mirror based on P(Th-Cbz-Th) and P(Th-Cbz-Th)-PEDOT films were fabricated and characterized. These devices also showed a reasonable multi-optical color contrast both in the visible and near IR regions, good optical memory, better optical switching stability and long-term electrochemical stability. The introduction of an electron-donating ethylenedioxy group into carbazole-thiophene based polymer main chain could effectively be improved in the redox stage, providing multi-colored electrochromism. Overall, the research presented in this thesis confirms that the highly promising ECDs based on conducting polymers can be commercialized and these electrochromic conducting polymers can also be used especially in the areas of solar cells, energy storage, and display applications.

7.2. Future Scope

This thesis described various specially synthesized electrochromic materials that are significantly used for developing solid-state electrochromic devices. However, new electrochromic materials and devices of higher efficiency are always in demand in optoelectronic applications. Further efforts to achieve black, broadly absorbing electrochromic material is highly desirable both in emissive and non-emissive opto-electronic technologies. This can be attained by the spectral engineering of conjugated polymers using alternate electron donor and electron acceptor groups along the polymer backbone that make dual band absorbing polymers. Though the EC performances of ECDs have been studied and improved in this thesis, strongly recommend further improvement of the quality and efficiency of the device by designing new materials and by optimizing the fabrication parameters. The electrochromic properties of single-type ECDs presented this research can also be enhanced by dual-type fabrication approach using compatible complementary EC materials.
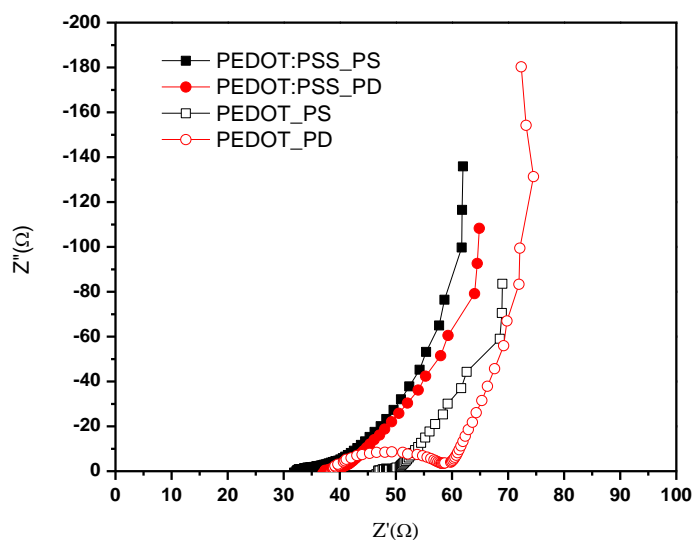
APPENDIX 1

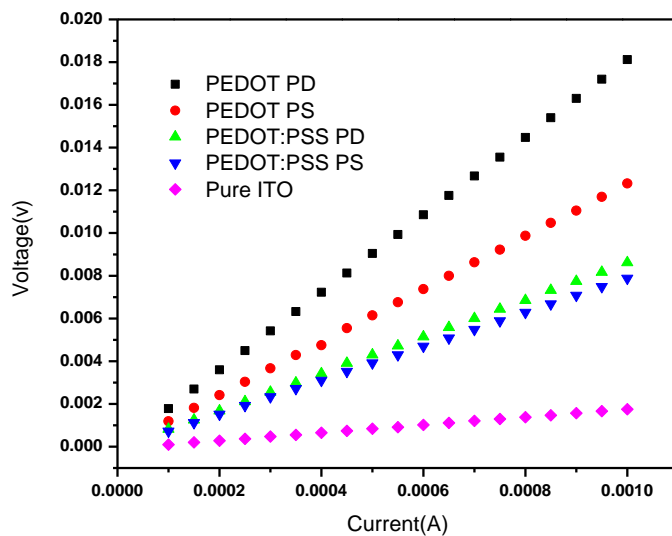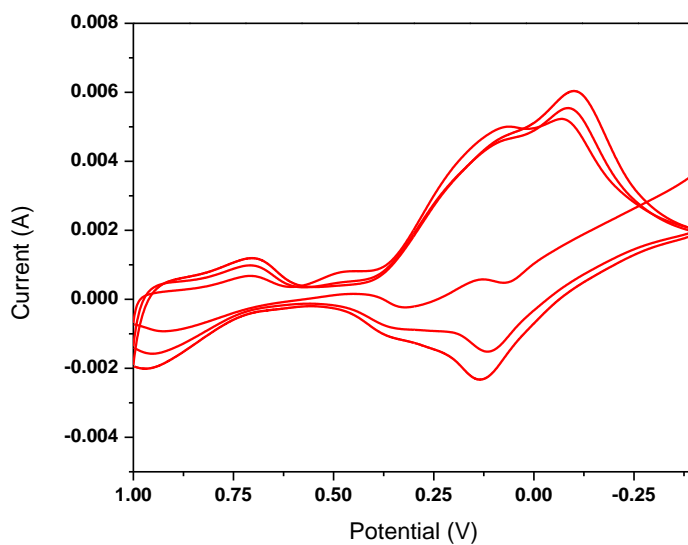# Electrochemical Performance of PEDOT and PEDOT: PSS Films
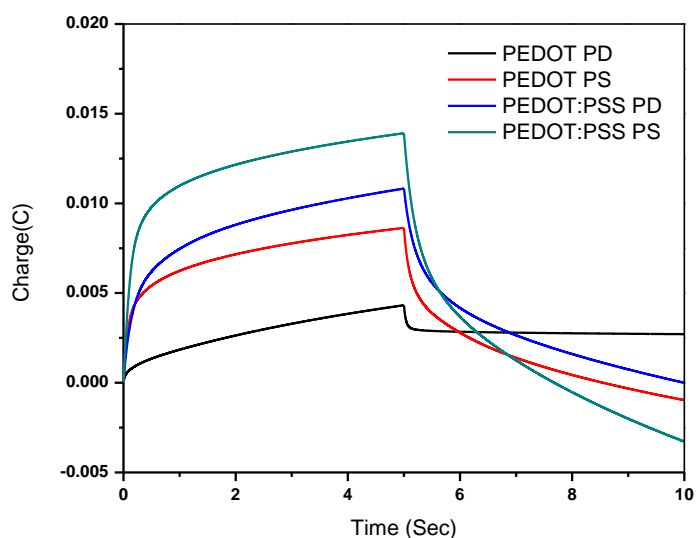
Figure A1.1: Chronocoulometry studies of Polymer films at different polymerization techniques (Potentiostatic and potentiodynamic methods)

Figure A1.2: Electrochemical impedance Spectra of PEDOT and PEDOT:PSS films prepared by PS and PD techniques.

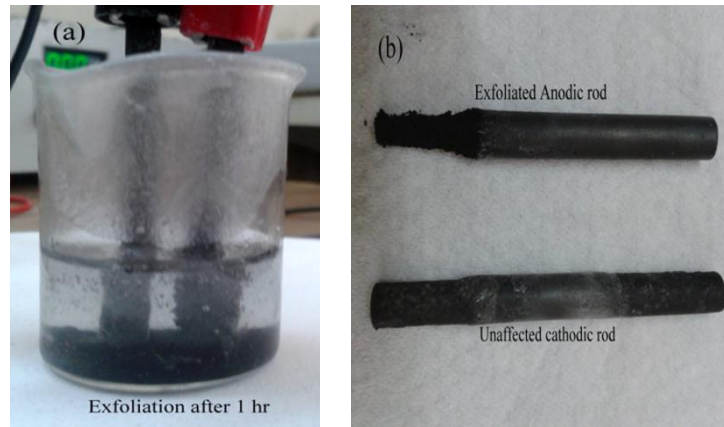**Figure A1.3:** I-V characteristics of PEDOT and PEDOT:PSS films prepared by PS and PD techniques.

Figure A1.4: Electropolymerization of Prussian blue from aqueous solution of K_3 Fe $(CN)_6$) (2 mM) and $FeCl_3$. $6H_2O$ (2 mM) using cyclic voltammetry.

APPENDIX 2

Optical Performance of PEDOT-IEGR Films

Figure A2.1: (a) Photographs of electrochemical exfoliation of graphite rod after 1 hr and (b) Cathodic and anodic graphite rods after exfoliation.
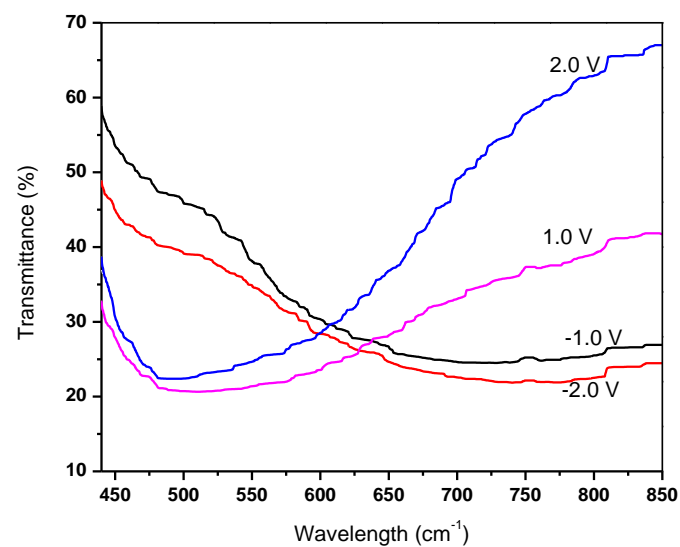
Figure A2.2: Transmittance spectra of PEDOT-IEGR films at different applied potentials.

APPENDIX 3

Structural Characterizations of Monomers and Polymers
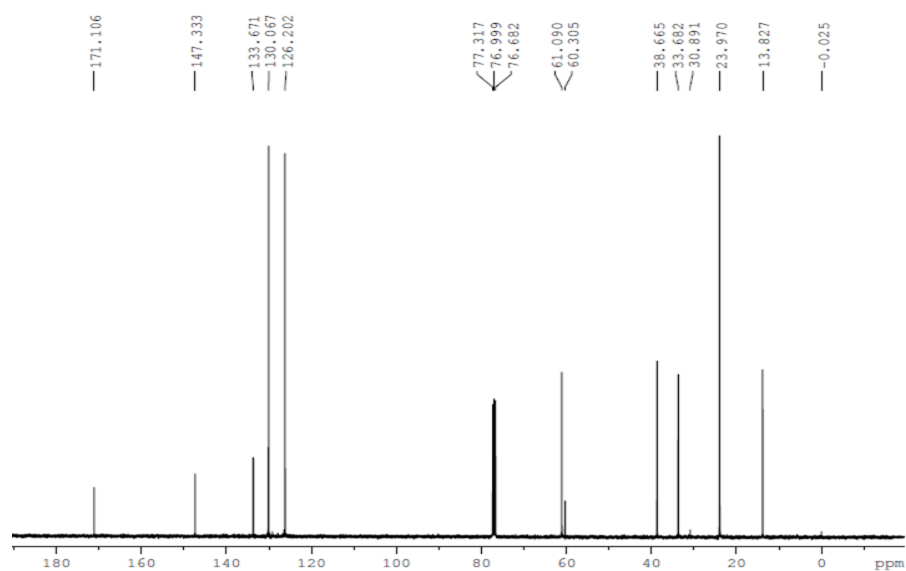
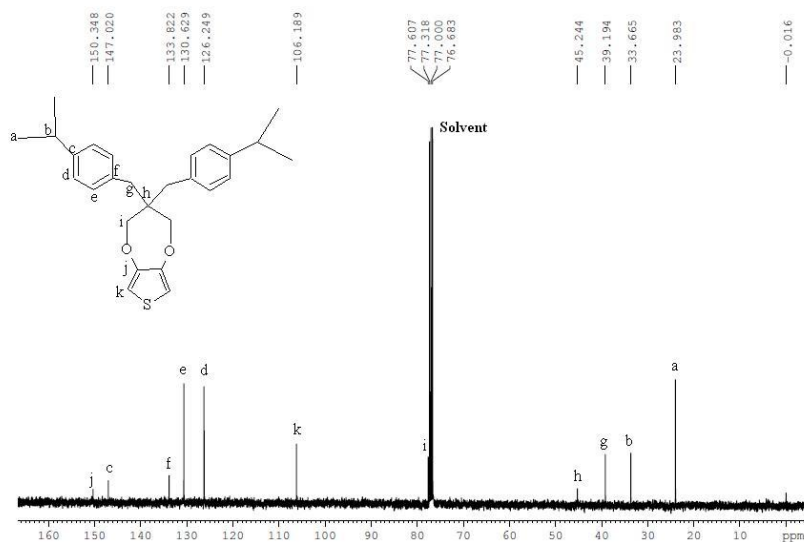**Figure A3.1:** ^{13}C NMR spectrum of 2,2 di isopropyl benzyl malonic acid diethyl ester.
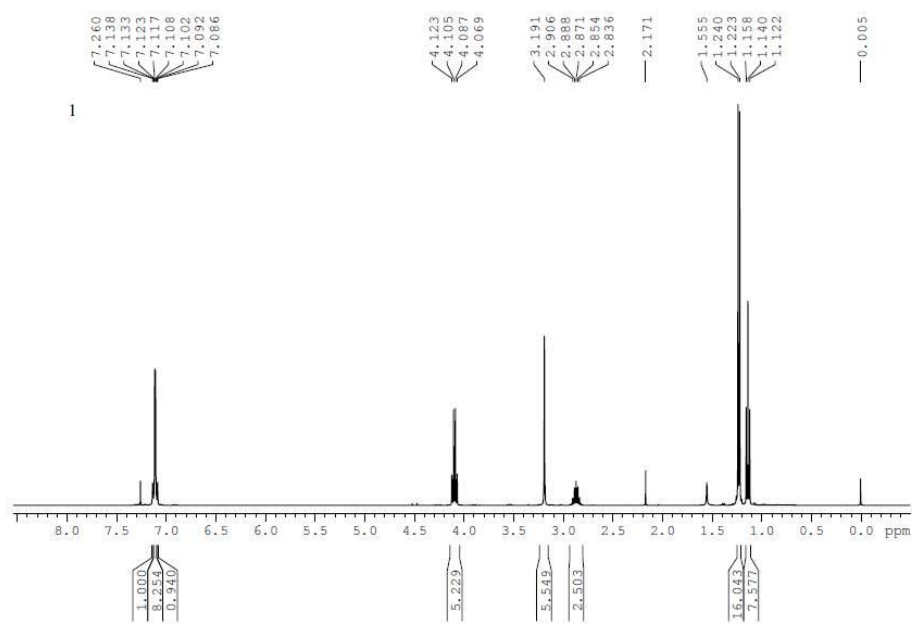
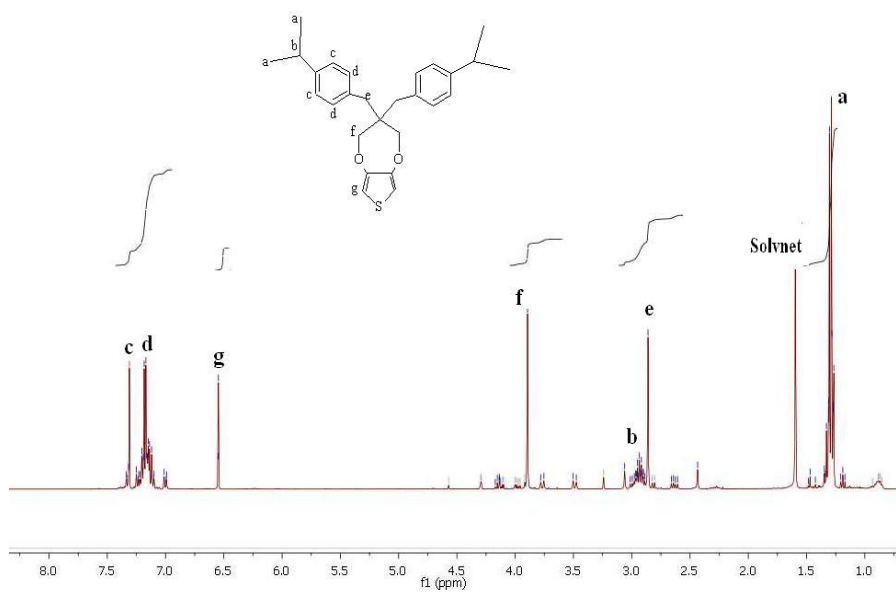**Figure A3.2:** ^{1}H NMR spectrum of 2,2 di isopropyl benzyl malonic acid diethyl ester.
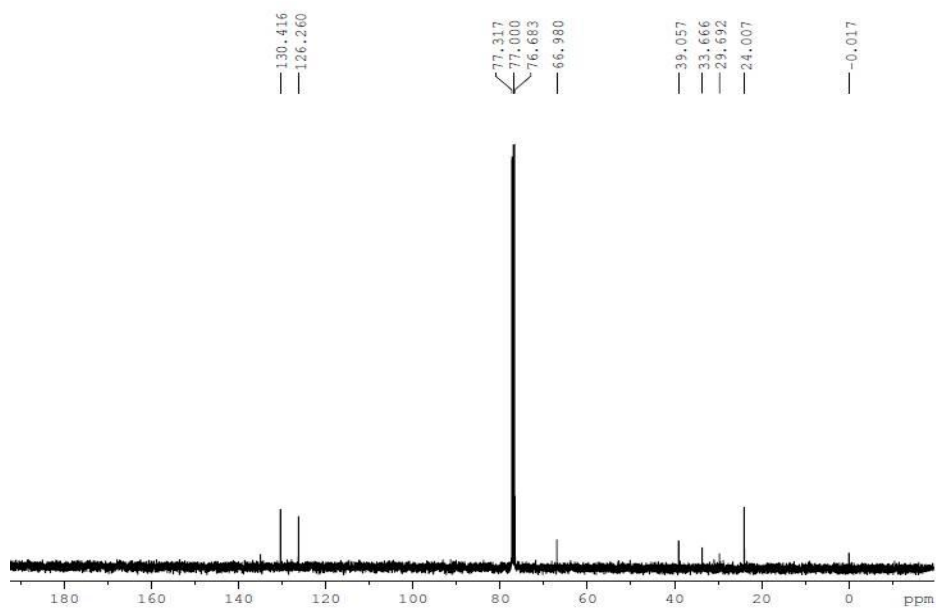
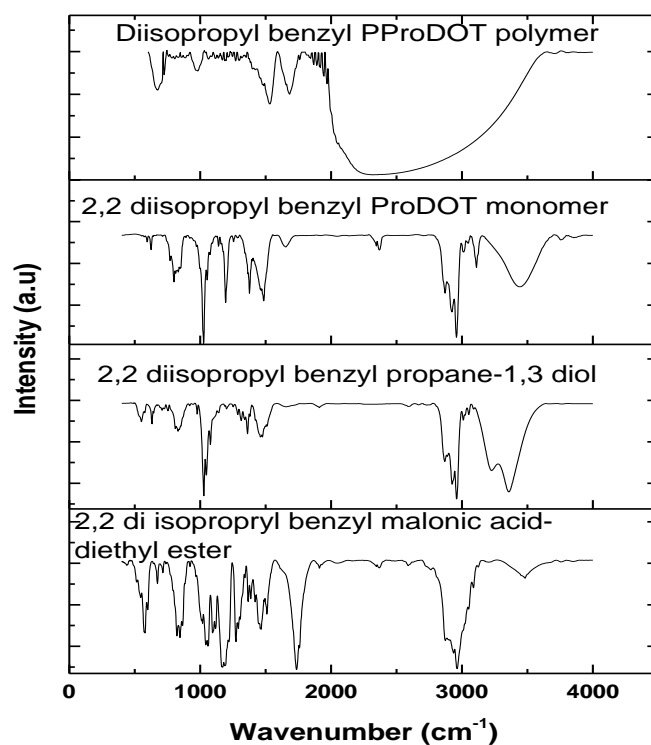**Figure A3.3:** ^{13}C NMR spectrum of 2,2 di isopropyl benzyl propane-1,3 diol.
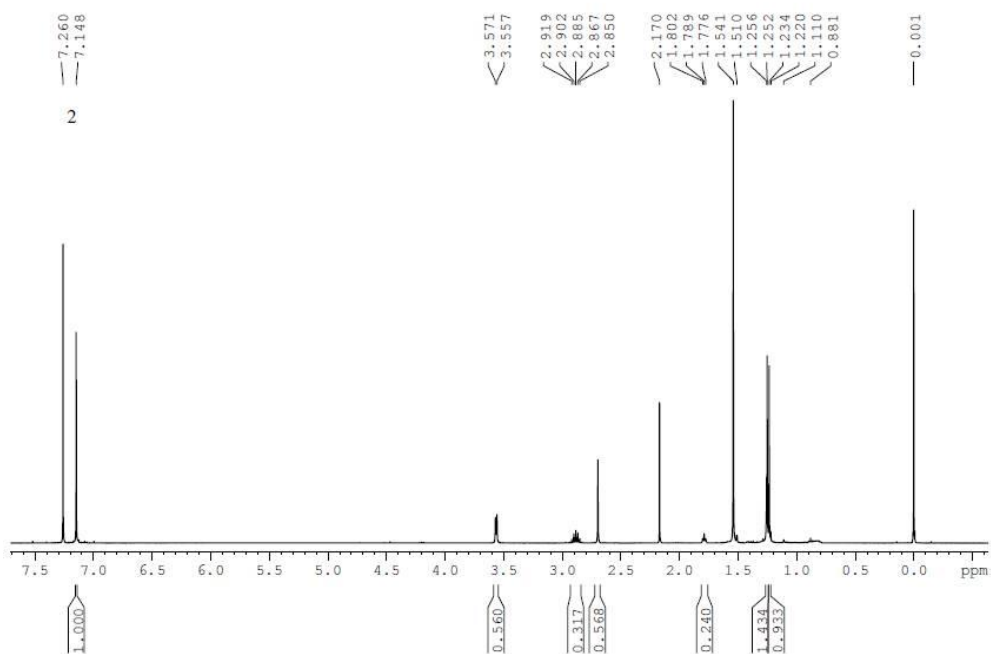
Figure A3.4: ^{1}H NMR spectrum of 2,2 di isopropyl benzyl propane-1,3 diol.

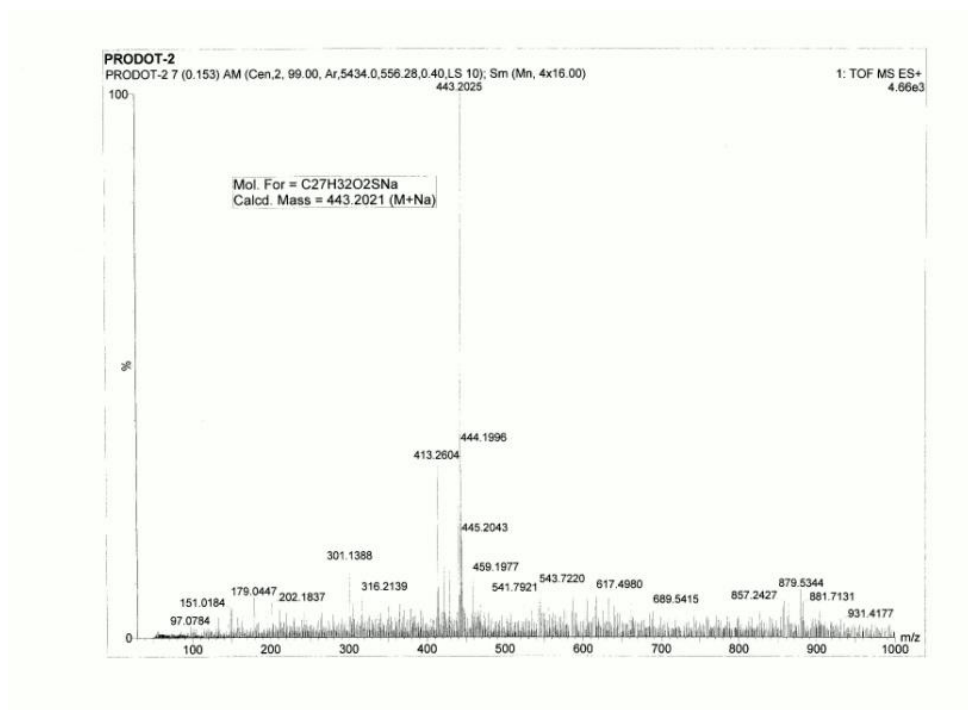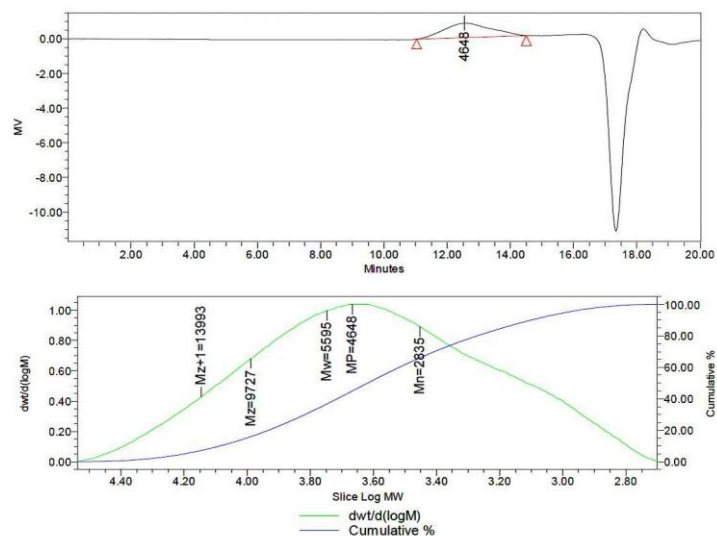**Figure A3.5:** ^{13}C NMR spectrum of di-isopropyl benzyl ProDOT.

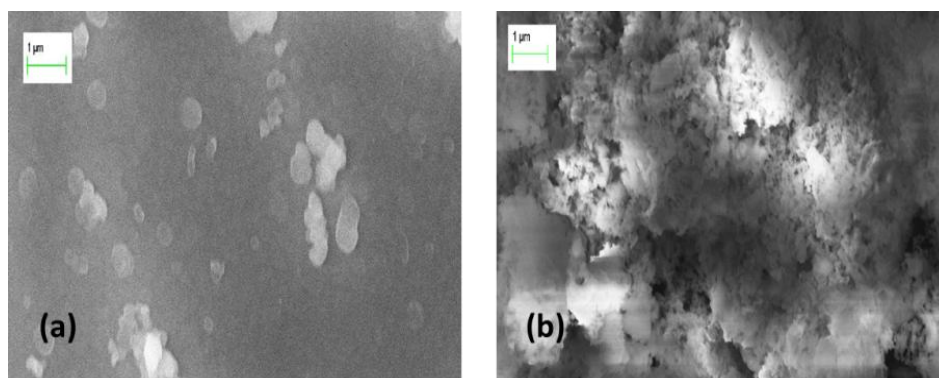**Figure A3.6:** ^{1}H NMR spectrum of di-isopropyl benzyl ProDOT.

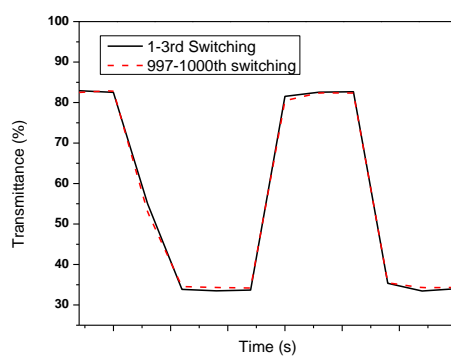**Figure A3.7:** FT-IR spectra of intermediate organic compounds, monomer and polymer

Figure A3.8: Mass spectrum of ProDOT-IPBz$_2$ monomer

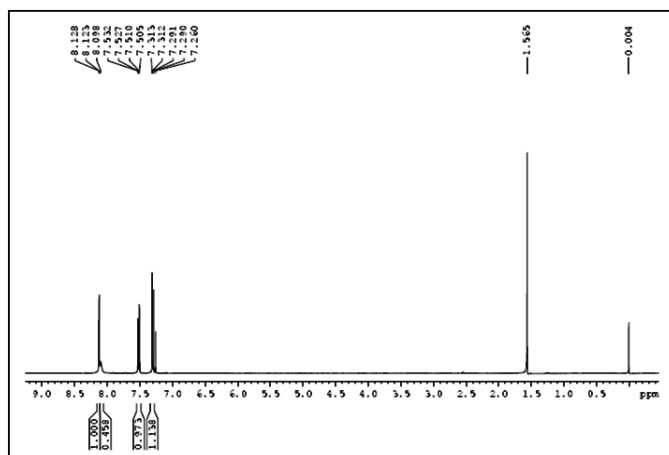**Figure A3.9:** GPC analysis of chemically polymerized ProDOT-IPBz$_2$

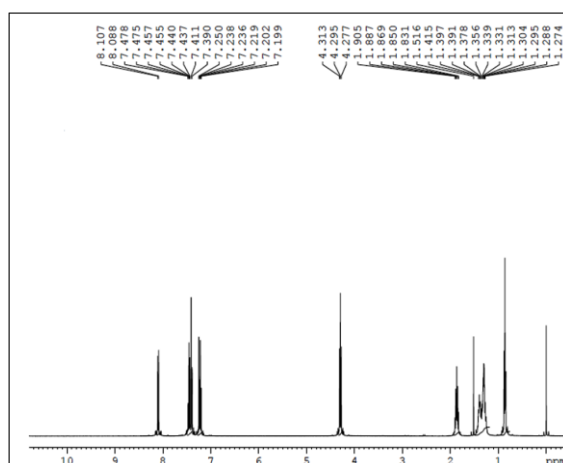**Figure A3.10.** SEM Images of (a) electropolymerized and (b) solution cast PProDOT-IPBz2 film

Figure A3.11. Optical switching stability of electropolymerized PProDOT-IPBz$_2$ film in 0.1 M LiClO$_4$/ACN solution after 1000 cycles.

Figure A3.12: ^{1}H NMR spectrum of 3,6-dibromo carbazole

Figure A3.13: ^{1}H NMR spectrum of tributyl(thiophen-2-yl)stannane
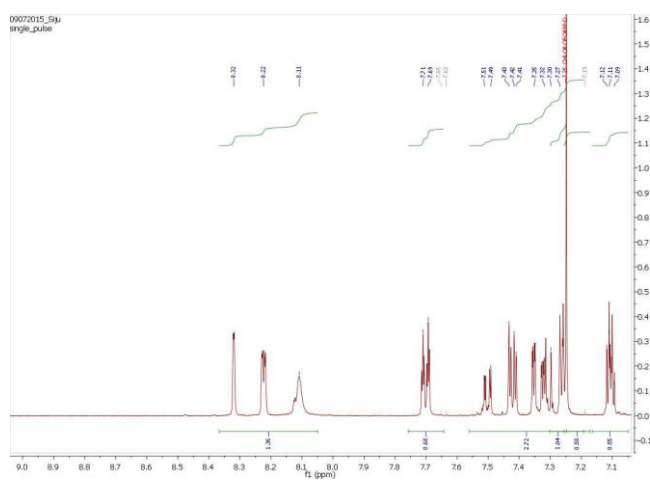
Figure A3.14: ^{1}H NMR spectrum of Th-Cbz-Th monomer

151
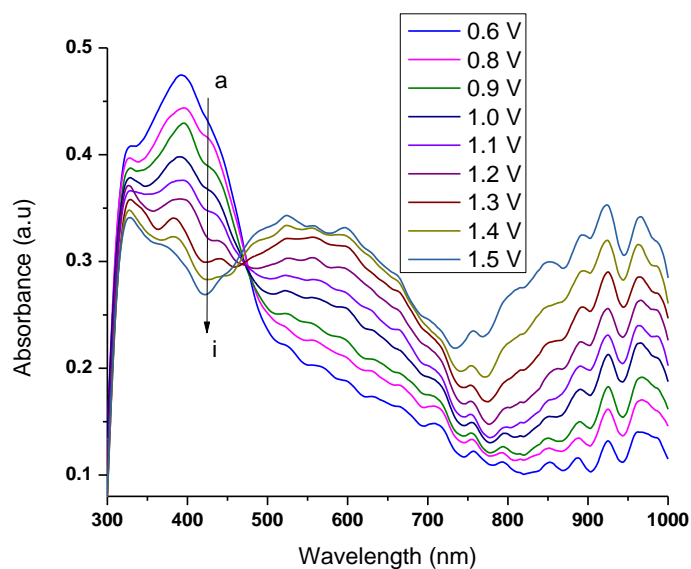
Figure A3.14: Spectroelectrochemical study of P(Th-Cbz-Th) film monitored in 0.1 M of LiClO$_4$/ACN solution at different applied potential.
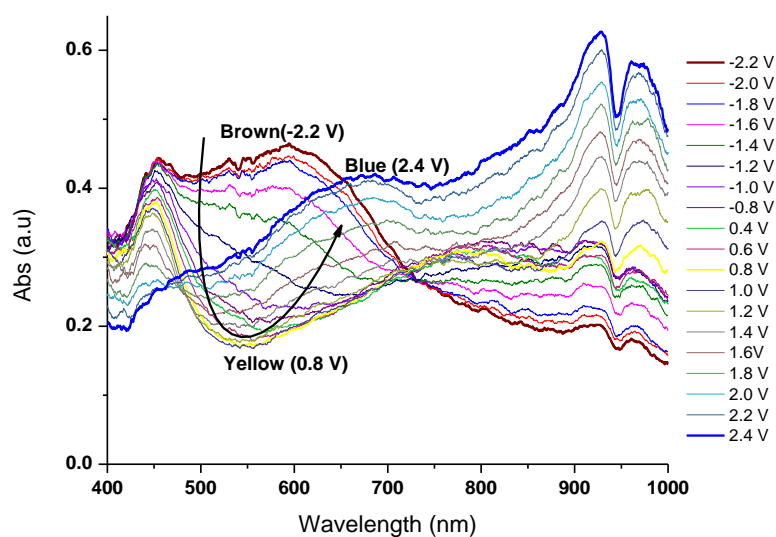
Figure A3.15: Spectroelectrochemical study of P(Th-Cbz-Th)-PEDOT film monitored in 0.1 M of LiClO$_4$/ACN solution at different applied potential.

LIST OF PUBLICATIONS IN INTERNATIONAL JOURNALS

1. Siju C.R., Rao K.N, Ganesan R., Gopal E.S.R., Sindhu S., Synthesis of poly(3, 4 ethylenedioxythiophene) nano structure using reverse microemulsion polymerization. *Phys. Status Solidi C*, 2011, 8: 2739–2741. DOI 10.1002/pssc.201084053.

2. Sindhu S., Siju C.R., Sharma S.K., Rao K.N., Gopal E.S.R., Optical, electrochemical and morphological investigations of poly(3,4 propylenedioxythiophene)-Sultone (PProDOT-S) thin films. *Bull. Mater. Sci*., 2012: 35: 611–616.

3. C.R. Siju., K. Narasimha Rao and S. Sindhu., Enhanced performance Characteristic of Electropolymerized PEDOT films on ITO by one step cyclic voltammetry. *J. Optics*, 2013, 42: 67–72. DOI 10.1007/s12596-012-0113-x.

4. Siju C.R., Saravanan T.R., Rao K.N., Sindhu S., Optical, electrochemical and structural properties of spray coated dihexyl substituted Poly(3, 4 propylene dioxythiophene) film for optoelectronics devices. *Int. J. Polym. Mater. Polym Biomater.* 2014, 63: 374-379.

5. Siju C.R., Shivaprakash N.C., Sindhu S., Gray to transmissive electrochromic switching based on electropolymerized PEDOT-ionic liquid functionalized graphene films. *J. Solid State Electrochem.* 2015, 19: 1393–1402, DOI 10.1007/s10008-015-2756-4.

6. Siju C.R., Shivaprakash N.C., and Sindhu S., Synthesis of Solution-Processable Poly(3,4 propylenedioxy thiophene) nanobelts for Electrochromic device applications, *J. Mater. Chem. C* (Under review).

7. Siju C.R., Shivaprakash N.C., and Sindhu S., Fabrication of Multi-Colored Electrochromic device based on Conjugated polymer bearing Carbazole and Thiophene groups, *Eur. Polym. J.* (Communicated).

LIST OF PAPERS/PROCEEDINGS PRESENTED IN CONFERENCES

1. "A Novel Electrochromic device based on Dihexyl derivatives of Poly(3,4 propylene dioxythiophene) Thin film" in International Workshop on Nanotechnology and Advanced Functional material, 2009 (NTAFM-09)", conducted by National Chemical Laboratory, Pune, India.

2. "Spectral and Electrochemical characterization of Dihexyl derivative of poly(3,4 Propylenedioxythiophene) thin films" in Emerging Trends in Nano biosciences and Workshop on Nano science and Engineering (NANATECH 2009), conducted at Dayanda Sagar college of Engineering, Bangalore, held on 19-20th November, 2009.

3. "Synthesis of poly(3,4 ethylenedioxythiophene) nano structure using reverse microemulsion polymerization in Fourth International Conference on Optical, Optoelectronics and Photonic materials and Applications held at Budapest, Hungary, August 2010.

4. "Enhanced performance characteristics of electropolymerized Poly(3, 4 ethylenedioxythiophene) films on ITO by one step cyclic voltammetry" in International Conference on Contemporary Trends in Optics and optoelectronics, jointly organized by Optical society of India and IIST,Trivandrum held on 17-19th January, 2011.

5. "Preparation and Characterization of Dibenzyl derivatives of Poly(3,4 Propylenedioxythiophene (PProDOT-Bz2) Film of PET substrate for the fabrication of Electrochromic Window" in 6th International Conference on Materials for Advanced Technologies (ICMAT 2011) held on 26th June-1st July 2011, at Suntech Singapore.

6. "Electropolymerization PEDOT thin films for the fabrication of Optoelectronic devices" in International Conference on Materials and Technology (ICMST 2012) held on 10-14 June 2012 at St.Thomas College Pala, Kottayam, Kerala.

7. "Low cost electrochromic Device Based on electropolymerized PEDOT:PSS films in aq.KNO_3 Solution" in 7th International Conference on Materials for Advanced Technologies (ICMAT 2013) held on 30th June-5th July 2013,Suntech Singapore.

8. "Electrochemically exfoliated Graphene on PEDOT films for Optoelectronic applications" in 7th International Conference on Materials for Advanced Technologies (ICMAT 2013) held on 30th June-5th July 2013, at Suntech, Singapore.

9. "Synthesis and Characterization of novel 2, 2 di isopropylbenzyl substituted Poly(3,4 propylenedioxythiophene) derivative for Opto-electronic applications" in International Union of materials Research societies- International Conference in Asia (IUMRS-ICA 2013) held on 16–20th Dec 2013 at Indian institute of Science, Bangalore, India.

10. "Good Optical Memory and Highly Stable Electrochromic Rear-view Mirror Based on New Poly(3,4 Propylenedioxythiophene) Derivative" in 8th International Conference on Materials for Advanced Technologies (ICMAT 2015) & IUMRS-ICA 2015 from 28 June to 3 July, at Suntech, Singapore.

11. "Fabrication and Characterization of Green Organic Light Emitting Diodes Based on Synthesized Tris-8-hydroxyquinoaluminum" in 8th International Conference on Materials for Advanced Technologies (ICMAT 2015) & IUMRS-ICA 2015 from 28 June to 3 July, at Suntech, Singapore.

Brief Biography of the Supervisor

Prof. S. Sindhu is an experimental and theoretical condensed matter physicist. She has completed Ph.D. from Mahatma Gandhi University, Kerala in the year 1998. She has worked as post-doctoral fellow at Department of Electrical Engineering, University of Twente, Netherlands since Jan 1999 to April 2000. She also worked as Postdoctoral research fellow at Department of Physics, Martin-Luther Universitat, Halle, Germany for more than two years (February 2002-May 2004). After that she joined as Research Associate at Dept. of Instrumentation, Indian Institute of Science, Bangalore, India till year 2007. Later, she joined in Dept. of Physics, BITS Pilani. At present, she is working as Associate Professor in Department of Physics and Associate Dean in Practice School division, BITS, Pilani. Her major research interests are in experimental and theoretical analysis of condensed matter phsics. She has wide range of research experience on surface and material science, lattice dynamics and magnetism. Currently she is working on fabrication of molecular electronic devices mainly electrochromic devices, and light emitting diodes using conducting polymers. She is the author and co-author for more than 20 articles published in reputed international journals. She has been serving position as editorial members, and reviewer of several journals. Currently, she has been working as Principal investigator in several ongoing projects which funded by DST and CSIR, India.

Brief Biography of the Candidate

Mr. Siju C.R has received Bachelor of Science in Chemistry from University of Calicut in the year 2002 and Master of Science in Polymer Chemistry from University of Calicut in the year 2005. He received the Master of Technology in Polymer Technology from Cochin University of Science and Technology (2008). Currently, he is working as Lecturer in Department of Chemistry, BITS Pilani. His research interests are design and synthesis of conjugated polymers for optoelectronic applications and organic electronics. He published his research work in 7 international journals and presented his research work in more than 10 international/national conferences held in India and abroad.